



HAL
open science

Synthesis, characterization and biomedical interest of amphiphilic biocompatible and bioeliminable (glyco)copolymers of various architectures

Rieger Jutta

► **To cite this version:**

Rieger Jutta. Synthesis, characterization and biomedical interest of amphiphilic biocompatible and bioeliminable (glyco)copolymers of various architectures. Other. Université Joseph-Fourier - Grenoble I, 2006. English. NNT: . tel-00076829

HAL Id: tel-00076829

<https://theses.hal.science/tel-00076829>

Submitted on 28 May 2006

HAL is a multi-disciplinary open access archive for the deposit and dissemination of scientific research documents, whether they are published or not. The documents may come from teaching and research institutions in France or abroad, or from public or private research centers.

L'archive ouverte pluridisciplinaire **HAL**, est destinée au dépôt et à la diffusion de documents scientifiques de niveau recherche, publiés ou non, émanant des établissements d'enseignement et de recherche français ou étrangers, des laboratoires publics ou privés.

UNIVERSITE DE LIEGE

Liège, Belgique

Faculté des Sciences

Département de Chimie

UNIVERSITE JOSEPH FOURIER

Grenoble, France

Ecole Doctorale Chimie et Sciences du Vivant

Spécialité: Sciences des Polymères

**Centre d'Etude et de Recherche sur
les Macromolécules (CERM)**

Professeur R. JEROME

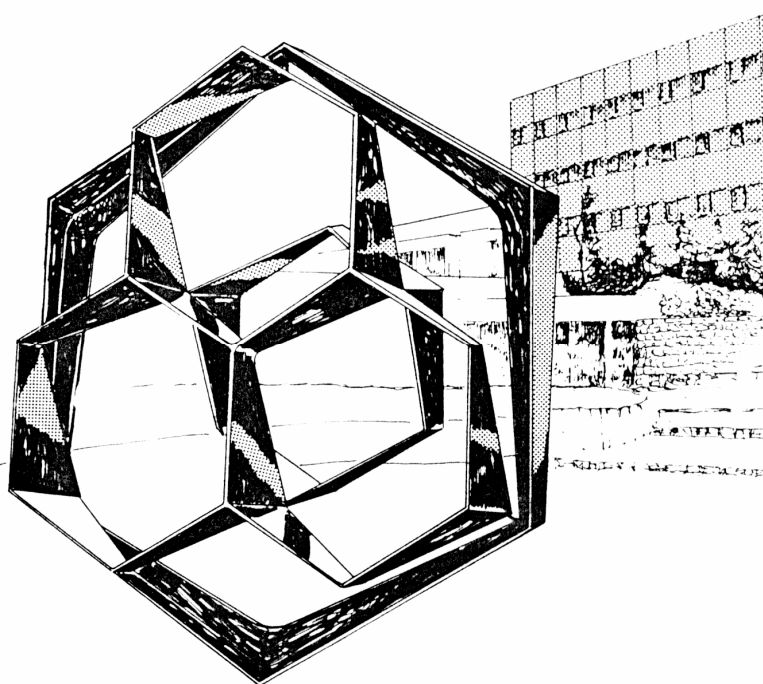
**Centre de Recherches sur les Macromolécules
végétales (CERMAV-CNRS)**

Professeur R. AUZELY-VELTY

THESE EN CO-TUTELLE

(Arrêtés ministériels du 06 janvier 2005 et du 25 avril 2002, France)

**SYNTHESIS, CHARACTERIZATION AND BIOMEDICAL
INTEREST OF AMPHIPHILIC BIOCOMPATIBLE AND
BIOELIMINABLE (GLYCO)COPOLYMERS OF VARIOUS
ARCHITECTURES**



Dissertation présentée par

Jutta RIEGER

pour l'obtention du grade de

Docteur en Sciences

Année académique 2005-2006

Abstract

This work mainly aims at modifying the surface of polymeric nanoparticles by novel biocompatible amphiphilic copolymers, composed of hydrophilic ethylene oxide (EO) units and hydrophobic ϵ -caprolactone (CL) units. Copolymers of different architectures have been considered, i.e., diblock copolymers, graft copolymers and star-shaped copolymers.

Firstly, poly(ethylene oxide) chains α -terminated by an ϵ -caprolactone group and ω -end-capped by a methoxy group (γ PEO.CL) were synthesized by living polymerization of ethylene oxide initiated by the para alkoxide derivative of protected cyclohexanone (*Chapter 1*). This versatile macromolecule was then used, (i) as a PEO macromonomer that was copolymerized by ring-opening polymerization (ROP) with ϵ -caprolactone (ϵ -CL) (*Chapter 2*), and (ii) as a precursor for a AB-double headed PEO chain, that was used to initiate selectively the polymerization of two different monomers and to form an ABC mikto-arm star copolymer (*Chapter 4*).

The copolymerization of γ PEO.CL with ϵ -CL was monitored by $^1\text{H-NMR}$ and the reactivity ratios of the comonomers were calculated. It was accordingly shown that these poly(ϵ -caprolactone)-*graft*-poly(ethylene oxide) copolymers (PCL-*g*-PEO) have a gradient, also called “palm-tree” molecular structure. The amphiphilic properties of the as-prepared copolymers were investigated by measurement of the interfacial tension with a pendant drop tensiometer and were compared to PEO-*b*-PCL diblock copolymers of similar composition and solubility (*Chapter 2*). A second pathway was also considered for the synthesis of poly(ϵ -caprolactone)-*graft*-poly(ethylene oxide) copolymers: the “Michael addition” of end-functional PEO chains onto a PCL backbone bearing mutually reactive groups. Thus, poly(γ -(acryloyloxy)- ϵ -caprolactone)-*co*-(ϵ -caprolactone) random copolymers were reacted with thiol end-capped PEO chains (*Chapter 3*).

A mikto-arm star-shaped copolymer was also prepared starting with the same γ PEO.CL chains. Therefore, a double-headed PEO macroinitiator was prepared by hydrolysis of the α -lactone end-group of the PEO chains. Then, the anionic polymerization of benzyl β -malolactonate (MLABz) was initiated by the α -potassium carboxylate end-group, prior to the ring opening polymerization of ϵ -caprolactone initiated by the hydroxyl group left at the junction of the two blocks of the PEO-*b*-PMLABz diblock copolymer (*Chapter 4*).

The amphiphilic PEO/PCL diblock and graft copolymers were used as stabilizers and surface modifiers of polymeric nanoparticles (NP). The effect of the copolymer structural features (architecture, composition and amount) on the formation and structure of the NP was investigated. As a rule, polymeric nanoparticles are known to activate the complement system, which is part of the human immune system, leading to the rapid elimination of the NPs from the blood circulation. PEO moderates this reaction and is able to make NPs “stealthy” towards the immune system. Thus, the ability of PEO/PCL copolymers to modify the surface of polymeric nanoparticles was confirmed by an *in vitro* test using human serum. This test actually measured the complement activation, i.e., the stealthiness of the nanoparticles, as a function of the composition and architecture of the copolymer used as a stabilizer (*Chapter 5*).

Another challenge of this work was to decorate the surface of such nanoparticles by mannose moieties, which are suitable targeting probes for dendritic, mannose-receptor expressing cells. Therefore, mannose derivatives were covalently attached as an α -end-group to poly(ϵ -caprolactone) and PEO-*b*-PCL diblock copolymers. These amphiphilic glycopolymers were then used as surface modifiers for polymeric NPs, that were characterized by $^1\text{H-NMR}$ spectroscopy and zeta potential measurements. Both the techniques showed that the NPs' surface properties were strongly related to the copolymer used (*Chapter 6*).

Finally, gold-nanodots (10 nm) were prepared and surface-modified by PLA chains. They were then successfully entrapped into polylactide (PLA) nanoparticles (200 nm), which allowed them to be labeled and detected *in vitro* and *in vivo* (*Chapter 7*).

Résumé

L'objectif principal de ce travail est la modification de la surface de nanoparticules polymères par de nouveaux copolymères amphiphiles et biocompatibles, de différentes architectures. L'ensemble des copolymères considérés dans cette étude sont composés d'une chaîne hydrophile de poly(oxyde d'éthylène) (POE) et d'une chaîne hydrophobe à base de poly(ϵ -caprolactone) (PCL).

Tout d'abord, du POE coiffé par une unité ϵ -caprolactone et par un groupement méthoxy en ses extrémités α et ω , respectivement, (γ POE.CL) a été synthétisé par polymérisation anionique amorcée par un alcoolate de cyclohexanone protégée, suivie de l'oxydation de la cyclohexanone en ϵ -caprolactone (*Chapitre 1*). Cette macromolécule polyvalente a été utilisée (i) comme macromonomère et copolymérisée par ouverture de cycle avec l' ϵ -caprolactone (ϵ -CL) (*Chapitre 2*), (ii) comme précurseur de chaînes de POE doublement fonctionnalisées en leur extrémité α , et capables d'amorcer la polymérisation sélective de deux monomères différents (*Chapitre 4*).

La copolymérisation de γ POE.CL avec l' ϵ -CL a été étudiée par RMN- ^1H , et les rapports de réactivité des monomères ont été calculés. Ceci a permis d'établir que les copolymères greffés PCL-*g*-POE présentaient une architecture de type « palmier », c'est-à-dire une distribution en gradient des comonomères. Les propriétés amphiphiles de ces copolymères ont été analysées et évaluées par des mesures de tension interfaciale en utilisant un tensiomètre à goutte pendante. Elles ont été comparées à celles de copolymères biséquencés POE-*b*-PCL de composition et solubilité similaires (*Chapitre 2*). Une deuxième voie de synthèse de copolymères greffés PCL-*g*-POE a encore été envisagée, à savoir l'addition de Michaël de chaînes de POE terminées par un groupement thiol sur des copolymères statistiques d' ϵ -caprolactone et de γ -(acryloyloxy)- ϵ -caprolactone (*Chapitre 3*).

En utilisant le même dérivé de POE (γ POE.CL), un copolymère ternaire avec une architecture en étoile a été synthétisé. Dans ce but, du POE coiffé en son extrémité α par deux fonctions, acide carboxylique et hydroxyle, a été préparé par hydrolyse du groupement terminal ϵ -caprolactone des chaînes γ POE.CL. La polymérisation anionique du β -malolactonate de benzyle (MLABz) a ensuite été amorcée par le groupement carboxylate de potassium. Dans un deuxième temps, la polymérisation de l' ϵ -caprolactone a été amorcée par le groupement hydroxyle formé au point de jonction entre les deux segments du copolymère biséquencé POE-*b*-PMLABz (*Chapitre 4*).

Les copolymères séquencés et greffés de POE et PCL, qui possèdent des propriétés tensioactives, ont été utilisés pour stabiliser et modifier la surface de nanoparticules polymères (NP), vecteurs potentiels pour la délivrance de principes actifs. L'effet des propriétés des copolymères (architecture, composition et quantité) sur la formation et la structure des nanoparticules, a été examiné. En général, les nanoparticules polymères sont réputées activer le « système du complément » faisant partie du système immunitaire, avec pour conséquence leur rapide élimination de la circulation sanguine. Le POE modère cette réaction et peut rendre des NP « furtives » vis-à-vis du système immunitaire. Par conséquent, la capacité de ces copolymères de modifier la surface des NP a été analysée par un test *in vitro* à base de sérum humain. Ce test a permis d'évaluer l'activation du complément, c.-à.-d. la furtivité des nanoparticules, en fonction de la composition et de l'architecture du copolymère utilisé (*Chapitre 5*).

Un autre défi relevé dans ce travail est la fonctionnalisation de la surface de nanoparticules par des molécules de mannose afin de cibler des cellules dendritiques, qui expriment à leur surface des récepteurs pour le mannose. A cet effet, des dérivés du mannose ont été fixés de manière covalente à l'extrémité de la poly(ϵ -caprolactone) et de copolymères biséquencés POE-*b*-PCL par trois voies différentes. Ces copolymères ont été utilisés pour modifier la surface des NP polymères, qui ont été ensuite caractérisées par spectroscopie RMN et mesures du potentiel zeta. Ces deux techniques ont confirmé la modification de la surface des NP (*Chapitre 6*).

Finalement, des nanoparticules d'or (10 nm) modifiées en surface par des chaînes de polylactide (PLA), ont été préparées et incorporées avec succès dans des nanoparticules de PLA (200 nm). Le marquage de ces dernières est un moyen aisé de détecter des vecteurs polymères de médicaments *in vitro* et *in vivo* (*Chapitre 7*).

This work is the result of a “Shared PhD Thesis” carried out at the “Center for Research and Education on Macromolecules” (CERM), laboratory of the “University of Liège” (ULg), Liège (Belgium), and at the “Centre de Recherches sur les Macromolécules Végétales” (CERMAV), laboratory of the CNRS associated to the “Université Joseph Fourier” (UJF), Grenoble (France).

First of all I express my thanks to the two tutors of this thesis, Pr. Robert Jérôme, professor at the ULg and director of the CERM, and Pr. Rachel Auzély-Velty, professor at the UJF and researcher at the CERMAV. I acknowledge Pr. Robert Jérôme for having welcomed a foreign pharmacist in his laboratory, furthermore I am grateful for his confidence and his meticulous examination of this work. All my thankfulness to Pr. Rachel Auzély-Velty who supervised my work in Grenoble and who involved me to the universe of carbohydrates. I have appreciated a lot her comprehension, her steady help and reliability.

I would like to express deep gratitude to Dr. Christine Jérôme, researcher “FNRS” at the CERM, who was the most closely involved in this project, for her constant support, her help and valuable advice during these four years, but also for her every day encouragements, and finally for her friendship.

It is an honor for me that Pr. Doris Klee, Pr. Filip Du Prez accepted to be the “rapporteurs” of this work. I thank Dr. Thierry Delair, Dr. Catherine Passirani and Dr. Christine Jérôme for the examination of this work and I am pleased that Pr. Moreno Galleni is the president of this jury.

This manuscript is the result of numerous collaborations that made the realization of an interdisciplinary study possible.

I would like to thank Pr. Philippe Dubois, Director of the “Service des Matériaux Polymères et Composites” at the University of Mons-Hainaut, for his kind reception in his laboratory and in particular Olivier Coulembier for his sound advice and help.

Thank you Catherine Passirani, Maitre de Conférences à “l’INSERM U646, Ingénierie de la Vectorisation Particulaire”, Angers (France), for the two pleasant and precious weeks in Angers.

I express my gratitude to Thierry Delair, researcher at “Unité mixte CNRS-Biomérieux”, Lyon, for his interest in my work and for his generous invitation to prepare and characterize polymeric nanoparticles with his assistance in Lyon.

All the MALDI-ToF measurements have been performed at the University of Ghent, at the Department of Organic Chemistry, in the Polymer Chemistry Research Group. I am grateful to Pr. Filip Du Prez, and to Katrien Bernaerts for her availability, promptness and sympathy. It was a real pleasure to work with her.

I would also like to thank Pr. Pierre Guénot of the “Centre Régional de Mesures Physiques de l’Ouest”, for the measurements by mass spectrometry.

I spent three pleasant years in Liège, and that thanks to all the members of the CERM. I am indebted to Philippe Lecomte and Christoph Detrembleur for her multiple assistance and scientific discussions, and to Philippe for our unforgettable trip to China. Thank you Krystyna Pezzetti, Enza Vesposito for your kindness and willingness to help, even when I was in Grenoble.

I thank the old crew of the “minus 2” (David, Sabine, Catherine, Hongjin, Abdel, Véro, Martine, Valérie, Sam, Milena, Patrick and Eric) for their warm-hearted reception and their help. A special mentioning is addressed to Kathy, with whom I spend my best time in the CERM. I won't forget Sandrine Gautier neither who familiarized me with the domain of nanoparticles during the first three months of my thesis.

Thanks to the members of the “U.D. chimie”, and especially to Philippe Mottet.

I acknowledge François the synthesis and supply of precious polymers during my stay in Grenoble.

It was not easy to leave Liège, but all the persons of the CERMAV, secretaries, technicians, researchers and students helped me to adapt myself rapidly to the new environment. I am especially grateful to Isabelle and Michel for their assistance during my RMN sessions, but also to Martine M., Magali, Martine B., Patrick and Claudius.

I thank Jean-Luc Putaux for the Cryo-TEM experiments and Frédéric Dubreuil for the AFM images, and I acknowledge their help for the finalization of Chapter 6. I am also grateful to Pr. Marguerite Rinaudo for the scientific discussions.

I express my everlasting gratitude to the lovable “foufous” of the “office 110”, Aurélia, Caroline and Shirin, who integrated me from the first minute of my arrival, who helped me through all imaginable situations and who made my laugh! Without them, my time in Grenoble would have been less cheerful, but more sad and lonely. I won't forget the others of the gang, above all LEMONIA and Pascal, but also Johann, Marie-Pierre, Lina, Stéphane, Sami, Roberto, Hélène, Gianluca, Fabien etc. Many thanks to Shirin and Caroline for their patience and support during the printing of the manuscript.

Finally, I cannot find the right words to express my gratefulness that I feel for my parents. I thank them infinitely for their support, their encouragements and their company in my life. I thank Alex for being and staying at my side, even in difficult situations, and for “proofreading” the General Introduction.

Danke !

Ce travail a été réalisé en co-tutelle au « Centre d'Etude et de Recherche sur les Macromolécules » (CERM), laboratoire de l'Université de Liège (ULg), Liège (Belgique), et au « Centre de Recherches sur les Macromolécules Végétales » (CERMAV), laboratoire propre du CNRS associé à l'Université Joseph Fourier (UJF), Grenoble (France).

Tout d'abord, mes sincères remerciements sont adressés à mes deux directeurs de thèse, le Pr. Robert Jérôme, professeur à l'ULg et directeur du CERM, et le Pr. Rachel Auzély-Velty, professeur à l'UJF et chercheur au CERMAV à Grenoble. Je remercie le Pr. Robert Jérôme pour avoir accueilli si facilement une pharmacienne étrangère dans son laboratoire pendant plus de trois ans, pour sa confiance et pour avoir examiné ce travail avec rigueur. Ma gratitude va également au Pr. Rachel Auzély-Velty qui m'a encadrée pendant mon année à Grenoble et qui m'a fait partager sa passion pour les glycopolymères. Je lui suis particulièrement reconnaissante pour sa disponibilité et son suivi permanent.

La réalisation de ma thèse de doctorat a été une expérience enrichissante mais parfois difficile. J'exprime ma profonde reconnaissance au Dr. Christine Jérôme, « Chercheur qualifié FNRS » au CERM, pour son soutien constant tout le long de ces quatre années, ses précieux conseils, ses encouragements quotidiens qui m'ont indiscutablement permis d'évoluer et finalement pour son amitié.

C'est un honneur pour moi que les Professeurs Doris Klee et Filip Du Prez aient accepté d'être rapporteurs de ce travail. Mes remerciements vont également aux Docteurs Thierry Delair, Catherine Passirani et Christine Jérôme pour leur participation à mon jury de thèse et au Professeur Moreno Galleni qui en est le Président.

Ce travail est le fruit des collaborations interdisciplinaires entre de nombreuses équipes qui ont contribué de manière importante aux résultats obtenus. Je tiens à remercier le Pr. Philippe Dubois, Directeur du « Service des Matériaux Polymères et Composites » à l'Université de Mons-Hainaut, de m'avoir accueilli à Mons et plus particulièrement Olivier Coulembier avec qui j'ai pu travailler pour ses conseils judicieux et sa disponibilité. Je souhaite exprimer ma sympathie et ma gratitude à Catherine Passirani, Maître de Conférences à l'INSERM U646, Ingénierie de la Vectorisation Particulaire, Angers (France), pour le séjour agréable et enrichissant à Angers. J'adresse également mes remerciements à Thierry Delair, chercheur à l'« unité mixte CNRS-Biomérieux », Lyon, pour l'intérêt qu'il a porté à ce travail et pour m'avoir accueillie dans son équipe si généreusement pendant plus qu'une semaine. L'ensemble de mesures de MALDI-ToF ont été réalisé à l'University of Ghent (Department of Organic Chemistry, Polymer Chemistry Research Group). J'exprime toute ma gratitude à son directeur le Pr. Filip Du Prez, et je remercie sincèrement Katrien Bernaerts pour sa disponibilité, sa rapidité et sa sympathie. C'était un vrai plaisir de travailler avec elle.

Je remercie également Pr. Pierre Guénot du Centre Régional de Mesures Physiques de l'Ouest, pour les analyses par spectrométrie de masse.

Si mes trois années à l'ULg se sont bien passées c'est grâce à l'ensemble des personnes du CERM. Un grand merci à Philippe Lecomte et Christoph Detrembleur pour leurs multiples conseils lors de nos discussions scientifiques, et à Philippe pour notre voyage inoubliable en Chine. Toute ma sympathie à Krystyna Pezzetti, Enza Vesposito pour leur gentillesse, disponibilité et l'aide qu'elles m'ont apportées, même quand j'étais partie à Grenoble.

Je remercie toute l'ancienne équipe du « moins 2 » (David, Sabine, Catherine, Abdel, Hongjin, Véro, Martine, Valérie, Sam, Milena, Patrick et Eric) pour leur accueil chaleureux et leur aide. Une mention spéciale est destinée à Kathy grâce à laquelle j'ai passé mes meilleurs mois à l'ULg. Je n'oublie pas non plus Sandrine Gautier, en effet, elle m'a fait profiter de ses expériences dans le domaine des nanoparticules les trois premiers mois de mon doctorat.

J'adresse mes remerciements aux membres de l'U.D. chimie, et plus particulièrement à Philippe Mottet pour sa disponibilité et sa gentillesse.

Merci à François pour les précieux produits qu'il m'a fournis lors de mon séjour à Grenoble.

Il n'a pas été facile de quitter mes Liégeois, et c'est grâce aux membres du CERMAV, secrétaires, techniciens, docteurs et permanents que j'ai pu m'adapter rapidement à mon nouvel environnement. Je remercie l'ensemble du personnel scientifique et technique du CERMAV, plus particulièrement Isabelle et Michel du service de RMN, mais aussi Martine M., Magali, Martine B., Patrick et Claudius.

Un tout grand merci à Jean-Luc Putaux pour les expériences Cryo-TEM et son aide pour la finalisation du Chapitre 6, et à Frédéric Dubreuil pour la relecture du même chapitre et le traitement des images AFM. Merci également au Pr. Marguerite Rinaudo pour nos discussions scientifiques.

J'aimerais tout particulièrement remercier les adorables « fufous » du « bureau 110 », Aurélia, Caroline et Shirin, qui m'ont, dès mon arrivée au CERMAV, intégrée et aidée dans toutes les situations imaginables, fait rire et appris à vivre sans lumière. Sans elles, les mois à Grenoble auraient été beaucoup moins drôles, plus tristes et seuls. Sans oublier les autres de la bande des Grenoblois, notamment LEMONIA, et puis Pascal, Johann, Marie-Pierre, Lina, Stéphane, Sami, Roberto, Hélène, Gianluca, Fabien etc. Un énorme merci à Shirin et Caroline pour leur soutien au moment de l'impression de ma thèse.

Et, ils me manquent les mots pour exprimer ma gratitude que j'éprouve pour mes parents. Je les remercie infiniment pour leur soutien, leurs encouragements et leur accompagnement dans ma vie. Et merci de tout mon cœur à Alex d'être à mes côtés, même dans les moments difficiles, et de la relecture de l'Introduction.

Danke !

Für meine lieben Eltern...

Table of Contents

General Introduction		1-44
Chapter 1	Synthesis and characterization of lactone end-capped poly(ethylene oxide) as new building block for biomaterials	45-72
Chapter 2	Controlled synthesis and interface properties of new amphiphilic poly(ϵ -caprolactone)- <i>graft</i> -poly(ethylene oxide) copolymers	73-104
Chapter 3	Versatile functionalization and grafting of poly(ϵ -caprolactone) by Michael-type addition	105-116
Chapter 4	Controlled synthesis of an ABC miktoarm star-shaped copolymer by sequential ring-opening polymerization of ethylene oxide, benzyl β -malolactonate and ϵ -caprolactone	117-144
Chapter 5	Synthesis of amphiphilic copolymers of poly(ethylene oxide) and poly(ϵ -caprolactone) with different architectures and their role in the preparation of stealthy nanoparticles	145-174
Chapter 6	Mannosylated poly(ethylene oxide)- <i>b</i> -poly(ϵ -caprolactone) diblock copolymers: synthesis, characterization, applications for surface modification of poly(D,L-lactide) nanoparticles and interaction with lectins	175-238
Chapter 7	PLA-coated gold nanoparticles for the labeling of PLA biocarriers	239-260
General Conclusions and Perspectives		261-267

General Introduction

Polymeric nanoparticles for drug delivery

Contents

I. PREFACE.....	5
(i) <i>First generation NPs</i>	6
(ii) <i>Second generation NPs – “passive targeting”</i>	7
(iii) <i>Third generation NPs – “active targeting”</i>	8
II. POLYMER MATERIALS USED FOR THE PREPARATION OF NPs	9
II.1. <i>Natural Polymers</i>	9
II.2. <i>“Degradable” synthetic polymers</i>	12
II.3. <i>“Non-degradable” synthetic polymers</i>	16
II.4. <i>Poly(ethylene oxide) (PEO)</i>	16
III. PREPARATION OF POLYMERIC NANOPARTICLES	19
III.1. <i>Preparation of nanospheres from preformed polymers</i>	19
III.1.1. <i>Emulsion-evaporation</i>	19
III.1.2. <i>Salting-out</i>	20
III.1.3. <i>Emulsification-diffusion</i>	21
III.1.4. <i>Nanoprecipitation</i>	21
III.2. <i>Synthesis of nanospheres by in-situ polymerization</i>	23
III.3. <i>Preparation of nanocapsules</i>	25
IV. SURFACE FUNCTIONALIZATION.....	27
IV.1. <i>Functionalization with biological (macro)molecules</i>	27
IV.2. <i>Functionalization with specific ligands: specific interaction through biological recognition</i>	27
IV.3. <i>Strategies for surface modification</i>	31
IV.3.1. <i>Adsorption on preformed nanoparticles</i>	31
IV.3.2. <i>Functional surfactants as stabilizers and surface-modifiers</i>	33
IV.3.3. <i>Emulsion, miniemulsion or dispersion polymerization</i>	36
IV.3.4. <i>Covalent linking of functional molecules to preformed NPs</i>	38

I. Preface

In the last decade, nanoparticles (NPs) have reached increasing interest both for drug delivery purposes and as diagnostic tools. The interest of NPs as drug carrier relies on the difficulties met in drug delivery. In fact, after extravascular administration of a drug, its fate is determined by the combination of several processes, i.e. its *absorption* to the blood stream, *distribution* in the organism, and finally *metabolism* and *elimination*. Regardless of the administration route, each of these processes depends mainly on the physicochemical properties of the drug. Drug delivery systems (DDS) have thus been developed to improve the pharmacological properties of conventional (“free”) drugs.

Among them, colloidal DDS, such as nanoparticles, are especially attracting, because of their multiple advantages.¹ They allow

- *solubilization* of poorly water soluble hydrophobic drugs,
- *protection* of sensitive drugs (e.g. proteins, nucleotides...) from premature enzymatic or metabolic degradation,
- altering the *pharmacokinetics* of drugs by controlled (prolonged/sustained) release,
- *avoiding the rapid renal clearance* of small drugs,
- changing the *biodistribution* of drugs in the organism and delivering them specifically to their pharmaceutical targets,
- *diminishing side effects* as a result of the gain of selectivity and thus providing the possibility to reduce the administered quantity of drug,
- *altering the conventional route of administration* of a drug (e.g. circumvent injections or infusions) and enhancing so the patient’s comfort.

Polymeric **nanoparticles** (NPs) are carriers in the nanometer range (with a diameter less than 1 μm) prepared from natural or synthetic polymers. This definition does not take into account any morphological and structural organization of the polymer. The term “**nanosphere**” is used to describe NPs that are constituted by a solid “homogeneous” polymeric matrix, as schematically represented in Figure 1. The delivery of the therapeutics proceeds either by diffusion through the polymer matrix or -in case of biodegradable particles- by degradation of the latter, or by both processes.

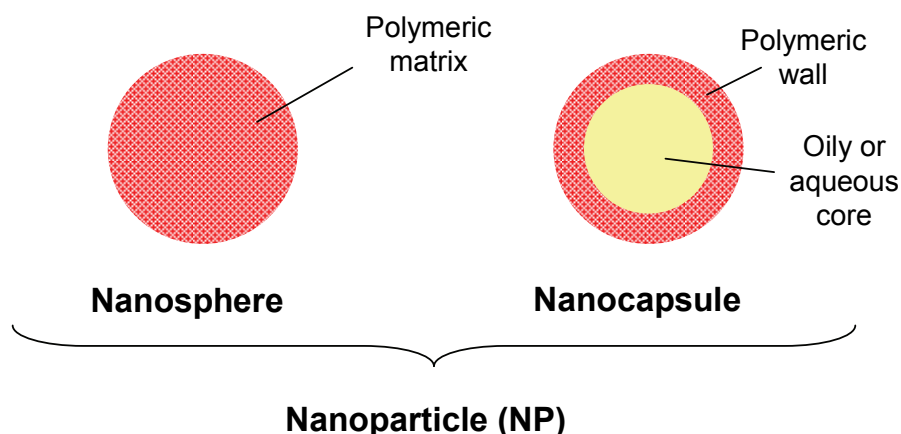


Figure 1. Schematic representation of nanospheres and nanoparticles.

In contrast, “**nanocapsules**” are NPs where a polymeric membrane surrounds a cavity filled by an oily or aqueous liquid, containing the drug. They are therefore considered as “reservoir” systems, where the diffusion of the hydrophilic or hydrophobic drug out of the nanocapsules’s core is controlled by the nature of the polymeric membrane. Both types of NPs can be administered via multiple routes, such as *intravenous*, *oral*, *pulmonary*, *nasal* and *ocular* routes, as a solid or suspension. It should be noted that most of the current systems are designed for *intravenous* and *oral* administration.

Polymeric nanoparticles (NPs) have been the subject of numerous studies for more than 20 years and have evolved and progressed since then, as presented hereafter.

(i) First generation NPs.

Whenever NPs are administered to the human body, they are rapidly recognized as foreign bodies and consequently removed from the blood circulation. In the organism, numerous plasma proteins adsorb at their surface, leading to the activation of the complement system. Consequently, the colloidal drug carriers are rapidly recognized by macrophages of the mononuclear phagocyte system (MPS) and removed within seconds from the blood stream. Organs with high phagocytic activity are the liver, spleen and bone marrow. These organs possess a discontinuous, i.e. more permeable, endothelium, where the blood is directly in contact with the immune active macrophages. Therefore, NPs of the “first generation” accumulate in and *passively target* liver, spleen and bone marrow. Such NPs have thus found application in the treatment of liver cancer and other liver-related diseases.²

As a rule, the protein adsorption on the NPs' surface, i.e. the key step to induce a cascade of biological processes leading to their elimination, is based on various interactions, but especially on interactions of *hydrophobic* domains of the proteins with hydrophobic domains present at the NPs' surface.

(ii) Second generation NPs – “passive targeting”.

In order to target other organs than tissues with high phagocyte activity, further developments strove for avoiding the rapid adsorption of blood proteins, i.e. the activation of the complement system. This has been achieved by modifying the surface of the NPs, especially by hydrophilic materials in order to circumvent hydrophobic protein-particle interactions. Indeed, the coating by hydrophilic chains leads to repulsion of proteins and consequently to prolonged residence times of the NPs in the blood stream. These surface-modified NPs are also called carriers of the “second generation” or “*stealthy*” NPs. The hydrophilic polymers that have been used for “protein-repellent” surface coating are synthetic polymers, particularly poly(ethylene oxide) (PEO),^{3,4} but also polysaccharides, such as **heparin**^{5,6} and **dextran**⁷.

Such long-circulating colloidal systems have reached interest in the field of cancer diagnosis and treatment. In general, cancerous tissues possess a defective vascular architecture, due to the rapid vascularization necessary to serve fast-growing cancers cells, coupled with poor lymphatic drainage. This phenomenon is known as the “enhanced permeation and retention effect” (**EPR effect**) (Figure 2) and allows long-circulating NPs to *passively target* cancerous tissues, due to their large size in comparison with free drugs.⁸ Actually, it has been shown in numerous studies that anticancer drugs encapsulated in PEO-coated NPs accumulate preferentially in cancer cells.^{9,10}

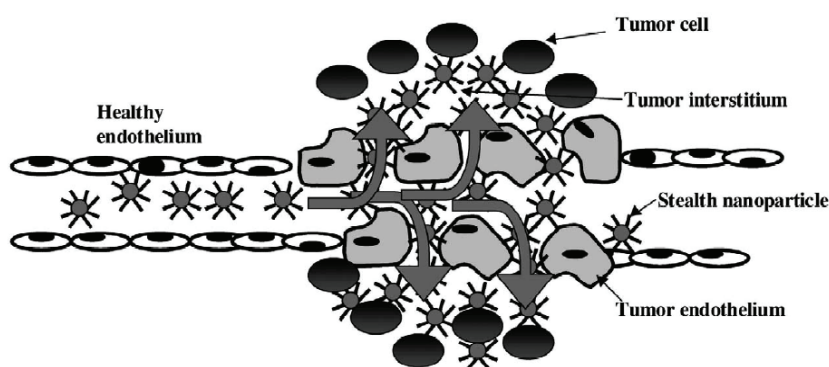


Figure 2. Extravasation of long-circulating stealthy nanoparticles in the tumor interstitium by passive diffusion or convection across the altered and hyperpermeable neoplastic endothelium.¹⁰

(iii) Third generation NPs – “active targeting”.

It is possible to give carriers affinity to specific tissues by decorating their surface with targeting ligands. This kind of carriers delivers a drug specifically to its pharmacological site in the organism and allows thus to decrease the administered quantity of drugs and to minimize side effects. Indeed, the latter are generally the result of the presence of the drug at other tissues than at the desired one.

Targeting ligands can be monoclonal antibodies, sugars, hormones, peptides (such as the tripeptide, arginine-glycine-aspartic acid¹¹), vitamins (e.g. biotin¹²) or other small organic molecules (e.g. folic acid⁹). Colloidal carriers, whose surface is decorated by targeting moieties, are also called “NPs of the third generation”, and today most studies tend to design such nanocarriers. The surface functionalization of polymeric NPs is thus the key point for *targeted drug delivery*.

II. Polymer materials used for the preparation of NPs

Depending on the route of administration (oral, intravenous, subcutaneous or topical etc.) and the application of polymeric NPs (drug carriers or diagnostic systems), the material used to produce the colloidal systems meets different physiological and biological requirements. Among these requirements, biocompatibility and safety are of crucial importance. Furthermore, it must be considered whether bioerosion or biodegradation is desired or not. *Bioerosion* refers to the solubilization of an initially water-insoluble material with or without changes in the chemical structure, while *biodegradation* refers to the solubilization that occurs as a consequence of the cleavage of bonds of the polymer backbone. The prefix “bio” is used since erosion or degradation takes place in a biological environment, either by biocatalytic processes (fungi, enzymes, etc.) or by chemical or radical processes (hydrolysis, oxidation etc.). Degradable polymers have great potential for drug delivery purposes. It must be noted, that not only the polymer itself used for the pharmaceutical formulation, but also the degradation products (metabolites) must be nontoxic, biocompatible and chemically inert. Synthetic biodegradable polymers are typically degraded by chemical hydrolysis whereas the degradation of natural polymers, i.e. polymers derived from animal or plant sources, generally requires enzymes to catalyze the hydrolysis.

In the following part, the main polymers used for the preparation of nanocarriers are described. Three groups of polymers can be distinguish, i.e. **(1) natural** polymers (“biopolymers”), **(2) synthetic** polymers which are “**degradable**” by biological or chemical processes in the human body and **(3) “non-degradable”** synthetic polymers.

II.1. Natural Polymers.

Polysaccharides (PS) represent - beside poly(peptides) - the most important group of **natural polymers**.¹³ Many polysaccharides are biocompatible and biodegradable.¹⁴ In addition, they display very attracting physico-chemical properties, in terms of gelation characteristics, chelating properties and biological activity. These properties as well as their interactions with living medium can be tuned by proper chemical modifications.

Several biocompatible polysaccharides such as chitosan, dextran, heparin and hyaluronic acid have been shown to be interesting candidates for the modification of NPs’ surfaces. This allows, for instance, reducing the uptake of NPs by the mononuclear phagocyte system (MPS) and also, in some cases, conferring specific biological

functions.¹⁵ In contrast to that, only few PS are used as matrix material for the preparation of nanospheres. They are briefly summarized in the following paragraphs.

Chitosan consists of a linear chain of (1-4) linked 2-amino-2-deoxy- β -D-glucopyranose and 2-acetamido-2-deoxy- β -D-glucopyranose units (Figure 3).

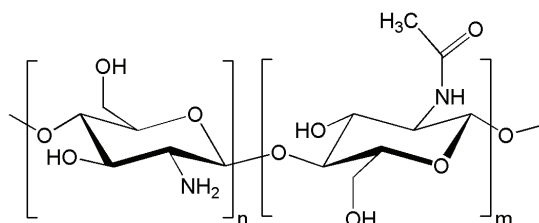


Figure 3. Chemical structure of chitosan.

In acidic conditions ($\text{pH} < 6$), most of the amino groups are protonated, and the polycation is easily water-soluble. Due to its special adhesive properties to mucosal surfaces, chitosan has largely been investigated as coating material of colloidal carriers for oral administration to the gastrointestinal tract,¹⁶ but also for nasal, ocular, buccal and vaginal routes. Besides its mucoadhesive properties, chitosan displays low toxicity, degradability by enzymes such as chitinase and lysozyme,¹⁴ anticoagulant properties, and antibacterial and antifungal action. It has also been demonstrated to be a promoter of wound healing in the field of surgery.^{17,18}

As mentioned above, taking advantages of the polycationic nature of chitosan, chitosan NPs have been prepared based on ionic gelation of chitosan with sodium tripolyphosphate. Furthermore, the polycationic character of chitosan makes it an interesting material for *nonviral gene delivery*. It forms polyelectrolyte complexes with the negatively charged DNA, condenses it and allows its protection against DNase.^{19,20} Finally, the properties of chitosan have been modified by chemical modifications such as deacetylation, N-sulfation or modification by organic molecules (e.g. sugars etc.), giving rise to other applications. Very recently, polyelectrolyte complex NPs were prepared from self-complexation of amphoteric N-sulfated chitosan.²¹

However it should be mentioned that the safety or toxicity of positively charged polymers for systemic application (e.g. intravenous administration) is currently discussed controversially. Indeed, it has been reported that chitosan induces the opening of the *tight junctions* between cells, enhancing their permeability.^{22, 23}

Dextran is an α -D-1,6-glucose-linked glucan with side-chains 1-3 or 1-4 linked to the backbone units, see Figure 4. The branches are mostly one to two glucose units long.

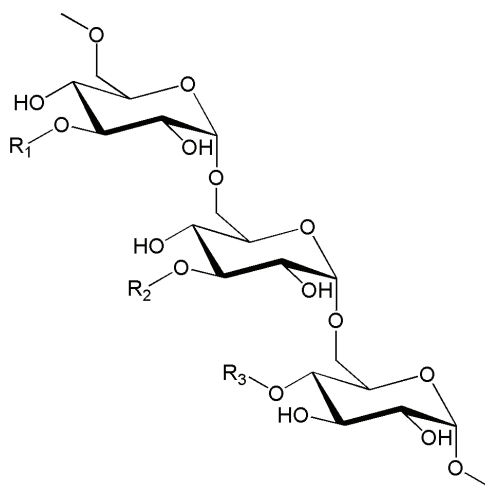


Figure 4. Chemical structure of dextran. R₁, R₂ and R₃ are positions of branching.

The clinical use of dextran over the past 50 years provides impressive proofs of its safety and quality. Due to its biocompatibility and hydrophilicity, it is often utilized as a coating material for NPs. Actually it has demonstrated protein repulsive properties. Moreover, the dextran macromolecule presents a large number of reactive hydroxyl groups for chemical attachment of functional molecules.

Hyaluronic acid (HA) is a linear polysaccharide composed of a repeating disaccharide unit of *N*-acetyl-D-glucosamine and D-glucuronic acid, belonging to the glycosaminoglycan family (Figure 5).

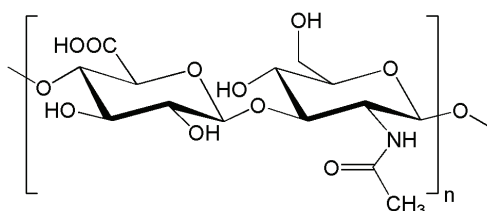


Figure 5. Repeating disaccharide units of HA.

It is a component of the synovial fluid, cartilage, vitreous humour and extracellular matrices.^{14,24} Protein interactions with HA play crucial roles in cell adhesion, cell mobility, inflammation, wound healing and cancer metastasis. Its carboxyl groups are mostly

deprotonated at physiological pH, thus conferring a polyanionic character to the polymer. Like chitosan, the advantage of using hyaluronic acid as a surface modifier relies on its *bioadhesive* properties, which have been particularly exploited for ophthalmic applications. Similar to other anionic polymers, such as poly(acrylic acid), the carboxylic groups are responsible for their adhesion to the mucus gel layer. It should be emphasized, that the biological activity of HA depends on its molecular weight.²⁵

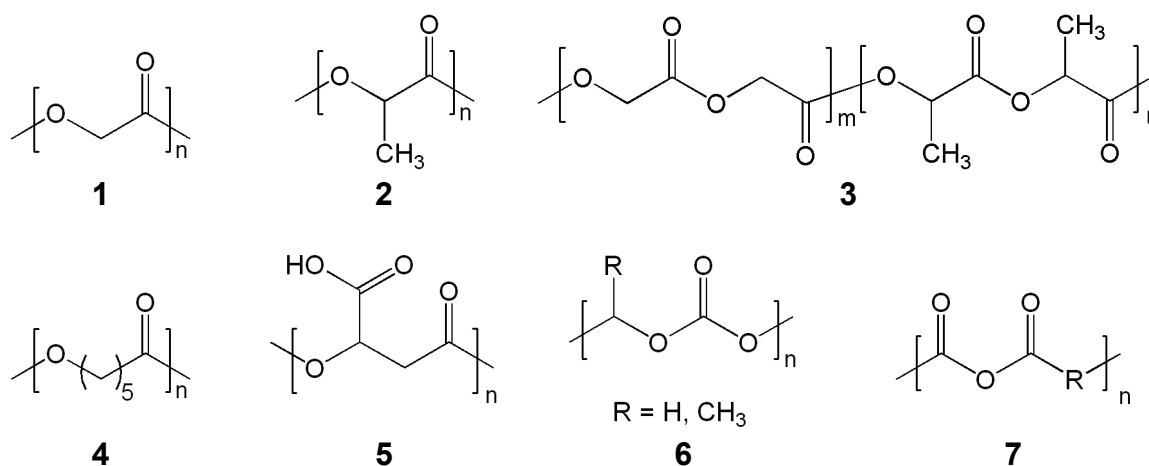
II.2. “Degradable” synthetic polymers.

In contrast to natural polymers, whose molecular weight and molecular weight distribution are determined by the fabrication and extraction procedures, *synthetic polymers* can be tailor-made. Hence, their physical and chemical properties can be varied over a wide range, in particular by copolymerization with appropriate (functional) comonomers. Additionally, using controlled polymerization techniques, the macromolecular characteristics can be adjusted and narrow molecular weight distribution (PDI) can be reached. Furthermore, some synthetic polymers can be prepared in oil-in-water (O/W) emulsion, which makes the *in situ* synthesis of NPs by emulsion-polymerization techniques possible.

Figure 6 presents the chemical structure of the main synthetic polymers used for the preparation of NPs.

The first and probably most important and frequently used group of biodegradable polymers comprises the *aliphatic linear polyesters*. (Co)polyesters based on poly(lactic acid) (or poly(lactide), PLA), poly(glycolic acid) (PGA) and poly(lactide-*co*-glycolide) (PLGA) have been used for more than three decades for a large variety of medical applications²⁶ and are considered as the best biomaterials with regards to design and performances. Indeed, they meet the biological requirements for safety and are biodegradable to nontoxic metabolites, and approved by the Food and Drug Administration (FDA) for biomedical application.

(A) “Degradable” synthetic polymers



(B) “Non-degradable” synthetic polymers

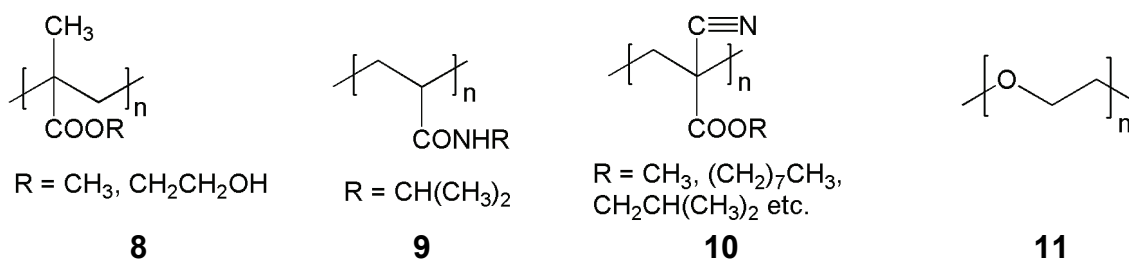


Figure 6. Chemical structure of (A) the main biodegradable synthetic polymers: (1) poly(glycolic acid), (2) poly(lactic acid), (3) poly(lactide-co-glycolide), (4) poly(ϵ -caprolactone), (5) poly(malic acid), (6) poly(ethylene carbonate) ($R = \text{H}$), poly(propylene carbonate) ($R = \text{CH}_3$), (7) poly(anhydride), and (B) some non-degradable synthetic polymers: (8) poly(methyl methacrylate) ($R = \text{CH}_3$), poly(hydroxyethyl methacrylate) ($R = \text{CH}_2\text{CH}_2\text{OH}$), (9) poly(*N*-isopropylacrylamide), (10) poly(alkylcyanoacrylate), (11) poly(ethylene oxide) used as core material for the preparation of polymeric nanoparticles.

Since **lactid acid** contains an asymmetric α -carbon atom, two different optical isomers exist, D- and L-lactid acid, giving rise to four distinct polymers. The polymers derived from the optically active monomers, i.e. poly(D-lactide), P(D-LA), and poly(L-lactide), P(L-LA), are semi-crystalline materials and exhibit identical physicochemical properties. Contrary the racemic P(D,L-LA) is purely amorphous and has striking different properties. Furthermore, these racemic and semi-crystalline polymers exhibit different degradation rates, as the (bio)degradation is dependent on the polymer crystallinity.²⁷ Despite of a chemically identical backbone structure and the same degree of hydrophobicity, devices made of poly(L-lactic acid) degrade much more slowly than

identical devices made of poly(D,L-lactic acid). The slower degradation of poly(L-lactic acid) is related to its semicrystalline morphology. Indeed, in the crystalline domains, the polymer chains are densely packed and organized in spherulites that resist the penetration of water. Amorphous regions are hydrated and thus hydrolyzed first, and then the crystalline regions undergo hydrolysis. This involves the enrichment of crystalline zones in the device during the degradation process leading to a change of its mechanical and biological properties.

Crystallinity is only one feature that determines the **biodegradation** of polymeric materials. The latter may be affected by many other important factors such as the chemical stability of the hydrolytically sensitive groups in the polymer backbone, the hydrophilic or *hydrophobic character* of the repeating units, the initial molecular weight and molecular weight distribution. The fabrication process, size, geometry (specifically the surface area to volume ratio), and porosity of the device have also a tremendous impact on the degradation rate.²⁷ Since the hydrolytic degradation is caused by the reaction of labile bonds with water, typically ester bonds in the polymer chain, the reaction rate is intimately connected with the ability of the polymer to absorb water. Thus, devices made of poly(glycolic acid) erode faster than identical devices made of the more hydrophobic poly(lactic acid) or even poly(ϵ -caprolactone) (see next paragraph), although the ester bonds have almost the same chemical reactivity toward water in both polymers. Vert *et al.*^{27,28} demonstrated the complexity of PLA, PGA and poly(lactic-co-glycolic acid) (PLGA) degradation, and emphasized the dependence of the hydrolytic process on the *size and morphology* of the biomedical device. Surprisingly, it has been demonstrated that PLA *microparticles*, degrade faster than PLA *nanoparticles*, and that this phenomenon relies on diffusion mechanisms.²⁹ Indeed, due to the large surface/volume ratio of NPs, the acid - produced during the degradation - can easily diffuse out of the NP. On the contrary, within *microparticles*, the produced acid accumulates inside the particles, as the diffusion is slower, and thus the local decrease of the pH has an *autocatalytic effect* on the degradation process. Indeed, after water uptake, the polymer chains degrade (corresponding to a decrease of the molecular weight) and finally weight loss of the material appears due to the diffusion of the degraded polymer chains out of the bulky material.

Another example of hydrolytically degradable polyester is **poly(ϵ -caprolactone) (PCL)**, which is widely used in the field in biomaterials or as degradable plastic. This polymer is semi-crystalline and therefore characterized by a slower (bio)degradation. As a rule, a device made of PCL degrades within several months up to some years, in contrast to

PLA, that degrades in the range of weeks or months, and PGA, which degrades within hours of days. This explains why PLGA or PLA are favored over PCL for the design of DDS intended to deliver quite high amounts of a drug for a limited period of time.

Furthermore, other biodegradable polyesters derived from naturally occurring, multifunctional hydroxy acids and amino acids, such as **malic acid** and **aspartic acid**, have been investigated by Lenz and Guerin.³⁰ **Poly(malic acid) (PMLA)** is biocompatible and degradable, and -in contrast to PLA and PCL- hydrosoluble due to its carboxylic acid groups. Biocompatibility tests indicated that poly(β -malic acid) is nontoxic and non-immunogen.³¹

Most of these polyesters lack functional groups, and efforts have thus been made to synthesize biodegradable aliphatic polyesters bearing functional groups that are available for further modification. Such copolymers can be reached by copolymerization of novel functional monomers with conventional ones.^{32,33,34,35,36} The features of such materials are affected by the choice of the comonomer, the polymer architecture and the molecular weight. Copolymers have been synthesized in order to adjust the degradation rate or the mechanical properties. For instance, poly(ethylene oxide)-*b*-poly(lactide) block copolymers (PEO-*b*-PLA) have been prepared and used to obtain NPs exhibiting faster degradation with respect to plain PLA NPs. Indeed, the introduction of a hydrophilic polymer (PEO) favors the hydration of the polyester NPs, which is the key requirement for hydrolytic degradation to take place. For the same reason, the ester functions next to the PEO segment degrade first, and thus PEO chains are lost rapidly.

Moreover, **polycarbonates**, such as poly(ethylene carbonate) and poly(propylene carbonate), have been explored in the design of new polyester-related structures for the preparation of NPs for drug delivery. For instance, they have been tested as biodegradable carriers for the delivery of 5-fluorouracil (5-FU)³⁷ and were found to be degraded enzymatically.³⁸

In addition to natural proteins, synthetic **(co)poly(amides)**, such as **poly(lysine)** and **poly(glutamic acids)** have also been studied as drug carriers.³⁹

Beside the described polymers, there are a lot of other classes of biodegradable polymers used for biomaterials, such as **poly(anhydrides)**, **poly(phosphate esters)**, **poly(phosphazenes)** and **poly(orthoesters)**. An exhaustive treatment on their properties, synthesis, degradation characteristics, biocompatibility and toxicity is out of the scope of this work and may be found in the literature.²⁶

II.3. “Non-degradable” synthetic polymers.

“Non-degradable” polymers are considered here as polymers that are not degraded by biological or chemical processes in biological environments. Polymers made of *acrylic* or *vinyllic* monomers constitute an important group of non-degradable materials used for the preparation of ‘biostable’ polymeric NPs. The interest in these materials relies mainly on the easiness of preparation and the availability of functional groups.

Poly(alkylcyanoacrylate) (PACA) represents an intermediate class between the synthetic biodegradable and non-biodegradable polymers.⁴⁰ Indeed, it has been shown that PACA particles are degraded by surface erosion process,⁴¹ through enzymatic hydrolysis of the ester side chains of the polymer. The polymer chains are therefore degraded to hydrophilic compounds, and the rate of elimination is dependent of the length of the non-degradable alkyl chain.⁴² It was demonstrated that materials based on PACA are well tolerated *in vivo*.

Finally, it is worth mentioning that *stimuli responsive polymers*, such as **poly(N-isopropylacrylamide)** (PNIPAAm), are promising materials for the preparation of stimuli responsive colloidal carrier systems.^{43,44}

II.4. Poly(ethylene oxide) (PEO).

Poly(ethylene oxide) (PEO) is a hydrophilic, neutral and very flexible polymer, which is widely used for surface modification of NPs. This polymer is FDA approved for biomedical application, and quite an important number of PEO-drug conjugates are on the market for intravenous administration. PEO is non-biodegradable, but bioeliminable, due to its hydrophilicity, whenever its molecular weight is inferior to 20000 g/mol.⁴⁵

The mechanisms of PEO-protein interactions have been proposed by Vermette *et al*, for instance.⁴⁶ Briefly, the protein repellence of PEO coatings was associated to ‘steric repulsion’ and/or ‘hydration’/ ‘water structuring’ of the chains. The flexibility of these PEO chains, which is particularly high in comparison to other hydrophilic polymers, is one explanation for its protein-repulsive or anti-fouling properties. Indeed, the reason for its flexibility must be found in the easy rotation of the ether bonds and in absence of any bulky substituent on the PEO skeleton. The rapid and transitory change of the conformation of PEO chains seems responsible for their poor interaction with proteins.

Whenever a protein or another surface approach with sufficient kinetic energy, PEO chains forming a dense brush at a surface will be compressed by the collision. This will increase the local concentration of polymer segments, thereby enhancing the free energy and inducing the repulsion of the protein from the surface.⁴⁶ The interaction is thus repulsive.

A lot of works tried to understand the influence of the density and length of PEO chains on the protein repulsive properties. The conformation of the PEO chains changes when the distance D that separates two neighboring PEO chains tethered at the surface becomes close to or smaller than the radius of gyration of the polymer (R_g), see Figure 7. In good solvents for PEO, such as water, and for long distances D ($D \gg R_g$), the polymer chains form “mushroom”-like structures, as illustrated in Figure 7A, whereas in bad solvents (Fig. 7B) flat “pancake”-like structures are expected. With decreasing distance ($D \sim R_g$), the chains start to interact with each other and approach the *mushroom* to *brush* transition (Figure 7, C and D). For $D < R_g$, the polymer chains strongly interact and stretch away from the surface getting the so-called “brush” conformation.⁴⁶ It is thus clear that one of the most important parameters in controlling the protein adsorption onto PEO layers is the grafting density of the PEO chains. It has been reported that a distance D of 1.5 nm between two terminally attached PEO chains at the NPs’ surface was found ideal for reducing protein adsorption. In addition, it has been demonstrated that rather long PEO chains (a MW of 2000 g/mol and 5000 g/mol has been proposed as ideal molecular weight earlier^{47,48,49}) are not necessarily a prerequisite for low protein adsorption.⁴⁶

These are the reasons why PEO is the polymer of choice for the design of NPs of the second generation and third generation.

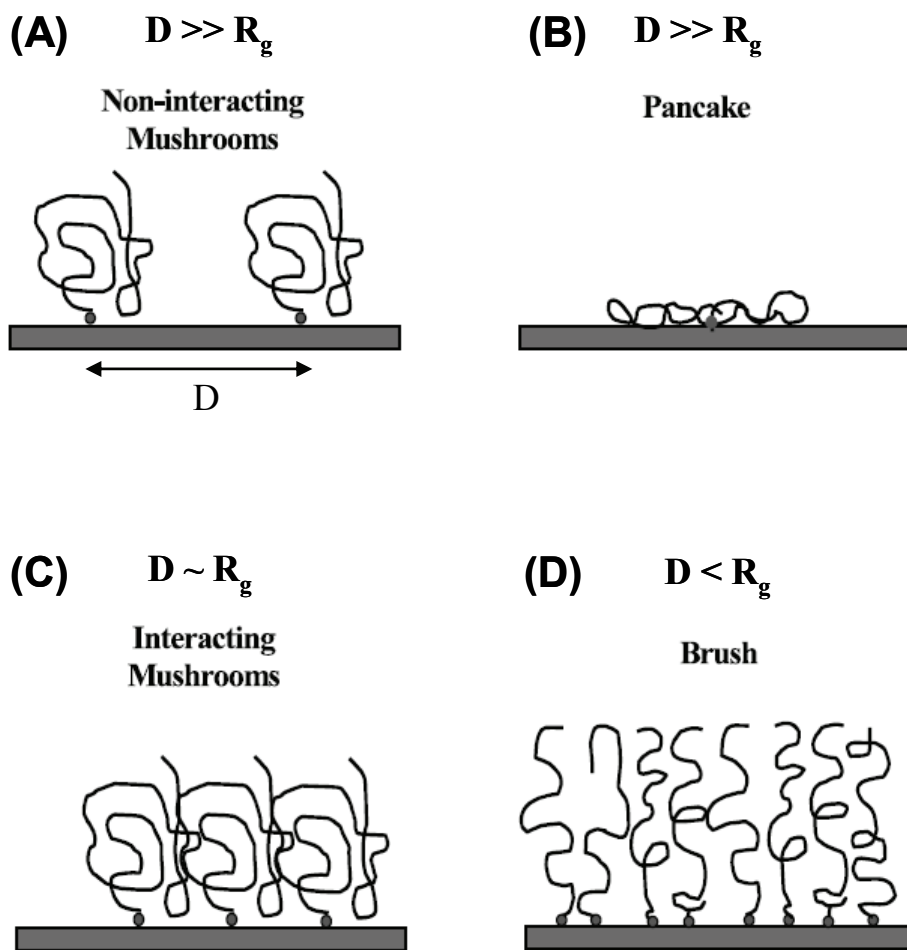


Figure 7. Schematic representation of polymer (PEO) structures at the interface.

III. Preparation of polymeric NPs.

In the last decades, several techniques have been developed to prepare colloidal carrier systems from polymeric materials. They can be obtained either (i) by association of preformed polymers (natural, modified natural or synthetic polymers, see section II) using techniques, such as *emulsion-evaporation*, *emulsion-diffusion*, *salting-out*, or (ii) by (mini)*emulsion* or micellar *polymerization* of polymerizable monomers dispersed in an aqueous phase. The preparation technique must be suitable for the material with regards to solubility and stability of the polymer. In case of emulsion polymerization, the availability of monomers polymerizable in O/W emulsion is the limiting factor.

III.1. Preparation of nanospheres from preformed polymers.

The use of preformed polymers for the preparation of nanospheres has several advantages, such as the availability of a large variety of materials with controlled and optimized macromolecular characteristics (molecular weight and polydispersity), as well as suitable physicochemical and biological properties. In fact, colloidal carriers should be prepared from well-defined macromolecular materials in order to favor reproducibility. In the following part, we briefly discuss the most popular methods to obtain nanospheres from preformed polymers, i.e. *emulsion-evaporation*, *emulsion-diffusion*, *salting-out* and *nanoprecipitation* techniques.

For the formation of dispersed colloidal systems in aqueous media, polymers that are insoluble in water are generally used. Thus, organic solvents are often required to dissolve the polymers, the first step on the way to nanoparticles. Depending on the preparation procedure described in the following sections, the organic solvents used are either miscible or not with water.

III.1.1. Emulsion-evaporation.

Organic *volatile* solvents, such as chloroform or dichloromethane, that are *poorly miscible* or immiscible with water, are suitable for the *emulsion-evaporation technique*, patented by Vanderhoff *et al.*⁵⁰ First, the polymer is dissolved in the organic solvent, and tiny solvent droplets are formed by emulsification in an aqueous phase containing an emulsifier (e.g. poly(vinyl alcohol) (PVA) or albumin). Then, the crude oil-in-water (O/W) emulsion is exposed to a high-energy source, such as ultrasonic devices or homogenizers etc.,⁵¹ and finally stable solid nanoparticles are formed from the emulsion droplets by

slight evaporation of the organic solvent (at reduced pressure). During the evaporation process, the organic solvent diffuses from the inner core of the droplets to the external phase, maintaining a saturation of the water phase by the organic solvent. The progressive elimination of the solvents induces the precipitation of the polymer and the NPs' formation. The size of the droplets and thus of the NPs can be adjusted by the nature and quantity of emulsifier, the viscosity of the dispersing phase, mechanical shear rate and stirring rate (a good homogenization leading to nanospheres of a diameter of 100 to 300 nm). Unfortunately, this method requires the use of large quantities of hydrosoluble surfactants (e.g. ranging from 0.5 up to 8 w/v % for poly(vinylalcohol)⁵¹) and high energy to form stable homogeneous emulsions. When ultrasonication is used instead of high-speed homogenizers, quite polydisperse nanosuspensions are obtained. Only hydrophobic drugs can be efficiently encapsulated by this O/W process. As far as hydrophobic drugs are concerned, a double emulsion (W/O/W) technique has been developed in order to obtain nanospheres of hydrophobic polymers (such as PLGA) loaded by hydrophilic biomolecules, such as proteins.⁵² Therefore, an inverse W/O emulsion is prepared first from an aqueous phase, containing the hydrophilic drug, and the organic phase, containing the matrix building polymer. Then this emulsion is emulsified in a second surfactant-containing aqueous phase to form the W/O/W emulsion. Finally the organic solvent is removed by evaporation at reduced pressure.

III.1.2. Salting-out.

Solvent immiscibility and polymer precipitation can be induced through changes in *temperature, pH* or the addition of *alcohol*, but also by the addition of *large quantities of salt* (“*salting-out*”). The salting-out method⁵³ uses *water-miscible organic solvents* and is based on the saturation of the aqueous phase by electrolytes in order to diminish drastically the miscibility of the organic solvent with the aqueous phase. At first, an O/W emulsion is formed between the organic phase and the surfactant (e.g. PVA, hydroxyethylcellulose or poly(vinyl pyrrolidone)) containing aqueous phase, which was previously saturated by the salt. Then, pure water is added in such an amount that the totality of the organic solvent becomes miscible with the aqueous phase. As a result, the organic solvent diffuses into the aqueous phase, leading to the precipitation of the polymer as nanospheres. Several factors, such as stirring rate and polymer concentration, have been reported to influence the mean size of the NPs. The salt is generally removed by cross-flow ultrafiltration/dialysis. This methodology allows using organic solvents of low toxicity (generally acetone) and which

can be easily removed at the end of the preparation process by ultrafiltration or evaporation. However, the use of large amount of surfactants and electrolytes is necessary.

III.1.3. Emulsification-diffusion.

The *emulsification-diffusion* method can be considered as a modification of the salting-out procedure, however avoiding the use of salts and hence intensive purification steps.⁵⁴ Before dissolution of the polymer, the *partially water-miscible organic solvent* (ethyl acetate, propylene carbonate, benzyl alcohol) is saturated in water to ensure the thermodynamic equilibrium of both liquids. Then, the polymer solution is emulsified (O/W emulsion) under vigorous stirring in an aqueous solution containing a stabilizer (e.g. PVA or *poloxamers*, that are copolymers composed of two poly(ethylene oxide) blocks separated by a poly(propylene oxide) block). The subsequent addition of water to the system causes the diffusion of the organic solvent to the external aqueous phase, resulting in the formation of NPs. Finally, the organic solvent is removed, depending on its boiling point, either by evaporation or cross-flow ultrafiltration. The size of the NPs depends on numerous factors, such as the concentration of the stabilizer (emulsifier), as well as the nature of the polymer and the stirring rate.⁵⁵

This method is only efficient for the encapsulation of lipophilic drugs. In addition, it requires the removal of large volumes of water because of the dilution induced diffusion process. However, the advantages of this approach rely on its good reproducibility and high loading efficiencies.

III.1.4. Nanoprecipitation.

In 1987, Fessi *et al.*⁵⁶ described and patented a simple technique to obtain polymeric NPs, which does not require the preliminary formation of an emulsion. It relies on the use of organic solvents that are *perfectly miscible* with water, such as acetone, ethanol, DMSO. Furthermore, the polymer must be insoluble in the aqueous phase, but also in the mixture of both phases. This method is called the “*nanoprecipitation*” or “*solvent displacement*” technique.

Thus, the organic polymer solution is added drop-by-drop into a large volume of an aqueous phase, typically containing a surfactant (e.g. PVA, poloxamers). Under these conditions, the NPs are formed instantaneously by the precipitation of the polymer induced by the diffusion of the organic solvent in the aqueous phase. Depending on its boiling point, the organic solvent is then eliminated by evaporation or dialysis. This technique has

been modified and adjusted by various research groups.^{57,58} Polymer precipitation has also been induced by gentle progressive *diffusion* of water to an organic polymer solution placed in tube of dialysis membranes.⁵⁹ The size of the NPs obtained by nanoprecipitation processes is typically about 200 nm depending on the nature, miscibility and viscosity of the solvent, the polymer and its concentration in the organic solvent, and the preparation conditions. This technique is especially attracting because it is barely energy consuming and very simple in handling.

The two nanoprecipitation techniques used in this work are schematized in Figure 8.

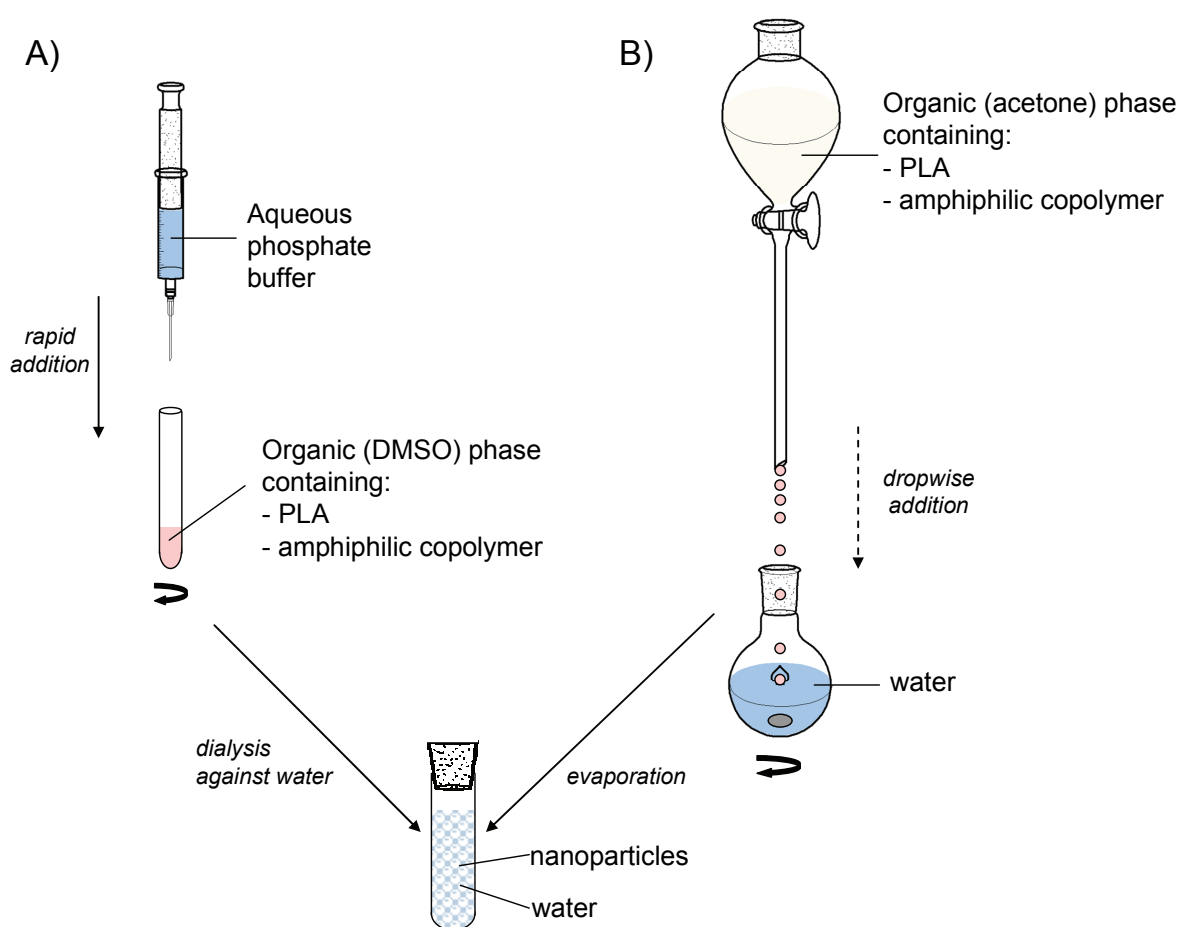


Figure 8. Schematic representation of nanoparticle preparation by A) nanoprecipitation-dialysis, B) nanoprecipitation-evaporation.

The conventional techniques described above rely on the use of surfactants in the aqueous phase, i.e. hydrosoluble (amphiphilic) polymers such as poly(vinyl alcohol) (PVA) or triblock copolymers of poly(ethylene oxide) and poly(propylene oxide) (PEO-*b*-

PPO-*b*-PEO, known as poloxamers) that exhibit interfacial activity, to guarantee the stability of the colloidal dispersions. On the contrary, the two techniques presented in Figure 8 employ amphiphilic copolymers that are not soluble in water. This feature is expected to enhance the affinity of the copolymer to the hydrophobic polymer nanoparticle (PLA) and to make the durable modification of the NPs' surface possible.

III.2. Synthesis of nanospheres by in-situ polymerization.

In contrast to techniques employing preformed polymers, NPs can also be synthesized by polymerization of suitable monomers in **(mini)emulsion**^{60,61} or **dispersion**.

Emulsion polymerizations employ water-insoluble monomers that are emulsified as micron-sized oil droplets (1-10 μm) in an aqueous phase stabilized by a surfactant. The initiators used in emulsion polymerizations are generally water-soluble and dissolved in the aqueous phase. Most emulsion polymerizations use a radical polymerization method. The drawback of such (macro)emulsion polymerizations is that the size of the latex particle does not correspond to the primary emulsion droplets but rather depends on polymerization kinetic parameters. A special class of emulsion polymerizations is the polymerization in **miniemulsion** (Fig. 9). In fact, miniemulsions consist of two immiscible liquids, a surfactant and a special co-surfactant (additive) that is only soluble in the dispersed phase. They are prepared by high-shear treatment of these mixtures, either by ultrasound or by a high-pressure microfluidizer, and consists of stable nanodroplets with a diameter of 30-300 nm. Indeed, the combination of the two surfactants makes the droplets extremely stable, inhibiting the diffusion of monomers out of the miniemulsion droplets and preventing their coalescence.⁶⁰ The size of the polymer NPs corresponds thus to that of the initially formed nanodroplets, which is controlled by the shear and the stabilizer system and not by the polymerization parameters (as for the (macro)emulsion). The active compound (drug) is generally incorporated in the dispersed phase, and therefore encapsulated in the NPs during the polymerization process. More seldom, it is adsorbed after the polymerization onto the surface of the as-prepared NPs.

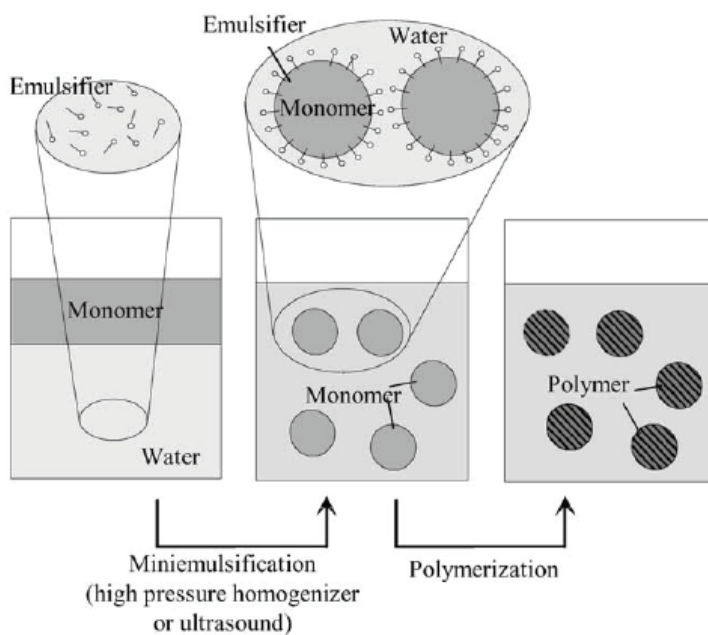


Figure 9. The principle of miniemulsion polymerization.⁶¹

NPs made of *poly(N-isopropylacrylamide)* (PNIPAAm), *poly(N-vinylacetamide)* (PNVA), *poly(vinylamine)* (PVAm), *poly(methacrylic acid)* (PMAA) have accordingly been prepared. The corresponding vinylic and (meth)acrylic monomers are generally polymerized under free radical conditions using, e.g. 2,2'-azobisisobutyronitrile (AIBN) as an initiator.⁶²

New processes based on the miniemulsion concept use amphiphilic polymers both as emulsifiers and surface modifiers of the final NPs. For instance, the radical polymerization of styrene has been carried out in miniemulsions stabilized by amphiphilic derivatives of dextran.⁶³ The size of the polysaccharide-coated polystyrene particles was directly correlated to that of the initial nanodroplet and depended on the monomer concentration.

Furthermore, other polymerization systems have also been used to prepare polymeric nanoparticles, such as dispersion or suspension polymerization. In the **suspension polymerization** process, the initiator is soluble in the monomer and larger particles ($> 1\mu\text{m}$) are obtained.

In addition, **dispersion polymerizations** have been rediscovered in recent years for the preparation of (sub)micron-size polymer particles with narrow size distributions. This process differs notably from emulsion and suspension polymerization as it starts with a *homogeneous* solution of monomer(s), stabilizer(s) and initiator in a polar solvent. The polymer precipitates as a colloidal dispersion during the polymerization process. As an interesting example, polystyrene core – glycopolymer corona nanospheres have been

obtained by free radical copolymerization of hydrophilic macromonomers and styrene (as hydrophobic comonomer) in dispersion in a polar solvent (e.g. ethanol/water mixture).^{64,65,66}

One of the advantages of emulsion polymerization for the preparation of polymeric nanoparticles is its reproducibility regarding size and drug loading rate, even at a semi-industrial level. On the other hand, the disadvantages of this approach are residual emulsifiers, monomers, but also oligomers, and the risk of drug interaction (with the reactives) and thus inactivation during polymerization.

III.3. Preparation of nanocapsules.

As mentioned in the introduction, nanocapsules are built of an oily or sometimes aqueous core, surrounded by a thin polymeric wall. Similar to nanospheres, nanocapsules can be obtained using either *preformed polymers* or by (interfacial) polymerization of *monomers*. Two main techniques for the synthesis of nanocapsules have been described: (i) the *interfacial deposition process* and (ii) an *emulsification diffusion technique*. Both techniques are related and rely on the use of a *water-miscible* organic solvent (generally solubilizing the polymer) and the *insolubility* of the polymer/monomer in both the oil (e.g. vegetable or mineral oil) and the aqueous phase. The miscibility of the organic solvent is thus the driving force for the diffusion of the polymer (or monomer) to the water/ oil interface.⁶⁷

(i) The *interfacial deposition process* can be applied to either preformed polymers or to monomers that polymerize at the oil-water interface. In both cases, the procedure generally consists of mixing the oily phase, i.e. an *oil* (vegetal or mineral) *containing a completely water-miscible organic solvent* such as an alcohol or a ketone, with the aqueous phase containing a hydrophilic (hydrosoluble) surfactant. In the case of *preformed polymers*, the first step consists in their solubilization in the organic phase (oil containing the organic solvent). Then, upon addition of the organic phase to the aqueous phase, the *polymer diffuses with the water-miscible organic solvent* and is stranded at the interface between oil and water. In the second case, *monomers* are solubilized in the organic phase, which is then dispersed in water inducing to the localization of the monomer at the interface. For instance, the polymerization of alkylcyanoacrylate has been initiated at the interface by hydroxyl ions present in the aqueous phase, leading to the formation of nanocapsules.⁶⁸

(ii) Very similar, the *emulsification diffusion technique* described by Quintanar *et al.*⁶⁹ is based on the initial formation of an O/W emulsion, where the oil phase contains the core-building oil, the preformed polymer, a drug and an *organic solvent*, which is *poorly miscible* with water. Upon addition of a large volume of water, this organic solvent diffuses to the external water phase, inducing the precipitation of the polymer and thus the formation of the nanocapsules. The advantages of this approach are the simplicity of the method, the need of only small quantities of organic solvents, the control of the size of the NPs (from 80 to 900 nm), the control of the thickness of the polymeric wall by the polymer concentration and the possibility of preparing nanocapsules with an inner aqueous core.⁷⁰ However, this technique requires the use of a large amount of water that has to be removed by evaporation.

Some of the advantages of nanocapsules over nanospheres are their low polymer content and the high loading capacity for lipophilic drugs. The percentage of encapsulation is generally related to the solubility of the drug in the core phase.⁷¹

IV. Surface functionalization

The NPs' surface characteristics have a crucial impact on the interactions of NPs with their biological environment, i.e. with living medium. In the last decade, numerous surface-modified carrier systems have thus been developed allowing the specific targeting of selected tissues. Polymeric materials functionalized with targeting moieties, such as sugars,⁷² peptides,⁷³ folic acid⁷⁴ and antibodies⁷⁵ have received considerable interest as means to generate intelligent delivery vehicles capable of specific binding interactions.

IV.1. Functionalization with biological (macro)molecules.

The first group of bioactive molecules comprises macromolecules (such as polysaccharides, oligopeptides), which interact *non-specifically* with tissues. Among them, polysaccharides are of great interest especially to confer NPs **bioadhesive** or **mucoadhesive** properties (cfr. section II). Therefore, NPs have been modified at their surface by polysaccharides, such as chitosan²² and hyaluronic acid.¹⁵ It could be demonstrated that NPs coated by such bioadhesive polymers, and especially by hyaluronic acid, increased significantly the ocular drug availability.⁷⁶

To overcome the fast capture of NPs by the MPS, they have not only been coated by poly(ethylene oxide) but also by **dextran** and **heparin**. Such NPs circulate for an enhanced period of time in the blood stream. The polysaccharide shell probably avoided complement activation and opsonisation of the NPs by preventing protein adsorption.^{77,78}

In the 80th, a tripeptide, arginine-glycine-aspartic acid (**RGD**), has been identified to promote cell attachment.⁷⁹ NPs decorated by RGD peptides have shown to induce a 50-fold increase in transport across the human intestine epithelial cells compared to blank PS NPs.^{80,81}

IV.2. Functionalization with specific ligands: specific interaction through biological recognition.

One of the greatest challenges is defining the optimal vector molecules or ligands to transport NPs *specifically* to the targeted tissue. The strategy relies on the ability of these targeting probes to bind specifically to cell surface receptors triggering receptor endocytosis, and thus to 'infiltrate' NP specifically into cells. A variety of specific ligands, such as mono- or oligosaccharides (mannose, galactose), biotin, folic acid, antibodies etc.

(Figure 10), has been identified and used hitherto for the functionalization of the NPs' surface.

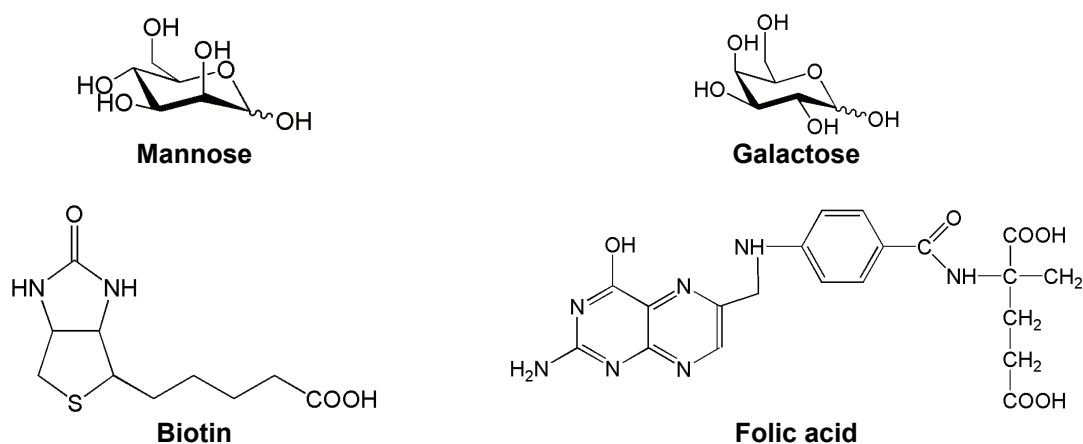


Figure 10. Chemical structure of some biological (macromolecules) as targeting probes.

Among them, **mono-** or **oligosaccharides** are of special interest. Indeed, cell surface carbohydrates from glycoproteins and glycolipids function as recognition sites between cells or cells and microorganisms.^{82,83,84} These recognition mechanisms are essentially based on specific interactions between the carbohydrates and soluble or membrane proteins called **lectins**. The communication network based on *carbohydrate-protein interactions* is crucial in a large variety of important biological phenomena such as cell growth, inflammation, cancer and viral and bacterial infections.

Taking advantage of these specific carbohydrate-lectin interactions, numerous glycomimetics have been developed for analytical, diagnostic and therapeutical purposes. In particular, sugar-mediated drug delivery (DD) allows targeting cells that possess *glyco-receptors* on their plasma membrane. Such kind of DD is considered as one of the most promising routes in cellular-specific targeting. Indeed, membrane lectins of some cell types are capable to internalize their ligands, and hence the glycoconjugates that are specifically recognized by these lectins can be used as efficient carriers of drugs.⁸⁵ Especially, *dendritic cells* of the human blood express cell-surface **mannose**-specific lectins, i.e. specific receptors for mannose (MR).^{86,87} In fact, these cells capture, process and present antigens to native T cells, inducing the cellular immune response.^{88,89} The possibility to target specifically dendritic cells makes thus mannose-coated NPs attractive delivery systems for *vaccines*. We would like to emphasize, that colloidal DDS might not only protect vaccines (in general peptides or proteins) from degradation, but they also possess

‘adjuvant’ properties - due to their “large” size – which means that they increase the specific immunity to an antigen (as compared to that introduced by the vaccine or antigen alone).⁹⁰ NPs are thus very promising carriers for *s.c.* or mucosal *vaccination*.^{91,92}

In contrast to mannose, **galactose** interacts with *hepatic cells* via a Gal/GalNAc-binding mammalian lectin. Galactose-conjugates have thus been synthesized, which have been used to carry antiparasitic⁹³ and antiviral drugs⁹⁴ specifically to liver cells. For the same purpose, polymeric NPs decorated by galactose,^{95,96} have been synthesized for hepatocyte-specific targeting.

It should be noted, that the binding of a particular sugar to its glycoreceptor occurs in a regioselective manner⁸³ and thus the introduction of glucidic ligands on polymers is generally performed by 1-*O* substitution of the sugar. Furthermore, it has been emphasized that sugar-lectin interactions depend on the “density” of the partners at a surface. Indeed, their affinity can be enhanced by multiple interactions between the binding proteins and the carbohydrate ligands, which is known as the *glycoside cluster effect*.⁹⁷ With respect to that, dendrimers end-capped by sugar moieties have been synthesized, and their enhancement of carbohydrate-lectin binding was shown by isothermal titration calorimetry (ITC).⁹⁸

Furthermore, the vitamin **folic acid** has been identified as a convenient targeting molecule for the specific delivery to *cancerous cells*. Briefly, all cells require folic acid for essential cell functions. They are equipped with several pathways for folate internalization. Folate-conjugates however were shown to enter cells only via the ‘alternative route’, which utilizes the folate receptor (FR). This cell-surface receptor is expressed in measurable quantities on activated macrophages and significantly over-expressed on the surface of many cancer cells, which needs large amounts of folic acid to enable their rapid proliferation. FR is thus a possible target for a number of types of cancer. In addition, their localization on activated macrophages, but not on their quiescent or resting counterparts, makes folate-conjugates promising in targeting inflammatory and autoimmune diseases since those specific macrophages cause or contribute to these diseases.

Beside ligand-receptor interactions, **antigen-antibody** interactions are highly specific molecular recognition processes and might be promising tools for specific targeted delivery. In fact, with the advent of monoclonal antibody technology, the utilization of antibodies increased dramatically. Monoclonal immunoglobulin G antibodies may thus

have potential as vector molecules to transport a colloidal carrier system specifically to the target tissue. For example, in the field of cancer, monoclonal antibodies have been shown to be capable of binding to specific tumor antigens.⁹⁹ Unlike monosaccharides and folic acid, which are chemically very stable, antibodies are very sensitive biomolecules. Each antibody consists of four polypeptides, two heavy chains and two light chains joined, forming a "Y-shaped" molecule. In order to circumvent difficulties related to the chemical conjugation of such sensitive macromolecules, antibodies¹⁰⁰ or antibody fragments were simply *adsorbed* at the NPs' surface. Recent studies however seek to attach them via biotin-avidin interactions, i.e. using biotinylated antibodies, or by covalent conjugation reactions on NPs or microcapsules bearing e.g. activated ester groups.^{101,102,103,104,105}

Beside their interest for targeted drug delivery, antibody-decorated NPs are useful tools for clinical analysis by immunoassays and medical diagnostics.¹⁰⁵

Finally, **biotin** (called also vitamin H), a little organic biomolecule, is widely used as a versatile linker molecule to which - via a biotin-avidin complex - a large variety of functional moieties can be bound. Actually, **biotin** is known to form very stable complexes with its tetravalent ligand, **avidin**. The avidin-biotin complex is known as one of the strongest studied non-covalent biological interaction (association constant $K_a = 10^{15} \text{ M}^{-1}$). In addition, a large variety of biotinylated targeting ligands are commercially available and they can be attached to the surface of biotin-coated NPs via biotin-avidin-biotin complexes (Figure 11).¹²

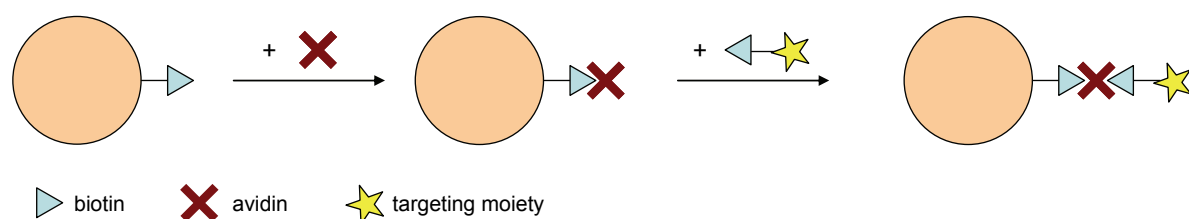


Figure 11. Surface functionalization via biotin-avidin-biotin complex formation.

Indeed, after complex formation with one of the sites of avidin, the residual three binding sites of avidin are still available for the binding of biotin-conjugates. A very versatile tool for surface modification was thus made available. It is however questionable whether the stability of colloidal dispersions of such NPs may be maintained after the addition of avidin, as interparticular cross-linking via free avidin binding sites might take place.

To avoid this problem, it might be advantageously to attach avidin (NeutrAvidine) directly in a covalent manner to the surface of NPs. This has been reached in the work of Balthasar *et al.*¹⁰² who prepared antibody-decorated cross-linked gelatin NPs as drug carriers for the specific targeting of T-lymphocytes (using biotinylated anti-CD3 antibodies).

IV.3. Strategies for surface modification.

On the basis of the methods described in section III, several approaches have been proposed to modify the surface of polymeric NPs. This can be reached by (i) *adsorbing* functional molecules on the surface of preformed NPs via hydrophobic or electrostatic interactions, (ii) *preparing* nanospheres from preformed polymers *in the presence* of “*functional surfactants*”, (iii) *in situ emulsion polymerization* using *functional emulsifiers* or *functional monomers* and (iv) finally by *covalent linking* of functional molecules to *preformed NPs*.

Most of these approaches require the synthesis of hybrid materials, i.e. materials containing both ‘natural’/biologically active and synthetic components. In this context, a great issue is to maintain the biomolecule-NP conjugates bioactive and to ensure the bio-availability of the bioactive entity. For this purpose, hydrophilic *spacer* molecules, such as **PEO** chains,¹² have often been introduced between the surface and the biological ligand, thereby allowing the accessibility of the biomolecule and its interaction. Furthermore, the conjugation reactions must be carried out under mild, non-degrading reaction conditions.

Examples of the different pathways to surface-functionalized NPs as well as the chemistry used to reach biomolecule-NP conjugates are discussed in the following paragraphs.

IV.3.1. Adsorption on preformed nanoparticles.

NPs have been surface-modified by simple adsorption of functional molecules on preformed NPs (Figure 12).¹⁰⁶

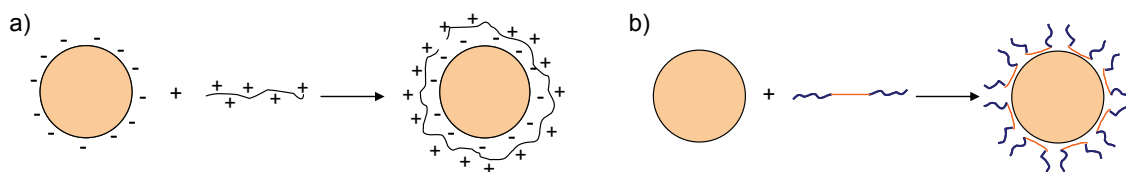


Figure 12. Adsorption of functional molecules by a) electrostatic, b) hydrophobic interactions.

The driving force for physisorption to happen is the affinity of at least part of the molecule to the NPs' surface.

Based on *electrostatic interactions* polyelectrolytes, such as chitosan,¹⁵ or charged molecules, such as cationized antigens, e.g. Tat(1-72)¹⁰⁷, have been adsorbed onto charged NPs of opposite charge (e.g. sodium alginate NPs). On the other hand, *hydrophobic* NPs have been surface-modified using hydrophobic or hydrophobically modified amphiphilic macromolecules.¹⁰⁸ Based on this approach, numerous studies have used amphiphilic block copolymers, such as poloxamers (PEO-*b*-PPO-*b*-PEO triblock copolymers).¹⁰⁹ Actually, the hydrophobic PPO block is the driving element for the adsorption onto the NPs' surface, while the hydrophilic PEO chains expand in the aqueous environment forming a steric barrier that stabilizes the NPs, prevents their aggregation and makes them 'stealthy' towards the MPS.

Furthermore, dextran bearing hydrophobic phenoxy groups and comb-like copolymers of dextran bearing pendant phenoxy groups and poly(ethylene oxide) chains (DexP-*g*-PEO) were synthesized.¹¹⁰ They were adsorbed on polystyrene NPs and the effect of the polymer composition and architecture on the protein adsorption were studied (see Figure 13).

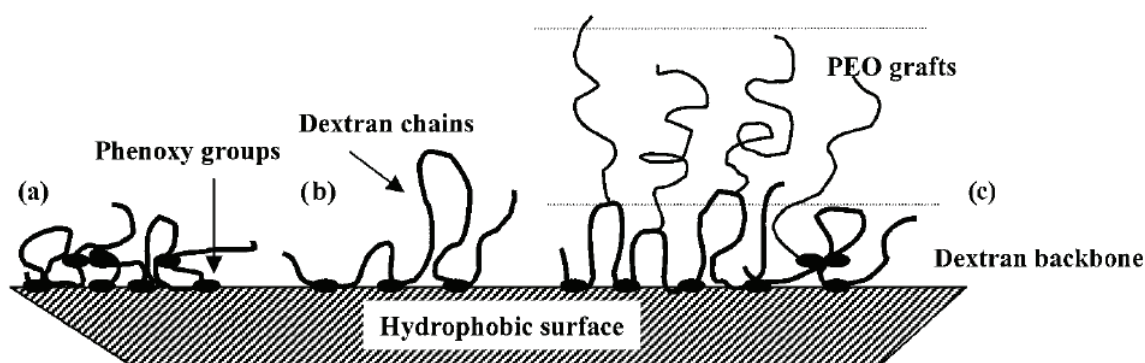


Figure 13. Adsorption of amphiphilic dextran (DexP) with (a) high and (b) low amounts of grafted phenoxy groups and (c) of graft DexP-PEO copolymer at the hydrophobic surface.¹¹⁰

It was found that the most important parameter in preventing the adsorption of bovine serum albumin (BSA) was the extent of the contact points between dextran and the surface, rather than the grafting density of PEO chains, in case of DexP-g-PEO.¹¹⁰

The advantage of surface-modification via **adsorption** relies on its simplicity. However, it must be considered that the post-modification of the surface of preformed NPs can alter their stability. The adsorption of material on NPs' surfaces influences their surface properties, and might diminish the interparticular repulsion inducing NPs' aggregation. In fact, the stability of colloidal systems relies generally on steric or electrostatic repulsion. Finally, the risk of desorption as a result of dilution and introduction into complex biological media must also be considered.

IV.3.2. Functional surfactants as stabilizers and surface-modifiers.

As explained in section III, most of the techniques to prepare polymeric NPs necessitate the use of surfactants, which play the role of emulsifiers and stabilizers. It was demonstrated that in case of hydrophobic NPs, the amphiphilic surfactant is located at the surface of the particles.^{49,15} *Amphiphilic copolymers* conjugated with bioactive molecules may thus serve as both emulsifiers and surface modifiers. Such copolymers may be synthesized with various architectures, for instance *block* (diblock (Fig. 14 A,B) or triblock) or *comb-like* structures (Fig. 14 C-E), employing controlled polymerization techniques. The functional biomolecule is rather attached on the hydrophilic part of the copolymers, in order to optimize its availability for interaction in the aqueous environment. Poly(ethylene oxide) (PEO) has preferentially been used because of its hydrophilicity and flexibility properties (see section II).

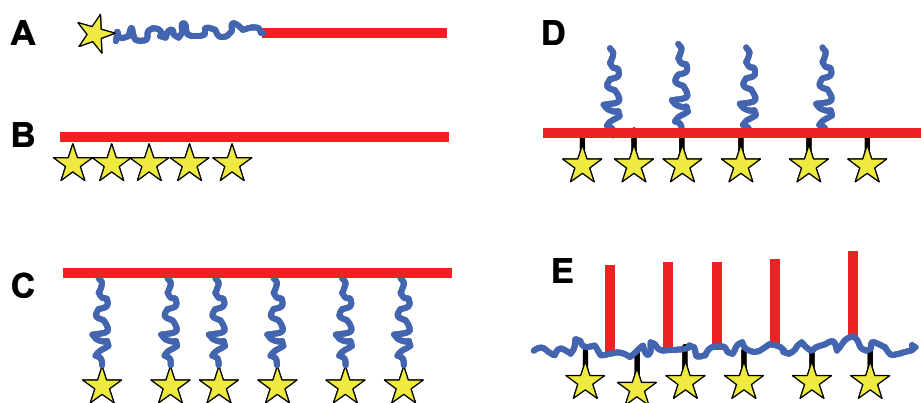


Figure 14. Amphiphilic copolymers, red/black: hydrophobic part; blue/grey: hydrophilic part; star: functional (bio)molecule.

A first group of copolymers used for surface functionalization, typically consists of amphiphilic **block copolymers** (Figure 14 A,B). Such copolymers can be obtained by four different strategies: (i) by *postpolymerization functionalization*, where the functional moiety is grafted to the hydrophilic end of the preformed amphiphilic block copolymer, (ii) by coupling the bioactive group at one end of an α,ω -*bifunctional hydrophilic* homopolymer, followed by the initiation of the polymerization of the second block from the residual reactive chain end,¹² (iii) by using (protected) *bioactive molecules as initiators* for the sequential polymerization of the diblock (hydrophilic block being polymerized first) or (iv) by using *polymerizable hydrophilic biomolecules*.

The first approach has mainly been applied for the functionalization of diblock copolymers by sugars and peptides. For instance, the hydrophilic chain end of amphiphilic poly(ethylene oxide)-*b*-poly(D,L-lactide) diblock copolymers (PEO-*b*-PLA) has been functionalized by mannose,¹¹¹ lactose,¹¹² or peptides¹¹³ using a *reductive amination reaction*. For this purpose, *aldehyde* (CHO)-capped copolymers and *amino-* or *aminophenyl-*derivatives of the biomolecule were synthesized. Then, the coupling of both compounds was carried out in the presence of reducing agents ($\text{NaBH}(\text{OAc})_3$ or NaBH_3CN).^{111,112,113}

On the other hand, biotin¹¹⁴ or protected monosaccharides⁸² have been used to initiate the polymerization of the hydrophilic block (approach iii). For instance, Qi *et al.*¹¹⁴ prepared NPs coated by biotin from biotin-terminated poly(acrylic acid)-*b*-poly(methyl acrylate) diblock copolymers (biotin-PAA-*b*-PMA). These functional copolymers were prepared using a biotinylated initiator for the sequential atom transfer radical polymerization (ATRP) of acrylic acid and methyl acrylate (Figure 15).

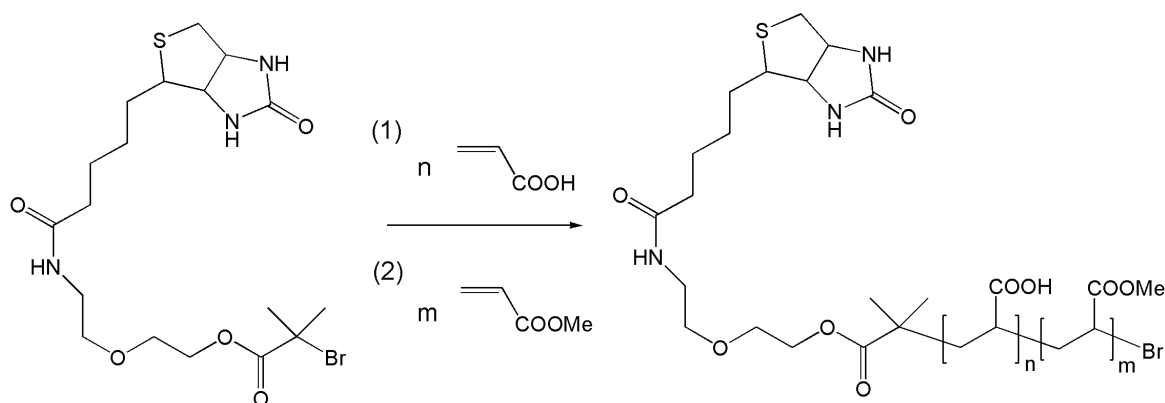


Figure 15. Synthesis of biotin end-capped poly(acrylic acid)-b-poly(methyl acrylate) by ATRP.

Not only radical polymerizations, but also ring opening polymerizations (ROP) have been successfully initiated by suitably protected molecules. Yasugi *et al.*⁸² synthesized amphiphilic biodegradable poly(ethylene oxide)-*b*-poly(D,L-lactide) (PEO-*b*-PLA) diblock copolymers that were end-functionalized by **galactose**. Therefore they initiated the anionic polymerization of ethylene oxide by a metal alkoxide of a regioselectively protected galactose, followed by ring opening polymerization of LA.

Finally, amphiphilic functional block copolymers were also prepared using *polymerizable carbohydrates as monomers*. Armes *et al.*¹¹⁵ synthesized new sugar-modified methacrylic monomers (2-gluconamidoethyl methacrylate and 2-2-lactobionamidoethyl methacrylate) suitable for the preparation of methacrylate-based diblock (see Figure 16) and triblock glycopolymers by ATRP starting from different (macro)initiators.

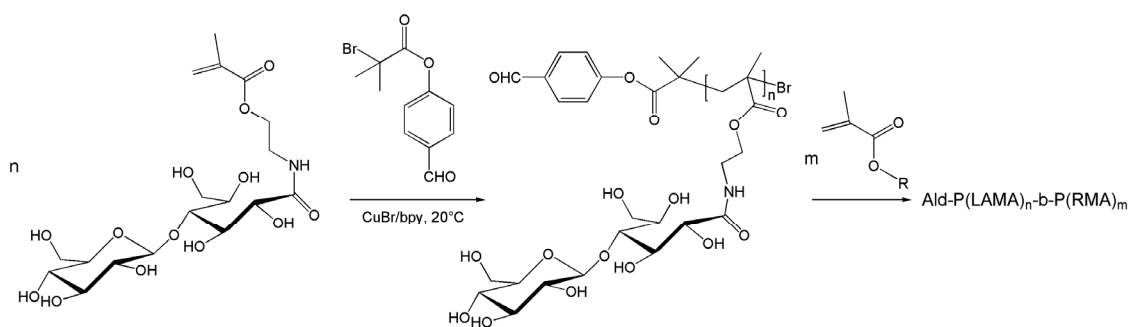


Figure 16. Sequential polymerization of 2-lactobionamidoethyl methacrylate (LAMA) with methacrylic monomers (R-MA) by ATRP at 20°C.

The most popular pathway to **functional amphiphilic random copolymers** (Figure 14, C-E) relies on the synthesis of copolymers bearing pendant functional groups that are prone to further chemical modification. In a second step, reactive biomolecule-derivatives

can be *grafted onto* the (hydrophobic or hydrophilic) polymer backbone (called “*grafting onto*” approach).

For example, the pendant carboxylic acid groups of poly(methyl methacrylate-*co*-methacrylic acid) copolymers have been successfully used as reactive sites for the covalent linking of biotin molecules. These random amphiphilic copolymers were efficient stabilizers and surface-modifiers of PLA NPs.¹¹⁶

With the purpose of obtaining fully biodegradable NPs, biodegradable amphiphilic copolymers bearing pendant reactive sites have also been synthesized. For instance, ϵ -caprolactone has been randomly copolymerized with γ -substituted functional ϵ -caprolactone (comonomers) (bromo-, hydroxyl-, carboxylic acid-substituted), allowing the posterior reaction with biologically active compounds. Fully biodegradable surface-modified NPs could be obtained by coprecipitation of PLA with these functional amphiphilic copolymers, and the presence of the amphiphilic copolymers at the surface of the NPs was demonstrated.¹¹⁷

IV.3.3. Emulsion, miniemulsion or dispersion polymerization.

As mentioned in chapter III. section 2, polymeric NPs can be prepared using emulsion, miniemulsion or dispersion polymerization. In order to modify the surface of NPs, two approaches have been proposed. The first one relies on the miniemulsion polymerization of monomers in the presence of *amphiphilic biopolymers as emulsifiers*. The second approach is based on the dispersion copolymerization of a hydrophilic *functional macromonomer* with a hydrophobic comonomer.

According to the first strategy, Dellacherie *et al.*⁶³ coated polystyrene NPs by dextran in a miniemulsion process, which did not necessitate the addition of any co-stabilizers and led to the formation of monodisperse NPs. For this purpose, they prepared dextran chains, which were hydrophobically modified by randomly grafting of phenoxy groups (see section IV.3.1.). This dextran derivative revealed strong interfacial activity. It could successfully be used as emulsion stabilizers and surface-modifier in a miniemulsion process to prepare polystyrene particles coated by dextran.⁶³

In contrast to that, the *macromonomer method* allows to covalently link biomolecules, such as monosaccharidic moieties, to the surface of NPs. To do so, a hydrophilic macromonomer end-capped by glucose moieties has been synthesized, as illustrated in Figure 17. An amine-terminated 2-glucosyloxyethyl methacrylate (GEMA)

oligomer was synthesized by radical initiation with ammonium peroxydisulfate (APS) and in the presence of 2-mercaptoethylamine as a chain transfer agent. In the next step, 4-vinylbenzoic acid (VBA) was coupled to the amine group of the GEMA oligomer in the presence of 3-(3-dimethylaminopropyl)-1-ethylcarbodiimide hydrochloride (EDC).⁶⁶

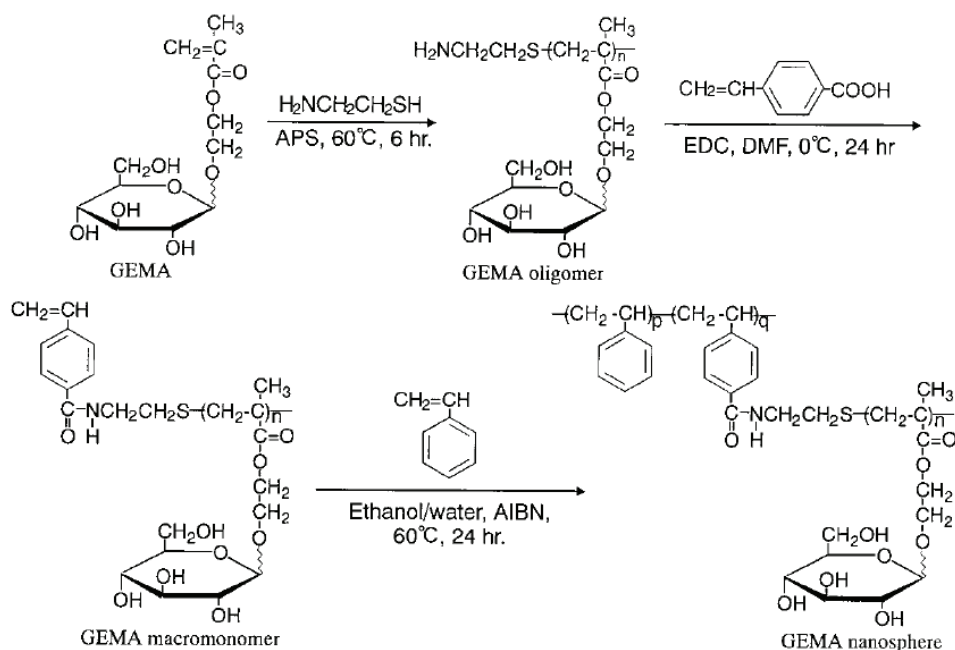


Figure 17. Synthesis and copolymerization of a glucose-capped macromonomer (GEMA macromonomer).

Nanospheres with a polystyrene core and a GEMA oligomer corona were then obtained by free radical copolymerization of the GEMA macromonomer with styrene in an ethanol/ water mixture. As mentioned in section IV.2.1, such glucose-decorated NPs were expected to increase the interaction with a glucose specific lectin (concanavalin A, Con A) due to the *cluster effect*. Hence, investigation of glucose-lectin interaction by Enzyme-Linked Lectin Assay (ELLA) demonstrated that the binding activity of the carbohydrate decorated NPs was less than that of the free GEMA macromonomer. It decreased even with increasing amount of glucose at the nanospheres. Steric hindrance was proposed as a possible explanation for the low bioavailability (Figure 18).⁶⁶

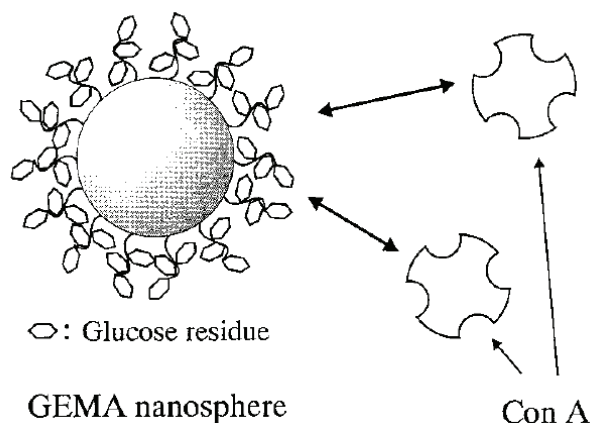


Figure 18. Schematic representation of a GEMA nanosphere and its interaction with ConA.⁶⁶

IV.3.4. Covalent linking of functional molecules to preformed NPs.

The surface functionalization of NPs by covalent grafting of functional molecules *on preformed* polymeric NPs is challenging (see Figure 19).

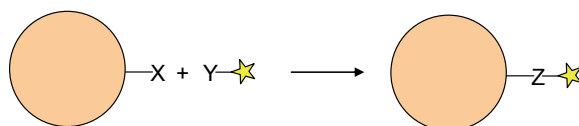


Figure 19. Covalent linking of functional molecules to preformed NPs.

Such reactions require (i) the availability of functional reactive groups at the NPs' surface, (ii) the synthesis of biomolecules bearing reactive groups, and (iii) the use of coupling reactions that are selective and efficient. Above all, they must be smooth not causing any denaturation of the biomolecules or degradation of the polymer material. These challenges led to the development of 'chemical ligation', that is the selective covalent coupling of mutually and uniquely functional groups under mild and aqueous conditions.¹¹⁸ Hitherto, only few of these methods have been applied to the chemical coupling of biomolecules onto preformed NPs. Among them, the **amine-acid coupling** is one of the most universally applied and efficient reaction. As an example, *folic acid*, which possesses a carboxylic acid group, has been conjugated onto NH_2 -coated NPs. Such NPs have been prepared using amine-functionalized comonomers, either in an *in situ* copolymerization process (III.2),⁷⁴ or for the synthesis of amphiphilic copolymers that

serve as surfactants and surface modifiers in a *nanoprecipitation technique* (III. 1).¹¹⁹ Folic acid was then successfully conjugated to the surface using 1,3-didecylcarbodiimide (DCC).

Furthermore, the introduction of thiol groups to the surface of NPs opens up a lot of new possibilities for ligand conjugation. Especially conjugation reactions between thiols and maleimides (**thiol-maleimide couplings**) have received increasing interest, due to their selectivity and reactivity under mild conditions. In fact, antibody or protein conjugation is commonly performed using bifunctional cross-linkers such as *m*-maleimidobenzoyl-*N*-hydroxysuccinimide ester (MBS) that offer two binding sites: one for primary amino groups (present in antibodies, drugs, specific peptides) and one for thiol functions.¹²⁰ Such coupling reactions have been found quantitative under physiological conditions.^{121,122, 123}

As an interesting example, **avidin** (NeutrAvidinTM), as a model protein and linker molecule, could be successfully conjugated onto thiolated PLA¹²³ and gelatin NPs¹²⁴ via sulfo-MBS (see Figure 20). Balthasar *et al.*¹⁰² further attached biotinylated antibodies at the surface via avidin-biotin-complex formation, and their bioavailability could be shown using indirect methods, such as immunoblotting or fluorimetry.

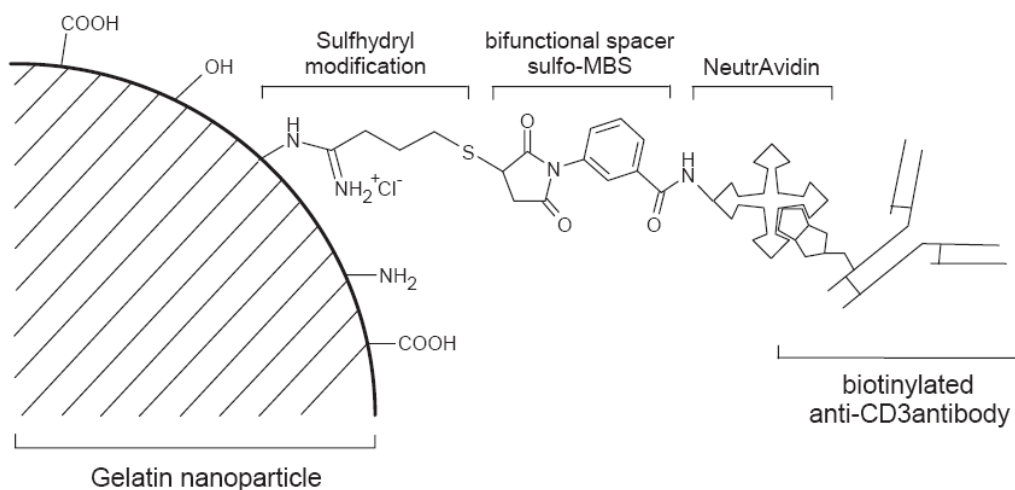


Figure 20. Schematic representation of antibody-loaded NeutrAvidinTM-modified gelatin nanoparticles: Sulfhydryl groups were introduced onto the particle surface by 2-iminothiolane followed by a conjugation reaction with NeutrAvidinTM using the heterobifunctional crosslinker sulfo-MBS. A biotinylated anti-CD3 antibody was attached to the particle surface by avidin-biotin-complex formation.¹⁰²

The choice of the appropriated technique for *surface* modification of NPs by biomolecules is thus crucial. It must be noted that biological recognition assays are however necessary to test the bioavailability of the molecules.

References.

- ¹ Allen, T.M.; Cullis, P.R.; *Science* **2004**, *303*, 1818-1822
- ² Passirani, C.; Benoit, J.P. in “Biomaterials for Delivery and Targeting of Proteins and Nucleic Acid”, ed. by Mahato, R. I. CRC Press, Inc., Boca Raton, Florida, USA, **2005**, Ch.6
- ³ Torchilin, V.P.; *J. Microencapsulation* **1998**, *15*, 1-19
- ⁴ Gref, R.; Minamitake, Y.; Peracchia, M.T.; Trubetskoy, V.; Torchilin, V.; Langer, R.; *Science* **1994**, *263*, 1600-1603
- ⁵ Labarre, D.; Vauthier, C.; Chauvierre, C.; Petri, B.; Müller, R.; Chehimi, M.M.; *Biomaterials* **2005**, *26*, 5075–5084
- ⁶ Passirani, C.; Barratt, G.; Devissaguet, J.-P.; Labarre, D.; *Life Sci.* **1998**, *62*, 775-785
- ⁷ Österberg, E.; Bergstrom, K.; Holmberg, K.; Schuman, T.P.; Riggs, J.A.; Burns, N.L.; Van Alstine, J.M.; Harris, J.M.; *J. Biomed. Mater. Res.* **1995**, *29*, 741-747
- ⁸ Maeda, H.; Wu, J.; Sawa, T.; Matsumara, Y.; Hori, K.; *J. Control. Release* **2000**, *65*, 271-284
- ⁹ Brannon-Peppas, L.; Blanchette, J.O.; *Adv. Drug Deliv. Rev.* **2004**, *56*, 1649-1659
- ¹⁰ Brigger, I.; Dubernet, C.; Couvreur, P.; *Adv. Drug Deliv. Rev.* **2002**, *54*, 631-651
- ¹¹ Ruoslathi, E.; Piersbacher, M.D.; *Science* **1987**, *238*, 491-497
- ¹² Gref, R.; Couvreur, P.; Barratt, G.; Mysiakine, E.; *Biomaterials* **2003**, *24*, 4529-4537
- ¹³ Janes, K.A.; Calvo, P.; Alonso, M.J.; *Adv. Drug Deliv. Rev.* **2001**, *47*, 83-97
- ¹⁴ Dumitriu, S.; “Polysaccharides as Biomaterials” in *Polymeric Biomaterials*, 2nd edition, ed. by Severian Dumitriu, Marcel Dekker, Inc., New York, **2002**, Chapt. 1, p.1-61
- ¹⁵ Lemarchand, C.; Gref, R.; Couvreur, P.; *Eur. J. Pharm. Biopharm.* **2004**, *58*, 327-341
- ¹⁶ Kawashima, Y.; Yamamoto, H.; Takeuchi, H.; Kuno, Y.; *Pharm. Dev. Technol.* **2000**, *5*, 77-85
- ¹⁷ Agnihotri, S.A.; Mallikarjuna, N.N.; Aminabhavi, T.M.; *J. Contr. Release* **2004**, *100*, 5-28
- ¹⁸ Takeuchi, H.; Yamamoto, H.; Kawashima, Y.; *Adv. Drug Deliv. Rev.* **2001**, *47*, 39-54
- ¹⁹ Hendricks, S.K.; Kwok, C.; Shen, M.; Horbett, B.D.; Ratner, B.D.; Bryers, J.D.; *J. Biomed. Mater. Res.* **2000**, *50*, 160-170
- ²⁰ Janes, K.A.; Calvo, P.; Alonso, M.J.; *Adv. Drug Deliv. Rev.* **2001**, *47*, 83–97
- ²¹ Schatz, C.; Bionaz, A.; Lucas, J.-M.; Pichot, C.; Viton, C.; Domard, A.; Delair, T.; *Biomacromolecules* **2005**, *6*, 1642-1647
- ²² Yamamoto, H.; Kuno, Y.; Sugimoto, S.; Takeuchi, H.; Kawashima, Y.; *J. Contr. Release* **2005**, *102*, 373–381
- ²³ Borchard, G.; Luen, H.L.; De Boer, A.G.; Verhoef, J.C.; Lehr, C.M.; Junginger, H.E.; *J. Contr. Release* **1996**, *39*, 131-138
- ²⁴ Felt, O.; Einmahl, S.; Gurny, R.; Furrer, F.; Baeyens, V.; “Polymeric Systems for Ophthalmic Drug Delivery” in *Polymeric Biomaterials*, second Edition, ed. By Severian Dumitriu, Marcel Dekker, Inc., New York, **2002**, Chapt. 15, p. 384ff

- ²⁵ Balazs, E.A.; “Why hyaluronan has so many biological activities ?” in *New Frontiers in Medical Sciences: Redefining Hyaluronan*; ed. by Abatangelo, G.; Weigel, P.H.; Elsevier Science B.V., Amsterdam, **2000**, Chapt.1, p. 3-10
- ²⁶ Domb, A.J.; Kumar, N.; Sheskin, T.; Bentolila, A; Slager, J.; Teomim, D.; “Biodegradable Polymers as Drug Carrier Systems” in *Polymeric Biomaterials*, 2nd edition, ed. by Severian Dumitriu, Marcel Dekker, Inc., New York, **2002**, Chapt. 4, p. 91-121
- ²⁷ Vert, M.; Mauduit, L.; Suming, L.; *Biomaterials* **1994**, *15*, 1209-1213
- ²⁸ Grizzi, I.; Garreau, H.; Li, S.; Vert, M.; *Biomaterials* **1995**, *15*, 305-311
- ²⁹ Park, T.G.; *Biomaterials* **1995**, *16*, 1123-1130
- ³⁰ Lenz, R.W.; Guerin, P.; “Polymers in Medicine: Functional Polyesters and Polyamides for Medical applications of Biodegradable Polymers”, ed. by E. Chiellini, P. Giusti, Plenum Press, New York, **1983**
- ³¹ Lee, B.-S.; Vert, M.; Holler, E. “Water-soluble aliphatic polyesters: Poly(malic acid)s”, in *Biopolymers*, ed. by. Doi, Y.; Steinbüchel, A.; Vol 3a, Wiley-VCH, Weinheim, Germany, **2002**, p.75-103
- ³² Tian, D.; Dubois, P.; Jérôme, R.; *Macromolecules* **1997**, *30*, 2575-2581
- ³³ Detrembleur, C.; Mazza, M.; Halleux, O.; Lecomte, P.; Mecerreyes, D.; Hedrick, J.L.; Jérôme, R.; *Macromolecules* **2000**, *33*, 14-18
- ³⁴ Latere, J.-P.; Lecomte, P.; Dubois, P.; Jérôme, R.; *Macromolecules* **2002**, *35*, 7857-7859
- ³⁵ Riva, R.; Schmeits, S.; Stoffelbach, F.; Jérôme, C.; Jérôme, R.; Lecomte, P.; *J. Chem. Soc. Chem. Commun.* **2005**, 5334-5336.
- ³⁶ Rieger, J.; Bernaerts, K.V.; Du Prez, F. E.; Jérôme, R., Jérôme, C.; *Macromolecules* **2004**, *37*, 9738-9745
- ³⁷ Kawaguchi, T.; Nakano, M.; Juni, K.; Inoue, S.; Yoshida, Y.; *Chem. Pharm. Bull.* **1982**, *30*, 1517-1520
- ³⁸ Kawaguchi, T.; Nakano, M.; Juni, K.; Inoue, S.; Yoshida, Y.; *Chem. Pharm. Bull.* **1983**, *31*, 1400-1403
- ³⁹ Anderson, J.M.; Spilizewski, K.L., Hiltner, A.; “Poly α -amino acids as biomedical polymers” in *Biocompatibility of tissue analogs*, Vol 1, ed. by Williams, D.F.; CRC Press, Boca Raton, FL, **1985**, p.67-88
- ⁴⁰ Webster, I.; West, P.J.; “Adhesives for Medical Applications” in *Polymeric Biomaterials*, 2nd edition, ed. by Severian Dumitriu, Marcel Dekker, Inc., New York, Chapt. 26, **2002**, p. 717-737
- ⁴¹ Müller, R.; Lherm, C.; Herbort, P.; Couvreur, P.; *Biomaterials* **1990**, *11*, 590-595
- ⁴² Leonard, F.; Kulkarni, R.K.; Brandes, G.; Nelson, J.; Mameron, J.J.; *J. Appl. Polym. Sci.* **1966**, *10*, 259-272
- ⁴³ Gil, E.S.; Hudson, S. M.; *Prog. Polym. Sci.* **2004**, *29*, 1173-1222
- ⁴⁴ De las Heras Alarcón, C.; Pennadam, S.; Alexander, C.; *Chem. Soc. Rev.* **2005**, *34*, 276-285
- ⁴⁵ Lee, J.H.; Lee, H.B.; Andrade, J.D.; *Prog. Polym. Sci.* **1995**, *20*, 1043-1979
- ⁴⁶ Vermette, P.; Meagher, L.; *Colloid Surf. B - Biointerfaces* **2003**, *28*, 153-198
- ⁴⁷ Peracchia, M.T.; *STP Pharm. Sci.* **2003**, *13*, 155-161
- ⁴⁸ Otsuka, H.; Nagasaki, Y.; Kataoka, K.; *Adv. Drug. Deliv. Rev.* **2003**, *55*, 403-419
- ⁴⁹ Gref, R.; Lück, M.; Quellec, P.; Marchand, M.; Dellacherie, E.; Harnisch, S.; Blunk, T.; Müller, R. H.; *Colloid Surf. B - Biointerfaces* **2000**, *18*, 301-313
- ⁵⁰ Vanderhoff, J.W.; El-Aasser, M.S.; Ugelstad, J.; U.S. Patent 4 177 177, **1979**

- ⁵¹ Quintanar-Guerrero, D.; Allémann, E.; Fessi, H.; Doelker, E.; *Drug Dev. Ind. Pharm.* **1998**, *24*, 1113-1128
- ⁵² Blanco, M.D.; Alonso, M.J.; *Eur. J. Pharm. Biopharm.* **1997**, *43*, 287-294
- ⁵³ Allémann, E.; Gurny, R.; Doelker, E.; *Int. J. Pharm.* **1992**, *87*, 247-253
- ⁵⁴ Fessi, H.; Puisieux, F.; Devissaguet, J.P.; Ammoury, N.; Benita, S.; *Int. J. Pharm.* **1989**, *55*, R1
- ⁵⁵ Quintanar-Guerrero, D.; Fessi, H.; Allémann, E.; *Int. J. Pharm.* **1996**, *143*, 133-141
- ⁵⁶ Fessi, H.; Puisieux, F.; Devissaguet, J.P.; Eur. Patent 274 961, **1986**
- ⁵⁷ Bilati, U.; Allémann, Doelker, E.; *Eur. J. Pharm. Sci.* **2005**, *24*, 67-75
- ⁵⁸ Qiu, H.; Rieger, J.; Gilbert, B.; Jérôme, R.; Jérôme, C.; *J. Chem. Mater.* **2004**, *16*, 850-856
- ⁵⁹ Vangeyte, P.; Gautier, S.; Jérôme, R.; *Colloid Surf. A – Physicochem. Eng. Asp.* **2004**, *242*, 203–211
- ⁶⁰ Antonietti, M.; Landfester, K.; *Chem. Phys. Chem.* **2001**, *2*, 207-210
- ⁶¹ Landfester, K.; *Macromol. Rapid Commun.* **2001**, *22*, 896-936
- ⁶² Kishida, K.; Akashi, A.; Sakuma, M.; Suzuki, S.; Kikuchi, N.; Hiwatari, H.; Arikawa, K.; *Int. J. Pharm.* **1997**, *149*, 93–106
- ⁶³ Durand, A.; Marie, E.; Rotureau, E.; Leonard, M.; Dellacherie, E. *Langmuir* **2004**, *20*, 6956-6963
- ⁶⁴ Uchida, T.; Seriwaza, T.; Akashi, M.; *Polymer J.* **1999**, *31*, 970-973
- ⁶⁵ Uchida, T.; Serizawa, T.; Ise, H.; Akaike, T.; Akashi, M.; *Biomacromolecules* **2001**, *2*, 1343-1346
- ⁶⁶ Serizawa, T.; Yasunaga, S.; Akashi, M.; *Biomacromolecules* **2001**, *2*, 469-475
- ⁶⁷ Gallardo, M.M.; Couarraze, G.; Denizot, B.; Treupel, L.; Couvreur, P.; Puisieux, F.; *Int. J. Pharm.* **1993**, *100*, 55-64
- ⁶⁸ Al Khouri, N.; Fessi, H.; Robot-Treupel, J.P.; Devissaguet, F.; Puisieux, F.; *Pharmaceutica acta Helveticae* **1986**, *61*, 274-281
- ⁶⁹ Quintanar-Guerrero, D.; Allémann, E.; Doelker, H.; Fessi, H.; *Pharm. Res.* **1998**, *15*, 1056-1062
- ⁷⁰ Vranckx, H.; De Moutier, M.; De Leers, M.; **1996**, U.S. patent 5.500.224
- ⁷¹ Fresta, M.; Cavallaro, G.; Giammona, G.; Wehrli, E.; Puglisi, G.; *Biomaterials*, **1996**, *17*, 751-758
- ⁷² Seymour, L. W.; Duncan, R.; Kopeckova, P.; Kopecek, J.; *J. Bioact. Compat. Polym.* **1987**, *2*, 97-119
- ⁷³ Arap, W.; Pasqualini, R.; Ruoslahti, E.; *Science* **1998**, *279*, 377-388
- ⁷⁴ Nayak, S.; Lee, H.; Chmielewski, J.; Lyon, L. A.; *J. Am. Chem. Soc.* **2004**, *126*, 10258-10259
- ⁷⁵ Seymour, L. W.; Flanagan, P. A.; Al-Shamkhani, A.; Subr, V.; Ulbrich, K.; Cassidy, J.; Duncan, R. *Sel. Cancer Ther.* **1991**, *7*, 59-73
- ⁷⁶ Langer, K.; Mutschler, E.; Lambrecht, G.; Mayer, D.; Troschau, G.; Stieneker, F.; Kreuter, J.; *Int. J. Pharmaceutics* **1997**, *158*, 219-231
- ⁷⁷ Passirani, C.; Barratt, G.; Dessaguet, J.-P.; Labarre, D.; *Pharm. Res.* **1998**, *15*, 1046-1050
- ⁷⁸ Chauvierre, C.; Labarre, D.; Couvreur, P.; Vauthier, C.; *Pharm. Res.* **2003**, *20*, 1786-1793
- ⁷⁹ Ruoslathi, E.; Piersbacher, M.D.; *Science* **1987**, *238*, 491-497
- ⁸⁰ Gullberg, E.; “Particle transcytosis across the human intestinal epithelium.” Model Development and Target Identification for Improved Drug Delivery, thesis universitatis upsaliensis, **2005**, ISBN 91-554-6145X

- ⁸¹ Andersson, M.; Fromell, K.; Gullberg, E.; Artursson, P.; Caldwell, K.D.; *Anal. Chem.* **2005**, *77*, 5488-5493
- ⁸² Yasugi, K.; Nakamura, T.; Nagasaki, Y.; Kato, M.; Kataoka, K.; *Macromolecules* **1999**, *32*, 8024-8032
- ⁸³ Varki, A. *Glycobiology* **1993**, *3*, 97-130
- ⁸⁴ Dwek, R. A. *Chem. Rev.* **1996**, *96*, 683-720
- ⁸⁵ Smart, J.D.; Nicholls, T.J.; Green, K.L.; Rogers, D.L.; Cook, J.D.; *Eur. J. Pharm. Sci.* **2000**, *9*, 93-99
- ⁸⁶ Waeckerle-Men, Y.; Groettrupa, M.; *Adv. Drug. Deliv. Rev.* **2005**, *57*, 475-482
- ⁸⁷ Foged, C.; Arigita, C.; Sundblad, A.; Jiskoot, W.; Storm, G.; Frokjaer, S.; *Vaccine* **2004**, *22*, 1903-1913
- ⁸⁸ McGreal, E.P.; Miller, J.L.; Gordon, S.; *Curr. Opin. Immunol.* **2005**, *17*, 18-24
- ⁸⁹ Jilek, S.; Merkle, H. P.; Walter, E.; *Adv. Drug Deliv. Rev.* **2005**, *57*, 377-390
- ⁹⁰ Warren, H.S.; Leclerc, C.; "Adjuvants" in Encyclopedia in Immunology, 2nd edition, Vol. 1, ed. by Delves, P.J.; Roitt, I. M., Academic press, San Diego, **1998**, p. 36-39
- ⁹¹ Illum, L.; Jabbal-Gill, M.; Hinchcliffe, M.; Fisher, A.N.; Davis, S.S.; *Adv. Drug Deliv. Rev.* **2001**, *51*, 81-96
- ⁹² Uchida, T.; Goto, S.; Foster, T.P.; *J. Pharm. Pharmacol.* **1995**, *47*, 556-60
- ⁹³ Trouet, A.; Masquelier, M.; Baurin, R.; Campeneere, D. D.-D.; *Proc. Natl. Acad. Sci. U.S.A.* **1982**, *79*, 626-629
- ⁹⁴ Fiume, L.; Bassi, B.; Busi, C.; Mattioli, A.; Spinosa, G.; *Biochem. Pharmacol.* **1986**, *35*, 967-972
- ⁹⁵ Cho, C.S.; Cho, K.Y.; Park, I.K.; Kim, S.H.; Sasagawa, T.; Uchiyama, M.; Akaike, T.; *J. Contr. Release* **2001**, *77*, 7-15
- ⁹⁶ Cade, D.; Ramus, E.; Rinaudo, M.; Auzély-Velty, R.; Delair, T.; Hamaide, T.; *Biomacromolecules* **2004**, *5*, 922-927
- ⁹⁷ Woller, E. K.; Cloniger, M.J.; *Organic Letters* **2002**, *4*, 7-10
- ⁹⁸ Dam, T.K.; Brewer, C.B.; *Chem. Rev.* **2002**, *102*, 387-429
- ⁹⁹ Nielsen, U.B.; Kirpotin, D.B.; Pickering, E.M.; Hong, K.; Park, J.W.; Shababy, M.R.; Shao, Y.; Benz, J.D.; Marks, J.D.; *Bioch. Bioph. Acta* **2002**, *1591*, 109-118
- ¹⁰⁰ Illum, L.; Jones, P.D.; Baldwin, R.W.; Davis, S.S.; *J. Pharmacol. Exp. Ther.* **1984**, *230*, 733-736
- ¹⁰¹ Rolland, A.; Bourel, D.; Genetet, B.; Le Verge, R.; *Int. J. Pharm.*, **1987**, *39*, 173-180
- ¹⁰² Balthasar, S.; Michaelis, K.; Dinauer, N.; Von Briesen, H.; Kreuter, J.; Langer, K.; *Biomaterials* **2005**, *26*, 2723-2732
- ¹⁰³ Pan, D.; Turner, J.L.; Wooley, K.L.; *Macromolecules* **2004**, *37*, 7109-7115
- ¹⁰⁴ Angelatos, A.S.; Radt, B.; Caruso, F.; *J. Phys. Chem. B.* **2005**, *109*, 3071-3076
- ¹⁰⁵ Park, J.; Kurosawa, S.; Watanabe, J.; Ishihara, K.; *Anal. Chem.* **2004**, *76*, 2649-2655
- ¹⁰⁶ Illum, L.; Jones, P.D.; Baldwin, R.W.; Davis, S.S.; *J. Pharmacol. Exp. Ther.* **1984**, *230*, 733-736
- ¹⁰⁷ Ciu, Z.; Patel, J.; Tuzova, M.; Ray, P.; Phillips, R.; Woodward, J.G.; Nath, A.; Mumper, R.J.; *Vaccine* **2004**, *22*, 2631-2640
- ¹⁰⁸ Borges, O.; Borchard, G.; Verhoef, J.C.; De Sousa, A.; Juninger, H.E.; *Int. J. Pharm.* **2005**, *299*, 155-166
- ¹⁰⁹ Redhead, H.M.; Davis, S.S.; Illum, L.; *J. Contr. Release* **2001**, *70*, 353-363
- ¹¹⁰ De Souza Delgado, A.; Léonard, M.; Dellacherie, E.; *Langmuir* **2001**, *17*, 4386-4391
- ¹¹¹ Studer, P.; Limal, D.; Breton, P.; Riess, G.; *Bioconjugate Chem.* **2005**, *16*, 223-229
- ¹¹² Jule, E.; Nagasaki, Y.; Kataoka, K.; *Langmuir* **2002**, *18*, 10334-10339

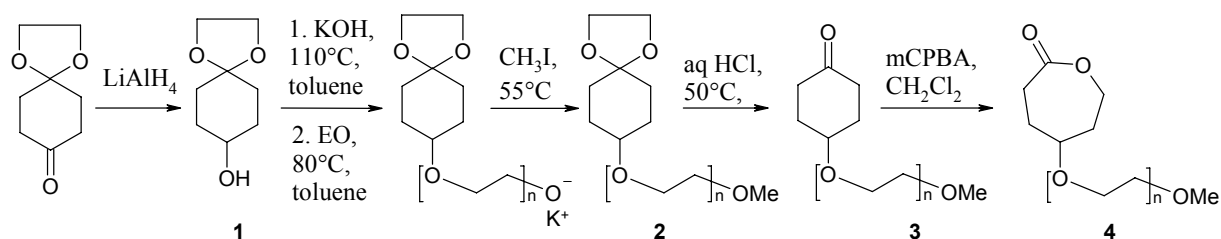
- ¹¹³ Yamamoto, Y.; Nagasaki, Y.; Kato, M.; Kataoka, K.; *Colloids Surf. B: Biointerfaces* **1999**, *16*, 135-146
- ¹¹⁴ Qi, K.; Ma, Q.; Remson, E.E.; Clark, C.G. Jr.; *J. Am. Chem. Soc.* **2004**, *126*, 6599-6607
- ¹¹⁵ Narain, R.; Armes, S. P.; *Biomacromolecules* **2003**, *4*, 1746-1758
- ¹¹⁶ Gautier, S.; Grudzielski, N.; Goffinet, G.; Henry de Hassonville, S.; Delattre, L.; Jérôme, R.; *J. Biomater. Sci. Polym. Edn.* **2001**, *12*, 429-450
- ¹¹⁷ Gautier, S.; D'Aloia, V.; Halleux, O.; Mazza, M.; Lecomte, Ph.; Jérôme, R.; *J. Biomater. Sci. Polym. Edn.* **2003**, *14*, 63-85
- ¹¹⁸ Lemieux, G.A.; Bertozzi, C.R.; *Tibtech.* **1998**, *16*, 506-513
- ¹¹⁹ Stella, B.; Arpicco, S.; Peracchia, M.T.; Desmaële, D.; Hoebeke, J.; Renoir, M.; D'Angelo, J.; Cattel, L.; Couvreur, P.; *J. Pharm. Sci.* **2000**, *89*, 1452-1464
- ¹²⁰ Jiang, F.N.; Jiang, S.; Liu, D.; Richter, A.; Levy, J.G.; *J. Immunol. Methods* **1990**, *134*, 139-149
- ¹²¹ Dufresne, M.H.; Gauthier, M.A.; Leroux, J.-C.; *Bioconjugate Chem.* **2005**, *16*, 1027-1033
- ¹²² Langer, K.; Coester, C.; Weber, C.; von Briesen, H.; Kreuter, J.; *Eur. J. Pharm. Biopharm.* **2000**, *49*, 303-307
- ¹²³ Nobs, L.; Buchegger, F.; Gurny, R.; Allémann, E.; *Int. J. Pharm.* **2003**, *250*, 327-337
- ¹²⁴ Nobs, L.; Buchegger, F.; Gurny, R.; Allémann, E.; *Eur. J. Pharm. Biopharm.* **2004**, *58*, 483-490

Chapter 1

**Synthesis and characterization
of lactone end-capped poly(ethylene oxide)
as new building block for biomaterials**

Abstract

This chapter reports on the synthesis of a novel poly(ethylene oxide) (PEO) macromonomer, which can be copolymerized with ϵ -caprolactone (ϵ -CL) by ring-opening polymerization (ROP). PEO chains end-capped by an ϵ -caprolactone unit (γ PEO.CL, **4**) have been synthesized by living anionic ring-opening polymerization of ethylene oxide (EO) initiated by the potassium alkoxide of 1,4-dioxaspiro[4.5]decan-8-ol, followed by derivatization of the acetal into a ketone and the Baeyer-Villiger oxidation of the ketone into a lactone. The end-capping of PEO by ϵ -CL was assessed by FTIR, MALDI-TOF and $^1\text{H-NMR}$ -spectroscopy. This type of macromonomer is a precursor of amphiphilic comb-like copolymers consisting of a biodegradable hydrophobic backbone of poly(ϵ -caprolactone) (PCL) and hydrophilic PEO-grafts. Copolymerization of γ PEO.CL with ϵ -CL was successfully initiated by aluminum alkoxide.



Contents

I. INTRODUCTION.....	51
II. EXPERIMENTAL PART.....	53
<i>Materials.....</i>	53
<i>Synthesis of the PEO macromonomer.....</i>	53
<i>Copolymerization of γPEO.CL and ϵ-caprolactone.....</i>	55
<i>Characterization techniques.....</i>	55
III. RESULTS AND DISCUSSION	56
<i>III.1. Synthesis of the PEO macromonomer.....</i>	56
<i>III.2. Copolymerization of γPEO.CL and ϵ-caprolactone.....</i>	65
IV. CONCLUSIONS	68

I. Introduction

Poly(ethylene oxide) (PEO) is known for solubility in both organic and aqueous media, hydrophilicity and biocompatibility.¹ It has great potential in biomedical applications, being for instance very efficient in preventing protein adsorption at surfaces as illustrated by reduction in cell adhesion in aqueous systems,² nonrecognition of surfaces by the mononuclear phagocyte system (MPS),³ and reduced complement activation in the human body.⁴ PEO-containing amphiphilic graft copolymers may therefore be useful to modify biomedical polymer surfaces^{5,6} and to design drug-delivery systems.⁷⁻¹⁰ Grafting of poly(ethylene oxide) brushes on a solid surface reduces efficiently the non-specific adsorption of biomolecules and bio-species, such as proteins and platelets.^{6,11} Griffith *et al.* prepared comb-like copolymers composed of a poly(methyl methacrylate) backbone and PEO grafts whose chain ends are partially capped by arginin-glycin-asparagin so called "RGD" tripeptides.¹² Functional surfaces were prepared by spin-coating a solution of these comb-like copolymers in a water/ethanol mixture on solid substrates (e.g., glass dishes and tissue culture polystyrene (TCPS)). RGD peptides then form nanoclusters on a protein-resistant (PEO) polymer surface, which allows for controlled cell adhesion.^{12,13}

Micelles of amphiphilic PEO graft copolymers have also been used for delivery of genes¹⁴ and sustained drug release.¹⁵ The PEO corona of the micelles inhibits protein adsorption, which prolongs the circulation time of the micelles in the blood (prolonged drug release).^{7,16}

Several techniques have been reported for the synthesis of amphiphilic graft copolymers of poly(ethylene oxide). The "grafting onto" method consists of grafting PEO chains onto a reactive backbone by traditional organic reactions. This method has been extensively reported for (meth)acrylic or styrene (co)polymers.¹⁷⁻¹⁹ For example, Wesslen *et al.* grafted poly(ethylene glycol) monomethyl alkoxides (MPEO-alkoxides) onto copolymers of acrylic and methacrylic ester by transesterification reactions in the melt or in solution.¹⁹ They also reported on the grafting of MPEO-alkoxides onto epoxy groups attached to the main chain. Although the grafting efficiency was higher compared to the transesterification strategy, occurrence of crosslinking was however a problem.¹⁹

In the so-called "grafting from" method, anions generated along a hydrophobic polymer backbone are used to initiate the anionic polymerization of ethylene oxide (EO). For instance, polystyrene-g-PEO copolymer was prepared from styrene chains containing 5-15% of (meth)acrylamide, whose amide units were metalated and used to initiate the

anionic polymerization of ethylene oxide.^{20,21} This method is restricted to backbones that are stable towards charged nucleophiles, which thus rules out ester containing chains such as poly(ϵ -caprolactone) and polylactide.

Because these two grafting techniques are usually time-consuming, attention has been paid to the copolymerization of PEO macromonomers (“grafting through”). Macromonomer copolymerization is a convenient and effective method to access amphiphilic graft copolymers without post-polymerization grafting. Controlled radical copolymerization, e.g., atom transfer radical copolymerization of vinylic monomers with poly(ethylene oxide) end-capped by a (meth)acrylate (PEO.AA or PEO.MA)²²⁻²⁵ or a p-vinylphenylalkyl group, has been reported.²⁶ Styrene has also been copolymerized with PEO macromonomers of the vinylbenzyl and acrylamide type, with potassium persulfate as an initiator.²⁷

Only few papers have been published about the preparation of PEO graft copolymers by ring-opening metathesis polymerization (ROMP). Breitenkamp *et al.*²⁸ synthesized novel poly(ethylene oxide) macromonomers with a cyclooctene end-group (co)polymerizable by ROMP. Polynorbornene-*graft*-poly(ethylene oxide) copolymers (PNB-*g*-PEO) were accordingly prepared.²⁹

All of the aforementioned amphiphilic graft copolymers consist of a non-(bio)degradable hydrophobic backbone. In contrast to diblock copolymers of PEO and biodegradable aliphatic polyesters, such as poly(ϵ -caprolactone) (PCL) and polylactide (PLA), PCL(PLA)-*g*-PEO copolymers have not been reported yet. Although they do not contain PEO, degradable amphiphilic copolyesters have been prepared by copolymerization of ϵ -CL with ϵ -CL comonomers substituted in the γ -position by a hydrophilic group, both charged or neutral.³⁰⁻³⁵

Because aliphatic polyesters are very sensitive to hydrolysis and transesterification reactions, grafting of PEO via the macromonomer technique is best suited. This paper reports on the synthesis of new PEO macromonomers (Scheme 1, **4**) copolymerizable with ϵ -CL by ring-opening polymerization (ROP) and therefore suitable for the preparation of amphiphilic comb-like copolymers with a (bio)degradable hydrophobic backbone.

II. Experimental Part

Materials.

ϵ -CL (Aldrich, 99%) was dried over calcium hydride for 48 h while stirring and distilled under reduced pressure before use. Triethylaluminum (AlEt₃) (Fluka, 1.9 M in toluene) was diluted in dry toluene, and the solution concentration was determined by addition of an excess of hydrogen chloride and measurement of the ethane released. Toluene was dried by refluxing it from Na/benzophenone for 48 h and distilled under nitrogen. Methylene chloride (CH₂Cl₂) was dried by refluxing it from calcium hydride for at least 48 h before distillation. 1,4-Dioxaspiro[4.5]decan-8-one (Fluka, >97 %), lithium aluminum hydride (LiAlH₄) (Aldrich, 95%), ethylene oxide (Messer), potassium hydroxide (KOH) (Acros, > 85 %), methyl iodide (CH₃I) (Aldrich, 99.5%), m-chloroperbenzoic acid (m-CPBA) (Fluka, 70 %) and diethyl ether (Vel) were used as received. p-Methoxy benzyl alcohol (Janssen Chimica, 98%) was dried by repeated azeotropic distillation of toluene just before use.

Synthesis of the PEO macromonomer.

Synthesis of 1,4-dioxaspiro[4.5]decan-8-ol (Scheme 1, 1).

1,4-Dioxaspiro[4.5]decan-8-ol was synthesized by reduction of 1,4-dioxaspiro[4.5]decan-8-one (1,4-cyclohexanedione monoethylene ketal) with lithium aluminum hydride in THF as published elsewhere.³⁶ The product was recovered by distillation in vacuo and characterized by ¹H-NMR. (Conversion: 100 %, Yield: 85 %) ¹H-NMR (CDCl₃, δ): 1.6 (m, 4H, CH₂-CH(OH)), 1.85 (m, 4H, CH₂-CH₂-CH), 3.77 (m, 1H, CH-CH₂), 3.92 (m, 4H, -O-CH₂-CH₂-O). FTIR: 3400 (OH), 2940 (CH), 1100 (C-O) cm⁻¹

Synthesis of α -(4-oxo-cyclohexy)- ω -methoxy-poly(oxy-1,2-ethanediyl) (2).

Compound 1 (30 g, 0.19 mol) was reacted with 80 mol% (8.53 g, 0.152 mol) of potassium hydroxide in 300 ml toluene in a "Dean-Stark" apparatus under nitrogen. The crude reaction product was transferred under nitrogen in a Zipperclave (Autoclave 316Ti) reactor together with 300 ml of dried toluene (theoretical concentration of 0.15 mol/l). For the synthesis of PEO 2a (Table 1, entry 1, M_{n,th} = 600), approximately 80g (84 g, 1.9 mol) of ethylene oxide (EO) was added and polymerized under vigorous stirring at 80°C for 5 h. The EO pressure decreased accordingly from 2 to 0.8 bar. The living chains were killed by

an excess of methyl iodide (35.5 ml, 0.57 mol) at 55°C for 20 h. The polymer was recovered by precipitation in heptane and dried in vacuo. Methylation was however partial (~45% for PEO **2b** (Table 1, entry 2, $M_{n,th} = 1100$) and **2c** (Table 1, entry 3, $M_{n,th} = 2200$) and ~75% for PEO **2a**, Table 1) and repeated as follows: PEO **2a**, **2b** and **2c** (0.19 mol) were reacted with 60 mol% of KOH with respect to PEO, followed by azeotropic distillation of toluene in order to convert the remaining hydroxyl groups into the potassium alkoxides. To the reaction mixture containing compound **2b** or **2c**, 0.7 equivalent of CH₃I (0.133 mol) in toluene (0.5 M solution) was added and let to react for 2 h at room temperature (“mild” conditions). On the other hand, the sample **2a** (114 g, 0.19 mol) was reacted with 2.5 equivalents of methyl iodide (30 ml, 0.475 mol) at 40 °C for 12 h (“stringent” conditions). In the first case, the methylation yield slightly increased (e.g., from 45% to 50%), in contrast to full methylation under the more stringent conditions. The excess of CH₃I was removed by precipitation in heptane, and the polymer dried under reduced pressure. (Conversion: 100%, Yield: 95%) ¹H-NMR (CDCl₃, δ): 1.4-1.9 (m, 8H, CH-CH₂-CH₂-), 3.36 (s, 3H, OCH₃), 3.6 (M, 4nH, -O-[CH₂-CH₂-O]_n), 3.9 (s, 4H, -O-CH₂-CH₂-O)

Synthesis of α -(4-ethylene ketal-cyclohexyl)- ω -methoxy-poly(oxy-1,2-ethanediyl) (α -4-cyclohexanone- ω -methoxy-poly(ethylene oxide)) (3**).**

The protecting acetal group of compound **2a** (40 g, 0.067 mol) was hydrolyzed in 300 ml 0.1 M HCl in water at 50°C for 90 min under nitrogen. NaHCO₃ was added until the pH was 7, and **3** was recovered by three-fold extraction with 250 ml dichloromethane. After removal of CH₂Cl₂, 29 g of compound **3a** were recovered. (Conversion: 100%, Yield: 75%) ¹H-NMR (CDCl₃, δ): 1.93 (m, 2H, C(O)CH₂-CH₂), 2.07 (m, 2H, C(O)CH₂-CH₂), 2.25 (m, 2H, C(O)CH₂-CH₂), 2.57 (m, 2H, C(O)CH₂-CH₂), 3.36 (s, 3H, OCH₃), 3.6 (M, 4nH, -O-[CH₂-CH₂-O]_n)

Synthesis of α -(4-oxo-5-oxepanyl)- ω -methoxy-poly(oxy-1,2-ethanediyl), (α - γ - ϵ -caprolactone)- ω -methoxy-poly(ethylene oxide)), (γ PEO.CL) (4**).**

A solution of 10 g (0.015 mol) of compound **3a** (10 w/v %) in 50 ml methylene chloride was reacted with 1.4 eq. of m-chloroperbenzoic acid (m-CPBA) (5.3 g, 0.0215 mol) at 25 °C for 72 h. After reaction, approximately half of the solvent was removed; the solution was cooled to -20 °C, filtered at -20 °C, and washed with 5 ml cold CH₂Cl₂. The CH₂Cl₂ solution was recovered. This procedure was repeated three times. The CH₂Cl₂

solution (40 ml) was then washed, first with 10 ml of a saturated aqueous solution of $\text{Na}_2\text{S}_2\text{O}_3$ (the aqueous phase was re-extracted with CH_2Cl_2), followed by 10 ml of a saturated solution of NaHCO_3 (the aqueous phase was re-extracted with CH_2Cl_2), and 5 ml of a saturated solution of NaCl , and finally dried over MgSO_4 . Compound **4** was precipitated in diethyl ether at 0°C (three times), and finally dried under reduced pressure at room temperature. It was stored under nitrogen at -20°C . (Conversion = 100%, Yield (**4a**) = 45%) $^1\text{H-NMR}$ (CDCl_3 , δ): 1.8-2.1 (m, 4H, $\text{CH-CH}_2\text{-CH}_2$), 2.40 (m, 1H, C(O)-CH_2), 2.98 (t, 1H, C(O)-CH_2), 3.36 (s, 3H, OCH_3), 3.6 (M, 4nH, $-\text{O}[\text{CH}_2\text{-CH}_2\text{-O}]_n$), 4.05 (m, 1H, C(O)-O-CH_2), 4.5 (t, 1H, C(O)-O-CH_2) (see also Figure 4). $^{13}\text{C-NMR}$ (CDCl_3 , δ): 28.3 ($\text{CH}_2\text{-CH}_2\text{COO}$), 28.7 ($\text{CH}_2\text{-CH}_2\text{-OCO}$), 34.9 (CH_2COO), 59.9 (OCH_3), 64.3 ($\text{CH}_2\text{-OCO}$), 71.7 ($\text{O}[\text{CH}_2\text{-CH}_2\text{-O}]_n$), 72.8 (CH-CH_2), 178 (COO)

Copolymerization of **4 ($\gamma\text{PEO.CL}$) and ϵ -caprolactone (Scheme 2).**

Diethyl aluminum alkoxide was prepared by reacting triethylaluminum (AlEt_3) with p-methoxy benzyl alcohol. A 0.36M solution of the previously dried alcohol (13.2 mg, 0.0001 mol) in CH_2Cl_2 was slowly added into a carefully dried Pyrex flask containing 1.1 equiv. of a 0.71 M solution of AlEt_3 in toluene. The reaction proceeded under nitrogen under vigorous stirring for 2 h at room temperature.

$\gamma\text{PEO.CL}$ **4a** (1 g, 0.001 mol, $M_{n,\text{th}} = 1000$) was dried by three azeotropic distillations of toluene and heated at 45°C under vacuum, overnight. A solution of dried $\epsilon\text{-CL}$ (0.02 mol, 2.2 ml) and $\gamma\text{PEO.CL}$ **4a** (1 g, 0.001 mol) in CH_2Cl_2 (10 w/v %) was added to the required amount of diethyl aluminum alkoxide (0.0001 mol). The copolymerization was conducted in 25 ml CH_2Cl_2 at room temperature and stopped after 20 h by addition of an excess of HCl (0.1 M solution). The copolymer was precipitated in heptane, filtered and precipitated again in methanol, in order to remove the non-reacted $\gamma\text{PEO.CL}$. The copolymer was recovered by centrifugation, dried in vacuo and stored in vacuo at -20°C . (Yield = 50%)

Characterization techniques.

MALDI-TOF spectra were recorded with a PerSeptive Biosystem Voyager-DE STR MALDI-TOF spectrometer equipped with 2 m linear and 3 m reflector flight tubes and a 337 nm nitrogen laser (3 ns pulse). Mass spectra were recorded at an accelerating potential of 20 kV in positive ion linear or reflectron mode. The data ($M_{n,\text{MALDI}}$ values in Table 1) were processed with the Polymerix software. To generate the isotopic distributions, the

isotope calculator tool of Data Explorer (software supplied by Applied Biosystems) was used. Dithranol (20 mg/ml THF) was used as a matrix and no cationating agent was added. Polymer was dissolved in THF (1 mg/ml THF). A PEG standard with a molecular weight of 1900 (1 mg/ml THF) was used for calibration, with dithranol as matrix (20 mg/ml THF) and without additional cation.

^1H NMR (400 MHz) and ^{13}C -NMR (400 MHz) spectra were recorded in CDCl_3 with a Bruker AM 400 apparatus at 25°C . The molecular weight of the PEO derivatives was calculated from the relative intensity of the methoxy end-group peak and the $-\text{CH}_2-\text{CH}_2-\text{O}$ peak. The completeness of the PEO end-group derivatization was estimated from the relative intensity of both the α and the ω end-groups.

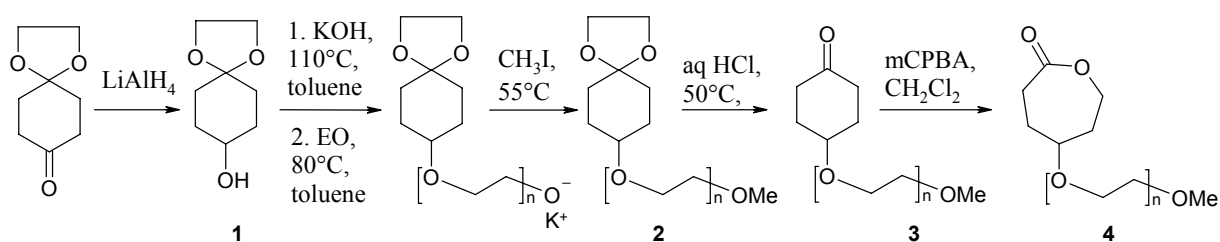
Size-exclusion chromatography (SEC) was carried out in THF at a flow rate 1ml/min at 45°C using a SFD S5200 Autosampler liquid chromatograph equipped with a SFD refractometer index detector 2000 and columns PL gel $5\mu\text{m}$ (columns porosity: 10^2 , 10^3 , 10^4 , 10^5\AA). PS and PEO standards were used for calibration.

FTIR spectra of polymer films deposited on NaCl were recorded with a Perkin Elmer FTIR 1720X spectrometer.

III. Results and Discussion

III.1. Synthesis of the PEO macromonomer.

In order to prepare comb-like copolymers of poly(ϵ -caprolactone) with poly(ethylene oxide) grafts, new macromonomers were synthesized, i.e., PEO chains prepared by living anionic polymerization and end-capped by an ϵ -caprolactone ring at one end (Scheme 1).



Scheme 1. Synthesis of the macromonomer (α -(γ - ϵ -caprolactone)- ω -methoxypoly(ethylene oxide)), (γ PEO.CL); mCPBA = meta-chloroperbenzoic acid

Copolymerization of these macromonomers with ϵ -caprolactone by a controlled ring-opening mechanism should be an efficient way to control the length of both the PEO graft and the polyester backbone. This route should be an improved alternative for the grafting of hydroxyl end-capped PEO onto carboxylic acid containing PCL chains. In the latter case, parasitic transesterification reactions would occur and increase the polydispersity of the PCL chains. Similarly, this type of side reaction could perturb the EO polymerization initiated by hydroxyl containing PCL chains.³⁰⁻³²

PEO macromonomers were synthesized by the multi-step process shown in Scheme 1. In order to control both the molecular weight and the end-group functionality, EO was polymerized by living anionic ring-opening polymerization initiated by a precursor of the polymerizable ϵ -CL end-group. Potassium alkoxide of 1,4-dioxaspiro[4.5]decan-8-ol (**1**) was used as the initiator because of its stability under the alkaline conditions of the anionic polymerization of EO. The cyclohexanone ethylene acetal is easily derivatized into lactone (Scheme 1). Compound **1** was prepared from the commercially available 1,4-cyclohexanedione monoethylene ketal as reported elsewhere.³⁶ By changing the ethylene oxide/ alcohol molar ratio, PEO of different M_n were synthesized (series a,b,c in Table 1: entries 1-3).

Table 1. Molecular characteristics of various functional PEO **2, **3** and **4** from Scheme 1**

<i>no.</i>	<i>product</i>	DP_{th}^a	$M_{n,th}$	$M_{n,NMR}$	$M_{n,MALDI}^b$	$M_{n,SEC}^c$	$M_w/M_{n,SEC}$
1	2a	10	600	600	n.d.	550	1.15
2	2b	21	1100	1200	n.d.	1100	1.11
3	2c	47	2200	1900	n.d.	1850	1.12
4	3a	10	550	650	750	600	1.18
5	3b	21	1050	1300	1150	1100	1.17
6	3c	47	2200	2000	1950	1900	1.13
7	4a^d	10	600	1000 ^d	850 ^e	800 ^e	1.09
8	4b^d	21	1100	1300	1350	1250	1.12

^aTheoretical degree of polymerization = $[M]_0/[I]_0$, ^bMALDI-TOF linear mode, ^ccalibration by poly(ethylene oxide) standards, ^dafter purification by three precipitations in diethyl ether, ^eafter purification by one precipitation in diethyl ether

The number-average molecular weight of these samples was determined by $^1\text{H-NMR}$ from the ratio of the integrated signal at 3.6ppm ($\text{CH}_2\text{-CH}_2\text{-O}$ from PEO) to the one at 3.36ppm (O-CH_3), by SEC with PEO standards and by MALDI-TOF, respectively. These experimental data at total monomer conversion are self-consistent and agree well with theoretical M_n . As reported by Vangeyte *et al.*³⁷, the KOH content has no noticeable influence on the EO polymerization, as result of a fast alcohol/alkoxide exchange and growth of all the chains at a comparable rate. In this work, 0.8 equivalent of KOH (with respect to the alcohol) was used, and the narrow molecular weight distribution (estimated by SEC, Table 1) confirms that the initiation step and the alcohol/alkoxide exchange are fast compared to propagation. At the end of the polymerization, the living PEO chains were end-capped by a methoxy group, by addition of CH_3I to the medium. Because this reaction is not complete (e.g., yield $\sim 75\%$ for PEO 2a; entry 1 in Table 1), it was repeated in order to get rid of the residual hydroxyl end groups that could interfere with subsequent reactions, including copolymerization of the macromonomer with ϵ -caprolactone. Completeness of the end-capping was determined by $^1\text{H-NMR}$ and by MALDI-TOF for samples 3, i.e., after deprotection of the acetal by reaction with 0.1 mol HCl for 90 min at 50°C (see Scheme 1).

As mentioned in the “experimental part”, methylation was carried out under “mild” and “stringent” conditions. Methylation under mild conditions remains incomplete as exemplified by the macromonomer 2b ($M_{n,\text{th}}\sim 1100$; Table 1), whose the methylation yield has increased from 45% to 50% during the second methylation step. In contrast, methylation is complete under the stringent conditions applied to macromonomer 2a ($M_{n,\text{th}}\sim 600$; Table 1). Both the partially (3b) and the fully (3a) methylated PEO-cyclohexanone chains were oxidized (Baeyer-Villiger reaction) and analyzed by MALDI-TOF. For all series of peaks in the MALDI-TOF spectrum, the mass and shape of the experimental isotope distribution fit the theoretical ones. A typical MALDI-TOF spectrum of the PEO 3b of 1050 molecular weight (Table 1, entry 5) and methylated under “mild” conditions (see “experimental part”) is shown in Figure 1a. Several series of peaks are observed, and the mass difference between two peaks of the same series is 44 Da (molar mass of EO). Figure 1b also shows a detail of Figure 1a in a mass window of 44 Da (EO monomer unit), which allows assigning the peaks more precisely.

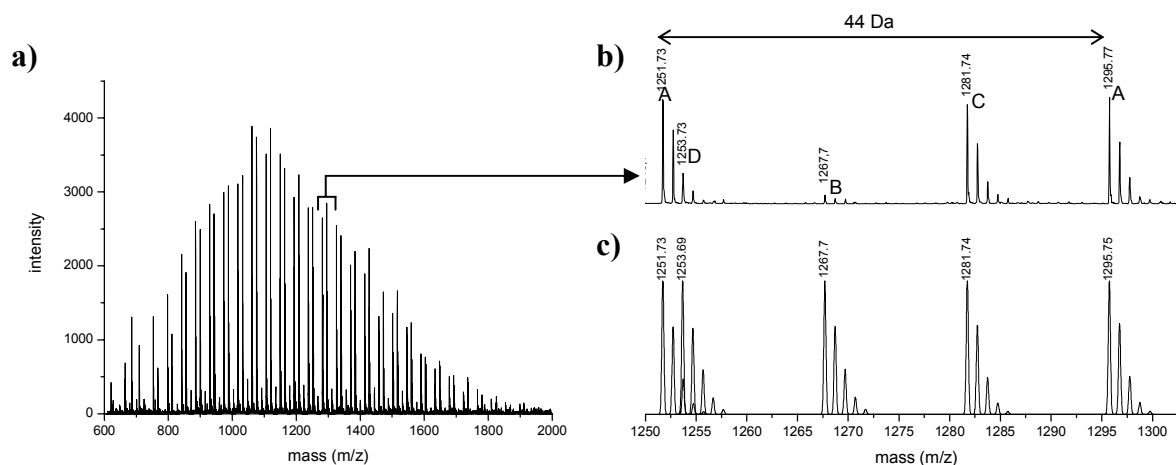


Figure 1. Reflectron mode MALDI-TOF spectrum of PEO 3b (Table 1) ($M_{n,th}=1050$), methylated under mild conditions: a) full spectrum, b) detail of the experimental isotope distribution and c) theoretical isotope distribution

The assignment of the different series of peaks is reported in Table 2. Several families of polymers can be discerned in Figure 1b: the main families can be attributed to the expected polymer (A, B), and to ω -hydroxyl terminated chains (signal C, D). For each family, the most intense peaks correspond to the Na adduct (A and C), whereas peaks with a much lower intensity (B and D) are K adducts because PEO 3b was initiated by KOH and treated with NaHCO_3 (see “experimental part”). The experimental isotope distribution of each signal (Fig 1b) is in good agreement with the theoretical simulation. (Figure 1c)

Table 2. Peak assignments of the MALDI spectra of Figure 1b (sample 3b) and Figure 2b (sample 3a)

<i>code</i>	<i>description</i>	<i>structure</i>
A	desired + Na	 <chem>COC(O)C1CCCC1(OCCO)n</chem>
B	desired + K	
C	ω -hydroxyl terminated chains + Na	 <chem>OCC(O)C1CCCC1(OCCO)n</chem>
D	ω -hydroxyl terminated chains + K	
E	α,ω -dimethoxy-PEO + K	<chem>COC(O)C1CCCC1(OCCO)nOC</chem>

Figure 2a shows the MALDI-TOF spectrum of PEO **3a** ($M_{n,th}=550$) methylated under “stringent” conditions (see “experimental part”).

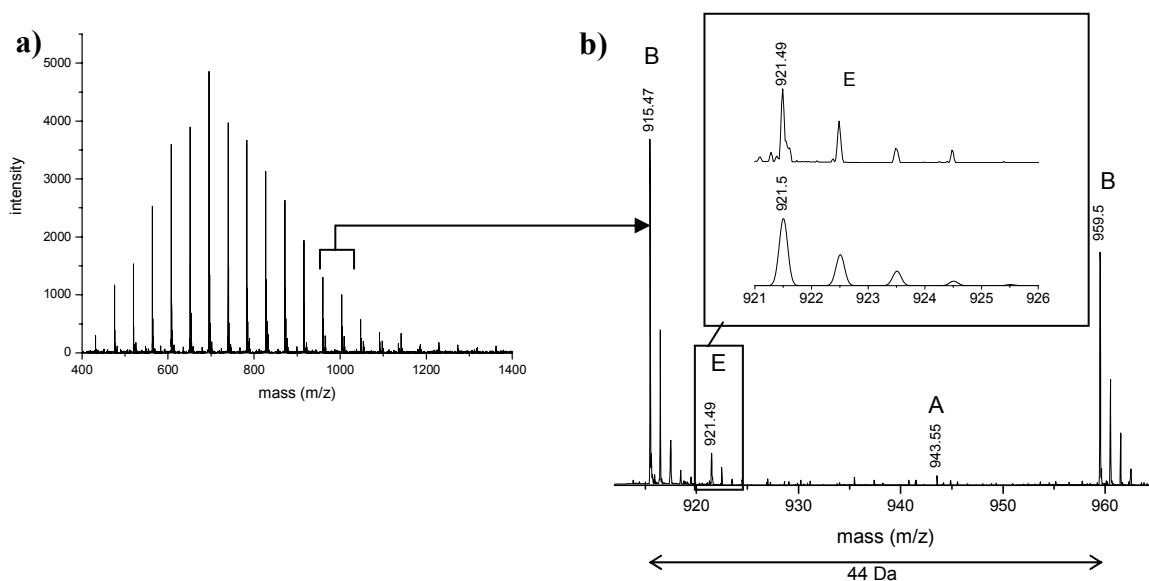


Figure 2. Reflectron mode MALDI-TOF spectrum of PEO **3a (Table 1) ($M_{n,th}=550$), methylated under stringent conditions: a) full spectrum, b) detail of the experimental isotope distribution with an insert for the comparison of the experimental (top) and the theoretical (bottom) isotope distribution for series E**

M_n of the PEO chains remains unchanged upon methylation as assessed by SEC. Compared to **3b**, **3a** shows a smaller number of peaks, consistent with a higher purity. Figure 2b illustrates the detailed isotope distribution of PEO **3a**, the peak assignment is reported in Table 2. Mainly, the K adduct of the desired ω -methylated PEO **3a** is observed (series B), the presence of the Na adduct is quasi negligible (series A). The reason lies in the polymer post-treatment by KHCO_3 (neutralization of the aqueous solution of **3a** after hydrolysis of the acetal by HCl) instead of NaHCO_3 in case of **3b**. Signals for the hydroxyl-terminated chains (C or D) are no longer observed. In addition, there is a new peak, E (K cationated), of lower intensity. The experimental isotope distribution of E agrees well with the theoretical isotope distribution of α,ω -dimethoxy PEO (see insert, Figure 2b). It possibly results from a loss of cyclohexanone end-groups during methylation under stringent conditions. These contaminating chains were not removed before polymerization, because of low content and lack of reactivity.

α - ϵ CL- ω -methoxy-PEO (**4**) was prepared by the Baeyer-Villiger oxidation of the cyclohexanone by *m*-chloroperbenzoic acid (*m*-CPBA). This reaction was performed on both the partially (PEO **3b**) and the fully methylated PEO-cyclohexanone chains (PEO **3a**).

The reaction progress was monitored by $^1\text{H-NMR}$ and stopped at 100% conversion. The PEO macromonomer was contaminated by excess of peracid (m-CPBA) and by m-chlorobenzoic acid (m-CBA) formed as a by-product. It was purified before polymerization because traces of acid have a detrimental effect on the control of the ROP process. Therefore, the crude product was carefully purified as reported in the “experimental part”. The major part of m-CBA was precipitated at 20°C. After filtration, residual m-CPBA was reduced by $\text{Na}_2\text{S}_2\text{O}_3$ to m-CBA, that was transferred to the water phase in presence of NaHCO_3 . Purity was checked by $^1\text{H-NMR}$, particularly the absence of residual acid. Only 45% of the original PEO 4a with $M_{n,\text{th}}=600$ was recovered as $\gamma\text{PEO.CL}$ by precipitation in cold diethyl ether³⁸ and centrifugation (15000 rpm at -5°C). After purification, the fully methylated (4a) and partially methylated (4b) macromonomers 4 ($\gamma\text{PEO.CL}$) were characterized by FTIR, SEC, $^1\text{H-NMR}$ and MALDI-TOF.

Figures 3a and 3b are the MALDI-TOF spectra for PEO 4b and PEO 4a, respectively. Figures 3c and 3d emphasize part of the spectra for sake of comparison of the experimental data and the theoretical isotope distribution (Figure 3e).

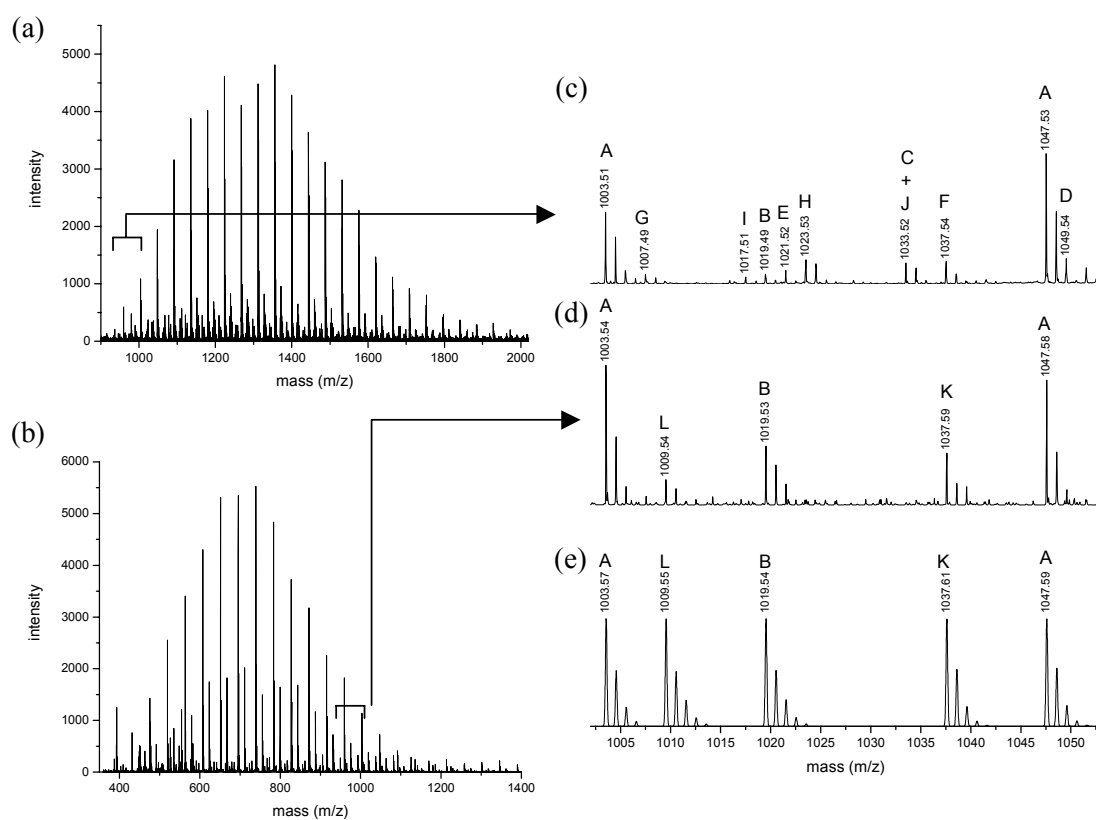
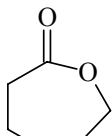
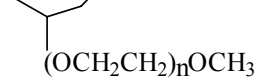
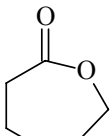
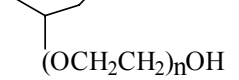
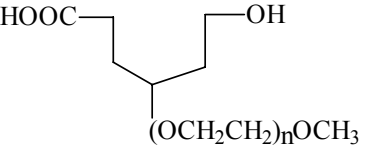
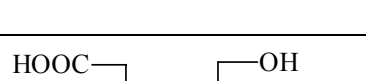
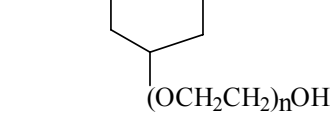

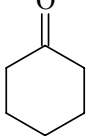
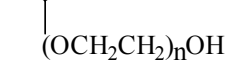


Figure 3. Reflectron mode MALDI-TOF spectra for $\gamma\text{PEO.CL}$: a) full spectrum for PEO 4b b) full spectrum for PEO 4a, c) experimental isotope distribution for sample 4b, d) experimental isotope distribution for sample 4a and e) theoretical isotope distribution

Table 3. Peak assignments for the MALDI spectra of Figure 3a (sample 4b) and Figure 3b (sample 4a)

<i>code</i>	<i>description</i>	<i>n</i>	<i>structure</i>
A	desired α -lactone- ω -methoxy PEO + Na	19	
B	desired α -lactone- ω -methoxy PEO + K	19	
C	ω -hydroxyl-terminated γ PEO.CL + Na	20	
D	ω -hydroxyl-terminated γ PEO.CL + K	20	
E	Hydrolyzed α -lactone ω -methoxy PEO + Na	19	
F	Hydrolyzed α -lactone ω -methoxy PEO + K	19	
G	Hydrolyzed α -lactone ω -hydroxyl PEO + Na	19	
H	Hydrolyzed α -lactone ω -hydroxyl PEO + K	19	
I	non-reacted ω -hydroxyl-terminated PEO <u>3</u> + Na	20	
J	non-reacted ω -hydroxyl-terminated PEO <u>3</u> + K	20	
K	α,ω -dimethoxy-PEO + Na	21	$\text{CH}_3\text{OCH}_2\text{CH}_2(\text{OCH}_2\text{CH}_2)_n\text{OCH}_3$
L	α,ω -dimethoxy-PEO + K	20	

The assignment of the series of peaks is reported in Table 3. The experimental isotope distribution for the partially methylated γ PEO.CL (4b) (Figure 3c) shows the main series A and B, assigned to the sodium and potassium forms of the desired α -lactone- ω -methoxy PEO (Table 3). ω -hydroxyl-terminated γ PEO.CL series (C and D) and series of non-reacted ω -hydroxyl-terminated PEO 3b (I and J) are also observed. Although it is out of the scope of this work, it must be noted that synthesis of ω -hydroxyl-terminated

γ PEO.CL is straightforward. Polymerization of this macroinimer can be initiated by Al or Sn alkoxide and lead to hyperbranched chains.

Figure 3c also confirms the sensitivity of the lactone end-group to hydrolysis. Indeed, signals for the hydrolyzed version of γ PEO.CL (**4b**) are observed for both the series of PEO chains, with the ω -methoxy end group (signals E and F) and the ω -hydroxyl end-group (signals G and H), respectively. Therefore, the contact time with water during purification of the Baeyer-Villiger oxidation product should be minimized. Furthermore, the final macromonomer should be dried by azeotropic distillation of toluene before storage under nitrogen at -20°C . Whenever these conditions were applied to the fully methylated γ PEO.CL chains, the MALDI-TOF spectrum (Figure 3d) shows the two main series (A and B) assigned to the desired α -lactone- ω -methoxy-terminated γ PEO.CL, together with peaks K and L which refer to the sodium and potassium forms of the unmodified α,ω -dimethoxy-PEO observed before the Baeyer-Villiger oxidation (Figure 2b, E). In contrast to macromonomer **4b** analyzed in Figure 3c, no ω -hydroxyl-terminated and no hydrolyzed products contaminate the macromonomer **4a** in Figure 3d. The experimental isotope distribution fits the theoretical one (Figure 3e). Moreover, the average molecular weight (M_n) and the molecular weight distribution (M_w/M_n) of the ω -methoxy-terminated γ PEO.CL (**4a**) are the same as before the Baeyer-Villiger reaction (**3a**), which confirms the stability of PEO during the functionalization process, in agreement with previous SEC analysis.

The average molecular weight calculated by MALDI-TOF is close to the data determined by SEC with PEO standards (Table 1). As far as sample **4a** is concerned, M_n determined by MALDI is lower compared to NMR data. The explanation is that the sample analyzed by MALDI was purified by only one precipitation in diethyl ether, whereas the sample analyzed by $^1\text{H-NMR}$ (Figure 4) was precipitated three times, with loss of the lower molecular weight chains.

Figure 4 shows a typical $^1\text{H-NMR}$ spectrum with peak assignment for the completely methylated macromonomer **4a**, precipitated three times in diethyl ether. The broad signal at 3.6 ppm is characteristic of the methylene protons of the PEO chain. Small peaks in the vicinity of the methylene protons of PEO at 3.45 and 3.8 ppm, are proton-carbon correlation peaks. The ω -methoxy protons are detected at 3.36 ppm (peak y). Six additional peaks are observed at 4.5, 4.05 (a and a') and 2.9 and 2.4 ppm (e, e'), each of them corresponding to one proton, and at 2.0 and 1.8 ppm which contribute altogether to four protons (b and d). These chemical shifts are typical of γ -substituted ϵ -caprolactone as was,

e.g., previously reported in case of a protected γ -hydroxyl- ϵ -caprolactone of a similar structure.^{39,32} The protons vicinal to the ester group (a and a', e and e') are not equivalent because of the asymmetry of the lactone ring after the Baeyer-Villiger reaction. The chemical shift of a, a' and e, e' differs by approximately 0.5 ppm, consistent with lactone-vicinal protons in ϵ -CL derivatives.³⁹

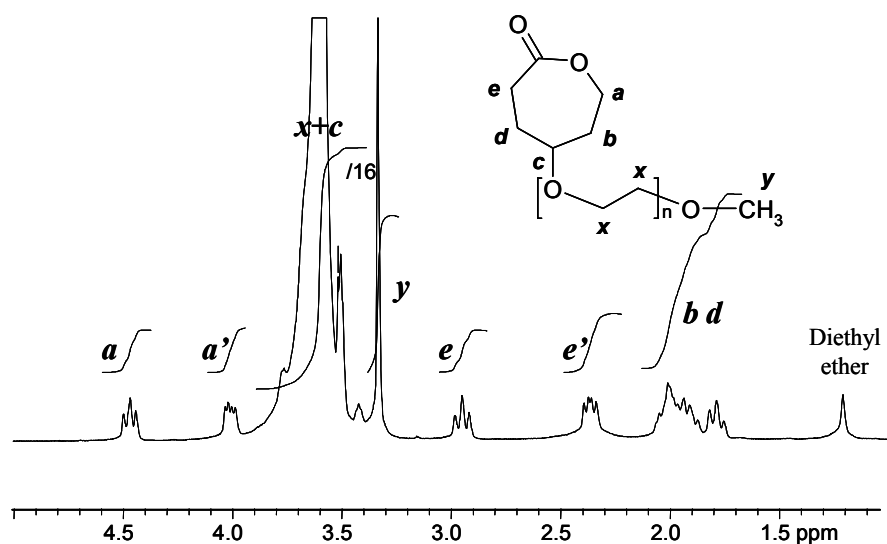


Figure 4. $^1\text{H-NMR}$ spectrum for the macromonomer $\gamma\text{PEO.CL 4a}$ (Table 1) in CDCl_3 , after precipitation in diethyl ether

From the relative intensity of peak a' (4.5 ppm, for the vicinal proton of the lactone) and peak y (3.34 ppm, for the methoxy end-group), the amount of α,ω -dimethoxy-PEO is estimated at approximately 10 %. The number average molecular weight (M_n) agrees well with the MALDI-TOF results (Table 1).

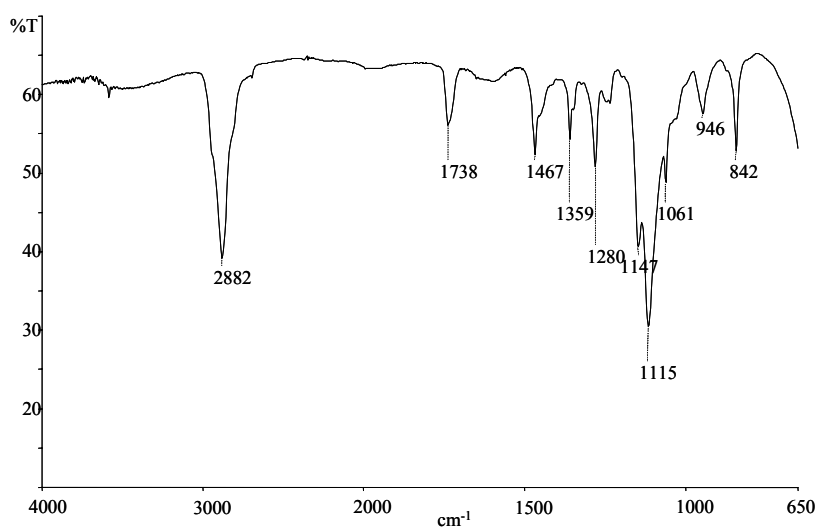
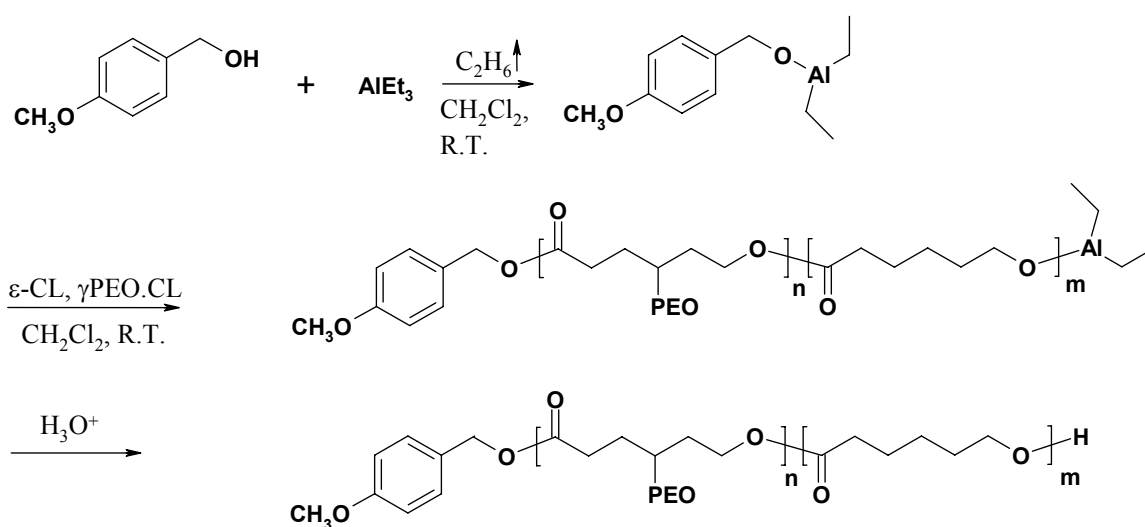


Figure 5. FTIR spectrum for the macromonomer $\gamma\text{PEO.CL 4a}$ (Table 1)

The FTIR spectrum for the new macromonomer is reported in Figure 5 and shows the expected main absorptions of the lactone ring at 1739 cm^{-1} (C=O stretching) and at 1280 cm^{-1} (C-O stretching). The strong absorption at 1115 cm^{-1} is characteristic of the ether bonding (C-O-C stretching) in the EO repeating units.

III.2. Copolymerization of γ PEO.CL and ϵ -caprolactone.

Ring-opening polymerization (ROP) of four, six and seven-membered lactones can be initiated by a variety of protic compounds and metal derivatives.⁴⁰ ROP of ϵ -CL was successfully carried out by coordination-insertion polymerization of the anionic type, for instance by aluminum alkoxide⁴¹ and tin octoate⁴². In the case of aluminum alkoxide, molecular weight is controlled not only by the monomer/ initiator molar ratio (and conversion) but also by hydroxyl containing additives as result of an alkoxide-alcohol exchange.⁴³ Therefore, it was mandatory to convert the ω -hydroxyl end-group of the PEO chains into methyl ether as quantitatively as possible, before copolymerization of the γ PEO.CL macromonomer with ϵ -CL. In order to identify easily the α -end-group of this copolymer (by $^1\text{H-NMR}$), the aluminum alkoxide of p-methoxy benzyl alcohol was used as an initiator in methylene chloride at room temperature (Scheme 2).



Scheme 2. Copolymerization of ϵ -CL and γ PEO.CL 4a into PCL-g-PEO copolymer

As a typical example, the fully ω -methylated γ PEO.CL, **4a**, ($M_{n,NMR} \sim 1000$) was copolymerized with ϵ -CL. The theoretical molar fraction of γ PEO.CL in the comonomer feed was 5 mol%, and the monomer/ initiator ratio was 220. After 3 h, a first sample was picked out and analyzed by $^1\text{H-NMR}$ and SEC. Copolymerization was stopped after 20 h by addition of 0.1 M HCl. Figure 6 compares the normalized SEC traces for the copolymer precipitated in heptane, a non-solvent for both the copolymer and the γ PEO.CL macromonomer, after 4 h (Figure 6, A) and 24 h (Figure 6, B) respectively.

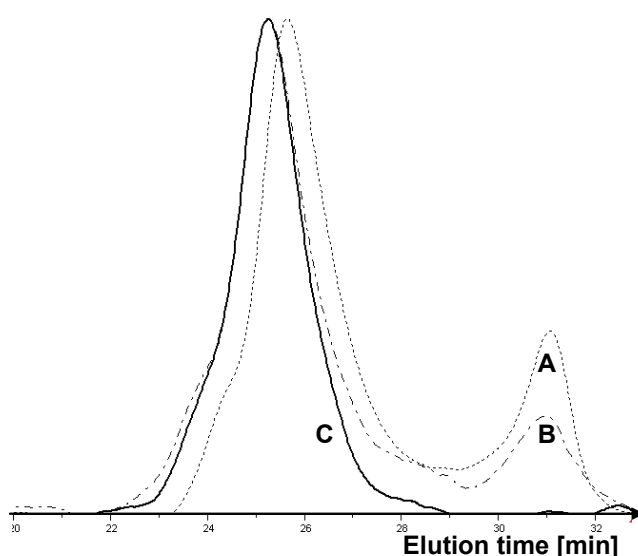


Figure 6. SEC traces of the copolymerization medium: (A) after 4 h (dotted line), (B) after 24 h (dotted broken line _ _ _), (C) after 24 h and purification by sequential precipitation in heptane and methanol (thick full line ___)

A bimodal molecular weight distribution is observed, as result of contamination of the copolymer by unreacted macromonomer. Indeed, the area of the higher elution volume peak decreases when the copolymerization time is increased (Figure 6, trace B), whereas the major peak of higher molecular weight is shifted towards lower elution volumes. The PEO chains, which are not incorporated into the copolymer after 20 h, are mixtures of non-reacted macromonomer and non reactive α,ω -dimethoxy PEO. These PEO chains are easily removed from the copolymer by precipitation in methanol, i.e., a good solvent for PEO and a non-solvent for PCL and the copolymer, as shown by curve C in Figure 6. The origin of the shoulder on the high molecular weight side of the copolymer peak is not clear yet. The molecular weight of the graft copolymer was estimated at $M_{n,SEC} = 35000$ g/mol by SEC with a polystyrene calibration.

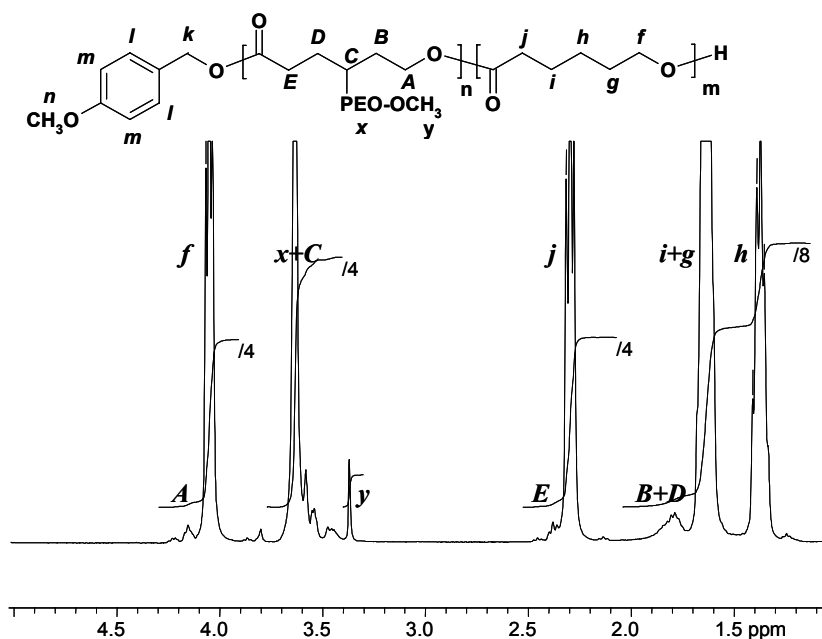


Figure 7. $^1\text{H-NMR}$ spectrum for the PCL-*g*-PEO copolymer in CDCl_3 , after precipitation in methanol

The $^1\text{H-NMR}$ spectrum for the purified copolymer (Figure 7) shows signals typical of PCL and PEO. The methylene protons of PEO are observed at 3.6 ppm, and resonances for the protons of PCL are detected at 4.05 (f) ($\text{C}(\text{O})\text{OC}-\underline{\text{C}}\text{H}_2$), 2.30 (j) ($\text{C}(\text{O})-\underline{\text{C}}\text{H}_2$), 1.63 (i+g) ($\text{C}(\text{O})-\text{C}\text{H}_2-\underline{\text{C}}\text{H}_2$) and 1.37 ppm (h) ($\text{O}-\text{C}\text{H}_2-\underline{\text{C}}\text{H}_2$), respectively. No resonance can be assigned to residual macromonomer. Indeed, the non chemically identical protons- a (4.0 ppm) and a' (4.5 ppm), e (2.4 ppm) and e' (2.95 ppm)- of the lactone group completely disappeared, whereas new peaks are observed as result of the lactone opening polymerization. Resonance of proton a is shifted from 4.0 to 4.15 ppm (Figure 7, proton A), and that one of b is also shifted to lower chemical shift, from 2.0 ppm (proton b) to 1.8 ppm (proton B).

The number average molecular weight (M_n) of the polyester backbone was determined by $^1\text{H-NMR}$ from the relative intensity of the signals at 4.05 ppm for PCL and at 6.9 ppm for the benzyl end-group (not shown). M_n of the PCL backbone ($M_{n,\text{NMR}}=30000$) is consistent with the theoretical value ($M_{n,\text{th}}=25000$), and the molecular weight distribution (M_w/M_n) is 1.21.

The experimental composition of the copolymer was calculated from the integration of the $^1\text{H-NMR}$ peaks at 4.05 ppm for PCL and at 3.65 ppm for PEO. Conversion of ϵ -caprolactone after 20 h is complete, whereas that one of $\gamma\text{PEO.CL}$ is approximately 66%. Conversion of $\gamma\text{PEO.CL}$ (at 100 % ϵ -CL conversion) was calculated by comparison of the

PEO/ PCL ratios (calculated by $^1\text{H-NMR}$) for the copolymer recovered by precipitation in heptane (removal of $\epsilon\text{-CL}$) and in methanol (removal of PEO), respectively. It appears that approximately 34% of the original PEO has not been copolymerized, which means a conversion of approximately 76% taking into account contamination of the macromonomer by approximately 10 % dimethoxy-PEO. From the $^1\text{H-NMR}$ spectrum recorded after precipitation in methanol, composition of the copolymer was estimated at PEO/PCL = 0.75. The molar fraction of $\gamma\text{PEO.CL}$ in the copolymer is therefore 3.5 mol% compared to 5 mol% in the comonomer feed. The total molecular weight of the copolymer can also be estimated from NMR ($M_{n,\text{NMR}}$ is about 39000 g/mol). Optimization of the copolymerization conditions, such as polymerization time, addition of pyridine³², and comonomer feed composition, is under current investigation.

IV. Conclusions

A well-defined PEO macromonomer ($\gamma\text{PEO.CL}$) was synthesized by polymerization of ethylene oxide (EO) initiated by a potassium alkoxide of 4-monoethylene acetal cyclohexanol with high control of the macromolecular parameters. After deprotection of the ketone and oxidation by the Baeyer-Villiger reaction (100% conversion), $\epsilon\text{-caprolactone}$ terminated PEO ($\gamma\text{PEO.CL}$) of controlled molecular weight was produced. This macromonomer was copolymerized with $\epsilon\text{-CL}$ with formation of amphiphilic graft copolymers. This copolymerization was initiated by Et_2Al alkoxide and found to be controlled. It could be carried out from hydroxylated surfaces of biomaterials in order to make them more hydrophilic and impart them a stealth behavior. This will be the topic of a forthcoming paper. Another prospect would be the quantitative hydrolysis of the $\alpha\text{-end-group}$ ($\epsilon\text{-caprolactone}$) of $\gamma\text{PEO.CL}$ in order to make a pair of hydroxyl and carboxylic acid groups available at one chain-end. Supramolecular assemblies might be built up by chelating ability of the dual end-groups. They could also be used to initiate the selective polymerization of two different monomers, with formation of mikto-arm ABC star copolymers. Finally, $\alpha\text{-caprolactone}$, $\omega\text{-hydroxy-PEO}$, could also be made available by the synthetic route reported in this work. Polymerization of this inimer could lead to amphiphilic hyperbranched macromolecules.

The ϵ -CL terminated PEO is thus an original elementary building block for the synthesis of novel amphiphilic biocompatible and biodegradable macromolecular architectures.

References.

- ¹ Lee, J.H.; Lee, H.B.; Andrade, J.D.; *Prog. Polym. Sci.*, **1995**, *20*, 1043-1079
- ² Vermette, P.; Meagher, L.; *Colloids Surf., B* **2003**, *28*, 153-198
- ³ Gref, R.; Lück, M.; Quellec, P.; Marchand, M.; Dellacherie, E.; Harnisch, S.; Blunck, T.; Müller, R.H.; *Colloids Surf. B* **2000**, *18*, 301-313
- ⁴ Peracchia, M.T.; Vauthier, C.; Passirani, C.; Couvreur, P.; Labarre, D.; *Life Sciences*, **1997**, *61*, 749-761
- ⁵ Lee, J. H.; Kopeckova, P.; Kopecek, J.; Andrade, J. D.; *Biomaterials* **1990**, *11*, 455-464
- ⁶ Walton, D. G.; Soo, P. P.; Mayes, A. M.; Sofia-Allgor, S. J.; Fujii, J. T.; Griffith, L. G.; Ankner, J. F.; Kaiser, H.; Johansson, J.; Smith, G. D.; Barker, J. G.; Satija, S. K. *Macromolecules* **1997**, *30*, 6947-6956
- ⁷ Gref, R.; Minamitake, Y.; Peracchia, M. T.; Trubetskoy, V.; Torchilin, V.; Langer, R. *Science* **1994**, *263*, 1600-1603
- ⁸ Nucci, M. L.; Shorr, R.; Abuchowski, A.; *Adv. Drug Deliv. Rev.* **1991**, *6*, 133-151
- ⁹ Delgado, C.; Francis, G. E.; Fisher, D.; *Crit. Rev. Ther. Drug Carrier Syst.* **1992**, *9*, 249-304
- ¹⁰ Ould-Ouali, L., Arien, A., Rosenblatt, J., Nathan, A., Twaddle, P., Matalenas, T., Borgia, M., Arnold, S., Leroy, D., Dinguizli, M., Rouxhet, L., Brewster, M. Pr at, V.; *Pharm. Res.*, **2004**, *21*, 1581-1590
- ¹¹ Harris, J. M. (ed.) in "Poly(ethylene glycol) Chemistry: Biotechnical and Biomedical Applications", Plenum Press, New York, **1992**
- ¹² Irvine, D. J.; Mayes, A. M.; Griffith, L. G.; *Biomacromolecules* **2001**, *2*, 85-94
- ¹³ Irvine, D. J.; Ruzette, A.-V. G., Mayes, A. M.; Griffith, L. G.; *Biomacromolecules* **2001**, *2*, 545-556
- ¹⁴ Toncheva, V.; Wolfert, M. A; Dash, P. R.; Oupicky, D.; Ulbrich, K.; Seymour, L. W., Schacht, E. H.; *Biochim. Biophys. Acta* **1998**, *1380*, 354-368
- ¹⁵ Vandorpe, J.; Schacht, E.; Stolnik, S.; Garnett, M. C.; Davies, M. C.; Illum, L.; Davis, S. S.; *Biotechnol. Bioeng.* **1996**, *52*, 89-95

-
- ¹⁶ Kwon, G.; Suwa, S.; Yokoyama, M.; Okano, T.; Sakurai, Y.; Kataoka, K.; *J. Controlled Release* **1994**, *29*, 17-23
- ¹⁷ Twaik, M. A.; Tahan, M.; Zilkha, A.; *J. Polym. Sci., Part A: Polym. Chem.* **1969**, *7*, 2469-2480
- ¹⁸ Thierry, A.; Skoulios, A.; *Makromol. Chem.* **1976**, *177*, 319-335
- ¹⁹ Wesslen, B.; Wesslen, K. B.; *J. Polym. Sci., Part A: Polym. Chem.* **1989**, *27*, 3915-3926
- ²⁰ Jannasch, P.; Wesslen, B.; *J. Polym. Sci., Part A: Polym. Chem.* **1993**, *31*, 1519-1529
- ²¹ Jannasch, P.; Wesslen, B.; *J. Polym. Sci., Part A: Polym. Chem.* **1995**, *33*, 1465-1474
- ²² Bo, G.; Wesslen, B.; Wesslen, K. B.; *J. Polym. Sci., Part A: Polym. Chem.* **1992**, *30*, 1799-1808
- ²³ Lee, J.H.; Kopeckova, P.; Zhang, J.; Kopecek, J.; Andrade, J. D.; *Polym. Mater. Sci. Eng.* **1988**, *59*, 234-238
- ²⁴ Neugebauer, D.; Zhang, Y.; Pakula, T.; Matyjaszewski, K.; *Polymer* **2003**, *44*, 6863-6871
- ²⁵ Neugebauer, D.; Zhang, Y.; Pakula, T.; Sheiko, S.; Matyjaszewski, K.; *Macromolecules* **2003**, *36*, 6746-6755
- ²⁶ Shen, R.; Akiyama, C.; Senyo, T.; Ito, K.; *C. R. Chimie* **2003**, *6*, 1329-1335
- ²⁷ Liu, X.-Y.; Ding, X.-B.; Zheng, Z.-H.; Peng, Y.-X.; Long, X.-P.; Wang, X.-C.; Chan, A. S. C.; Yip, C. W.; *J. Appl. Polym. Sci.* **2003**, *90*, 1879-1884
- ²⁸ Breitenkamp, K.; Simeone, J.; Jin, E.; Emrick, T.; *Macromolecules* **2002**, *35*, 9249-9252
- ²⁹ Chemtob, A.; Heroguez, V.; Gnanou, Y.; *Macromolecules*, **2002**, *35*, 9262-9269
- ³⁰ Tian, D.; Dubois, P.; Jérôme, R.; *Macromolecules* **1997**, *30*, 2575-2581
- ³¹ Tian, D.; Dubois, P.; Jérôme, R.; *Macromol. Symp.* **1998**, *130*, 217-227
- ³² Stassin, F.; Halleux, O.; Dubois, P.; Detrembleur, C.; Lecomte, P.; Jérôme, R.; *Macromol. Symp.* **2000**, *153*, 27-39
- ³³ Detrembleur, C.; Mazza, M.; Halleux, O.; Lecomte, P.; Mecerreyes, D.; Hedrick, J. L.; Jérôme, R.; *Macromolecules* **2000**, *33*, 14-18
- ³⁴ Detrembleur, C.; Mazza, M.; Lou, X.; Halleux, O.; Lecomte, P.; Mecerreyes, D.; Hedrick, J. L.; Jérôme, R.; *Macromolecules* **2000**, *33*, 7751-7760
- ³⁵ Gautier, S.; D'Aloia, V.; Halleux, O.; Mazza, M.; Lecomte, P.; Jérôme, R.; *J. Biomater. Sci., Polym. Ed.* **2003**, *14*, 63-85
- ³⁶ Majewski, M.; MacKinnon, J.; *Can. J. Chem.* **1994**, *72*, 1699-1704
- ³⁷ Vangeyte, P.; Jérôme, R.; *J. Polym. Sci., Part A: Polym. Chem.* **2004**, *42*, 1132-1142
- ³⁸ Latere J.-P.; Lecomte P., Dubois P., Jérôme R.; *Macromolecules* **2002**, *35*, 7857-7859

- ³⁹ Pitt, C. G.; Gu, Z. W., Ingram, P.; Hendren, R. W.; *J. Polym. Sci., Part A: Polym. Chem.* **1987**, *25*, 955-966
- ⁴⁰ Loefgren, A.; Albertsson, A.C.; Dubois, P.; Jérôme, R.; *J. Macromol. Sci., Rev. Macromol. Chem. Phys.* **1995**, *C35*, 379-418
- ⁴¹ Duda, A.; Penczek, S.; *Makromol. Chem., Macromol. Symp.* **1991**, *47*, 127-140
- ⁴² Duda, A.; Penczek, S.; *Macromol. Rapid Commun.* **1994**, *15*, 559-566
- ⁴³ Penczek, S.; Duda, A.; *Macromol. Symp.* **1996**, *107*, 1-15

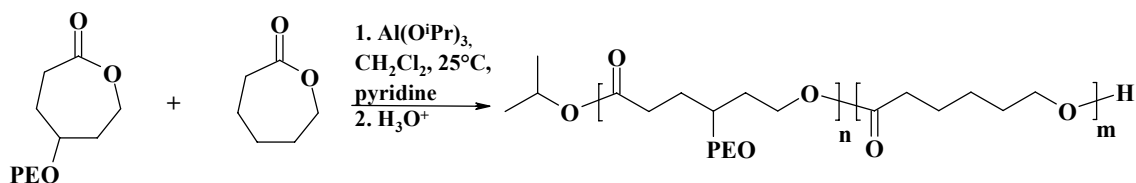
Chapter 2

**Controlled synthesis and interface properties
of new amphiphilic poly(ϵ -caprolactone)-*graft*-poly(ethylene oxide)
copolymers**

Abstract

Novel biodegradable and biocompatible poly(ϵ -caprolactone)-graft-poly(ethylene oxide), PCL-g-PEO, copolymers consisting of biocompatible blocks have been synthesized by ring-opening copolymerization of ϵ -caprolactone (ϵ CL) and a poly(ethylene oxide) (PEO) macromonomer, i.e., PEO end-capped by an ϵ -caprolactone unit (γ PEO.CL), with efficient control over the composition and length of both the hydrophobic polyester backbone and the hydrophilic PEO grafts. The reactivity ratios have been determined by monitoring the copolymer composition in relation to the comonomer conversion. The PCL-g-PEO copolymers have a tapered (gradient) rather than a random structure consistent with $r_{\epsilon\text{CL}} = 3.95$ and $r_{\gamma\text{PEO.CL}} = 0.05$.

The amphiphilic graft copolymers, which are soluble in organic solvents but not in water, display surfactant properties similar to PEO-b-PCL diblock copolymers of similar composition and solubility, as shown by measurements of the CHCl_3 /water interfacial tension by the pendant drop method.



Contents

I. INTRODUCTION.....	79
II. EXPERIMENTAL PART.....	81
<i>Materials.....</i>	<i>81</i>
<i>Synthesis of the PEO macromonomer (γPEO.CL).....</i>	<i>82</i>
<i>Polymerization of γPEO.CL.....</i>	<i>82</i>
<i>Copolymerization of γPEO.CL and ϵ-caprolactone (ϵCL).....</i>	<i>82</i>
<i>Determination of reactivity ratios of γPEO.CL and ϵCL.....</i>	<i>83</i>
<i>Synthesis of PEO-b-PCL diblock copolymers.....</i>	<i>84</i>
<i>Characterization techniques.....</i>	<i>84</i>
<i>Interfacial tension measurements.....</i>	<i>85</i>
III. RESULTS AND DISCUSSION	85
<i>III.1. Homopolymerization of γPEO.CL.....</i>	<i>85</i>
<i>III.2. Copolymerization of γPEO.CL and ϵCL.....</i>	<i>87</i>
<i>III.3. Determination of the reactivity ratios of ϵCL and γPEO.CL.....</i>	<i>89</i>
<i>III.4. Synthesis of PEO-b-PCL diblock copolymers</i>	<i>93</i>
<i>III.5. Interfacial activity and amphiphilic properties of the copolymers.....</i>	<i>94</i>
IV. CONCLUSION	100

I. Introduction

Aliphatic polyesters, such as poly(ϵ -caprolactone) (PCL), have great potential as biomaterials due to a unique combination of biodegradability and biocompatibility. However, these polymers do not exhibit any amphiphilic/surfactant properties. Therefore, the introduction of hydrophilic groups or grafts along these hydrophobic backbones is of great interest. Hydrophilic poly(ethylene oxide) (PEO) units are of special interest for the synthesis of copolymers with particular interest for biomedical application. In fact, PEO is a biocompatible and bioeliminable hydrophilic polymer. It is well-known for preventing very efficiently protein adsorption at surfaces.

Amphiphilic block and graft copolymers are commonly used as stabilizers of liquid/liquid dispersions and immiscible polymer blends. For instance, amphiphilic diblock copolymers composed of poly(ethylene oxide) (PEO) and polyesters, such as poly(ϵ -caprolactone) (PCL) or polylactides (PLA), have found extensive utilization due to their biocompatibility and surface / interfacial activity.^{1,2} They have already found biomedical applications, e.g. for the surface modification of polymeric scaffolds for tissue engineering³ and as new stabilizers for drug delivery systems.⁴ As an example, amphiphilic water-soluble poly(ethylene glycol)-poly(lactide) diblock copolymers (PEO-*b*-PLA) have been used to stabilize nanoemulsions. It was reported that the emulsifying ability of such copolymers mainly depended on the length of the PLA block.²

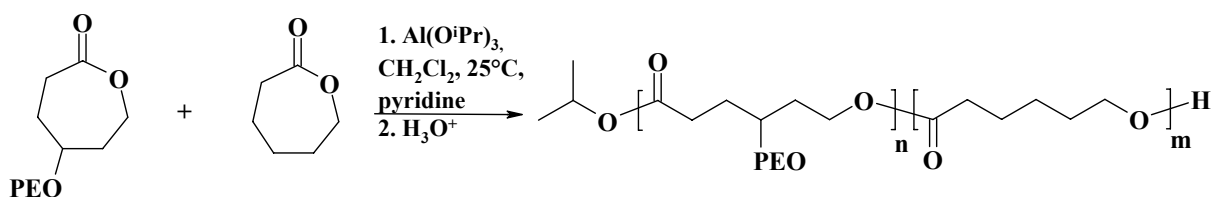
There are only few examples in the literature that discuss the influence of the polymer architecture on the amphiphilic properties, e.g. measured by their ability in stabilizing emulsions. However, recent developments in polymer chemistry allow the controlled synthesis of copolymers of various architecture, e.g. comb or star-shape copolymers, dendrimers, architecture employing controlled/living polymerizations.^{5,6}

Several works investigated PEO-containing copolymers as emulsion stabilizers. March and Napper⁷ reported that the hydrophobic segment of the graft or block amphiphile should surpass a critical length, because it seems responsible for the efficient anchoring in the dispersed phase. Furthermore, the weight ratio of the hydrophobic segment to hydrophilic segment should exceed a critical value, e.g., 0.4 in the case of the poly(styrene) / PEO pair. Similarly, Piirma and Lenzotti⁶ investigated the emulsifying properties of poly(*p*-methylstyrene)-*graft*-poly(ethylene oxide) copolymers. For the investigated system (styrene in water), the emulsion stability was mostly determined by the average distance between the PEO grafts. In fact, long hydrophobic loops were required for the effective

anchoring in the dispersed phase. Furthermore, Sela et al. compared the surface and interfacial activity of water-soluble poly(hydrogenmethyl siloxane)-*graft*-poly(ethylene oxide) copolymers (PHMS-*g*-PEO) with the corresponding copolymers of a mixed block/*graft* structure: poly(dimethylsiloxane) (PDMS)-*b*-[PHMS-*g*-PEO].⁸ The interfacial activity of the PHMS-*g*-PEO copolymers at air/water and dodecane/water interfaces diminished with increasing water-solubility of the copolymer. The latter was determined by the EO content, thus the grafting density and length of PEO grafts. In contrast, the performance of the PDMS-*b*-[PHMS-*g*-PEO] copolymers was improved with increasing graft density of PEO. Generally, the interfacial activity of these copolymers in O/W emulsions was better than that of the corresponding PHMS-*g*-PEO *graft* copolymers. It seems probable that a dangling PDMS block has got a higher anchoring capacity than PHMS loops. These experimental observations illustrate the strong dependence of the surfactant properties of copolymers on their macromolecular architecture.

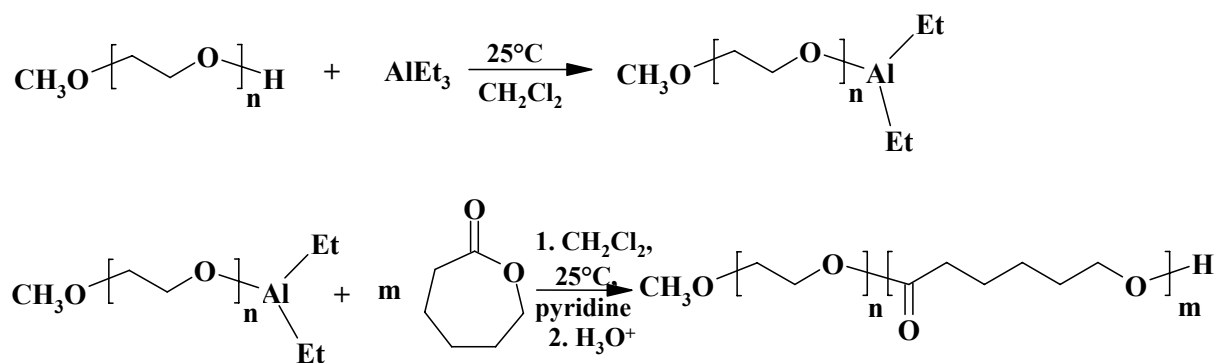
To our best knowledge, the interfacial activity of non-water soluble PCL-*graft*-PEO *graft* copolymers has not been investigated yet. However, the demand for such biocompatible and eliminable copolymers increases steadily, especially for the surface modification of biodegradable scaffolds/ implants^{3,9} or for new drug delivery systems for intravenous injection.¹⁰ Indeed, several recent papers have reported on the particularly high efficiency of branched PEO structures, as compared to linear ones, in protein repellency by increasing the packing density of the PEO chains at the surface.^{3,11}

This paper aims at reporting on the controlled synthesis, characterization and interfacial properties of novel “branched” amphiphilic poly(ϵ -caprolactone)-*graft*-poly(ethylene oxide) (PCL-*g*-PEO) copolymers and their comparison to diblock copolymers of similar composition. The original synthesis of the *graft* copolymers relies on the ring-opening copolymerization of ϵ -caprolactone (ϵ CL) with a PEO macromonomer, i.e., ϵ CL substituted by a PEO chain in γ -position (γ PEO.CL macromonomer¹²) (Scheme 1). The copolymer structure obtained by this synthesis pathway was determined by calculation of the comonomer reactivity ratios.



Scheme 1. Copolymerization of ϵ CL and γ PEO.CL (poly(ϵ CL-*co*- γ PEO.CL))

In addition, PEO-*b*-PCL diblock copolymers of similar PEO/PCL composition have been synthesized, according to Scheme 2, in order to determine the influence of the copolymers' macromolecular architecture on the interfacial activity.



Scheme 2. Synthesis of PEO-*b*-PCL diblock copolymer

II. Experimental Part

Materials.

ϵ -caprolactone (ϵ CL) (Aldrich, 99%) was dried over calcium hydride for 48 h and distilled under reduced pressure before use. Methylene chloride (CH_2Cl_2) and pyridine were dried by refluxing over calcium hydride for at least 48 h before distillation. Aluminum triisopropoxide ($\text{Al}(\text{O}^i\text{Pr})_3$, Aldrich) was purified by distillation under reduced pressure, dissolved in dry toluene, and the solution was titrated by complexometry of Al with ethylenediaminetetraacetic acid (EDTA), as reported elsewhere.¹³

Synthesis of the PEO macromonomer (γ PEO.CL).

The synthesis of the macromonomer (γ PEO.CL) was reported elsewhere.¹² Briefly, ethylene oxide was polymerized by living anionic ring-opening polymerization, initiated by the potassium alkoxide of 1,4-dioxaspiro[4.5]decan-8-ol, followed by derivatization of the α -acetal end-group into a ketone and the Baeyer-Villiger oxidation of the ketone into lactone. The ω -hydroxyl end-group of PEO was methylated by reaction with CH₃I in order to prevent it from interfering with the copolymerization reaction. The macromonomer (γ PEO.CL) was purified by repeated precipitations (4 times) from CH₂Cl₂ into diethyl ether. Purity and chain-end functionalization were assessed by MALDI-Tof and ¹H-NMR. MALDI-Tof analysis proved that methylation of the hydroxyl end-groups was quantitative. ¹H-NMR (CDCl₃, 400 MHz, δ (ppm): 1.8-2.1 (m, 4H, CH-CH₂-CH₂), 2.40 (m, 1H, C(O)-CH₂-), 2.98 (m, 1H, C(O)-CH₂-), 3.36 (s, 3H, OCH₃), 3.6 (M, 4nH, -O-[CH₂-CH₂-O]_n), 4.05 (m, 1H, C(O)-O-CH₂-), 4.5 (t, 1H, C(O)-O-CH₂-).

The same γ PEO.CL macromonomer was used in all the experiments with a molecular weight of 1000 g/mol (determined by ¹H-NMR) and low polydispersity (Mw/Mn = 1.09, as determined by SEC). It was dried by three azeotropic distillations of toluene and heated at 45°C *in vacuo* overnight, just prior to use.

Polymerization of γ PEO.CL.

Polymerization of γ PEO.CL was initiated by aluminum triisopropoxide, Al(OⁱPr)₃, in CH₂Cl₂ in the presence of 1 equivalent of pyridine with respect to Al, under nitrogen at room temperature. In a typical polymerization experiment, 0.2 ml of a 0.247 M solution of pyridine (0.05 mmol) and a 0.33 M solution of Al(OⁱPr)₃ (0.05 mmol) were added to 20 ml of a CH₂Cl₂ solution of 1 g (1 mmol) dried γ PEO.CL. Polymerization was stopped after 4 h, by addition of an excess of 0.1 M HCl solution. The polymer was analyzed by SEC and ¹H-NMR analysis.

Copolymerization of γ PEO.CL and ϵ -caprolactone (Scheme 1).

Copolymerization of the PEO macromonomer (γ PEO.CL) and ϵ -caprolactone (ϵ CL) was initiated by aluminum triisopropoxide (Al(OⁱPr)₃), in the presence of 1 equivalent of pyridine with respect to aluminum (Al). Copolymerization was conducted in a previously flamed glass reactor under nitrogen at room temperature. Copolymers of various compositions were synthesized by changing the monomer to initiator molar ratio as well as the composition of the comonomer feed. These conditions are summarized in Table 1.

In a typical copolymerization experiment (copolymer 3, Table 1), 0.54 ml of a 0.247M solution of pyridine (0.133 mmol) and 0.4 ml of 0.33 M $\text{Al}(\text{O}^i\text{Pr})_3$ (0.133 mmol) were added to 50 ml of CH_2Cl_2 containing 9 mmol of dried ϵCL (1.0 ml) and 0.9 mmol of dried $\gamma\text{PEO.CL}$ (0.9 g). Copolymerization was stopped after 4 h 30 by addition of a slight excess of HCl (0.1 M solution).

The copolymers were precipitated in heptane, filtered off and precipitated again in methanol, in order to eliminate the unreacted $\gamma\text{PEO.CL}$ as assessed by SEC. They were recovered by centrifugation, dried *in vacuo* and stored *in vacuo* at -20°C .

$^1\text{H-NMR}$ (CDCl_3 , 400 MHz, δ (ppm)): 1.2 (m, 6H, $(\text{CH}_3)_2\text{-CH-}$), 1.35 (m, 2H, $\text{CH-CH}_2\text{-CH}_2$), 1.65 (m, 4H, $-\text{CH}_2\text{-CH}_2\text{-CH}_2\text{-CH}_2\text{-O}$), 2.3 (m, 2H, $\text{OC(O)-CH}_2\text{-}$), 3.35 (s, 3H, OCH_3), 3.6 (M, 4H, $-\text{O-}[\text{CH}_2\text{-CH}_2\text{-O}]_n$), 4.05 (m, 2H, $-\text{CH}_2\text{-O-CO-}$), 5.0 (m, 1H, $(\text{CH}_3)_2\text{-CH-}$) (Figure 1).

Determination of reactivity ratios of the PEO macromonomer and ϵ -caprolactone / $^1\text{H-NMR}$ monitoring of the copolymerization.

The progress of the conversion of the PEO macromonomer and ϵ -caprolactone has been monitored by $^1\text{H-NMR}$ (400 MHz) analysis of samples picked out regularly during 4h30 from the reaction medium, at time t (and before addition of $\text{Al}(\text{O}^i\text{Pr})_3$ ($t = 0$)). After sampling, the copolymerization was stopped by addition of a slight excess of 0.1M HCl. The solvent (CH_2Cl_2) was easily removed under reduced pressure at room temperature, before analysis. It was ascertained that the $[\text{n}(\epsilon\text{CL}) + \text{n}(\text{PCL})] / [\text{n}(\text{EO}) + \text{n}(\text{PEO})]$ ratio did not change for the different samples as a result of this treatment, i.e. that no unreacted ϵCL monomer was lost. Conversion of the $\gamma\text{PEO.CL}$ was determined on the basis of the methylene protons in α and ϵ positions of the carbonyl ester of the lactone ring (4.50(1H) and 2.98 ppm (1H)) and the methylene protons of PEO at 3.6 ppm which remain constant during polymerization and can thus be used as an internal standard. Indeed, upon ring-opening the intensity of the four signals of the chemically-distinct methylene protons at 4.5 (1H) & 4.0 ppm (1H) and 3.0 (1H) & 2.35 ppm (1H), respectively, decreases and two new signals appear at 4.15(2H) and 1.75ppm (2H), which overlap at least partially with the PCL protons. Conversion of ϵ -caprolactone was monitored by integration of the methylene protons adjacent to the carbonyl ester of the lactone ring at 4.20 and 2.63 ppm (before polymerization), and at 4.05 and 2.29 ppm after polymerization.

Synthesis of PEO-*b*-PCL diblock copolymers (Scheme 2).

Diblock copolymers were synthesized by ring-opening polymerization of ϵ -caprolactone (ϵ CL) initiated by α -methoxy- ω -hydroxy poly(ethylene oxide) (MPEO) as reported elsewhere.¹⁴

Briefly, MPEO of different molecular weights were prepared by anionic polymerization of ethylene oxide (EO) initiated from the potassium alkoxide of triethylene glycol monomethyl ether. They were purified by dialysis against water and dried first by three azeotropic distillations of toluene, and then *in vacuo* at 45°C overnight. The macromolecular characteristics (M_n and M_w/M_n) of the α -methoxy- ω -hydroxy poly(ethylene oxide) are summarized in Table 2.

The diethyl aluminum alkoxide macroinitiator of the ring-opening polymerization of ϵ -caprolactone was prepared by reaction of dried α -methoxy- ω -hydroxy poly(ethylene oxide) with 1.1 equivalent of triethylaluminum ($AlEt_3$) in CH_2Cl_2 , in a flamed glass reactor under nitrogen. The reaction was complete within 2 or 3 h, under vigorous stirring, at room temperature.

The ϵ CL polymerization was carried out under nitrogen atmosphere in CH_2Cl_2 in the presence of 1 equivalent of pyridine with respect to Al, at room temperature. Monomer conversion was monitored by 1H -NMR analysis based on the resonance peaks at 4.06 ppm for PCL and at 3.65 ppm for PEO. Copolymerization was stopped by addition of HCl excess (0.1 M solution). The copolymers were purified by precipitation in heptane, filtered off and dried *in vacuo*. They were dissolved in a water/THF mixture (80/20), and the solution was dialyzed against water using spectra-por (Spectra Por, Cut-off 3500 and 6000-8000, Polylab) membranes. The purified copolymers were recovered by lyophilization for 24 h and stored *in vacuo*.

1H -NMR ($CDCl_3$, 400 MHz, δ (ppm)): 1.35 (m, 2H, $CH-CH_2-CH_2$), 1.65 (m, 4H, $-CH_2-CH_2-CH_2-O$), 2.3 (m, 2H, $OC(O)-CH_2-$), 3.35 (s, 3H, OCH_3), 3.6 (M, 4H, $-O-[CH_2-CH_2-O]_n$), 4.05 (m, 2H, $-CH_2-O-CO-$) (Figure 5).

Characterization techniques.

1H NMR spectra were recorded with a Bruker AM 400 apparatus in $CDCl_3$ at 400 MHz and 25°C. Size-exclusion chromatography (SEC) was carried out in THF at a flow rate 1ml/ min at 45°C, with a SFD S5200 Autosampler liquid chromatograph equipped with a SFD refractometer index detector 2000 and 5 μ m PL gel columns (columns porosity: 10², 10³, 10⁴, 10⁵Å). Polystyrene and PEO standards were used for calibration.

Interfacial tension measurements.

The interfacial (chloroform/water) tension was measured at 20°C (293K) with a pendant drop tensiometer (drop shape analysis system DSA 10 Mk2 (Krüss)) equipped with a thermostated chamber and a Circulator Thermo HAAKE DC 10. Chloroform solutions of different copolymer concentrations were prepared with chloroform previously saturated with doubly distilled water (mixing for 24h). A drop of constant volume (10 μ l) of each solution has been formed in water (8 ml) and the dynamic interfacial tension $\gamma(t)$ has been determined from the shape of the organic drop in doubly distilled water previously saturated with chloroform. All the samples were let to equilibrate for a sufficiently long time (minutes to hours) in order to reach constant readings, i.e. the equilibrium interfacial tension γ_{eq} . Data from at least three measurements were averaged for each concentration and displayed a maximum variation lower than 2 %.

III. Results and Discussion

The end-capping of PEO chains by a cyclic ϵ -caprolactone (ϵ CL) unit (via the γ -position of the ring with respect to the carbonyl) has been reported elsewhere¹², so making a new type of macromonomer available (γ PEO.CL) for polymerization by a ring-opening mechanism with formation of comb-shaped macromolecules. In this work, a macromonomer of M_n 1000 g/mol has been synthesized in order to investigate its homopolymerization initiated by Al isopropoxide in the presence of pyridine, and its random copolymerization with ϵ CL (including determination of the reactivity ratios).

III.1. Homopolymerization of γ PEO.CL.

Previous studies reported on the successful homopolymerization of PEO macromonomers of the (meth)acrylic and the vinylbenzylic types with molecular weights higher than 1000 g/mol, by free-radical polymerization initiated by AIBN and potassium peroxodisulfate^{15,16} and by controlled radical polymerization (RAFT).¹⁷ High molecular weight (up to 5000 g/mol) ω -methacryloyloxy PEO macromonomers have also been polymerized by an anionic route¹⁸, although with poor control. On the other hand, no mention of the coordinative ring-opening polymerization of PEO macromonomers could

be found in the scientific literature, which prompted us to test their polymerizability in the presence of Al triisopropoxide ($\text{Al}(\text{O}^i\text{Pr})_3$) which is known to be an effective initiator for the highly controlled ring-opening polymerization of ϵ -caprolactone (ϵCL).¹⁹ Indeed, it has been reported that the coordinative ring-opening polymerization of ϵ -caprolactone (ϵCL) can be successfully initiated with (mono)hydroxyl-end-capped PEO in the presence of aluminum alkoxide such as diethylaluminum alkoxide^{20,21}, but bimodal molecular weight distributions have been observed.²⁰ Further work was done in order to optimize the conditions of this ring-opening polymerization of ϵCL in the presence of PEO chains, which proceeds via a coordination-insertion mechanism requiring the coordination of the Al to the ester carbonyl.¹⁴ This work pointed out that the oxygen of the EO units is an electron-donating ligand, which is able to compete with the monomer for the coordination to aluminum. That is the reason why aluminum alkoxides are at least partially hindered from being active in the coordinative polymerization. The addition of a Lewis base, such as pyridine, which is a better ligand for the Al atom than the ether function and known to increase the polarity and reactivity of the bonding,^{22,23,24} was found to prevent the formation of bimodal weight distributions. In addition, aggregates of PEO chains were observed in most of the common solvents, except in CH_2Cl_2 .¹⁴

In the present study, the polymerization of $\gamma\text{PEO.CL}$ macromonomers was conducted in the presence of pyridine (1eq with respect to aluminum), and CH_2Cl_2 was chosen as solvent, in order to prevent aggregation of the macromonomer. Firstly, the homopolymerization of this functional PEO macromonomer ($\gamma\text{PEO.CL}$) has been tested in the presence of Al triisopropoxide in CH_2Cl_2 at room temperature (and in the presence of 1 equivalent of pyridine with respect to Al). $^1\text{H-NMR}$ analysis of the polymerization medium after 4h showed only the resonance signals typical of the original macromonomer (data not shown), i.e., signals of the methylene protons adjacent to the carbonyl ester of the lactone α -end group (at 4.5 (1H), 4.05 (1H) and at 2.9 (1H) and 2.4 ppm (1H)). Moreover, the intensity of these signals compared to those of the PEO chain was unaltered, indicating that no polymerization occurred, as confirmed by SEC analysis (only the elution peak of the macromonomer was observed). This failure of polymerization has been repeatedly observed.

Whenever the ring-opened macromonomer $\gamma\text{PEO.CL}$, i.e. $\gamma\text{PEO.CL}$ where the lactone end-group had been previously hydrolyzed to the ring-opened compound, was subject to azeotropic distillation with toluene followed by heating at 50°C under reduced pressure, the condensation of two or three monomer units was observed by SEC in THF.

Therefore, steric effects are not the major limitation for homopolymerization of this macromonomer. The strong competition between ϵ CL and the EO units for the coordination to Al, despite the addition of pyridine, has rather to be considered. To clarify this point, the copolymerization of γ PEO.CL with ϵ CL, i.e., in conditions where the amount of ϵ CL units becomes similar to the EO units, has then been investigated under the same conditions.

III.2. Copolymerization of γ PEO.CL and ϵ -caprolactone.

The ring-opening copolymerization of γ PEO.CL with ϵ -caprolactone (ϵ CL) has been tested under the same conditions as for the homopolymerization of the macromonomer. In sharp contrast to the homopolymerization that systematically failed, copolymerization of the γ PEO.CL mixtures of various compositions (Table 1) was effective, as assessed by $^1\text{H-NMR}$ (Figure 1) and SEC analyses.

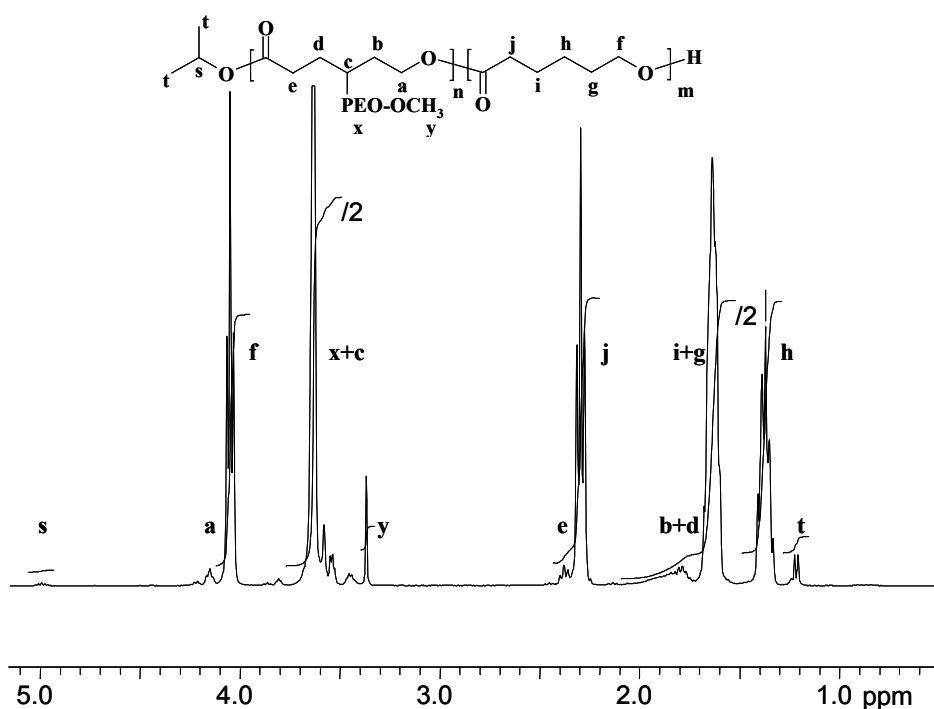


Figure 1. 400 MHz $^1\text{H-NMR}$ spectrum of poly(ϵ CL-*co*- γ PEO.CL) copolymer 3 (Table 1, sample 3)

Table 1. Molecular characteristics of PEO macromonomer “ γ PEO.CL” and poly(ϵ CL-*co*- γ PEO.CL)

#	PEO ^a		copolymer									
	Mn ^b	Mw/	DP ^{th,c}	DP ^{exp,d}	M _{n,NMR}	M _{n,SEC} ^f	M _w /	f ^g	F ^h	n(EO)/	N ⁱ	
		Mn ^b		PCL	PCL	tot ^e		M _n ^f	[mol%]	[mol%]	n(ϵ CL)	
1	1000	1.09	90	70	10000	18000	1.30	5	3	0.65	2.3	
2	1000	1.09	220	250	37000	20000	1.24	5.5	4	0.77	9.6	
3	1000	1.09	75	60	10600	14700	1.33	10	7	1.4	4.2	

^a characteristics of the PEO macromonomer γ PEO.CL; ^b determined by SEC with PEO standards; ^c theoretical degree of lactone-polymerization = $[M]_0/[I]_0$ (M = ϵ CL + γ PEO.CL); ^d degree of polymerization of ϵ CL calculated by ¹H-NMR; ^e total Mn calculated by ¹H-NMR and Mn of PEO; ^f calibration by polystyrene standards; ^g molar content of γ PEO.CL in the feed; ^h molar content of γ PEO.CL in the copolymer; ⁱ N stands for the number of PEO grafts with Mn (PEO) = 1000 g/mol (D.P. = 20)

As a rule, the conversion of ϵ CL, as monitored by ¹H-NMR, was complete after less than 20 h. Unreacted γ PEO.CL could be completely removed by precipitation of the crude copolymerization product in methanol, as assessed by ¹H-NMR (no residual peaks at 4.05 or 2.98 ppm, typical for the lactone ring) and size exclusion chromatography. The elution chromatogram of the purified copolymer is monomodal and consistent with a narrow molecular weight distribution (Table 1). On the basis of the copolymer composition, as determined by ¹H-NMR, and the Mn of the PEO macromonomer, the molecular characteristics of the poly(ϵ CL-*co*- γ PEO.CL) copolymers (PCL-*g*-PEO) (1, 2 and 3) have been calculated and are collected in Table 1, i.e., total molecular weight (M_{n,tot}), molar composition and average number of PEO grafts per copolymer chain. The average degree of polymerization, and thus the molecular weight of the polyester backbone, have been determined from the ¹H-NMR resonances of the α -methylene protons of PCL (2.29 ppm, 2H) (peak j, Figure 1) and the methyl protons (1.2 ppm, 6H) of the isopropyl α -end-group (peak t). Compositions of the purified copolymer (F) are generally found to be slightly lower than the theoretical ones, due to incomplete conversion of the macromonomer. The composition of the purified copolymer (F) and the comonomer feed (f) are reported in Table 1. As previously mentioned, the conversion of the ϵ CL was complete, in contrast to the macromonomer, which was incorporated in the copolymer up to 70% (F/f \times 100), at least in the composition range investigated here. Nevertheless, although the molar content of PEO grafts was limited, e.g., 7mol% for copolymer 3 (Table 1), the molar ratio of the comonomer units, EO/ ϵ CL was higher than 1. This EO / ϵ CL ratio has been determined from the intensity of the ¹H-NMR signals for the methylene protons in the α -position of the

carbonyl ester of the ϵ CL units (2.29 ppm) (peak j, Figure 1) and the methylene protons of the PEO (3.6 ppm) (peak x, Figure 1).

The success of the copolymerization in contrast to the homopolymerization of γ PEO.CL, can be explained as follows; for both types of polymerization (homopolymerization and copolymerization), 1 equiv. of pyridine with respect to Al was used. Considering that the molar ratio of PEO chains to Al (and pyridine) was 20 in the case of the homopolymerization versus than 6.8 in the case of the copolymerization, this ratio is clearly higher than for the copolymerization experiments (PEO/ Al molar ratio = 1). Despite the fact that pyridine is a better ligand than the polyether, the large quantity of PEO might favor the coordination of PEO rather than pyridine to the Al. This might be the reason for the coordination of Al with the lactone-end group of PEO to be hindered in the case of the homopolymerization. In conclusion, the failure of the homopolymerization seems to be the result of coordination problems of the Al to the lactone ring of the PEO macromonomer, due to the high amount of PEO chains present in the reaction medium.

III.3. Determination of the reactivity ratios of ϵ CL and γ PEO.CL.

Qualitatively, the macromonomer appears to be less reactive than ϵ CL, consistent with its inability to homopolymerize, thus k_{22} (2 standing for the macromonomer) being close to 0.²⁵

In order to gain more insight into the macromolecular structure of the graft copolymers, the reactivity ratios of the comonomers have been determined by monitoring the copolymerization with ¹H-NMR (see experimental section). Because the ¹H-NMR resonances characteristic of each comonomer and their polymerized counterparts are well resolved (no overlap), the composition of the copolymerization medium as well as the amounts of residual comonomers could be determined versus time.

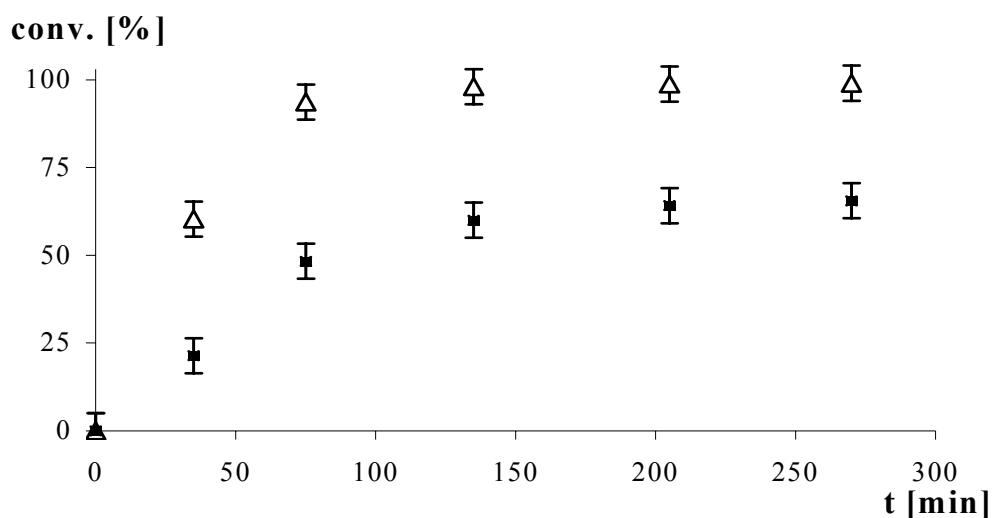


Figure 2. Monomer conversion with time ($\Delta = \epsilon\text{CL}$, $\blacksquare = \gamma\text{PEO.CL}$)

Figure 2 shows the time dependence of the conversion for each comonomer in a typical copolymerization of ϵCL with 5 mol% of $\gamma\text{PEO.CL}$ in the original comonomer feed (cfr. sample 1, Table 1). As expected, ϵCL is consumed much more rapidly than $\gamma\text{PEO.CL}$. As soon as the ϵCL conversion is complete, that of $\gamma\text{PEO.CL}$ levels off, consistent with the unsuccessful homopolymerization of the macromonomer. Thus, the copolymer basically consists of poly(ϵ -caprolactone) (PCL) at the beginning of the copolymerization and then, with progress of the copolymerization and thus increase of the $\gamma\text{PEO.CL} / \epsilon\text{CL}$ ratio along with the consumption of ϵCL , the macromonomer ($\gamma\text{PEO.CL}$) is incorporated in the copolymer.

Several methods have been proposed to determine the reactivity ratios of two comonomers. The methods based on the analysis of the copolymer composition at low conversion²⁶ have been disregarded because not enough copolymer would be incorporated for the analysis to be accurate enough. Therefore, the extended Kelen-Tüdös method²⁷, which is valid up to high conversion, has been used, where an average monomer composition is assigned to the corresponding experimental average copolymer composition. This approximation extends the use of the well-known linearization technique developed for low conversions²⁶ and is reliable for practically all copolymerization systems.²⁷ The reactivity ratios of ϵCL (monomer 1) and $\gamma\text{PEO.CL}$ (monomer 2) have been calculated according to the following equation (eqn.1):

$$\eta = r_1 \xi - (r_2/\alpha) (1 - \xi) \quad (1)$$

where $\eta = G / (\alpha + F) = z(y-1) / (\alpha z^2 + y)$ and $\xi = y / (\alpha z^2 + y) = F / (\alpha + F)$; with $F = y / z^2$ and $G = (y - 1) / z$; where

$y = \Delta m_1 / \Delta m_2 = (m_1^0 - m_1) / (m_2^0 - m_2)$ stands for the average composition of the copolymer up to the conversion ξ , with m_1 = concentration [mol/l] of monomer 1 at time t , where the superscript zero stands for the initial value of the monomer concentration.

$\bar{x} = y/z^0$ is the “average” composition dm_1/dm_2 of the comonomer feed and

$z = \log (m_1 / m_1^0) / \log (m_2 / m_2^0)$, average z value

and auxiliary parameter $\alpha = (F_{\min} F_{\max})^{1/2}$; F_{\min} stands for the lowest F value and F_{\max} for the highest F value, respectively.

In this study α was determined to be 0.70, and the experimental dependence of η on ξ is linear (Figure 3).

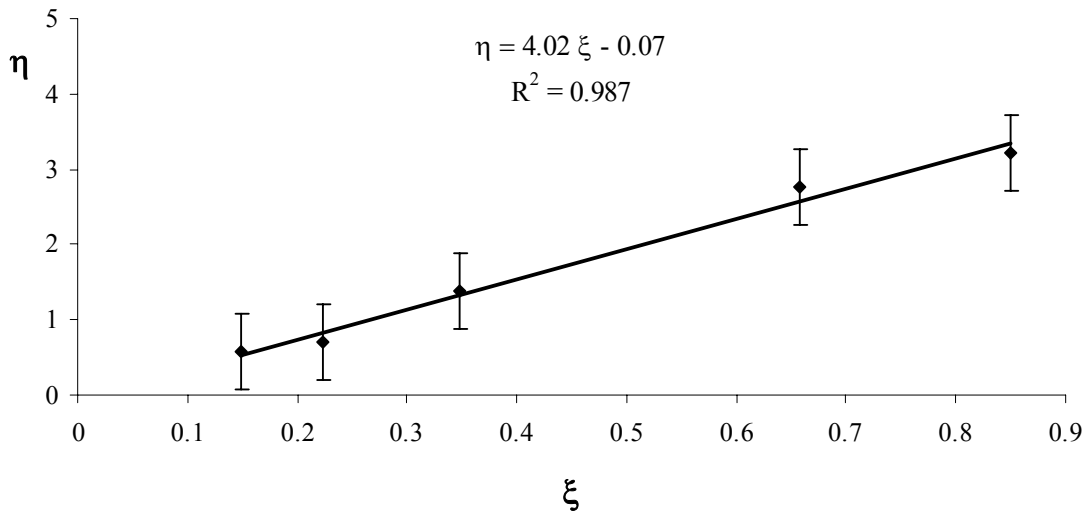


Figure 3. Kelen-Tüdös plot calculated for high conversion for the copolymerization of ϵ CL and γ PEO.CL with $Al(O^iPr)_3$ as initiator ($M_0/I_0 = 90$) at 25°C in presence of pyridine

Extrapolation of this straight line to $\xi = 0$ and $\xi = 1$, yields $-r_2 / \alpha$ (as intercept) and r_1 , respectively. The copolymerization is typically non-ideal, with $r_{\epsilon CL} (r_1) = 3.95$ and $r_{\gamma PEO.CL} (r_2) = 0.05$ and $r_1 r_2 \sim 0.2$. $r_{\gamma PEO.CL} (r_2)$ being very low, k_{21} is much higher than k_{22} , in agreement with the strong tendency of the macromonomer to alternate. As previously suggested, ϵ CL is extensively polymerized before the macromonomer has a chance to be incorporated as a lonely graft. The incorporation of ϵ -caprolactone is thus overwhelmingly

favoured leading to a tapered copolymer structure (or a gradient distribution) rather than a random one. Along the same line, Bo *et al.* reported on the radical copolymerization of acrylate monomers with poly(ethylene oxide) monomethacrylate (PEGMA) ($M_n = 400$ or 1000 or 2000 g/mol) initiated by AIBN, which resulted in the partial conversion of the macromonomer (30 to 50 %) and a heterogeneous structure of the copolymer.²⁸

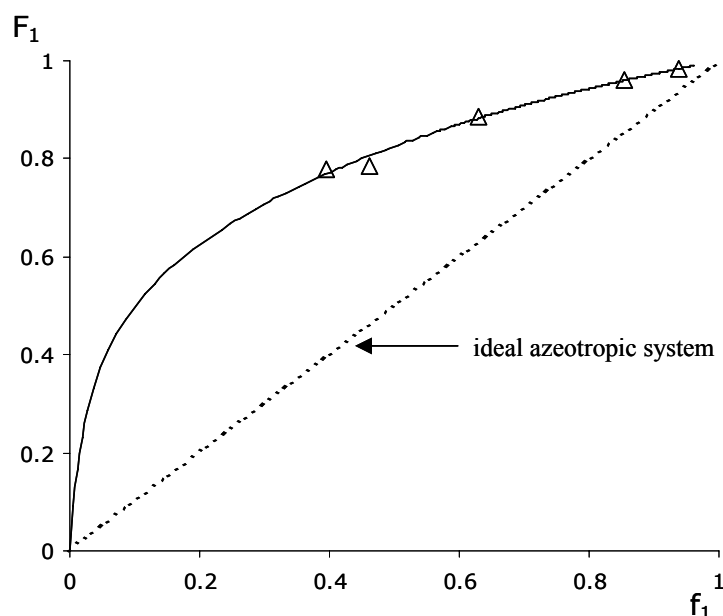


Figure 4. Plot of the instantaneous composition, with f_1 = molar fraction of monomer 1 (ϵ CL) in the feed and F_1 = molar fraction of monomer 1 (ϵ CL) in the copolymer

Figure 4 shows the instantaneous copolymer composition (molar fraction of monomer 1). The diagram shows that the plot fits well the experimental results (Figure 4) and gives access to the instantaneous copolymer composition, which could not be measured experimentally or determined from direct measurement results. The curve is typical for non-ideal copolymerizations, where one of the monomers (here ϵ -caprolactone, monomer 1) is always preferentially added to the growing polymer chain, whatever the terminal monomer. The structure of the copolymer is therefore a tapered structure.

III.4. Synthesis of PEO-*b*-PCL diblock copolymers (Scheme 2).

For sake of comparison of their interfacial properties, the equivalent diblock copolymers have been synthesized as described elsewhere.¹⁴ A typical ¹H-NMR spectrum of a diblock copolymer is shown Figure 5 and the composition of the various diblock copolymers are summarized in Table 2.

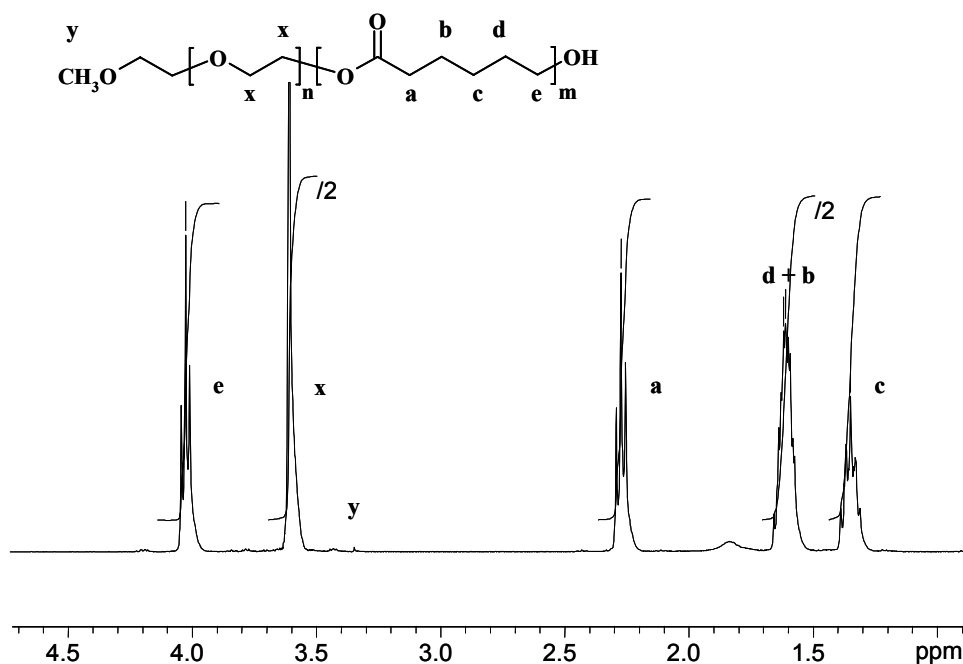


Figure 5. 400 MHz ¹H-NMR spectrum of PEO-*b*-PCL diblock copolymer (Table 2, sample 6)

Table 2. Molecular characteristics of α -monomethoxyPEO and PEO-*b*-PCL block copolymers

#	PEO ^a		copolymer					
	M_n^b	M_w/M_n	$DP^{th,c}$	$DP^{exp,d}$	$M_{n,NMR}^e$	$M_{n,SEC}^f$	M_w/M_n SEC,f	$n(EO)/n(\epsilon CL)$
4	900	1.05	43	44	5900	12500	1.22	0.47
5	9500	1.12	280	250	38100	31100	1.36	0.86
6	5000	1.04	80	75	13600	20300	1.25	1.52
7	9500	1.12	43	44	14500	18500	1.17	4.92

^a characteristics of the PEO macroinitiator; ^b determined by SEC with PEO standards; ^c theoretical degree of polymerization of ϵ -CL = $[M]_0/[I]_0$; ^d degree of polymerization of ϵ CL calculated by ¹H-NMR; ^e total M_n calculated by ¹H-NMR and M_n of PEO; ^f calibration by polystyrene standards

III.5. Interfacial activity and amphiphilic properties of the copolymers.

Copolymers composed of PCL and PEO segments combine hydrophilic (PEO) and hydrophobic (PCL) components in the same macromolecule making them potentially amphiphilic.²⁹ The amphiphilic properties of hydrosoluble PEO-*b*-PCL block copolymers, typically with a PEO block of $M_n = 5000$ g/mol and PCL blocks ranging from 350 to 2000 g/mol, have already been extensively studied, e.g. by surface tension measurements.¹ Whenever the PCL block exceeded 2000 g/mol, the CMC of those copolymers were $< 1 \cdot 10^{-6}$ mol/l. In the same line, the interfacial and emulsifying properties of hydrosoluble copolymers of PLA and PEO have been investigated.² On the other hand, there are several examples in the literature, considering the interfacial properties and adsorption behavior of hydrophobic copolymers soluble in organic solvents, such as polylactid-grafted dextrans³⁰ or ammonio polymethylmethacrylates, known as Eudragits RL or RS³¹, at the methylene chloride (MC)/water interface.

In this work, the interfacial activity of not/poorly hydrosoluble graft (PCL-*g*-PEO) copolymers and diblock (PEO-*b*-PCL) copolymers composed of hydrophilic PEO segments and hydrophobic PCL segments has been investigated in a water/chloroform system with a pendant drop tensiometer. Actually, the copolymers are quite soluble in chloroform (a common solvent for PCL and PEO), but rather insoluble in water. The relative hydrophobicity of the copolymers listed in Table 1 and 2 was expressed by their hydrophilic-lipophilic balance (HLB), calculated by the Griffin's relationship (eqn. 2):

$$HLB = 20 \times M_H / (M_L + M_H), \quad (2)$$

where M_L and M_H are the total molecular weights of the lipophilic (CL) and the hydrophilic (EO) segments, respectively.³² Table 3 summarizes the HLB data for the different diblock and graft PCL-PEO copolymers and compares the molecular weight and hydrophilicity of the graft and diblock copolymers. Graft copolymers "1" and "2" have comparable HLB (Table 1). The third copolymer "3" is more hydrophilic with a M_n similar to copolymer "1". As for the diblock copolymers, diblock copolymer 5 corresponds in molecular weight and HLB to graft copolymer 2, and 6 is comparable to 3 (graft copolymer). Diblock copolymer 4 consists of a PEO segment of $M_n = 900$ with a HLB comparable to the graft copolymers 1 and 2, which contain grafts of a similar length (1000 g/mol). Finally, block copolymer 7 has been synthesized with a PEO block length comparable to graft copolymer 2 and block copolymer 5, in order to assess the influence of the PCL block length.

In the experiments, the dynamic water/ CHCl_3 interfacial tension of the different copolymers dissolved in CHCl_3 was recorded by the pendant drop method (DSA), until a constant value was reached, corresponding to the equilibrium interfacial tension, γ_{eq} . We found that the dynamic interfacial tension diminishes with time depending on the copolymer and the copolymer concentration (data not shown). At low polymer concentrations ($c < 10^{-7}$ mol/l), equilibrium was only reached after several hours, in agreement with the literature.^{33,34} Indeed, whenever a fresh interface is created, the copolymer molecules diffuse from the “bulk” CHCl_3 solution to the interface, where they adsorb whilst also achieving the correct orientation, which decreases accordingly the interfacial tension. This accounts for the finite time that is necessary to reach the interfacial equilibrium tension.³⁵ The driving force for the adsorption of the hydrophobic copolymers at the interface is probably the gain of enthalpy upon hydration of the hydrophilic PEO chains when they immerse in the water phase.³¹ Contrary, PCL homopolymers are expected and known not to diminish the interfacial CH_2Cl_2 / H_2O tension.³¹ Consistently, PCL homopolymers are known not to diminish the interfacial CH_2Cl_2 / H_2O tension.³¹ Above a certain concentration, C_s , the copolymer concentration for which saturation of the surface by copolymer molecules is reached, no further significant decrease of γ_{eq} is observed upon increase of the copolymer concentration. For concentrations close to C_s , the steady-state value (equilibrium) of the interfacial tension (γ) was reached within several minutes. For concentrations higher than the C_s , only a couple of minutes were needed.

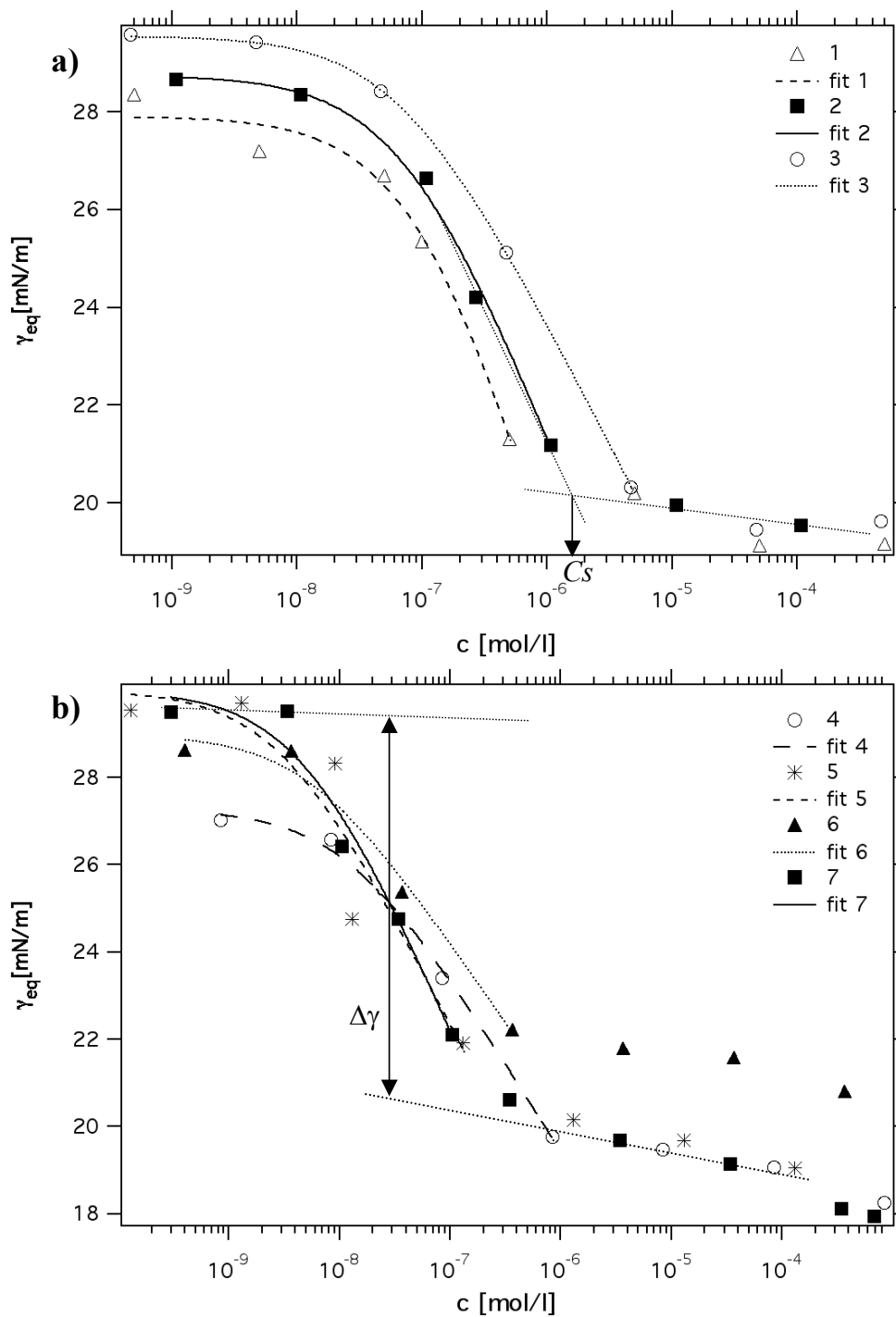


Figure 6. Equilibrium interfacial tension, γ_{eq} , versus a) poly(ϵ CL-co- γ PEO.CL) copolymer (1-3) concentration, b) PEO-*b*-PCL diblock (4-7) copolymer concentration, c [mol/l], at the water/chloroform interface at 20°C. Curves fitted to eqn. 2 together with Gibbs equation eqn. 4.

Figure 6A (graft copolymers) and 6B (diblock copolymers) show plots of the equilibrium (steady-state) CHCl₃/water interfacial tension (γ_{eq}) vs. the copolymer concentration (c lying in the 10^{-10} to 10^{-3} mol/l range) (adsorption isotherms). All semi-

logarithmic plots have the same (sigmoidal) shape showing the decrease of the interfacial tension, which indicates that the copolymers investigated here, adsorb at the interface and exhibit interfacial activity. The shape of the curves is similar to those of conventional non-ionic surfactants where a sharp inflection point is observed at the critical micelle concentration (CMC). At low copolymer concentrations, the effect on the interfacial tension reduction is negligible (γ remains nearly constant), since only few macromolecules migrate to and accumulate at the interface. Upon increasing copolymer concentration, the interfacial tension, γ , drops rapidly until the water / chloroform interface is saturated by a dense copolymer layer, thus until an upper concentration above which the interfacial tension changes no longer significantly. This critical saturation concentration, C_s , was graphically determined, as illustrated in Figure 6A, at the intersection of the tangents to the sigmoidal plot at high concentration and reported in Table 3.

Table 3. Macromolecular copolymer characteristics of P(ϵ CL-*co*- γ PEO.CL) graft copolymers and PEO-*b*-PCL block copolymers and their interfacial properties.

#	$M_{n, NMR}$ PEO <i>tot</i> ^a	$M_{n, NMR}$ PCL ^b	HLB ^c	$\Delta\gamma$ ^d [mN/m]	C_s ^e [mol/l]	Γ_{max} ^f [mol/m ²]	a_L ^g [mol/l]	A^h [nm ²]
1	2300	7700	4	8.5	$9 \cdot 10^{-7}$	$1.6(7) \cdot 10^{-6}$ ⁱ	$1.1(9) \cdot 10^{-7}$	1.0(4)
2	9600	27400	4.5	8.5	$1 \cdot 10^{-6}$	$1.2(2) \cdot 10^{-6}$	$8(4) \cdot 10^{-8}$	1.4(2)
3	4200	6400	7.5	10	$6 \cdot 10^{-6}$	$9.01(8) \cdot 10^{-7}$	$7.1(2) \cdot 10^{-8}$	1.84(2)
4	900	5000	3	6	$9 \cdot 10^{-7}$	$7(1) \cdot 10^{-7}$	$1.2(7) \cdot 10^{-8}$	2.3(3)
5	9500	28600	5	9	$2 \cdot 10^{-7}$	$9(5) \cdot 10^{-7}$	$6(6) \cdot 10^{-9}$	2(1)
6	5000	8600	7.5	6	$3 \cdot 10^{-7}$	$7(2) \cdot 10^{-7}$	$6(6) \cdot 10^{-9}$	2.5(7)
7	9500	5000	13	9	$2 \cdot 10^{-7}$	$1.1(4) \cdot 10^{-6}$	$5(5) \cdot 10^{-9}$	1.6(5)

^a for poly(ϵ CL-*co*- γ PEO.CL): number of grafts \times Mn (PEO); with Mn PEO = 1000 g/mol; ^b for poly(ϵ CL-*co*- γ PEO.CL): Mn PCL backbone; ^c HLB = $20 \cdot [\text{Mn}(\text{hydrophilic}) / (\text{Mn}(\text{lipophilic}) + \text{Mn}(\text{hydrophilic}))]$; ^d $\Delta\gamma = \gamma_{C_s} - \gamma_0$, where γ_{C_s} is the equilibrium interfacial tension γ at the critical saturation concentration and γ_0 the interfacial tension at the interface of pure chloroform/water, respectively; ^e C_s = "saturation concentration" was determined as the intersection of the tangents at high concentration of the sigmoidal plot (Figures 6a and 6b); ^f Γ_{max} = saturation adsorption; ^g a_L = Langmuir constant, representing the concentration at which half of the interfacial coverage is reached; ^h A = area occupied per molecule; ⁱ standard deviation values given in parentheses refer to the last digit. For example 9.01(8) is equivalent to 9.01 ± 0.08

For the graft copolymers, C_s is on the order of 10^{-6} mol/l, whereas, for the diblock copolymers, the surface is already saturated in the range of 10^{-7} mol/l. The difference between the initial and the lower interfacial tension, $\Delta\gamma$, reflects the interfacial activity of

the copolymer and has also been estimated graphically at the inflexion point (see example in Figure 6B) as summarized in Table 3. The graft copolymers 1 and 2, which are characterized by a similar EO to ϵ CL ratio (HLB, hydrophilicity) trigger a comparable decrease in the interfacial tension (~ 8.5 mN/m). The more hydrophilic graft copolymer 3 shows the largest decrease in the interfacial $\text{CHCl}_3/\text{H}_2\text{O}$ tension $\Delta\gamma = 10$ mN/m). All these graft copolymers are composed of PEO grafts with the same length of 1000 g/mol, which would explain the similar interfacial activity. For the diblock copolymers, copolymers 4 to 7 in Table 3, $\Delta\gamma$ is in the range of 6 to 9 mN/m and lower for the copolymers that contain shorter PEO blocks indicating that $\Delta\gamma$, thus the interfacial activity, is probably mostly controlled by the length of the hydrophilic block rather than the HLB. The observation that the decrease of the interfacial tension γ is strongest for the copolymers with the longest PEO segment could be explained considering that PEO is responsible for the migration of the copolymer to the interface, which is driven by the gain of enthalpy by the hydration of the PEO chains. When the molecular architecture is compared, at comparable HLB (e.g., copolymer 3 and 6), the tapered graft copolymer shows a higher interfacial activity.

The Langmuir isotherm (eqn. 3) is most commonly used to account for the interfacial adsorption of surfactants.³⁵

$$\Gamma = \Gamma_{\max} \times \frac{c}{a_L + c} \quad (3)$$

where Γ_{\max} is the amount of adsorbed copolymer at saturation in mol/m² and a_L is the Langmuir constant in mol/l, which is actually the concentration at which half the interface is covered by the surfactant. The dependence of adsorbed amount Γ on the surfactant concentration is expressed by the Gibbs adsorption equation.³⁵(eqn. 4)

$$\Gamma = -\frac{1}{RT} \times \frac{d\gamma}{d(\ln c)} \quad (4)$$

where R is the gas constant, T is the absolute temperature, γ is the equilibrium interfacial tension, and c is the copolymer concentration [mol/l]. The area occupied per molecule, A in nm², can be calculated by equation 5:³⁶

$$A = \frac{10^{18}}{N_A \Gamma_{\max}} \quad (5)$$

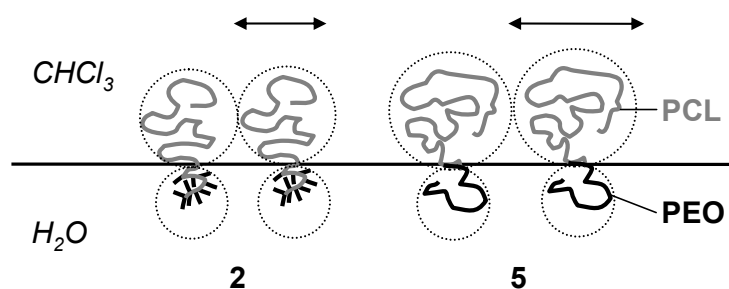
where N_A is the Avogadro constant.

Γ_{\max} (Langmuir), a_L and thus A have been determined by fitting the experimental data by eqn. 3 combined with the Gibbs equation (eqn. 4) up to the Cs concentration (the

results are collected in Table 3). Figures 6A and B show a good agreement between the experiments and the theoretical curves, corresponding to a model of a quasi “ideal” adsorption layer at the interface. Comparing block and graft copolymers, from Table 3, it appears that Γ_{\max} of both the graft and the diblock copolymers is in the range of 10^{-6} to 10^{-7} moles/m², the number of graft copolymers (of 10^{-6} mol/m²) at the saturated interface (Γ_{\max}) being moderately higher compared to the diblock copolymers (10^{-7} mol/m²). In other terms, the area occupied by one molecule, A , ranges from 1 to 3 nm² and is in general slightly lower for the graft copolymers compared to diblock copolymers. These results are in line with the results for Cs: the saturation of the interface is reached at lower copolymer concentration for diblock copolymers, i.e., fewer copolymer molecules are present (at saturation of the interface) and the area occupied by one diblock molecule is larger compared to graft copolymer molecules. With increasing HLB, i.e. with increasing number N of PEO grafts, the area occupied by one adsorbed molecule at saturated interface is increased (Table 3, copolymer 1 and 3).

These observations might be related to the copolymer architecture and the conformation that the polymer chains exhibit at the interface. As supported by the reactivity ratios, the graft copolymers have a gradient or “palm-tree” structure. Indeed, the asymmetric distribution of the PEO grafts along the PCL backbone results in chains with a hydrophobic head-segment and a hydrophilic tail-segment quite reminiscent of pure diblock copolymers. The branched structure of the hydrophilic tail is expected to increase the hydrophilicity of the originally hydrophobic PCL segment. Thus, the resemblance of the graft copolymers to diblocks may explain that the calculated physico-chemical parameters for both copolymers are in the same range for both architectures.

Indeed, after diffusion to the interface, both segments (PCL and PEO) must adopt the most energetically favorable conformation. The conformation of hydrosoluble PEO-*b*-PLA copolymers at the decane/water interface has been reported extensively; it has been found that the occupied area strongly depended on the length of the PLA segment.² In that system, PLA is not soluble neither in water nor in the organic phase; therefore the PLA chains are lying flat at the interface, which determines directly the occupied interfacial area A . In contrast, the present study describes a system where the hydrophobic segment (PCL) is soluble in the organic phase (CHCl₃) and PEO is soluble in water. Therefore, both segments have probably a coil conformation in each phase, rather than “lying” flat at the interface as expected for random graft copolymers.³¹



Scheme 3. Adsorption of the PCL/PEO copolymers at the $\text{CHCl}_3/\text{H}_2\text{O}$ interface (PCL (in grey) /PEO (in black); numbers correspond to copolymer references in table 1 and 2)

Scheme 3 shows a tentative proposal for the conformation of graft copolymer 2 ($M_{n,\text{tot}} = 39000 \text{ g/mol}$, HLB = 4.5) and diblock copolymer 5 ($M_{n,\text{tot}} = 39000 \text{ g/mol}$, HLB = 5) to explain why graft copolymers occupy a smaller surface and are apparently more densely packed than the corresponding diblock copolymers. Indeed, both copolymer types are composed of a PCL segment of $M_n \sim 28000 \text{ g/mol}$. As for the graft copolymer however, a part of the PCL is most probably located in the aqueous phase because of the densely packed PEO grafts, so that the remaining “pure” hydrophobic PCL part, i.e., the PCL segment that is generated at first during copolymerization, is shorter, thereby occupying a smaller area.

In conclusion, in each case (graft and block polymers), the amphiphilic hydrophobic PCL-PEO showed interfacial activity, revealing emulsifying or surfactant properties.

IV. Conclusion

Well-defined hydrophobic PCL-*graft*-PEO copolymers have been synthesized by ring-opening copolymerization of a previously synthesized ϵ -caprolactone-terminated PEO macromonomer ($\gamma\text{PEO.CL}$). $^1\text{H-NMR}$ monitoring of the copolymerization gave access to the reactivity ratios and revealed that the macromonomer is not randomly distributed along the PCL backbone but the copolymers rather have a blocky structure.

These graft copolymers showed surfactant properties as investigated in a water/chloroform system by the pendant drop method, comparable to those of hydrophobic PEO-*b*-PCL diblock copolymers of similar composition. The interfacial activity of different graft copolymers with the same graft length of 1000 g/mol was found to depend hardly on the substitution degree or the total molecular weight. The maximum molar

adsorption of PCL-*graft*-PEO copolymers at the CHCl₃/H₂O interface was higher compared to the diblock copolymers of similar hydrophilicity and total molecular weight.

These new amphiphilic and biocompatible copolymers are thus promising materials for biomedical applications, when protein-repellent surfaces are needed, as in the field of drug delivery as emulsifiers for colloidal drug carriers (nanoparticles), or for surface modification of biodegradable scaffolds (implants). In a forthcoming paper, both graft and diblock copolymers will be used and compared as surfactants for the stabilization and surface-modification of polymeric nanoparticles for drug delivery, in order to make them “stealthy”. Their complement activation in human serum and biocompatibility is currently under investigation with respect to the copolymer structure.

References.

- ¹ Vangeyte, P.; Leyh, B.; Heinrich, M.; Grandjean, J.; Bourgaux, C.; Jérôme, R. *Langmuir* **2004**, *20*, 8442-8451.
- ² Gref, R.; Babak, V.; Bouillot, P.; Lukina, I.; Bodorev, M.; Dellacherie, E. *Colloid Surf. A: Physicochem. Eng. Aspects* **1998**, *143*, 413-420.
- ³ Walton, D. G.; Soo, P. P.; Mayes, A. M.; Sofia-Allgor, S. J.; Fujii, J. T.; Griffith, L. G.; Ankner, J. F.; Kaiser, H.; Johansson, J.; Smith, G. D.; Barker, J. G.; Satija, S. K. *Macromolecules* **1997**, *30*, 6947-6956.
- ⁴ Torchilin, V. P.; *J. Microencapsulation* **1998**, *15*, 1-19.
- ⁵ Iatrou, H.; Hadjichristidis, N.; *Macromolecules* **1992**, *25*, 4649-4651.
- ⁶ Piirma, I.; Lenzotti, J. R. *Br. Polym. J.* **1989**, *21*, 45-51.
- ⁷ March, G. C.; Napper, D. H. *J. Colloid Interface Sci.* **1977**, *61*, 383-387.
- ⁸ Sela, Y.; Magdassi, S.; Garti, N. *Colloid Polym. Sci.* **1994**, *272*, 684-691.
- ⁹ Lee, J. H.; Kopeckova, P.; Kopecek, J.; Andrade, J. D. *Biomaterials* **1990**, *11*, 455-464.
- ¹⁰ Gref, R.; Minamitake, Y.; Peracchia, M. T.; Trubetskoy, V.; Torchilin, V.; Langer, R. *Science* **1994**, *263*, 1600-1603.
- ¹¹ Harris, J. M. In *Poly(ethylene glycol) chemistry: Biotechnical and Biomedical Applications*, Harris, J. M., Eds.; Plenum Press: New York, 1992.
- ¹² Rieger, J.; Bernaerts, K. V.; Du Prez, F. E.; Jérôme, R.; Jérôme, C. *Macromolecules* **2004**, *37*, 9738-9745.

-
- ¹³ Lofgren, A.; Albertsson, A.-C.; Dubois, P.; Jérôme, R.; Teyssié, P.; *Macromolecules* **1994**, *27*, 5556-5562.
- ¹⁴ Vangeyte, P.; Jérôme, R.; *J. Polym. Sci., Part A: Polym. Chem.* **2004**, *42*, 1132-1142.
- ¹⁵ Ito, K.; Kobayashi, H. *Polym. J.* **1992**, *24*, 199-204.
- ¹⁶ Schmitt, B.; Alexandre, E.; Boudjema, K.; Lutz, P.J.; *Macromol. Symp.* **1995**, *93*, 117-124.
- ¹⁷ Khoussakoun, E.; Gohy, J.-F.; Jerome, R.; *Polymer* **2004**, *45*, 8303-8310.
- ¹⁸ Hadjichristidis, N; Poulos, Y.; Avgeropoulos, A.; *Macromol. Symp.* **1998**, *132*, 207-220.
- ¹⁹ Ouhadi, T.; Stevens, C.; Teyssie, P.; *Makromol. Chem., Suppl.* **1975**, *1*, 191-201.
- ²⁰ Dubois, P.; Degée, P.; Jérôme, R.; Teyssie, P.; *Macromolecules* **1993**, *26*, 2730-2735.
- ²¹ Yu, Y.; Eisenberg, A.; *Polym. Mater. Sci. Eng.* **1998**, *79*, 288-289.
- ²² Dubois, P.; Barakat, I.; Jerome, R; Teyssie, P.; *Macromolecules* **1993**, *26*, 4407-4412.
- ²³ Degée, P.; Dubois, P.; Jérôme, R.; *Macromol. Chem. Phys.* **1997**, *198*, 1973-1984.
- ²⁴ Dubois, P.; Degée, P.; Ropson, N.; Jérôme, R. in "Macromolecular Design of Polymeric Materials"; Hatada, K., Eds.; Marcel Dekker, New York, **1996**; Ch. 4, p 247.
- ²⁵ Braun, D.; *Macromol. Symp.* **2001**, *174*, 127-135.
- ²⁶ Kelen, T; Tüdös, F.; *J. Macromol. Sci., Chem.* **1975**, *A9*, 1-27.
- ²⁷ Kelen, T; Tüdös, F.; Földes-Berezsnich, T; Turcsanyi, B.; *J. Macromol. Sci., Chem.*, **1976**, *A10*, 1513-1540.
- ²⁸ Bo, G.; Wesslen, B.; Wesslen, K.B.; *J. Polym. Sci., Part A: Polym. Chem.* **1992**, *30*, 1799-1808.
- ²⁹ Tuzar, Z.; Kratochvil, P.; *Surf. Colloid Sci.*, **1993**, *15*, 1-83.
- ³⁰ Nouvel, C.; Frochot, C.; Sadtler, V.; Dubois, P.; Dellacherie, E.; Six, J. L.; *Macromolecules* **2004**, *37*, 4981-4988.
- ³¹ Babak, V.G.; Boury, F.; *Colloid. Surf. A. Physicochem. Eng. Aspects* **2004**, *243*, 33-42.
- ³² Becher, P., Schick, M. J. in "Nonionic Surfactants", Schick, M. J., Eds.; Marcel Dekker, New York, **1987**; Vol. 23; p. 435.
- ³³ Daniels, R.; Barta, A.; *Eur. J. Biopharm.*, **1994**, *40*, 128-138.
- ³⁴ Wollenweber, C.; Makievski, A.V.; Miller, R. Daniels, R.; *Colloid. Surf. A. Physicochem. Eng. Aspects* **2000**, *172*, 91-101.
- ³⁵ Easton, J.; Dalton, J.S.; *Adv. Colloid Interface Sci.* **2000**, *85*, 103-144.

-
- ³⁶ Rosen, M. J. *in* “Surfactants and Interfacial Phenomena”, 2nd ed.; Wiley-Interscience, New-York, **1989**.

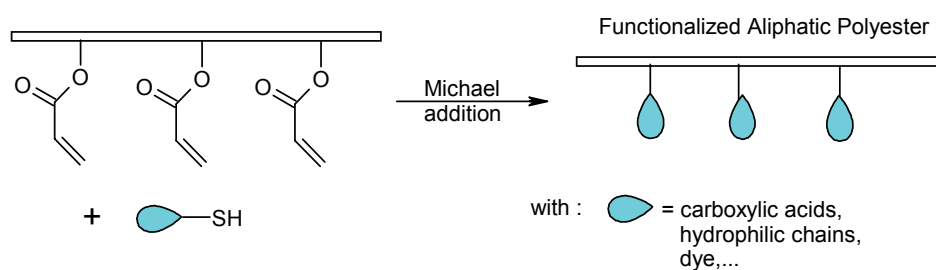
Chapter 3

Versatile functionalization and grafting of poly(ϵ -caprolactone)

by Michael-type addition

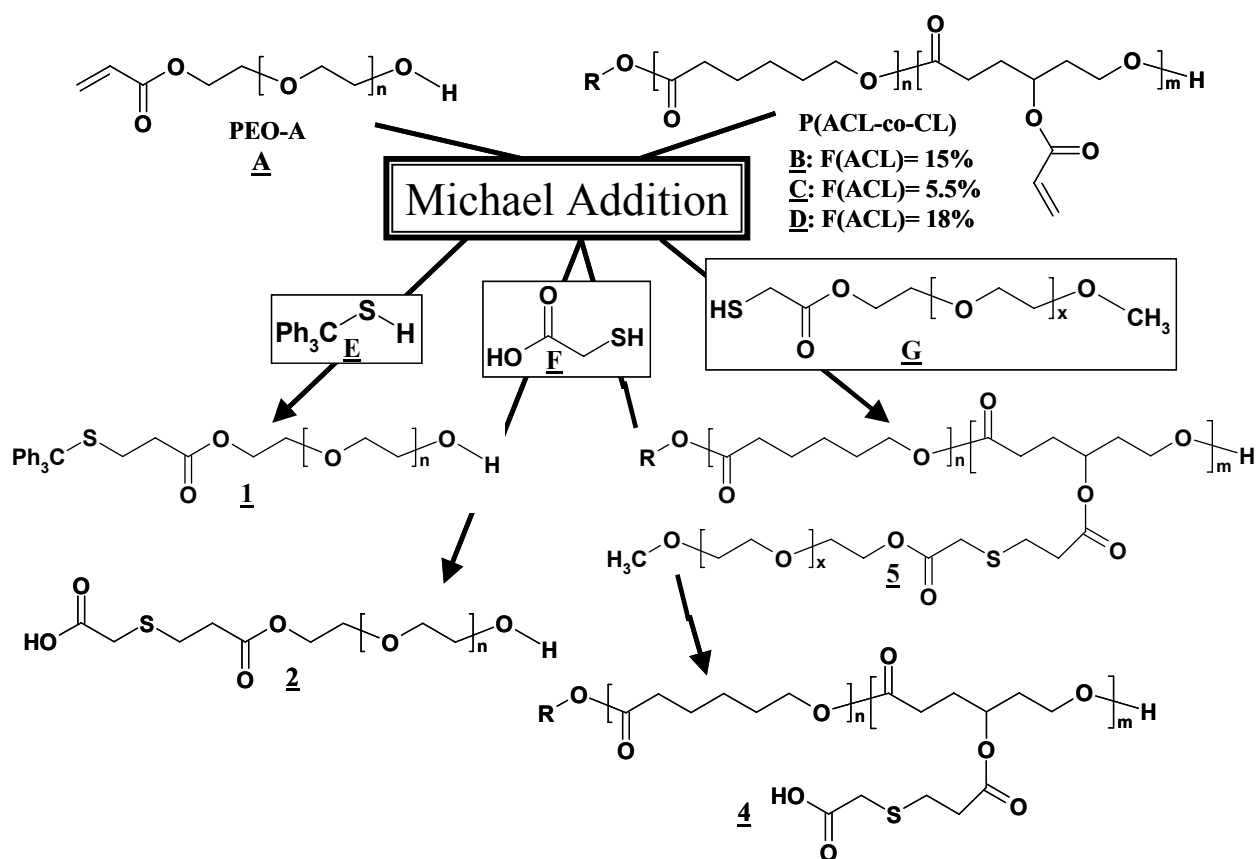
Abstract

The Michael-type addition is a very straightforward technique of functionalization and grafting, which is tolerant to a variety of functional groups and does not require intermediate protection/deprotection steps. Based on this versatile reaction a large variety of molecules could be grafted onto γ -acryloyloxy ϵ -caprolactone units of aliphatic (co)polyesters, so providing them with new properties, including reactivity and amphiphilicity.



Aliphatic polyesters, such as poly(ϵ -caprolactone) (PCL), have great potential as biomaterials due to a unique combination of biodegradability and biocompatibility. Attaching reactive groups or hydrophilic grafts along these preformed backbones is usually a problem because of the sensitivity of the ester units to nucleophilic attack followed by chain degradation. One strategy to tackle this problem consists of the synthesis and copolymerization with ϵ -caprolactone, of γ -substituted ϵ -caprolactones. Bromide, activated bromide, (protected) carbonyl, protected hydroxyl and carboxyl groups, and acryloyloxy are examples of γ substituents that have been reported.¹⁻³ Polymerization and copolymerization of these γ -substituted ϵ -caprolactones are living and permit long chains to be prepared because the γ -substitution does not perturb the reactivity of the cyclic monomer.¹⁻³ The major drawback of this method is that any protic function reactive towards the metal alkoxides used in (co)polymerization must be protected and that the deprotection has to be carried out under mild conditions. For these specific cases, a more direct functionalization technique is highly desirable.

In this paper, we report on the use of the Michael-type addition⁴ to synthesize functional and/or amphiphilic poly(ϵ -caprolactone) (PCL). The characteristic features of this reaction are (i) occurrence under very mild conditions (preventing the polyester degradation), (ii) tolerance to a wide range of functional groups (avoiding protection/deprotection steps), (iii) no need for metallic catalyst, and thus no contamination that could be a problem for biomedical applications. The easy synthesis and living (co)polymerization of γ -acryloyloxy- ϵ -caprolactone (ACL) makes it easy to have double bonds distributed along polyester backbones of different architectures⁵ and enable Michael-type addition. The addition of thiol derivatives to pendent acrylate groups has been investigated in this paper, as a versatile method of functionalization and grafting of PCL with the advantage of high reactivity and chemoselectivity of the reactants.⁶



Scheme 1. Synthesis pathways to amphiphilic and/ or reactive polymers by Michael-type addition

The Michael-type addition was first tested with commercially available poly(ethylene oxide) end-capped by an α -hydroxy group and an ω -acrylate one, respectively (PEO-A, $M_n = 375$ g/mol, from Aldrich) (Scheme 1, **A**). This preliminary reaction aimed at optimizing the reaction conditions for the grafting of thiols before being extended to pendent acrylate containing poly(ϵ -caprolactone) (Scheme 1). The experimental data are reported in Table 1.

Triphenylmethanethiol (Scheme 1, **E**) was first considered because its strong UV absorption makes quantification of the grafting efficiency quite easy. The reaction was carried out in toluene, a good solvent for poly(ϵ -caprolactone) that will be used further, at room temperature under nitrogen and in the dark.

Table 1. Experimental data and yields for the Michael-type additions

<i>Entry^a</i>	<i>Acrylic deriv.^a (equiv.)</i>	<i>R-SH^a (equiv.)</i>	<i>Solvent</i>	<i>Catalyst (equiv.)</i>	<i>Reaction time (h)</i>	<i>Reaction yield (%)</i>
1a	A (1)	E (0.5)	Toluene	TBAF (1)	5	100
1b	A (1)	E (1)	Toluene	NEt ₃ (1)	5	100
1c	A (1)	E (1)	Toluene	Pyridine (1)	5	100
2a	A (1)	F (1.5)	Toluene	Pyridine (2)	20	< 10
2b	A (1)	F (1.5)	Toluene	Pyridine (2)	100	40
2c	A (1)	F (10)	THF	Pyridine (15)	30	50
2d	A (1)	F (10)	THF	Pyridine (15)	50	80
2e	A (1)	F (10)	THF	Pyridine (15)	75	100
3a	A (1)	G (20)	THF	Pyridine (25)	25	60
3b	A (1)	G (20)	THF	Pyridine (25)	60	80
4a	B (1)	F (10)	THF	Pyridine (15)	30	25
4b	B (1)	F (10)	THF	Pyridine (15)	50	40
4c	B (1)	F (10)	THF	Pyridine (15)	75	70
5a	C (1)	G (10)	THF	Pyridine (15)	80	25
5b	C (1)	G (10)	THF	Pyridine (15)	150	35
5c	C (1)	G (10)	THF	Pyridine (15)	300	60
5d	D (1)	G (10)	THF	Pyridine (15)	80	30
5e	D (1)	G (10)	THF	Pyridine (15)	150	45
5f	D (1)	G (10)	THF	Pyridine (15)	300	65

^a The letters refer to compounds shown in Scheme 1; *acrylic deriv.* stands for acrylic derivatives.

The effect of three catalysts (Table 1, entries 1a-c) was compared. Finally, poly(ϵ -caprolactone) was added to the reaction medium in order to assess its stability under these conditions (GPC analysis before and after reaction). The Michael addition was systematically complete within 5 h (Table 1, entries 1a-c), and no degradation of PCL was observed whatever the catalyst. Pyridine was selected as a catalyst for the addition of mercaptoacetic acid (Scheme 1, F) (Table 1, entries 2a-e). The reaction was then much slower with only 40 % yield after 100 h (Table 1, entry 2b) even if an excess of thiol (1.5 equiv.) and catalyst (2 equiv.) was used. The higher reactivity of the triphenylmethanethiol might be explained by the three phenyl-substituents that increase the nucleophilicity and

thus the reactivity of this thiol derivative. However, conversion of the acrylate end-group of PEO-A into a carboxylic acid one was quantitative after 75 h in a more polar solvent, such as THF (Table 1, entries **2c-e**) with a large excess of the reactant (Table 1, entry **2e**). Once again, PCL that was added to the reaction medium was recovered without any degradation. Similarly, the unprotected hydroxyl end-group of PEO-A remained unmodified, as assessed by ¹H-NMR analysis of the reacted PEO-A (spectrum not shown). This reaction is thus a straightforward efficient pathway for the synthesis of α -hydroxy- ω -carboxy-PEO, a macromonomer well-suited to polycondensation with low molecular weight hydroxy-acids.

Finally, an oligomeric thiol, α -methoxy- ω -mercapto-poly(ethylene oxide) (PEO-SH, Scheme 1, **G**), was added to PEO-A. This PEO-SH was synthesized by esterification of MeO-PEO-OH ($M_{n,NMR} = 900\text{g/mol}$) with mercaptoacetic acid in toluene in a Dean-Stark apparatus as reported elsewhere.⁷ The yield of the Michael addition of PEO-A (**A**) and PEO-SH (**G**) was 80 % after 60 h (Table 1, entries **3a-b**), which is quite comparable to the addition of mercaptoacetic acid to PEO-A (**A**).

Thus, under mild reaction conditions, high coupling yields of hydrophilic thiol derivatives (mercaptoacetic acid **F** and PEO-SH **G**) and PEO-acrylate are observed, whereas poly(ϵ -caprolactone) is not degraded at all. These experimental conditions have been extended to a random poly(ACL-*co*-CL) copolymer in order to make amphiphilic copolymers available (Scheme 1, **4** and **5**). Synthesis of γ -acryloyloxy- ϵ -caprolactone has been reported elsewhere,⁵ as well as copolymerization with CL.⁸ In this work, copolymers with various ACL contents (15, 5.5 and 18 mol% ACL; Scheme 1, **B**, **C** and **D**) were reacted with the mercapto-derivative **F** (Table 1, entries **4a-c**) and PEO-SH (**G**) (Table 1, entries **5a-f**), the SH/acrylate and catalyst/acrylate molar ratios being 10 and 15, respectively. In case of mercaptoacetic acid (**F**) (Table 1, entries **4a-c**), 70 % of the pendent acrylates reacted after 75 h providing the hydrophobic polyester with hydrophilicity and water solubility. A comparable grafting efficiency is observed for PEO-SH, but after 300 h (Table 1, entry **5f**). As expected the size of the hydrophilic thiol (**F** *versus* **G**) has clearly an effect on the kinetics of the addition onto the hydrophobic polyester backbone, the reaction between two polymeric partners being unfavorable. Indeed, in the case of graft copolymers, steric hindrance of the firstly grafted chains limits further addition. The reaction is then incomplete.

Figure 1 shows the $^1\text{H-NMR}$ spectra for P(ACL-*co*-CL) (Scheme 1, **D**) ($M_n = 24000$ g/mol, $F_{\text{ACL}, \text{H-NMR}} = 18\%$) before (Fig. 1a) and after reaction (Fig. 1b) with PEO-SH ($M_n, \text{H-NMR} = 900$ g/mol).

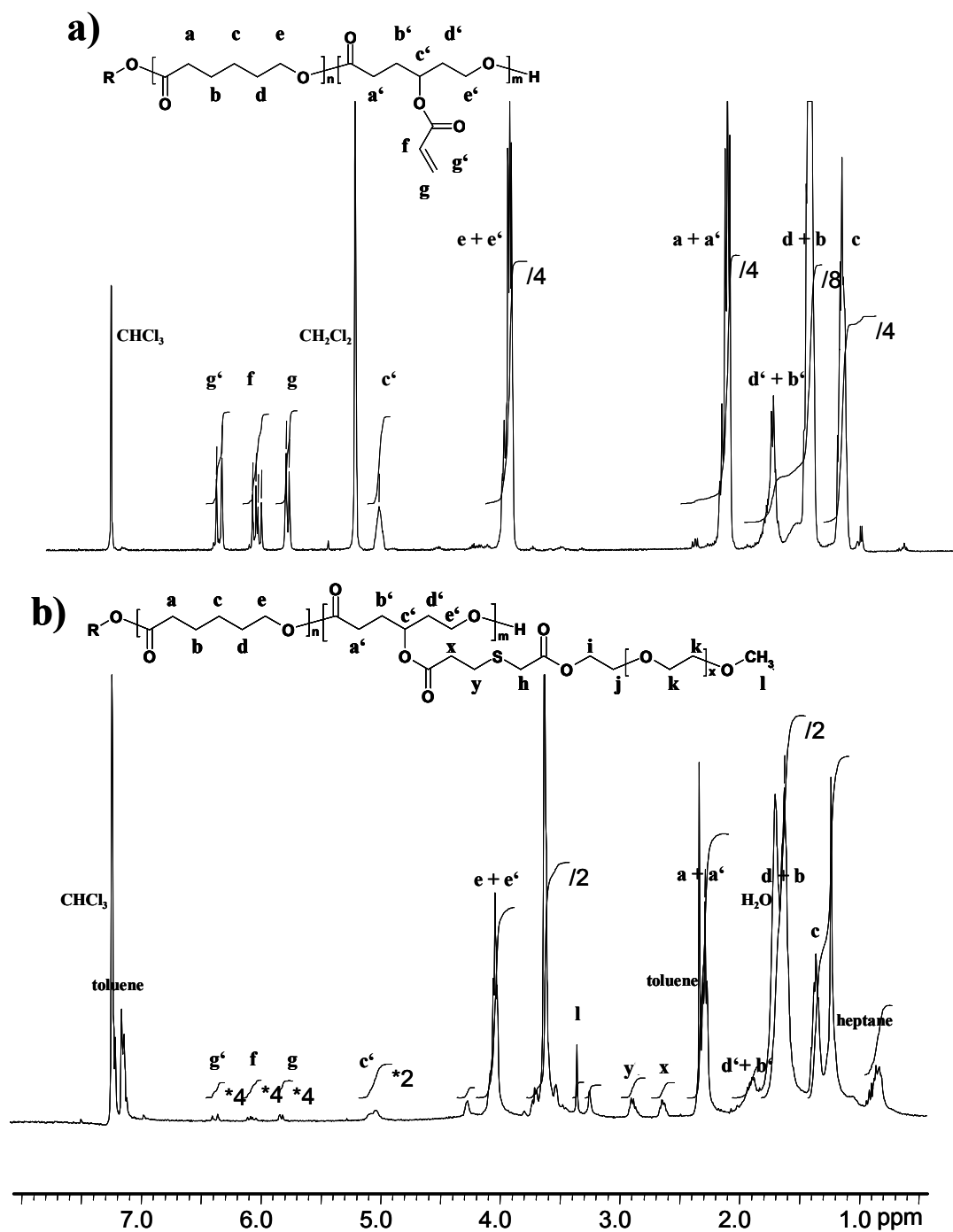


Figure 1. $^1\text{H-NMR}$ spectra for P(ACL-*co*-CL), $F_{\text{ACL}, \text{H-NMR}} = 18\%$, a) before, b) after reaction with PEO-SH (Table 1, 5f)

The PCL-*g*-PEO comb-like copolymer was purified by precipitation in water, followed by dialysis against water and recovery by ultracentrifugation. The methylene protons (**x** and **y**, see figure 1b) adjacent to the sulfur atom are observed at 2.6 ppm (proton **y**) and 2.9 ppm (proton **x**), respectively. Moreover, the intensity of the acryloyloxy-protons (5.8-6.4 ppm) is much lower. From the relative intensity of the protons **x** and **e** + **e'**, copolymer composition has been calculated. As an average, one PEO graft is attached to PCL each 10 units (PCL_{0.9}-*g*-PEO_{0.1}).

Success of the grafting was confirmed by TEM observation of the copolymer self-associated in water. When one drop of an aqueous solution was evaporated on a TEM grid, micelles with an average diameter of 20 nm were observed, as shown in Figure 2.

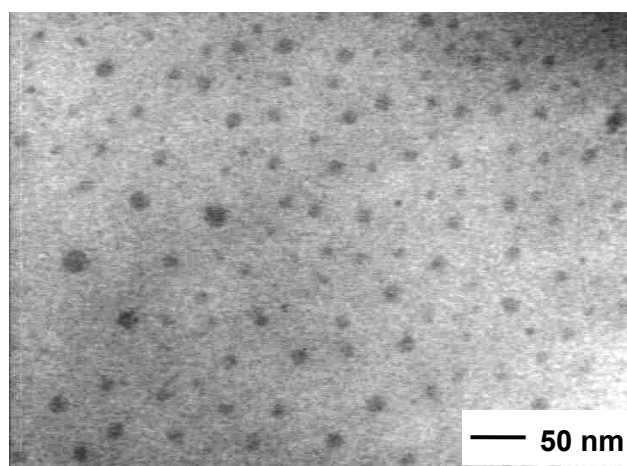


Figure 2. TEM picture of PCL-*g*-PEO self-assembled in water (5f)

These preliminary experiments have shown that the Michael-type addition is a straightforward, effective and versatile reaction for the functionalization and grafting of PACL and copolymers, so making an originally biodegradable and biocompatible polyester reactive and amphiphilic. The incompleteness of the reaction with PEO-SH leads to few remaining pendant acrylic functions on the graft copolymers that can be reacted further with small size thiols to avoid cross-linking and confer them additional functionality. Tolerance of the Michael addition to urea or protic functions, such as carboxylic acid and alcohol, must be noted. This would allow the grafting of α -biotinylated- ω -mercapto PEO onto PCL and ultimately the targeting of specific organs based on biotin-avidin complexation.⁹ Similarly, the α -hydroxy group of the grafted ω -mercapto-PEO could be used to attach molecules with biological activity, *e.g.*, in diagnostics, sensing devices, *etc.*

References.

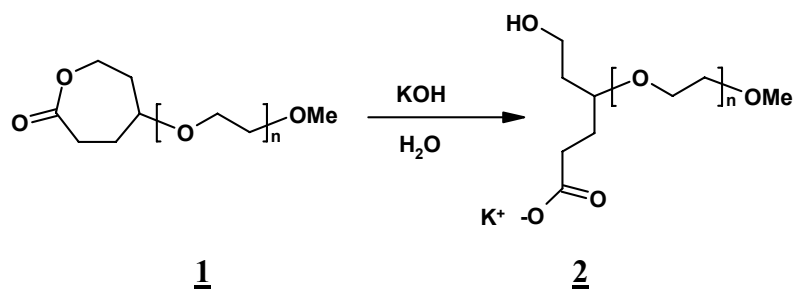
- ¹ Tian, D.; Dubois, P.; Jérôme, R.; *Macromolecules* **1997**, *30*, 2575
- ² Tian, D.; Dubois, P.; Jérôme, R.; *Macromol. Symp.* **1998**, *130*, 217
- ³ Lecomte, P.; d'Aloia, V.; Mazza, M.; Halleux, O.; Gautier, S.; Detrembleur, C.; Jérôme, R.; *ACS Polymer Preprint* **2000**, *41*, 1534
- ⁴ Heggli, M.; Tirelli, N.; Zisch, A.; Hubbell, J. A.; *Bioconjugate Chem.* **2003**, *14*, 967
- ⁵ Mecerreyes, D.; Humes, J.; Miller, R. D.; Hedrick, J. L.; Detrembleur, C.; Lecomte, P.; Jérôme, R.; San Roman, J.; *Macromol. Rapid Commun.* **2000**, *21*, 779
- ⁶ Tirelli, N.; Lutolf, M. P.; Napoli, A.; Hubbell, J. A.; *Rev. Molecular Biotechnol.* **2002**, *90*, 3
- ⁷ Vidal, F.; Hamaide, T.; *Polym. Bulletin* **1995**, *35*, 1
- ⁸ Lou, X.; Jérôme, C.; Detrembleur, C.; Jérôme, R.; *Langmuir* **2002**, *18*, 2785
- ⁹ Gref, R.; Couvreur, P.; Barratt, G.; Mysiakine, E.; *Biomaterials* **2003**, *24*, 4529

Chapter 4

**Controlled synthesis of an ABC miktoarm star-shaped copolymer by
sequential ring-opening polymerization of
ethylene oxide, benzyl β -malolactonate, and ϵ -caprolactone**

Abstract

This chapter reports on the synthesis of an amphiphilic miktoarm ABC star-shaped copolymer, $s[(PEO)(PMLABz)(PCL)]$, consisting of biocompatible/ bioresorbable arms. Indeed, PEO is a hydrophilic biocompatible poly(ethylene oxide) arm, PMLABz is a poly(benzyl β -malolactonate) arm precursor of a pH-sensitive bioresorbable poly(β -malic acid) block, and PCL is a hydrophobic bioresorbable poly(ϵ -caprolactone) arm. Each constitutive arm was prepared by ring-opening polymerization. A double-headed PEO macroinitiator [PEO-(OH)-COO⁻K⁺] (2) was first prepared by selective hydrolysis of the α -lactone (2-oxepanone) end-group of PEO chains end-capped by a ω -methoxy group (1). The anionic polymerization of benzyl β -malolactonate (MLABz) was selectively initiated by the α -potassium carboxylate end-group of PEO in the presence of 18-crown-6 ether. The polymerization of ϵ -caprolactone (ϵ -CL) was initiated by the hydroxyl group left at the junction of the two blocks of the as-prepared PEO-*b*-PMLABz diblock copolymer, in the presence of tin (II) bis(2-ethylhexanoate) (Sn(Oct)₂). The macroinitiator, the intermediate diblock and the final miktoarm star-shaped copolymer were analyzed by ¹H-NMR spectroscopy and size exclusion chromatography (SEC).



Contents

I. INTRODUCTION.....	123
II. EXPERIMENTAL PART.....	124
<i>Materials</i>	124
<i>Synthesis of ϵ-caprolactone end-capped PEO</i>	124
<i>Synthesis of the α-hydroxy, α'-carboxylate PEO macroinitiator</i>	125
<i>Synthesis of the [PEO-<i>b</i>-PMLABz]-OH diblock copolymer</i>	125
<i>Synthesis of the s[(PEO)(PMLABz)(PCL)] star-shaped copolymer</i>	126
<i>Characterization</i>	127
III. RESULTS AND DISCUSSION.....	128
<i>III.1. Synthesis of the α-hydroxy, α'-carboxylate poly(ethylene oxide) macroinitiator</i>	128
<i>III.2. Synthesis of the [PEO-<i>b</i>-PMLABz]-OH copolymer</i>	135
<i>III.3. Synthesis of the s[(PEO)(PMLABz)(PCL)] miktoarm star-shaped copolymer by ring-opening polymerization of ϵ-CL</i>	139
IV. CONCLUSIONS.....	141

I. Introduction

Increasing attention is paid nowadays to the synthesis and characterization of ABC miktoarm star-shaped copolymers that consist of three different polymer chains emanating from a central junction point.^{1,2,3-9} Whenever the three arms are sufficiently long and immiscible, a nanophase separation occurs, with formation of long range nanostructures different from those formed by the linear counterparts of the same composition.^{4,5,6} Adsorption of triarm star-block copolymers of polystyrene, poly(ethylene oxide) and poly(ϵ -caprolactone) at the surface of titanium dioxide particles in toluene is significantly different from that of the parent diblock copolymers.⁷ Micellization of this type of ABC copolymers in organic solvents^{4,8}, and, recently, in water has also been investigated.⁹

Several methods have been used to synthesize ABC star-shaped terpolymers, including the use of a trifunctional initiator and the sequential polymerization of the parent monomers.² An alternative method consists of adding a living polymer A to the reactive end-group of a preformed polymer B with formation of an initiator species for the polymerization of the third comonomer C at the junction point of the diblock copolymer.¹⁰ The sequential polymerization of the comonomers A and B can also be initiated by an α, α' -bifunctional macroinitiator C.¹¹ This strategy has been used in this work to prepare an ABC miktoarm star-shaped terpolymer, in which the three arms are biocompatible/bioresorbable. Indeed, hydrophilic α -hydroxy, α' -carboxylate- ω -methoxy-poly(ethylene oxide) [PEO-(OH)-COO⁻] has been designed as a macroinitiator for the sequential synthesis of two biocompatible/ biodegradable polyesters, i.e., poly(benzyl β -malolactonate) (PMLABz), and poly(ϵ -caprolactone) (PCL). Although these two polyesters are hydrophobic, PMLA is easily converted into hydrophilic pH-responsive poly(β -malic acid) (PMLA). Some of us previously reported the anionic polymerization of ethylene oxide initiated by the potassium alkoxide of 1,4-dioxaspiro[4.5]decan-8-ol, followed by the Bayer-Villiger oxidation of the cyclohexanone end-group into an ϵ -caprolactone one.¹² The hydrolysis of the lactone end-group can release the desired carboxylate and hydroxyl species, as shown in Scheme 1. Polymerization of benzyl β -malolactonate (MLABz) is initiated by potassium carboxylate even in the presence of hydroxyl groups.¹³ Moreover, the polymerization of ϵ -caprolactone is commonly initiated by alcohols in the presence of a tin catalysts.^{14,15}

The composition of the envisioned copolymer makes it unique. It is indeed potentially biocompatible,^{14,16} two of the constitutive blocks are biodegradable,^{17,18} and the

third one (PEO) can be eliminated from the human body if it is of low enough molar mass. Moreover, the amphiphilicity of this copolymer is largely tunable because one block is hydrophilic (PEO), another one is hydrophobic (PCL) and the third one (PMLABz) can be made hydrophilic upon hydrogenation into a pH-responsive block. Because of the unique combination of different blocks in a star-shaped architecture, the new $s[(\text{PEO})(\text{PMLABz})(\text{PCL})]$ copolymer is expected to have potential in the biomedical field.

II. Experimental Part

Materials.

ϵ -Caprolactone (ϵ -CL) (Aldrich, 99%) was dried over calcium hydride under stirring at room temperature for 48 h and distilled under reduced pressure before use. Methylene chloride (CH_2Cl_2) and pyridine were dried by refluxing over calcium hydride for at least 48 h and distilled prior to use. 1,4-Dioxaspiro[4.5]decan-8-one (Fluka, > 97 %), lithium aluminum hydride (LiAlH_4) (Aldrich, 95%), ethylene oxide (EO) (Messer), potassium hydroxide (KOH) (ChemLab, > 85 %), methyl iodide (CH_3I) (Aldrich, 99,5%), *m*-chloroperbenzoic acid (*m*-CPBA) (Fluka, 70%), diethyl ether (Vel) were used as received. (*R,S*)-Benzyl β -malolactonate (MLABz) was synthesized from aspartic acid and purified as reported elsewhere.¹⁹ It was stored at -18°C , distilled under reduced pressure, and dried by three successive distillations of toluene prior to use. 18-Crown-6 ether (ChemLab, 99%) was dried by three successive azeotropic distillations of toluene. A 0.06M solution of tin (II) bis(2-ethylhexanoate) ($\text{Sn}(\text{Oct})_2$) (ABCR) was prepared in dry toluene. Toluene and tetrahydrofuran (THF) (Labscan, 99%) were dried by refluxing over CaH_2 and Na/benzophenone complex, respectively. THF was further dried over lithium polystyryl oligomers and distilled under reduced pressure, just prior to use.

Synthesis of ϵ -caprolactone end-capped PEO (γ PEO.CL), (1).

The living anionic polymerization of ethylene oxide was initiated by the potassium alkoxide of 1,4-dioxaspiro[4.5]decan-8-ol, followed by derivatization of the α -acetal end-group of PEO into a ketone, followed by the Baeyer-Villiger oxidation of this ketone into a lactone, as detailed elsewhere.¹² The ω -hydroxyl end-group was methylated by reaction with 2.5 equiv of CH_3I in toluene at 40°C for 12 h. The macromonomer (γ PEO.CL) was purified by repeated precipitations (4 times) in diethyl ether in order to remove impurities

(e.g., residual acid after the Baeyer-Villiger reaction). γ PEO.CL was dried by three azeotropic distillations of toluene, heated at 45°C in *vacuo* overnight, and stored at -20°C. Purity and end-functionalization were assessed by Matrix-Assisted Laser Desorption/Ionization Time-of-flight (MALDI-Tof) analysis and $^1\text{H-NMR}$ spectroscopy (Figure 1). MALDI-Tof analysis confirmed the complete methylation of the ω -chain-ends.¹²

Yield: 31 %, $M_{n, \text{NMR}} = 600 \text{ g/mol}$, $M_w/M_n = 1.10$. $^1\text{H-NMR}$ (CDCl_3 , δ ppm, Figure 1): 1.8-2.1 (*m*, $4\text{H}_{\text{b+b'+d+d'}}$), 2.40 (*m*, $1\text{H}_{\text{e'}}$), 2.98 (*m*, 1H_{e}), 3.36 (*s*, 3H_{y}), 3.6 (*M*, $n \times 4\text{H}_{\text{x}}$), 4.05 (*m*, $1\text{H}_{\text{a'}}$), 4.5 (*t*, 1H_{a}).

Synthesis of the α -hydroxy, α' -carboxylate PEO macroinitiator [PEO-(OH)-COO $^-$ K $^+$], (2**) - Scheme 1.**

In a typical experiment, 0.8 ml of a 1M aqueous KOH solution (0.8 mmol) was added to 0.5 g of γ PEO.CL **1** (0.83 mmol) previously dissolved in 5 ml of double-distilled water. The reaction proceeded under vigorous stirring at room temperature for 2 h. The solution was filtered through a 0.2 μm Millex syringe filter unit, then lyophilized for one night, and dried by repeated azeotropic distillation of toluene. The product (0.4 g) was stored under nitrogen at -20°C.

Yield: 80 %, $M_{n, \text{NMR}} = 600 \text{ g/mol}$, $M_w/M_n = 1.34$. $^1\text{H-NMR}$ ($\text{D}_2\text{O} + \text{KOH}$, δ ppm, Figure 4): 1.7-1.85 (*m*, $4\text{H}_{\text{b+d}}$), 2.25 (*m*, 2H_{e}), 3.35 (*s*, 3H_{y}), 3.5-3.8 (*m*, $2\text{H}_{\text{a}} + 1\text{H}_{\text{c}} + n \times 4\text{H}_{\text{x}}$).

Synthesis of the [PEO-*b*-PMLABz]-OH diblock copolymer, (3** and **4**) - Scheme 2.**

In a previously flame-dried and nitrogen-purged round bottom flask, 0.12 g of **2** ($2.0 \times 10^{-4} \text{ mol}$) was dried by three azeotropic distillations of toluene, then dried at 50°C in *vacuo* overnight, and dissolved in 6 ml of dried THF. This solution was added to 0.058 mg of previously dried 18-crown-6 ether ($2.2 \times 10^{-4} \text{ mol}$) and thermostated at 0°C for 20 minutes. The polymerization of (R,S)- benzyl β -malolactonate (0.626 g, $3.0 \times 10^{-3} \text{ mol}$) was typically conducted in a previously flame-dried and nitrogen-purged round bottom flask equipped with a three-way stopcock and a septum by initiation with the complex formed between **2** and the 18-crown-6 ether in 14 ml THF at 0°C. The monomer conversion was monitored by IR spectroscopy until completeness (170 min) (disappearance of the signal of the carbonyl characteristic of the lactone at $1846 \text{ cm}^{-1}(\nu_{\text{C=O}})$).¹³ After addition of a few

drops of aqueous HCl (0.1M), the solvent was evaporated, the solid residue was dissolved in chloroform (10 ml) and the solution was extracted three times with a saturated aqueous solution of KCl (3 x 10 ml) and with deionized water (2 x 10 ml). Finally, the organic phase was poured into 8 volumes of cold heptane (100 ml), the polymer was recovered by filtration and dried under reduced pressure at 35°C until constant weight, i.e., 0.625 g.

Yield: 89 %, $M_{n, \text{NMR}} = 3700 \text{ g/mol}$, $M_w/M_n = 1.32$. $^1\text{H-NMR}$ (CDCl_3 , δ ppm, Figure 9): 1.6-1.9 (*m*, $4\text{H}_{\text{b+d}}$), 2.9 (*m*, $p \times 2\text{H}_{\text{h}}$), 3.35 (*s*, 3H_{y}), 3.6 (*M*, $n \times 4\text{H}_{\text{x}}$), 5.15 (*m*, $p \times 2\text{H}_{\text{i}}$), 5.51 (*m*, $p \times 1\text{H}_{\text{g}}$), 7.30 (*m*, $p \times 5\text{H}_{\text{j}}$).

The carboxylic acid end-group of the diblock copolymer (**3**) was esterified to (**4**), as follows. In a previously flame-dried and nitrogen-purged round-bottom flask, 0.30 g of **3** ($8.11 \times 10^{-5} \text{ mol}$, $M_n = 3700 \text{ g/mol}$) was dried by three azeotropic distillations of toluene ($3 \times 5 \text{ ml}$), and then dissolved in a mixture of 20 ml toluene and 2 ml of anhydrous methanol. Nine equivalents of trimethylsilyldiazomethane (0.50 ml, $9.84 \times 10^{-4} \text{ mol}$) were added and the reaction was carried out under nitrogen at room temperature.²⁰ Nitrogen was evolved through an oil valve. After three hours, the reaction was stopped by addition of a few drops of 0.1M acetic acid, and the volatile compounds were removed under reduced pressure. The copolymer was recovered by precipitation in cold heptane, filtered and dried under reduced pressure at 35°C until constant weight (0.26 g).

Yield: 85 %. $^1\text{H-NMR}$ (CDCl_3 , δ ppm): 1.6-1.9 (*m*, $4\text{H}_{\text{b+d}}$), 2.9 (*m*, $p \times 2\text{H}_{\text{h}}$), 3.35 (*s*, 3H_{y}), 3.6 (*M*, $n \times 4\text{H}_{\text{x}}$), 3.7 (*s*, 3H_{z}), 5.15 (*m*, $p \times 2\text{H}_{\text{i}}$), 5.51 (*m*, $p \times 1\text{H}_{\text{g}}$), 7.30 (*m*, $p \times 5\text{H}_{\text{j}}$).

Synthesis of the $s[(\text{PEO})(\text{PMLABz})(\text{PCL})]$ star-shaped copolymer, (**5**) - Scheme 2

In a previously flame-dried and nitrogen-purged round-bottom flask, 0.16g of **4** (0.043 mmol, $M_n = 3700 \text{ g/mol}$, $M_w/M_n = 1.32$) was dried by three azeotropic distillations of toluene (3 x 10 ml), kept *in vacuo* at 45°C overnight, dissolved in 10 ml of dry toluene and finally added with 0.11 ml of freshly distilled ϵ -caprolactone (1 mmol). After heating under stirring at 80°C, 0.36 ml of 0.06 M $\text{Sn}(\text{Oct})_2$ (0.5 equiv with respect to the hydroxyl groups) was rapidly injected through a septum, and the polymerization occurred for 24 h. After addition of a few drops of 0.1M aqueous HCl solution, the polymer solution was filtered and poured into 10 volumes of cold heptane (100 ml). After one night at -20°C , the polymer was recovered by filtration and dried *in vacuo* until constant weight (0.18 g).

Yield: 66 %, $M_{n, \text{NMR}} = 6200 \text{ g/mol}$, $M_w/M_n = 1.50$. $^1\text{H-NMR}$ (CDCl_3 , δ ppm, Figure 11): 1.38 (*m*, $q \times 2\text{H}_{\text{m}}$); 1.64 (*m*, $q \times 4\text{H}_{\text{n,i}}$); 1.6-1.9 (*m*, $4\text{H}_{\text{b+d}}$); 2.30 (*t*, $q \times 2\text{H}_{\text{o}}$); 2.9 (*m*,

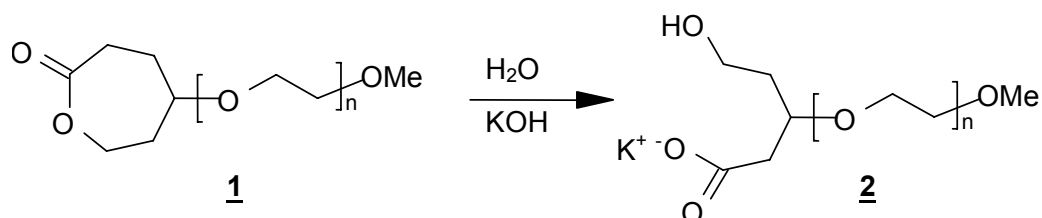
$p \times 2H_h$); 3.35 (*s*, $3H_y$); 3.64 (*M*, $n \times 4H_x$); 4.05 (*t*, $q \times 2H_k$); 5.15 (*m*, $p \times 2H_i$); 5.51 (*m*, $p \times 1H_g$); 7.30 (*m*, $p \times 5H_j$).

Characterization.

$^1\text{H-NMR}$ (400 MHz) spectra were recorded in CDCl_3 at 25°C with a Bruker AM 400 apparatus. The molecular weight of the PEO chains was calculated from the relative intensity of the protons of the methoxy end-group ($I_{3.35\text{ppm}} : 3$) and the methylene protons ($-\text{CH}_2-\text{CH}_2-\text{O}$) ($I_{3.6\text{ppm}} : 4$) of the monomer unit. The completeness of the conversion of the PEO hydroxyl end-group into a methoxy one as assessed by the relative intensity of the protons characteristic of both the α ($I_{4.5\text{ppm}}$) and the ω ($I_{3.35\text{ppm}} : 3$) end-groups and confirmed by Matrix-Assisted Laser Desorption/Ionization Time-of-flight (MALDI-Tof) analysis. MALDI-Tof spectra were recorded with a PerSeptive Biosystem Voyager-DE STR MALDI-Tof spectrometer equipped with 2 m linear and 3 m reflector flight tubes and a 337 nm nitrogen laser (3 ns pulse). Mass spectra were recorded at an accelerating potential of 20 kV in positive ion linear or reflectron mode. The data ($M_{n,\text{MALDI}}$ values in Table 1) were processed with the Polymerix software, and the isotope calculator tool of Data Explorer (software supplied by Applied Biosystems) was used for making the isotopic distributions available. A PEO standard with a molecular weight of 1900 g/mol (1 mg/ml THF) was used for calibration. Polymer samples were dissolved in THF (1 mg/ml THF). Dithranol (20 mg/ml THF) was used as a matrix and no cationating agent was added. Size-exclusion chromatography (SEC) was carried out in THF at a flow rate of 1 ml/min at 45°C using a SFD S5200 Autosampler liquid chromatograph equipped with a SFD refractometer index detector 2000 and columns PL gel $5\mu\text{m}$ (columns porosity: 10^2 , 10^3 , 10^4 , 10^5\AA). Polystyrene (PS) and PEO standards were used for calibration. FTIR analysis was carried out with a Bio-Rad Excalibur FTIR spectrometer (resolution: 0.2 cm^{-1}). Spectra were recorded (from 4000 to 700 cm^{-1}) with a single reflection crystal system (Split PEA from Harrick) and a DTGS detector. Films of PEO and derivatives were solvent-cast on NaCl and analyzed with a Perkin Elmer FTIR 1720X spectrometer.

III. Results and discussion

III.1. Synthesis of the α -hydroxy, α' -carboxylate poly(ethylene oxide) (PEO) macroinitiator [PEO-(OH)-COO⁻K⁺], (**1**) and (**2**) - Scheme 1



Scheme 1. Hydrolysis of γ -(ϵ -caprolactone) poly(ethylene oxide) [γ PEO.CL] to α -hydroxy, α' -carboxylate poly(ethylene oxide) [PEO-(OH)-COO⁻K⁺]

An α,α' -heterobifunctional PEO macroinitiator was designed for the synthesis of a $s[(\text{PEO})(\text{PMLABz})(\text{PCL})]$ miktoarm star-shaped copolymer, in which PEO stands for poly(ethylene oxide), PMLABz stands for poly(benzyl β -malolactonate) and PCL for poly(ϵ -caprolactone). This macroinitiator is actually a PEO chain with two functional α end-groups: (i) a potassium carboxylate function, which selectively initiates the ring-opening polymerization (ROP) of benzyl β -malolactonate, and (ii) a hydroxyl group, which is commonly used for the controlled polymerization of ϵ -caprolactone (ϵ -CL) in the presence of a tin octoate catalyst (Sn(Oct)₂). Some of us reported elsewhere the α -end-capping of ω -methoxy PEO by an ϵ -caprolactone unit (**1**), or conversely the substitution of ϵ -caprolactone in γ -position by a PEO chain (γ PEO.CL), so leading to a PEO macromonomer.¹²

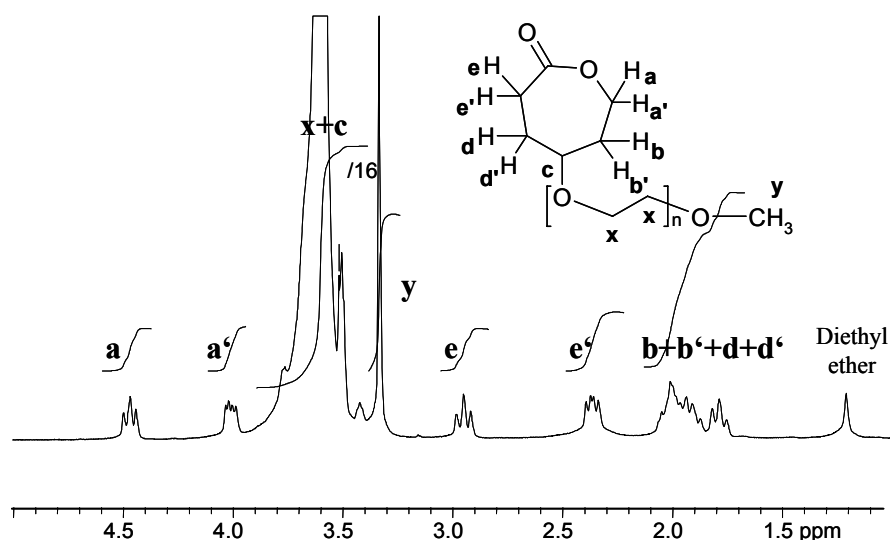


Figure 1. ¹H-NMR spectrum for the γ -(ϵ -caprolactone) poly(ethylene oxide) macromonomer [γ PEO.CL] **4a** (Table 1) in CDCl₃, after precipitation in diethyl ether

A typical ¹H-NMR spectrum of γ PEO.CL is shown in Figure 1 with peak assignment. The broad signal at 3.6 ppm is characteristic of the methylene protons (H_x) of the PEO chain. Because of substitution by the PEO segment, the quick interconversion of the axial and equatorial protons (H_a and H_{a'} or H_e and H_{e'}) of the CL ring is limited. Therefore, these four protons (a and a' and e and e') next to the ester group are not magnetically equivalent, which is quite consistent with the structure expected for the macromonomer and are evidence for the polymerizable lactone head. Figure 1 shows also two multiplets for protons b, b' and d, d'. The first multiplet at 1.7 ppm (triplet) corresponds to one proton, the second at about 2.0 ppm corresponds to three protons, as result of inequivalent chemical shift for protons (b, b', d, d') in the α -position of an asymmetric carbon that cannot be exchanged by rotation. Upon hydrolysis of the lactone ring by KOH, the γ PEO.CL macromonomer has been converted into the desired dual macroinitiator (**2**, Scheme 1). An excess of KOH (2.5 equiv., with respect to the lactone end-group) was used in the first experiments and this excess was neutralized by HCl after hydrolysis, followed by dialysis against distilled water (desalting). The polymer was recovered by lyophilization, dried by azeotropic distillations of toluene, heated at 40°C for one night in *vacuo*, and finally analyzed by SEC, MALDI-Tof and ¹H-NMR spectroscopy. The SEC chromatogram is bimodal with a shoulder on the high molecular weight side and a main peak at the same elution volume as the initial γ PEO.CL (chromatogram not shown).

Table 1. Macromolecular characteristics of poly(ethylene oxide) (PEO) derivatives: γ -(ϵ -caprolactone) poly(ethylene oxide) [γ PEO.CL] (1**) and (**2**) γ PEO.CL after hydrolysis with KOH**

	<i>PEO derivative</i>	$M_{n,NMR}^a$	$M_{n,MALDI}^b$
1	γ PEO.CL	780	750
			760
2a	PEO-(OH)-COOH	800	1400 ^c
			2200 ^d
2b	PEO-(OH)-COOH	800	760

^a M_n calculated by ¹H-NMR, ^b determined by MALDI-Tof, linear mode, ^c second population observed by MALDI-Tof, linear mode, ^d third population observed by MALDI-Tof, linear mode

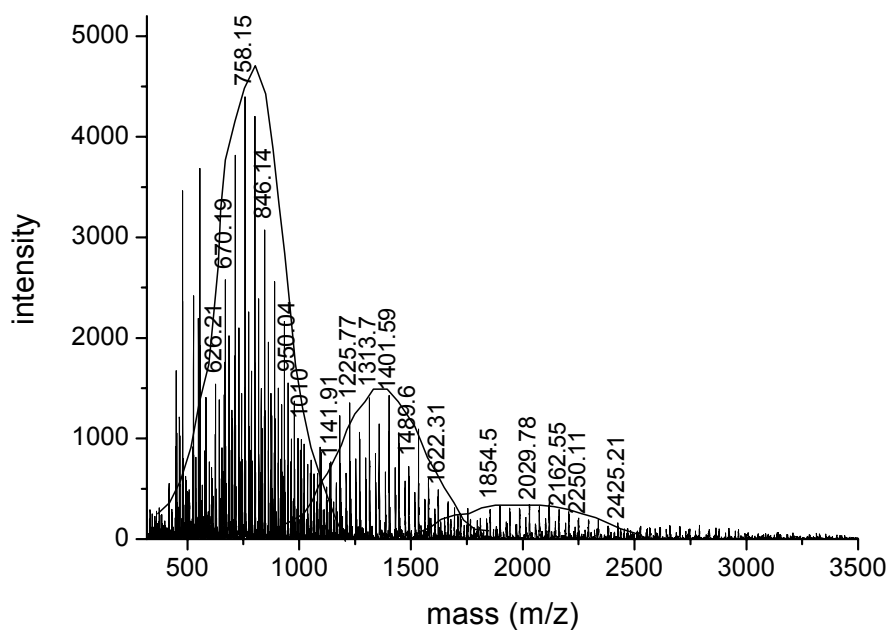


Figure 2. MALDI-Tof spectrum (linear mode) of γ -(ϵ -caprolactone) poly(ethylene oxide) [γ PEO.CL] treated by KOH according to non optimized conditions (product **2a, table 1)**

Consistently, higher molecular weight species have been observed by MALDI-Tof. Figure 2 shows the MALDI-Tof spectrum in the 319 to 3000 m/z mass range, which emphasizes that three mass populations coexist. The first one has the expected molecular weight ($M_{n,NMR} = 800$ g/mol; $M_{n,MALDI} = 760$ g/mol, Table 1 entry 2a and Figure 2), the second population appears at the double molecular weight ($M_{n,MALDI} = 1400$ g/mol, Table 1 entry 2a) and the molar mass of the third population is three times the molar mass of the

first distribution ($M_{n, \text{MALDI}} = 2200 \text{ g/mol}$). The molecular weight and shape for the main series of the first population fit the Na^+ and K^+ adducts of the α -hydroxy- α' -carboxylate- ω -methoxy PEO [PEO-(OH)-COO $^-$] (detailed spectrum not shown). The main series of the higher molecular weight compounds shown in Figure 3 (detailed experimental isotope distribution of the second (Figure 3a) and third (Figure 3b) mass population) can be accounted for by the dimerization and trimerization of the γ PEO.CL macromonomer (assignment in Table 2).

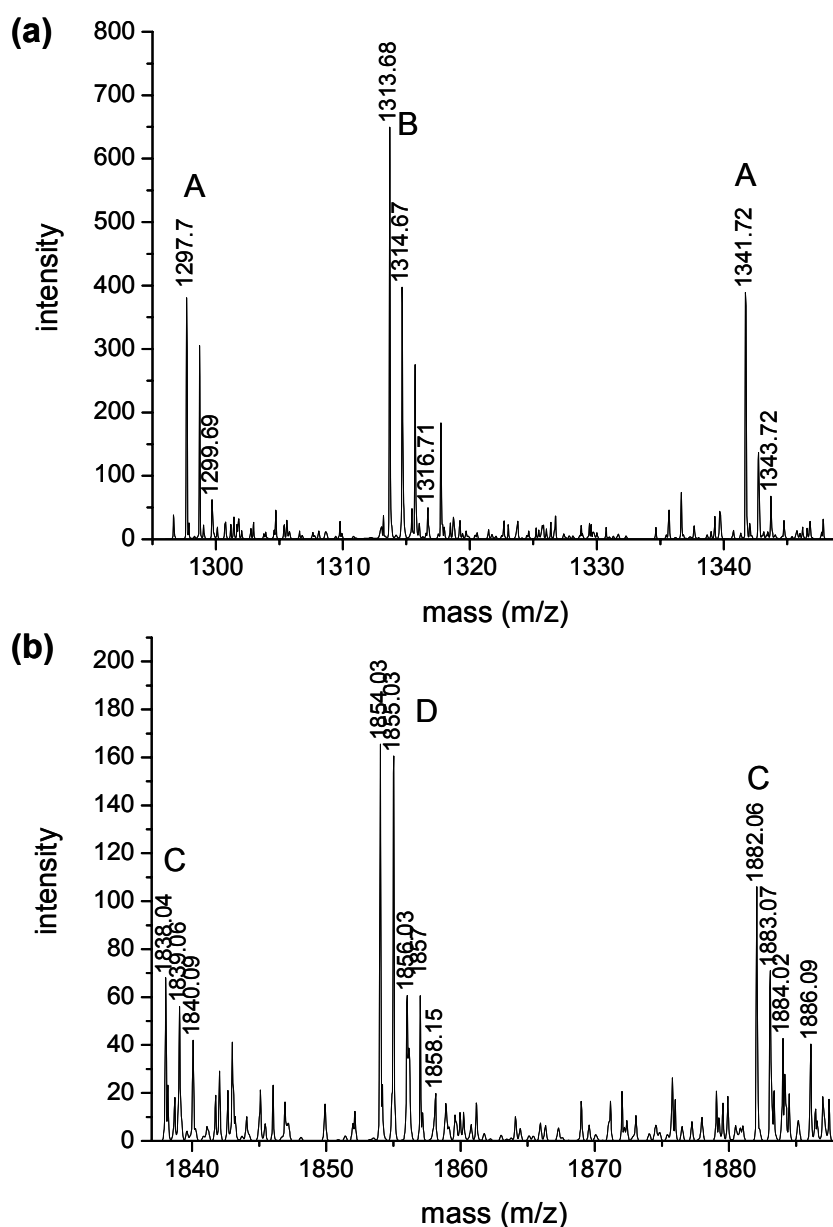
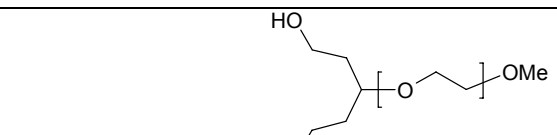
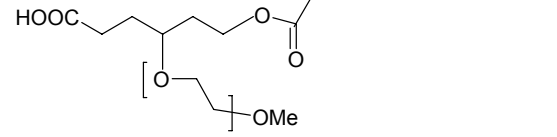
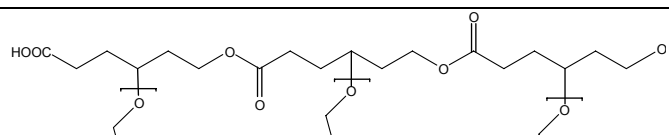
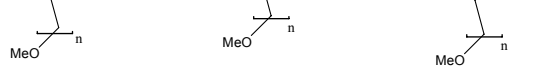


Figure 3. Detail of the experimental isotope distribution MALDI-ToF spectrum for the sample 2a (Table 1) (reflectron mode): (a) second molecular weight population (dimerization), (b) third molecular weight population (trimerization)

Table 2. Peak assignments for the second and third molecular weight population of sample 2a (Table 1) in Figure 3 a) and b)

<i>code</i>	<i>cation</i>		<i>structure</i>	<i>bruto formula</i>
A	dimer	Na		$(C_2H_4O)_{22}C_{14}H_{26}O_7Na$
B	dimer	K		$(C_2H_4O)_{22}C_{14}H_{26}O_7K$
C	trimer	Na		$(C_2H_4O)_{31}C_{21}H_{38}O_{10}Na$
D	trimer	K		$(C_2H_4O)_{31}C_{21}H_{38}O_{10}K$

To prevent this undesired condensation reaction from occurring, the experimental conditions were modified. KOH (1 equiv) was used instead of an excess previously used. Just after hydrolysis, the polymer was recovered, dried (cf. supra) and directly used to initiate the polymerization of benzyl β -malolactonate (MLABz) in the presence of 18-crown-6-ether.

The 1H -NMR spectrum of the lactone end-capped PEO after treatment with ca. 1 equiv of KOH (Figure 4) is significantly different from the initial 1H -NMR spectrum (Figure 1).

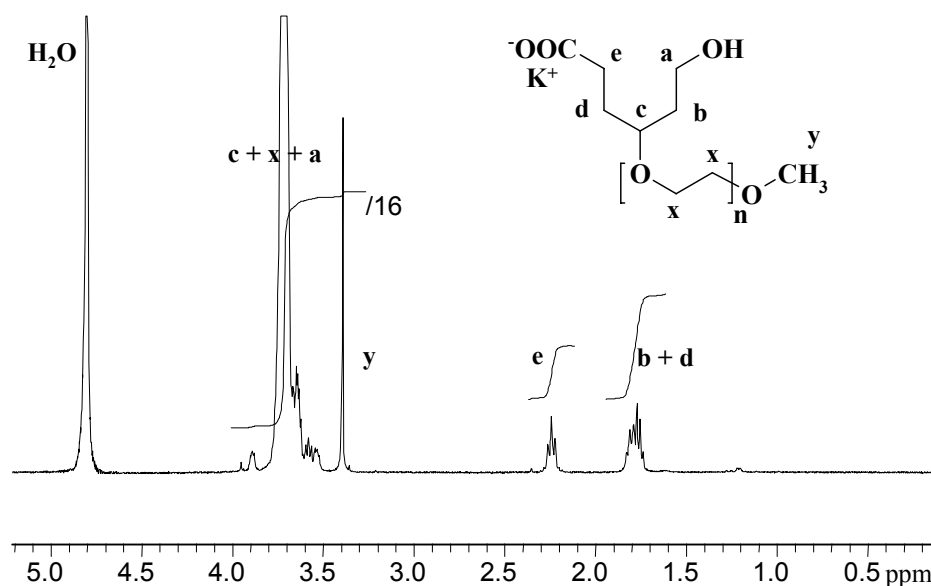


Figure 4. 1H -NMR spectrum for α -hydroxy, α' -carboxylate poly(ethylene oxide) [PEO-(OH)-COO $^-$ K $^+$] recorded in D_2O after hydrolysis with KOH

Fewer peaks are observed because of more rotation freedom for the alkyl chains as result of the ring-opening. Therefore, only one signal is observed for the protons H_a and H_e, respectively, instead of the original splitting. These peaks are observed at lower chemical shifts, the signal of proton H_a being hidden by the broad peak of PEO. ¹H-NMR spectroscopy confirms the completeness of the ring-opening of the lactone by the complete disappearance of the initial protons H_e and H_a. Similarly, the two protons H_b and H_{b'}, and H_d and H_{d'} (Figure 1) are now chemically equivalent and observed as a broad peak at 1.7 ppm (Figure 4). However, whenever an excess of KOH is used, the hydrolysis product is contaminated by condensation products, an additional peak is observed at 4.15 ppm, as previously observed for copolymers of the γ PEO.CL macromonomer with ϵ -caprolactone.¹²

SEC analysis of γ PEO.CL before and after alkaline hydrolysis with 1 equiv of KOH shows that M_n remains quasi unchanged with a slight shift towards smaller M_n and a slight increase in M_w/M_n (Table 4, chromatograms not shown). Moreover, MALDI-Tof analysis of the as-prepared PEO-macroinitiator shows only one population at M_{n, MALDI} = 760 g/mol (Table 1, entry 2b) and no chains of higher molecular weight (Figure 5).

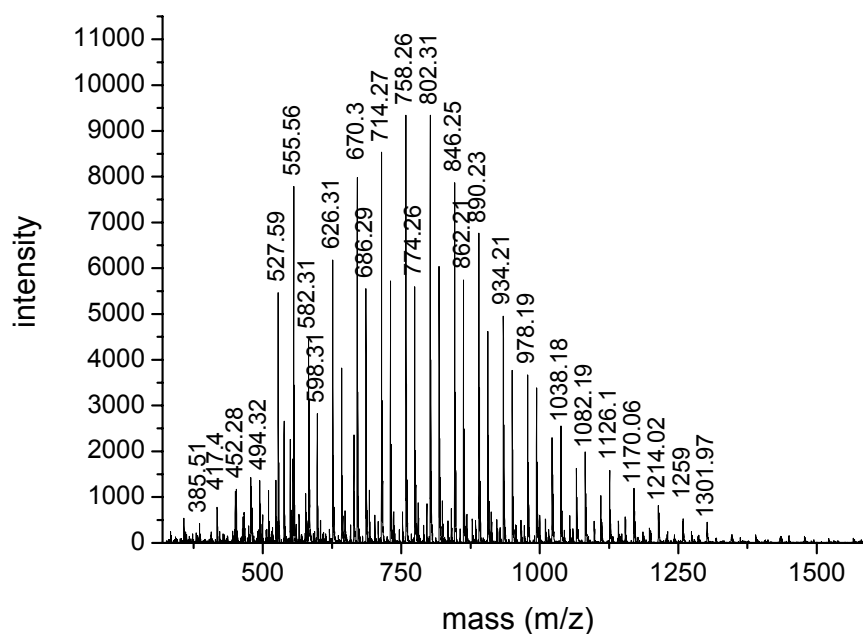


Figure 5. MALDI-Tof spectrum (linear mode) for γ PEO.CL treated by KOH according to optimized conditions (Table 1, product 2b)

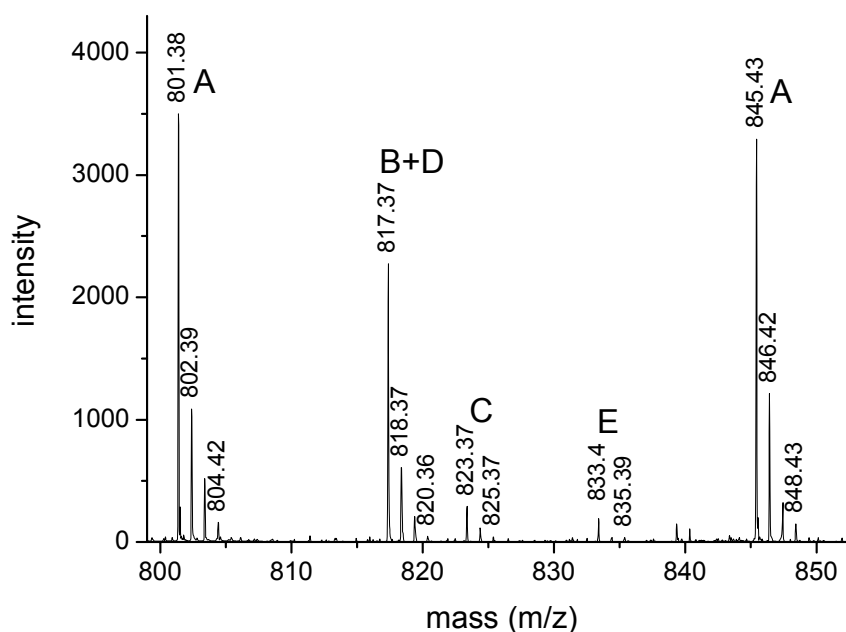


Figure 6. Detail of the experimental isotope distribution MALDI-ToF spectrum for the sample 2b (Table 1) (reflectron mode)

Figure 6 shows a detail of the experimental isotope distribution of the MALDI-ToF spectrum, and the peak assignment is reported in Table 3. The main series have the shape and isotope distribution expected for the desired product, which confirms the success of the lactone-hydrolysis.

Table 3. Peak assignments for the MALDI spectrum of Figure 6 (sample 2b)

<i>code</i>	<i>description</i>	<i>cation</i>	<i>structure</i>	<i>bruto formula</i>
A	desired	Na		$(C_2H_4O)_{14}C_7H_{14}O_4Na$
B	desired	K		$(C_2H_4O)_{14}C_7H_{14}O_4K$
C	desired	H		$(C_2H_4O)_{15}C_7H_{14}O_4H$
D	unmodified PEG	Na	$CH_3OCH_2CH_2(OCH_2CH_2)_nOCH_3$	$(C_2H_4O)_{16}C_4H_{10}O_2Na$
E	unmodified PEG	K	$CH_3OCH_2CH_2(OCH_2CH_2)_nOCH_3$	$(C_2H_4O)_{16}C_4H_{10}O_2K$

Finally, the IR spectrum of the γ PEO.CL (Figure 7, trace A) shows a strong absorption at 1740 cm^{-1} , characteristic of the C-O stretching to the lactone group. Upon hydrolysis by KOH, this absorption disappears in favor of a peak at 1576 cm^{-1} , assigned to the C-O stretching of the carboxylate group (Figure 7, trace B). Furthermore, the broad absorption from 2700 cm^{-1} to 3500 cm^{-1} in spectrum B confirms the formation of hydroxyl groups.

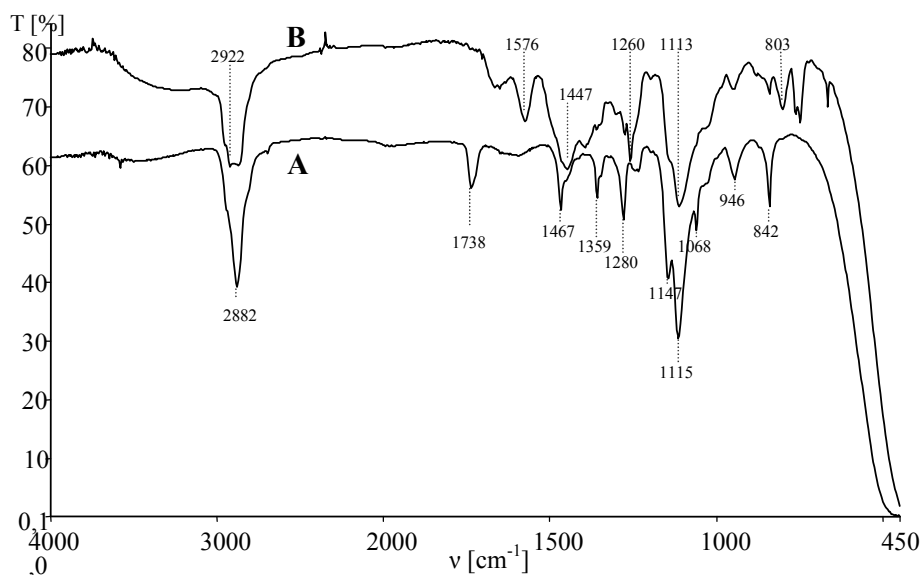


Figure 7. IR spectrum of A) γ PEO.CL; B) γ PEO.CL after treatment with KOH

Therefore, an equimolar amount of KOH (~ 1 equiv) with respect to the PEO end-group has been systematically used in this work, and the hydrolysis products have been characterized by SEC, $^1\text{H-NMR}$ and MALDI-Tof in order to confirm systematically the structure of the dual macroinitiator.

III.2. Synthesis of the [PEO-*b*-PMLABz]-OH copolymer (3) and selective esterification of the carboxylic acid end-group. (4).

Poly(benzyl β -malolactonate), i.e., an aliphatic polyester with pendant protected carboxylic acid groups, can be prepared by an anionic ring-opening polymerization of benzyl β -malolactonate, initiated by either tetraalkylammonium benzoate²¹ or potassium alkanoate added with a ligand, such as 18-crown-6-ether.²² In this work, polymerization of carefully purified MLABz was initiated by PEO-(OH)-COO⁻ K⁺ ligated by 18-crown-6 ether in THF.¹³ Indeed, the potassium carboxylate species are unable to initiate the

polymerization of ϵ -CL²³. A 0.2 mol/l MLABz solution was polymerized in THF at 0°C, with a $[M]_0/[I]_0$ ratio of 15. The progress of polymerization was monitored by FTIR, based on the carbonyl absorption at 1846 cm⁻¹ for the monomer and at 1748 cm⁻¹ for the polymer. Figure 8 shows the FTIR spectra for samples withdrawn from the reaction medium after 80 min (Figure 8, trace A) and 160 min (Figure 8, trace B), respectively, without any purification). Because the absorption by the lactone at 1846 cm⁻¹ was weak after 160 min, the polymerization was stopped 10 min later.

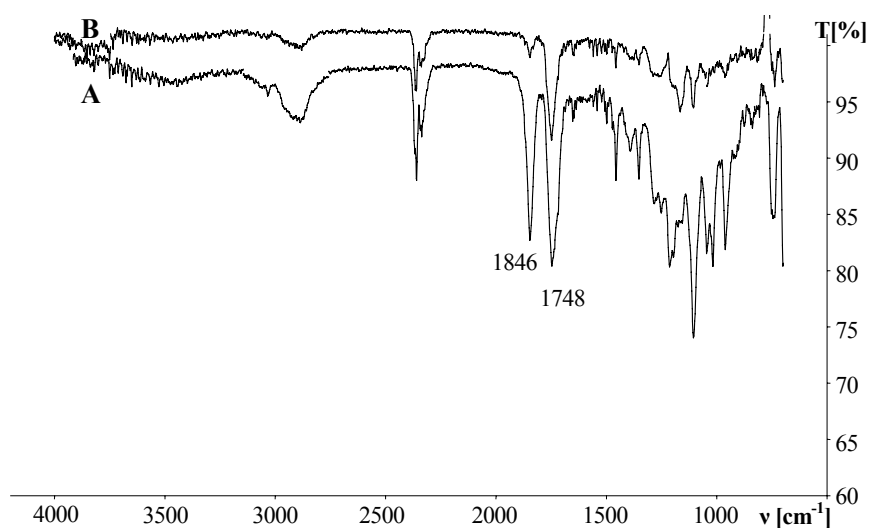


Figure 8. IR spectrum for the benzyl β -malolactonate [MLABz] polymerization initiated by α -hydroxy, α' -carboxylate poly(ethylene oxide) [PEO-(OH)-COO⁻K⁺]/18-crown-6-ether in THF at 0°C under nitrogen, (A) after 80 min of polymerization and (B) after 160 min

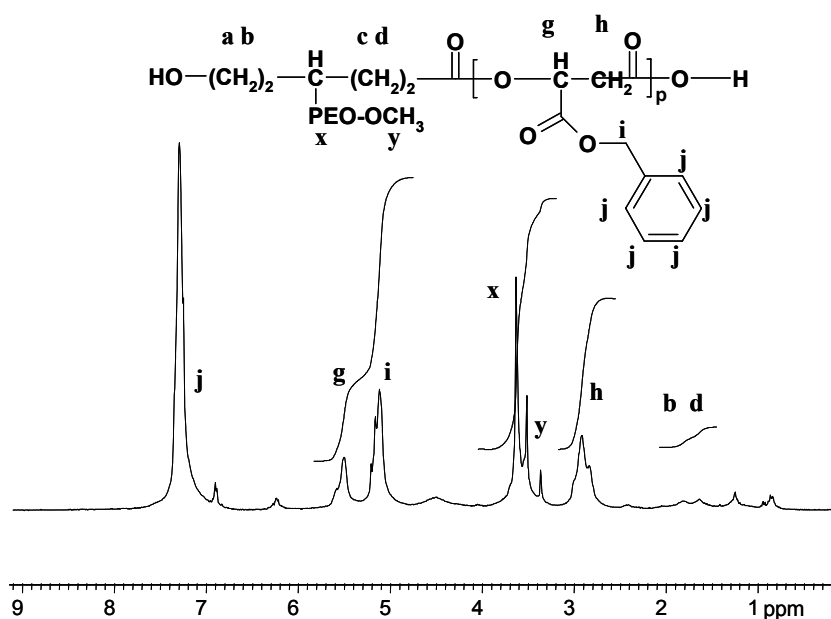


Figure 9. ¹H-NMR spectrum for the [PEO-*b*-PMLABz]-OH copolymer in CDCl₃

Figure 9 shows the $^1\text{H-NMR}$ spectrum of the [PEO-*b*-PMLABz]-OH copolymer after purification by precipitation in heptane. Peaks H_g and H_h present at 5.5 ppm and 2.9 ppm, respectively, can be assigned to the methine and methylene protons of the PMLABz chain. The methylene protons H_i of the protecting benzyl group are observed at 5.1 ppm. The aromatic protons overlap the CHCl_3 protons at 7.3 ppm. The intensity of the methylene protons H_i is two times higher than that one of proton H_g , which indicates that the protecting group is preserved during polymerization. The number-average molecular weight ($M_{n,\text{NMR}}$) of the diblock copolymer has been calculated by eqn. 1, and the result is listed in Table 4.

$$M_{n,\text{NMR}}([\text{PEO-}b\text{-PMLABz}]\text{-OH}) = I_{5.5} / (I_{3.6}/4) \times \text{DP}(\text{PEO}) \times 206 + M_{n,\text{NMR}}(\text{PEO}) \quad (1)$$

Table 4. Macromolecular characteristics of the (co)polymer formed at each synthesis step

#	description	$M_{n,\text{theor}}$	$M_{n,\text{NMR}}^b$	M_w/M_n^e
<u>1</u>	γ PEO.CL	-	600	1.10
<u>2</u>	PEO-(OH)-COO $^-\text{K}^+$	-	600	1.34
<u>3a</u>	[PEO- <i>b</i> -PMLABz]-OH	3700 ^a	3750 ^c	1.32
<u>3b</u>	[PEO- <i>b</i> -PMLABz]-OH	3150 ^a	2800 ^c	1.28
<u>5</u>	$s[(\text{MPEO})(\text{PMLABz})(\text{PCL})]$	6350 ^b	6200 ^d	1.50

^a $M_{n,\text{theor}} = M_n(\text{PEO}) + [\text{MLABz}]_0/[\text{PEO}] \times \text{MW}_{\text{MLABz}}$; ^b $M_{n,\text{theor}} = M_n(\text{PEO}) + M_n(\text{PMLABz}) + [\epsilon\text{-CL}]_0/[[\text{PEO-}b\text{-PMLABz}]\text{-OH}] \times \text{MW}_{\epsilon\text{-CL}}$, at 100% of conversion; ^c calculated by $^1\text{H-NMR}$ according to eqn. 1; ^d calculated by $^1\text{H-NMR}$ according to eqn. 2, ^e As determined by SEC calibrated by PS standards

$I_{5.5}$ and $I_{3.6}$ are the intensities of the peaks for the protons H_g of PMLABz at 5.5 ppm (see Figure 9) and at 3.6 ppm for the methylene protons of PEO. The molecular weight of the MLABz monomer is 206 g/mol; DP (PEO) and $M_{n,\text{NMR}}$ (PEO) are the degree of polymerization and molecular weight of the PEO block, respectively. The experimental M_n agrees well with the theoretical value at 100% conversion (Table 4, samples 3a and 3b). As previously reported, polymerization of MLABz is sensitive to temperature and monomer concentration.¹³ Therefore, polymerization has been carried out at 0°C with an initial MLABz concentration of 0.2 mol/l, in order to restrict undesirable transfer and termination reactions.¹³ Nevertheless, small quantities of fumarate derivatives, i.e., transfer reaction products, are formed as observed by $^1\text{H-NMR}$ spectroscopy (vinyl protons of fumaric

esters: ROOC-CH=CH-COO^-) at 6.8 ppm. High conversion (higher than 90%) and long polymerization time might be an explanation. The success of copolymerization has been assessed by SEC.

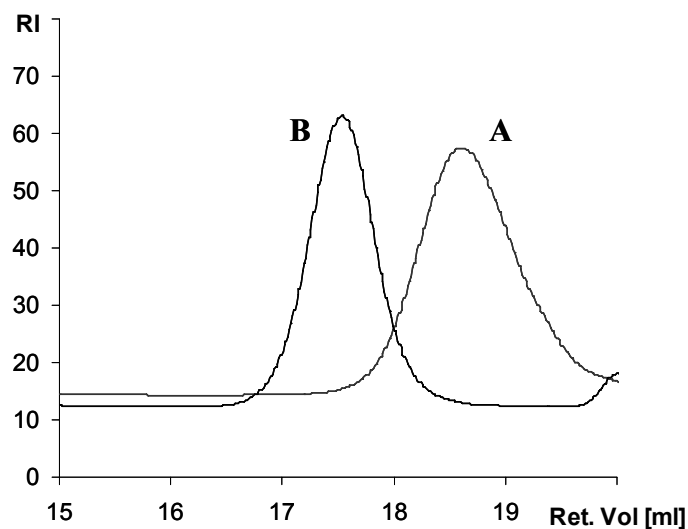
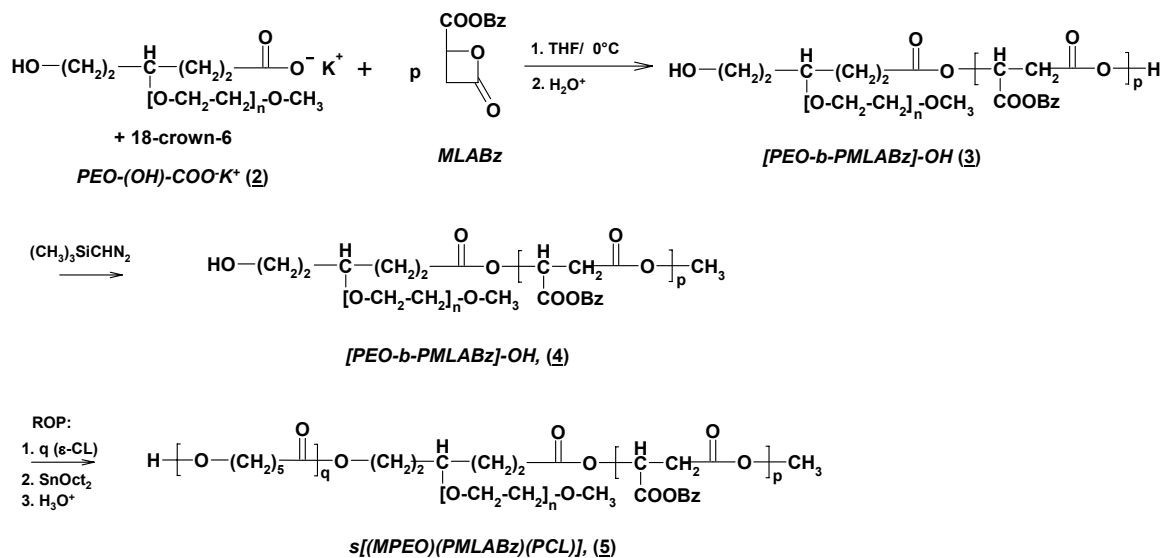


Figure 10. SEC traces for PEO-(OH)-COO-K⁺ (A) and [PEO-*b*-PMLABz]-OH (B)

Figure 10 compares the SEC traces for the PEO macroinitiator (trace A) and the [PEO-*b*-PMLABz]-OH diblock (trace B), respectively. The final chromatogram (trace B) is monomodal, symmetric and completely shifted to smaller elution volumes compared to the initial trace A, consistent with apparently complete initiation by the macroinitiator. It must be noted that the unreacted lactone-end capped PEO (γ PEO.CL) was completely eliminated by precipitation and washing with water. The polydispersity index (Table 4) is quasi the same before (1.34) and after (1.32) polymerization of MLABz.

Prior to synthesis of the third block, the carboxylic acid end-group has been esterified in order to avoid any interference with the subsequent ϵ -caprolactone (ϵ -CL) polymerization. For being selective in the presence of a hydroxyl group at the junction point of the diblock, esterification has been carried out with 9 equivalents of trimethylsilyldiazomethane²⁰ (with respect to the carboxylic group). Resonance of the ω -methoxycarbonyl end-group has been observed by ¹H-NMR at 3.7 ppm.

III.3. Synthesis of the s[(PEO)(PMLABz)(PCL)] miktoarm star-shaped copolymer by ring-opening polymerization of ϵ -CL, (5) – Scheme 2.



Scheme 2. Synthesis of the star-shaped s[(PEO)(PMLABz)(PCL)] copolymer

Ring-opening polymerization of ϵ -caprolactone (ϵ -CL) has been initiated by the pendant hydroxyl group at the junction of the PEO and PMLABz blocks using tin (II) bis(ethyl hexanoate) (Sn(Oct)₂) as a catalyst. Sn(Oct)₂ has been reported to react with hydroxyl groups with the fast and reversible formation of tin(II)alkoxide initiating species.^{14,15} So, for a [ROH]/[Sn(Oct)₂] ratio higher than 2, ROH is not only an initiator but also a chain transfer agent.¹⁴

The ϵ -CL polymerization has been initiated in toluene at 80°C, with an initial monomer to hydroxyl molar ratio of 23 and with 0.5 equivalent of Sn(Oct)₂ with respect to the hydroxyl groups. After 5 h, the ϵ -CL conversion is only 10% as estimated by ¹H-NMR, which points out a much slower polymerization compared to the ϵ -CL homopolymerization initiated by α -hydroxy-monomethoxyPEO. After 24 h, the polymer has been collected by precipitation in heptane. A typical ¹H-NMR spectrum for the star-shaped copolymer recorded in CDCl₃ is shown in Figure 11.

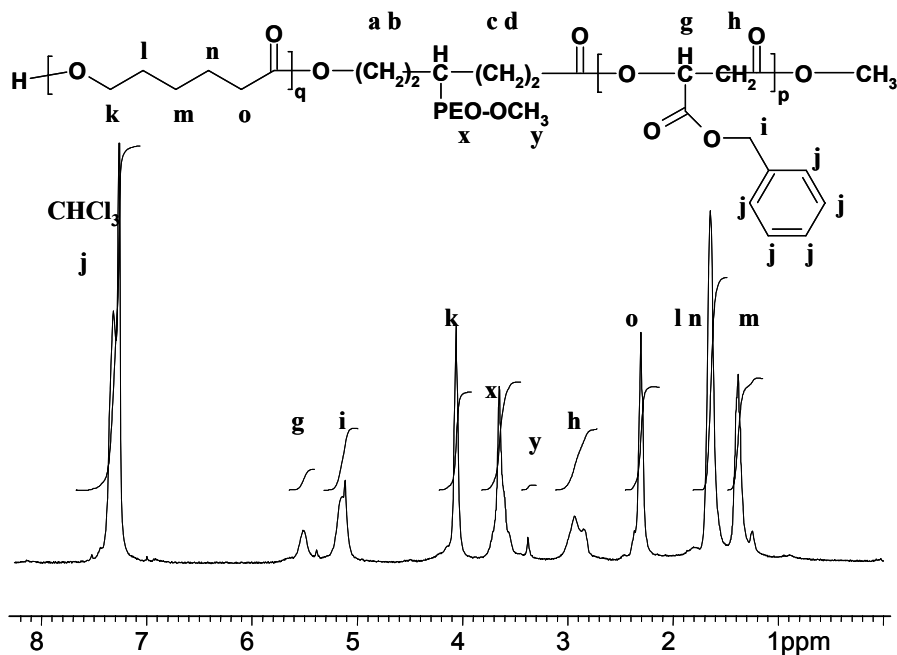


Figure 11. $^1\text{H-NMR}$ spectrum for the ABC $s[(\text{PEO})(\text{PMLABz})(\text{PCL})]$ star-shaped copolymer in CDCl_3

The characteristic methylene protons of PCL appear at 4.05 (H_k), 2.3 (H_o), 1.7 (H_l, H_n) and 1.4 ppm (H_m). On the basis of the molecular weight of the initiating diblock copolymer, the number average molecular weight of the terpolymer has been calculated by eqn. 2

$$M_{n,\text{NMR}} (s[(\text{PEO})(\text{PMLABz})(\text{PCL})]) = [(I_{4.05}/2) / (I_{3.6}/4)] \times \text{DP} (\text{PEO}) \times 114 + M_{n,\text{NMR}} ([\text{PEO-}b\text{-PMLABz}]\text{-OH}) \quad (2)$$

where $I_{4.05}$ and $I_{3.6}$ are the intensities for the protons H_k of PCL values of the peaks at 4.05 ppm (see Figure 11) and for the methylene protons of PEO at 3.6 ppm. 114 is the molecular weight of $\epsilon\text{-CL}$, DP (PEO) is the degree of polymerization of the PEO block and $M_{n,\text{NMR}} ([\text{PEO-}b\text{-PMLABz}]\text{-OH})$ the molecular weight of the diblock copolymer. The experimental degree of $\epsilon\text{-CL}$ polymerization agrees well with the theoretical value (Table 4, sample 5).

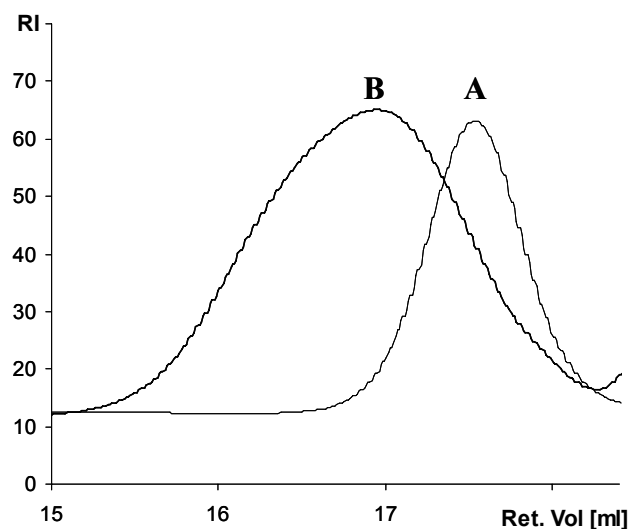


Figure 12. SEC traces for (A) the [PEO-*b*-PMLABz]-OH and (B) the star-shaped $s[(PEO)(PMLABz)(PCL)]$

Figure 12 shows the traces for the [PEO-*b*-PMLABz]-OH diblock copolymer (trace A) and the $s[(PEO)(PMLABz)(PCL)]$ star-shaped copolymer (trace B). The chromatogram B is monomodal with a maximum of the peak shifted towards smaller elution volumes, and a substantially increased polydispersity, more likely in relation to a slow initiation. The slow polymerization of the second and the third block might result from interactions of the propagating species with the first PEO block, which needs however further investigation.

IV. Conclusions

The envisioned ABC miktoarm star-shaped copolymer consisting of PEO, PMLABz and PCL was successfully synthesized, by using a dual PEO macroinitiator. Although the anionic polymerization of the first two segments (PEO and PMLABz) is well controlled and leads to blocks with low polydispersity, the synthesis of the third arm, PCL is more touchy. This polymerization failed in the presence of $AlEt_3$ (not discussed herewith). Although it occurred with $Sn(Oct)_2$, it is slow and the molecular weight distribution is broad. This step needs optimization, before considering the catalytic hydrogenolysis of the benzyl ester functions of the PMLABz block. Then, a pH-sensitive ABC star-shaped copolymer will be formed, with a polyacid block soluble at high pH, and able to trigger micellization at low pH as result of insolubility.

References.

- ¹ Iatrou, H.; Hadjichristidis, N.; *Macromolecules* **1992**, *25*, 4649-4651
- ² He, T.; Li, D.; Sheng, X.; Zhao, B.; *Macromolecules* **2004**, *37*, 3128-3135
- ³ Shi, P.-J.; Li, Y.-G.; Pan, C.-Y.; *Europ. Polymer J.* **2004**, *40*, 1283-1290
- ⁴ Sioula, S.; Hadjichristidis, N.; Thomas, E. L.; *Macromolecules* **1998**, *31*, 5272-5277
- ⁵ Pispas, S.; Hadjichristidis, N.; Potemkin, I.; Khokhlov, A.; *Macromolecules* **2000**, *33*, 1741-1746
- ⁶ Ludwigs, S.; Schmidt, K.; Stafford, C. M.; Amis, E. J.; Fasolka, M. J.; Karim, A.; Magerle, R.; Krausch, G.; *Macromolecules* **2005**, *38*, 1850-1858
- ⁷ Lambert, O.; Amane, J.; Dumas, P.; *Colloids Surfaces A: Physicochem. Eng. Aspects* **1998**, *136*, 263-272
- ⁸ Sotiriou, K.; Nannou, A.; Velis, G.; Pispas, S.; *Macromolecules* **2002**, *35*, 4106-4112
- ⁹ Zhibo, Li; Kesselmann, E.; Talmon, Y.; Hillmyer, M. A.; Lodge, T.P.; *Science* **2004**, *306*, 98-101
- ¹⁰ Fujimoto, T.; Zhang, H.; Kazama, T.; Isono, Y.; Hasegawa, H.; Hashimoto, T.; *Polymer* **1992**, *33*, 2208-2213
- ¹¹ Lambert, O.; Reutenauer, S.; Hurtrez, G.; Dumas, P.; *Macromol. Symp.* **2000**, *161*, 97-102
- ¹² Rieger, J.; Bernaerts, K. V.; Du Prez, F. E.; Jérôme, R.; Jérôme, C.; *Macromolecules* **2004**, *37*, 9738-9745
- ¹³ Coulembier, O.; Degée, Philippe; Cammas-Marion, S.; Guérin, P.; Dubois, P.; *Macromolecules* **2002**, *35*, 9896-9903
- ¹⁴ Storey, R. F.; Sherman, J.W.; *Macromolecules* **2002**, *35*, 1504-1512
- ¹⁵ Kowalski, A.; Duda, A.; Penczek, S.; *Macromol. Rapid Comm.* **1998**, *19*, 567-572
- ¹⁶ Torchilin, V. P.; *Adv. Drug. Deliv. Rev.* **2002**, *54*, 235-252
- ¹⁷ Domurado, D.; Fournié, P.; Braud, C.; Vert, M.; *J. Bioact. Compat. Polym.* **2003**, *18*, 23-32
- ¹⁸ Lee, B.-S.; Vert, M.; Holler, E. in "Biopolymers"; Doi, Y., Steinbüchel, A., Eds.; Wiley-VCH: Weinheim, Germany, **2002**; 3a, p.76-100
- ¹⁹ Cammas, S.; Renard, I.; Langlois, V.; Guérin, P.; *Polymer Chem.* **1986**, *6*, 305-311
- ²⁰ Braud, C; Vert, M.; *Polym. Bull.* **1992**, *29*, 177-183
- ²¹ Mabile, C.; Masure, M.; Hémerly, P.; Guérin, P.; *Polym. Bull.(Berlin)* **1998**, *40*, 381-387

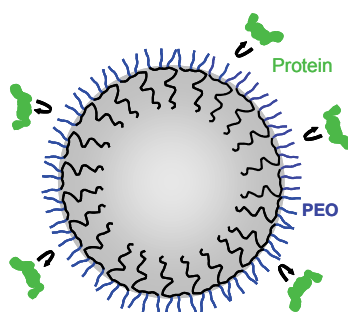
- ²² Cammas-Marion, S.; Béar, M.M.; Harada, A.; Guérin, P.; *Macromol. Chem. Phys.* **2000**, *201*, 355-364
- ²³ Löfgren, A.; Albertsson, A.-C.; Dubois, Ph.; Jérôme, R.; *J. Macromol. Sci. – Rev. Macromol. Chem. Phys.* **1995**, *C35(3)*, 379-418

Chapter 5

Synthesis of amphiphilic copolymers of poly(ethylene oxide) and poly(ϵ -caprolactone) with different architectures and their role in the preparation of stealthy nanoparticles

Abstract

Well-defined copolymers of biocompatible poly(ϵ -caprolactone) (PCL) and poly(ethylene oxide) (PEO) have been synthesized by two methods. Graft copolymers with a gradient structure have been prepared by ring-opening copolymerization of ϵ -caprolactone (ϵ CL) with a PEO macromonomer of the ϵ -caprolactone-type. The ϵ CL polymerization has also been initiated by a PEO macroinitiator with the purpose to prepare diblock copolymers. These amphiphilic copolymers have been used as stabilizers for biodegradable poly(D,L-lactide) (PLA) nanoparticles prepared by a nanoprecipitation technique. The effect of the copolymer characteristic features (architecture, composition and amount) on the nanoparticle formation and structure has been investigated. Average size, size distribution and stability of aqueous suspensions of the nanoparticles have been measured by dynamic light scattering. For sake of comparison, an amphiphilic random copolymer, poly(methylmethacrylate-co-methacrylic acid) (P(MMA-co-MA)), has been synthesized. Stealthiness of the nanoparticles has been analyzed in relation to the copolymer used as stabilizer. For this purpose, the activation of the complement system by nanoparticles has been investigated in vitro, using human serum. This activation is much less important whenever the nanoparticles are stabilized by a PEO containing copolymer rather than by the P(MMA-co-MA) amphiphile. The graft copolymers with a gradient structure and the diblock copolymers with similar macromolecular characteristics (molecular weight and hydrophilicity (HLB)) have been compared on the basis of their capacity to coat PLA nanoparticles and to make them stealthy.



Contents

I. INTRODUCTION.....	151
II. EXPERIMENTAL PART.....	153
<i>Synthesis of PCL-g-PEO graft copolymers.</i>	153
<i>Synthesis of PEO-b-PCL diblock copolymers.</i>	153
<i>Synthesis P(MMA-co-MA) copolymer.</i>	153
<i>Characterization of the amphiphilic copolymers.</i>	154
<i>Preparation of poly(D,L-lactide) nanoparticles.</i>	154
<i>Characterization of polymeric nanoparticles.</i>	155
<i>Determination of the structural composition of the nanoparticles by $^1\text{H-NMR}$.</i>	155
<i>Complement activation.</i>	155
III. RESULTS AND DISCUSSION	157
<i>III.1. Amphiphilic PCL-g-PEO and PEO-b-PCL copolymers.</i>	158
<i>III.2. Preparation of nanoparticles.</i>	162
<i>III.3. Size and charge of the nanoparticles.</i>	166
<i>III.4. Stability of the nanoparticle dispersion.</i>	167
<i>III.5. Complement activation.</i>	168
IV. CONCLUSION	170

I. Introduction

Poly(D,L-lactide) (PLA) and poly(ϵ -caprolactone) (PCL) are synthetic polymers of special interest because of unique properties of biocompatibility and biodegradability. They are commonly used in biomedical applications, including resorbable bone pins and screws, scaffolds for cells in tissue engineering, and drug delivery systems.^{1,2,3} A variety of bioactive principles have been successfully encapsulated into biodegradable nanoparticles of PCL and PLA⁴⁻⁹ prepared by different techniques, such as emulsification-evaporation, salting-out and solvent displacement also known as “nanoprecipitation”.¹⁰ The nanoprecipitation process has been reported and patented for the first time by Fessi *et al.* in 1987.¹⁰ In this technique, the core building polymer (here PLA) and an amphiphilic stabilizer are dissolved in a semi-polar water-miscible solvent. This solution is poured or injected in an aqueous solution containing a stabilizer under magnetic stirring. As soon as PLA precipitates, it is stabilized by the copolymer with formation of nanoparticles. Non-degradable stabilizer, e.g., poly(vinyl alcohol) (PVA), polysorbate,⁴ and poloxamer are commonly used in this technique,¹⁰ of which the incomplete removal may cause problems. Another issue is the surface functionalization of the nanoparticles by the stabilizer itself, that must contain appropriate moieties, including charges,¹¹ poly(ethylene oxide) chains^{12,13} or targeting molecules.^{13,14} For instance, Barbault-Foucher *et al.* prepared PCL nanospheres coated by a bioadhesive polymer (hyaluronic acid) by a nanoprecipitation technique, in the presence of cationic surfactants.¹¹ Gref *et al.* used an emulsion-evaporation technique to prepare nanoparticles of PLA or PLA/PLA-PEO mixtures using sodium cholate as surfactant.¹² Recently, some of us reported on the successful use of functional biodegradable amphiphilic copolymers of ϵ -caprolactone (ϵ CL) and ϵ CL-derivatives, in order to stabilize and modify the surface of PLA nanoparticles (100-200 nm diameter) prepared by a co-precipitation technique in the absence of additional stabilizers.^{15,16} These copolymers have a dual role of surfactant and surface modifier, on top of being biodegradable.

However, the rapid uptake of intravenously injected nanoparticles by the mononuclear phagocytic system (MPS) remains a pending problem.¹⁷ Therefore there is a quest for drug carriers that are hardly detectable by the MPS cells, that circulate for a prolonged period of time in the blood compartment and that allow for the targeting of other sites than the immune active ones in the human body. At the time being, the hydrophilic

and biocompatible poly(ethylene oxide) (PEO) is approved by FDA for parenteral use in humans.^{18,19} It is the most efficient material known to modify the surface of nanoparticles, in order to make them stealthy, i.e., not or hardly detectable by the immune system either through humoral reactions or, at the cell level, through opsonins. Indeed, the highly hydrated and flexible PEO chains can form a steric barrier against the adsorption of proteins at the nanoparticle surface.²⁰ Preventing this protein adsorption (opsonization), phagocytosis of the nanoparticles is avoided which results in an increased lifetime in the blood circulation.^{8,12,17} The components of the complement system, which is part of the immune system, seem to act synergistically with the other opsonins in making foreign surfaces prone to phagocytosis.^{18,19} Because of this important role of the complement system, quantitative consumption of the proteins of the human complement system, as consequence of adsorption on the nanoparticle surface, is a stealthiness criterion. Basically, in an established test (CH50 test), the hemolytic capacity of the residual, non-adsorbed complement proteins can be evaluated, after contact of human serum with different amounts of nanoparticles.²¹⁻²³

PEO-*b*-PCL diblock copolymers have been extensively used to prepare PEO-coated nanoparticles.^{8,12,13,24,25} Recently, some of us reported on poly(ethylene oxide) (PEO) chains end-capped by an ϵ -caprolactone unit (γ PEO.CL).²⁶ This novel macromonomer has been successfully copolymerized with ϵ -caprolactone (ϵ CL), which is a direct way to prepare amphiphilic PCL-*g*-PEO graft copolymers.²⁷

This paper aims at reporting on the formation of PEO-coated biodegradable nanoparticles by nanoprecipitation of PLA with the assistance of well-defined diblock (PEO-*b*-PCL) and graft (PCL-*g*-PEO) copolymers as stabilizers and surface-modifiers. These amphiphilic copolymers are indeed expected to form a steric barrier at the surface of the nanoparticles, the PCL component being entrapped within the PLA chains. The activation of the complement system by the as-prepared particles (100-200 nm) has been investigated, as a stealthiness criterion, in relation to the molecular architecture and composition of the PEO containing copolymers and compared to nanoparticles stabilized by a non-(bio)degradable P(MMA-*co*-MA) copolymer.¹⁶

II. Experimental Part

Synthesis of PCL-*g*-PEO graft copolymers.

This synthesis was reported elsewhere.²⁶ Briefly, the ring-opening copolymerization of ϵ -caprolactone with a PEO macromonomer (γ PEO.CL), i.e., PEO end-capped by an ϵ -caprolactone unit,²⁶ was initiated by aluminum isopropoxide, $\text{Al}(\text{O}^i\text{Pr})_3$, in CH_2Cl_2 in the presence of 1 equivalent of pyridine with respect to Al (Figure 2, eqn. 1).²⁷ Copolymerization was stopped by a few drops of HCl (0.1 M), and Al was extracted with an aqueous solution of ethylenediaminetetraacetic acid (EDTA) (0.1 M) buffered at pH 4.8, followed by washing with deionized water. The copolymer was recovered by repeated precipitation, first in cold heptane and then in methanol, in order to remove the unreacted ϵ CL and γ PEO.CL, respectively. Size exclusion chromatography (SEC) assessed the successful removal of the residual macromonomer. The copolymer was recovered by centrifugation, dried *in vacuo* and stored *in vacuo* at -20°C . Three copolymers with a constant graft length (M_n , PEO = 1000 g/mol) were synthesized (Table 1, G1 to G3, and Figure 3). Yield = 50-60%, depending on the macromolecular characteristics.

Synthesis of PEO-*b*-PCL diblock copolymers.

α -Methoxy, ω -hydroxy poly(ethylene oxide) (MPEO) was first synthesized by living anionic polymerization of ethylene oxide initiated by the potassium salt of triethylene glycol monomethyl ether. Five samples of MPEO of different molecular weight were prepared, i.e., 900, 2100, 3900, 5000 and 9000 g/mol. In the second step, the hydroxyl group of the MPEO was reacted with AlEt_3 and used as a macroinitiator for the ring-opening polymerization of ϵ -caprolactone at 25°C (Figure 2, eqn. 2), as reported elsewhere by Vangeyte *et al.*²⁸ The length of the PCL block was varied by changing the ϵ -caprolactone over MPEO-Al alkoxide molar ratio. The Al residues were extracted by EDTA (cfr supra). The copolymers were recovered by precipitation in heptane and dialyzed against water. Seven block copolymers of different composition and molecular weight were synthesized (Table 1, B4 to B10). Yield = 85%

Synthesis P(MMA-*co*-MA) copolymer.

A poly(methyl methacrylate-*co*-methacrylic acid) random copolymer, P(MMA-*co*-MA₂₅) (where 25 is the molar fraction of the methacrylic acid (MA) units), was synthesized by atom transfer radical copolymerization (ATRP) of methyl methacrylate

(MMA) and trimethylsilyl methacrylate initiated by 2-bromo-ethylisobutyrate and catalyzed by dibromobis(triphenylphosphine) nickel bromide ($\text{NiBr}_2(\text{PPh}_3)_2$). The pendant silylated groups were hydrolyzed as reported elsewhere.^{15,29}

Characterization of the amphiphilic copolymers.

Structure, composition, molecular weight and molecular weight distribution of the copolymers were determined by $^1\text{H-NMR}$ spectroscopy and SEC. $^1\text{H-NMR}$ spectra were recorded in CDCl_3 at 400 MHz with a Bruker AM 400 apparatus at 25°C. Figure 1 and 5 in Chapter 2 show typical $^1\text{H-NMR}$ spectra for the graft (Chapter 2, Figure 1) and diblock (Chapter 2, Figure 5), respectively. Molecular weight and composition ($n(\text{EO})/n(\text{CL})$) were determined by $^1\text{H-NMR}$ in CDCl_3 from the intensity of the signals for the methylene protons in α -position of the carbonyl ester of the ϵ -CL units (2.29 ppm), the methylene protons characteristic of PEO (3.6 ppm) and the end-groups ($\delta = 1.2, 5.0$ ppm and 3.35 ppm). These data together with the polydispersity estimated by SEC (M_w/M_n) are collected in Table 1. SEC was carried out in tetrahydrofuran (THF) with a flow rate of 1ml/min at 45°C, with a SFD S5200 Autosampler liquid chromatograph equipped with a SFD refractometer index detector 2000 and columns from Polymer Laboratories (gel 5 μm ; columns porosity: 10², 10³, 10⁴, 10⁵Å). PEO and polystyrene (PS) standards were used for calibration.

Preparation of poly(D,L-lactide) nanoparticles.

Nanoparticles were prepared by a nanoprecipitation technique,³⁰ as reported elsewhere.^{6,15,16} Typically, 1 ml of solutions of poly(D,L-lactide) (PLA) and increasing amounts of copolymers (PCL-*g*-PEO, PEO-*b*-PCL, or P(MMA-*co*-MA₂₅)) in dimethylsulfoxide (DMSO) (Merck, 99.5%) were prepared (total concentration = 16 mg/ml). 6 ml of phosphate buffer (pH = 7.4, 0.14 M) (Milli-Q filtered water Millipore Synthesis) were then rapidly added to the polymer solution, under agitation, in order to precipitate of the PLA (Purasorb[®], Purac, $M_n = 77500$, $M_w/M_n = 2.2$). The weight percent (wt%) of the copolymer (with respect to PLA) was varied from 10 to 500 in order to know the minimum amount necessary to reach complete conversion of PLA into nanoparticles. The nanosuspensions were dialyzed against water for 24 h, in order to eliminate DMSO, followed by centrifugation at 3500 rpm for 15 min of any residual solids including unstable aggregated particles or precipitated polymer. The nanoparticle content (~ 2-3 mg/ml) was

accurately determined by lyophilization of 1 ml of nanosuspension for 24 h and weighing. The nanoparticle suspensions were stored at 4°C.

Characterization of polymeric nanoparticles.

Dynamic light scattering (DLS) was carried out with a Brookhaven instrument (Ar laser, 488 nm) fitted with a photon correlation spectrometer. The intensity of the light scattered by 150 μ g/ml solution (original suspensions diluted by filtered deionized water) was measured at 90° to the incident beam. The hydrodynamic diameter and size distribution were calculated by the CONTIN method and data of at least five measurements were averaged for each nanosuspension.

Zeta potential was measured with a Zetasizer 2000 (Malvern Instruments Ltd, UK), at a voltage of 150 V. The ionic strength and pH of the nanoparticle suspensions were 1mM of NaCl and 7.4, respectively.

Determination of the structural composition of the nanoparticles by $^1\text{H-NMR}$.

With the purpose to determine the amount of amphiphilic copolymer exposed at the NPs' surface, $^1\text{H-NMR}$ analysis were performed on these colloidal systems as previously described by Vila *et al.*³¹ The NP suspensions were concentrated by three successive centrifugations, also allowing for the exchange of water against D_2O . In detail, 10 ml of NP dispersions were centrifuged at 13200 rpm for 30 min; after each centrifugation step, the supernatant was removed and the solid homogenized in 1 ml of D_2O . After the last washing step, the NPs were homogenized in 0.5 ml of D_2O . The whole was transferred in a NMR tube, a known amount of naphthalene-2-sulfonic acid (dissolved in D_2O) was added as an internal standard, and analyzed by $^1\text{H-NMR}$. Under these conditions, only mobile PEO chains at the outer phase of the NPs were detected. Then, the whole content of the NMR tube was recovered (by addition of organic solvent, THF), the solvents evaporated to constant weight. Finally, the solid was dissolved in CDCl_3 and the PLA/ copolymer composition of the NPs checked by $^1\text{H-NMR}$. The quantification of the portion of PEO (i.e., copolymer) at the surface of the NPs was thus achieved by comparing the results in both solvents.

Complement activation.

Complement activation was measured as the lytic capacity of a normal human serum (NHS) towards antibody-sensitized sheep erythrocytes after exposure to the nanoparticles.

Aliquots of NHS were incubated with increasing amounts of nanoparticles. The amount of serum, able to haemolyse 50% of a fixed number of the sheep erythrocytes after exposure to the nanoparticles, was determined (“CH50 units”) for each sample. NHS was provided by the “Etablissement Français du Sang” (Angers, France) and stored as aliquots at -80°C until use. Veronal-buffered saline containing 0.15 mM Ca^{2+} and 0.5 mM Mg^{2+} (VBS++) was prepared as reported elsewhere.³² Firstly, sheep erythrocytes were sensitized by rabbit anti-sheep erythrocytes antibodies (Sérum hémolytique, Biomérieux, Marcy-l’Etoile, France) and diluted by the veronal-buffered saline at a final concentration of 2.10^9 cells/ml in VBS++. Increasing amounts of particle suspension were added to NHS diluted in VBS++ such that the final dilution of NHS in the mixture was 1/4 (v/v) in a final volume of 1 ml. After 1 h of incubation at 37°C under gentle agitation, the suspension was diluted 1/25 (v/v) in VBS++, and aliquots of 8 different dilutions were added to a given volume of sensitized sheep erythrocytes. After 45 min of incubation at 37°C , the reaction mixture was slightly centrifuged at 2000 rpm for 10 min. The absorption of the supernatant was determined at 414 nm with a microplate reader (Multiskan Anscant, Labsystems SA, Cergy-Pontoise, France) and compared to the results obtained with control serum in order to evaluate the amount of haemolysed erythrocytes. Positive and negative controls were made in each series of experiments in order to account for any difference in the hemoglobin response from a given erythrocyte preparation. Furthermore, corrections for particle light-scattering and spontaneous erythrocyte haemolysis were estimated by UV/VIS measurements using blanks containing only particles and only erythrocytes, respectively. In order to compare nanoparticles of different average diameters, their surface area was calculated as follows: $S = 3 m/\rho r$, where S is the surface area [cm^2], m the weight [μg] in 1 ml nanosuspension, r the average radius [cm] determined by DLS, and ρ the voluminal mass [$\mu\text{g}/\text{cm}^3$] of the nanoparticles estimated at $10^6\text{ }\mu\text{g}/\text{cm}^3$.²¹⁻²³ The experimental data are the average of 3 independent experiments with a 10% standard deviation.

III. Results and Discussion

Nanoparticles of aliphatic polyesters are commonly prepared with the assistance of water-soluble polymeric stabilizers,¹⁰ such as PVA and Poloxamers. In this study, PLA nanoparticles (NPs) have been prepared by the nanoprecipitation technique,^{6,15,16} that consists generally in dissolving a polymer in a water miscible organic solvent, which is poured, under stirring, into a large volume of water. The organic solution is supposed to form droplets when poured into the aqueous phase, due to interfacial turbulence.¹⁰ Nanoparticles are formed instantaneously, as result of the fast diffusion of the organic solvent from the droplets to the aqueous phase which makes PLA insoluble. Gross precipitation of PLA is prevented from occurring, whenever the amphiphilic copolymer forms an effective coalescence barrier around the particles. The advantage of the nanoprecipitation technique is that it does not require any specific equipment and that quite monodisperse NPs are formed with an average size in the 100 to 200 nm range.^{6,15,16} In this work, hydrophobic PLA is actually co-precipitated with amphiphilic copolymers, whose (water-insoluble) anchoring block (PCL) is entrapped within the core of the particles and the stabilizing (hydrosoluble) component forms either an electrostatic (methacrylate groups) or a steric (PEO blocks) barrier against aggregation (Figure 1a and Figure 1b).

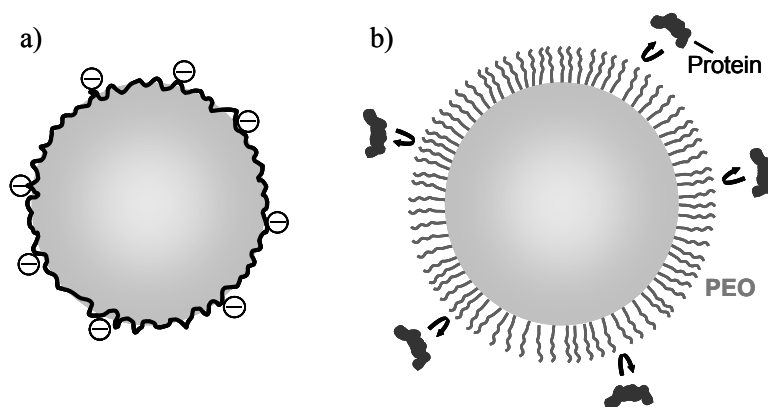


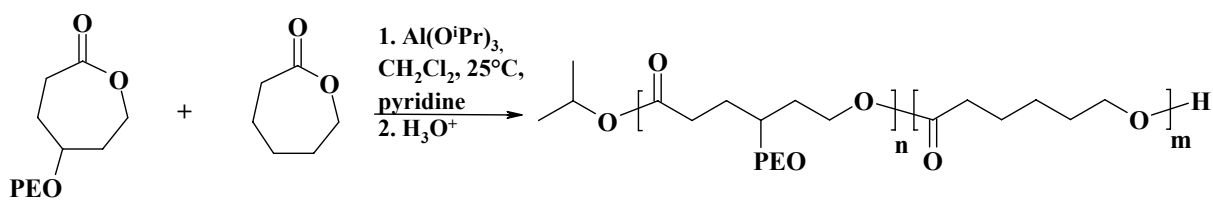
Figure 1. Schematic representation of nanoparticles stabilized by a) a charged amphiphilic copolymer (e.g., P(MMA-co-MA)), b) a PEO containing amphiphilic copolymer (protein repulsive)

Measurements of the zeta potential of the as-prepared NPs have shown that the surface properties of the NPs are directly governed by the copolymer used in the process, thus by its propensity of being located at the NPs' surface.^{15,16} With the purpose to make PLA NPs stealthy, PEO containing amphiphilic copolymers have been used in conjunction and co-precipitated with PLA. Indeed, a brush of PEO, well-known for protein-repulsive properties,^{12,20,33} is expected to be formed at the surface of the NPs, which would prevent them from being detected and rapidly removed from the blood circulation (Figure 1b). For this concept to be implemented, a series of amphiphilic copolymers have been synthesized that contain PEO chains chemically linked to a PLA homologous aliphatic polyester, i.e., poly(ϵ -caprolactone) (PCL).^{26,27} For sake of comparison, an amphiphilic random copolymer of methylmethacrylate (MMA) and methacrylic acid (MA), P(MMA-*co*-MA), has been synthesized and used to prepare NPs without any PEO at the surface. This type of random copolymer had already been reported as a stabilizer for the nanoprecipitation of PLA nanoparticles.^{6,15}

III.1. Amphiphilic PCL-*g*-PEO and PEO-*b*-PCL copolymers.

In a first step, the effect of the macromolecular architecture of copolymers consisting of PCL and PEO on the formation and properties of PLA-containing nanoparticles has been investigated. Copolymers with a PCL backbone and PEO grafts (PCL-*g*-PEO), have been synthesized according to the equations shown in Figure 2, and compared to conventional PEO-*b*-PCL diblock copolymers.

Equation 1:



Equation 2:

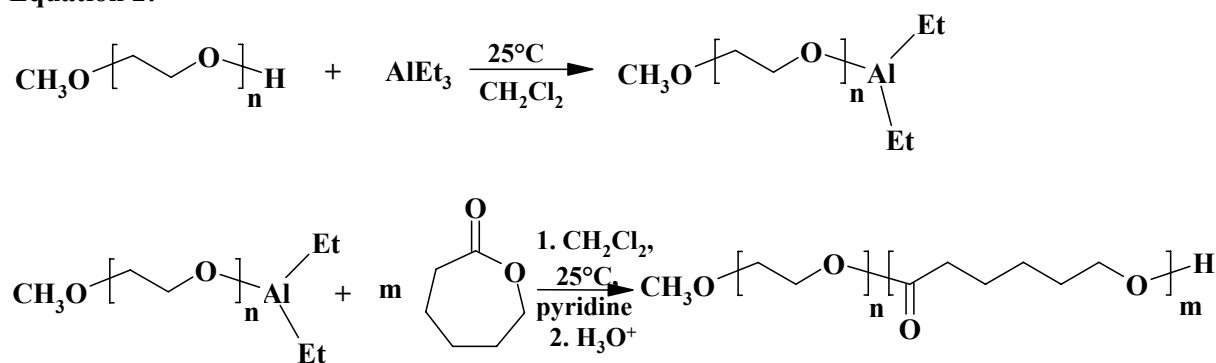


Figure 2. Synthesis of PCL-*g*-PEO graft copolymers with a gradient structure (eqn. 1) and PEO-*b*-PCL diblock copolymers (eqn. 2)

The molecular structure of these amphiphilic copolymers is schematized in Figure 3 and their molecular characteristic features are listed in Table 1.

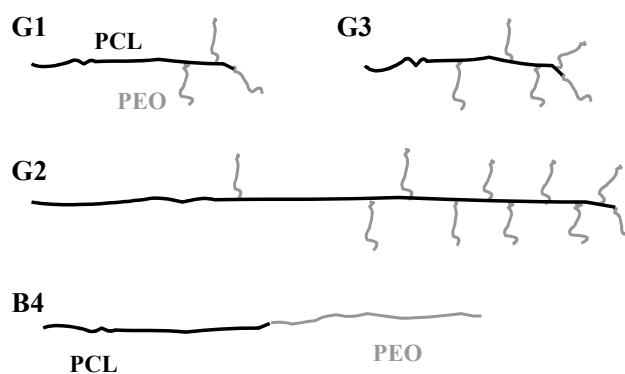


Figure 3. Schematic structures of the PCL-*g*-PEO graft copolymers with a palm-tree architecture and the PEO-*b*-PCL block copolymer B4 (symbols refer to Table 1)

Table 1. Molecular characteristics of amphiphilic PEO/PCL copolymers

# ^a	PEO ^b		PCL	Copolymer				
	Mn ^c	Mw/Mn ^c	M _{n, NMR} ^d	M _{n, tot}	M _w /M _n	n(EO)/n(εCL)	HLB	N ^e
G1	1000	1.09	7700	10000	1.30	0.65	4	2.3
G2	1000	1.09	27400	37000	1.24	0.77	4.5	9.6
G3	1000	1.09	6400	10600	1.33	1.4	7	4.2
B4	900	1.05	5000	5900	1.22	0.47	3	-
B5	9500	1.12	28600	38100	1.36	0.86	5	-
B6	9500	1.12	22800	32300	1.18	1.08	6	-
B7	2100	1.03	4000	6100	1.33	1.38	7	-
B8	5000	1.04	8600	13600	1.25	1.52	7.5	-
B9	3900	1.13	3800	7700	1.28	2.68	10	-
B10	9500	1.12	5000	14500	1.17	4.92	13	-

[a] "G" corresponds to PCL-*g*-PEO graft copolymer, "B" corresponds to PEO-*b*-PCL diblock copolymers, [b] PEO is the macromonomer included in the graft copolymers, and the macroinitiator included in the diblocks, [c] determined by SEC with PEO standards, [d] Mn calculated from the copolymer composition (1H-NMR analysis) and Mn of PEO, [e] N stands for the average number of PEO grafts (Mn = 1000 g/mol or D.P. = 20)

The graft copolymers were synthesized by living ring-opening copolymerization of ε-caprolactone with a poly(ethylene oxide) macromonomer of the same type (Mn = 1000 g/mol) and their structure was confirmed by ¹H-NMR (see Chapter 2, Figure 1).^{26,27} Macromonomer conversion was up to 70%, depending on the macromonomer content in the feed. For instance, the molar content of the macromonomer in the copolymer is 7% (Copolymer G3) for a macromonomer content of 10% in the comonomer feed. Three copolymers (G1, G2 and G3) containing the same macromonomer were prepared. The copolymers G1 and G2 were prepared with a comonomer feed of the same composition and different comonomer/initiator molar ratios. Parallel to the increase in molecular weight (M_{n, tot}, Table 1) from G1 to G2, the average number of PEO grafts per chain is also increased (2.3 to 9.6). The final composition is comparable although not exactly the same, because the comonomer conversion is not the same neither. Copolymer G3 was prepared with the same comonomer/initiator molar ratio as G1 but with a high macromonomer content, such that the average number of PEO grafts is higher in G3 than in G1 at constant M_{n, tot}. It must be noted that the macromonomer is less reactive than ε-caprolactone (r_{εCL} = 3.95; r_{PEO, CL} = 0.05),²⁷ which results in graft copolymers with a gradient structure as

schematized in Figure 3. Indeed, ϵ -caprolactone is preferentially polymerized at the beginning of the copolymerization and the macromonomer content increases in the comonomer feed with the conversion, which dictates the extent to which the macromonomer is incorporated in the growing chains.²⁷ As tentatively shown in Figure 3, the graft copolymers have a "palm tree" structure, with a hydrophobic trunk of PCL and hydrophilic PEO branches.

The hydrophilicity of the copolymers is expressed by the hydrophilic-lipophilic balance (HLB), as reported in Table 1. It was calculated by the Griffin's relationship:

$$HLB = 20 \times M_H / (M_L + M_H),$$

where M_L and M_H are the molecular weights (M_n) of the lipophilic (PCL) and hydrophilic (PEO) chains, respectively.³⁴ The HLB value of predominantly hydrophobic materials is in the 1-10 range, compared to 10-20 for hydrophilic materials. The graft copolymers listed in Table 1 are thus predominantly hydrophobic with a HLB in the 4-7 range. G1 and G2 have quite a similar hydrophilicity, whereas G3 is more hydrophilic than G1 of quasi the same $M_{n, tot}$.

PEO-*b*-PCL diblock copolymers were synthesized as reported elsewhere.²⁸ Their composition was determined by ¹H-NMR spectroscopy (see chapter 2, Figure 5). The average molecular weight and the composition were varied by changing both the macroinitiator to ϵ -caprolactone molar ratio and the length of the macroinitiator (Table 1, B4 to B10). A large range of HLB was accordingly covered, and the hydrophilicity of the copolymers increased from B4 to B10.

Similarities in molecular weight and HLB must be noted for the graft and diblock copolymers in Table 1. For instance, the diblock B5 has similar molecular weight and HLB as the graft copolymer G2. Diblock copolymers B7 and B8 have comparable HLB as the graft copolymer G3. Finally, the PEO block of the diblock B4 has a molecular weight ($M_n = 900$ g/mol) close to that of the PEO brushes of the graft copolymers ($M_n = 1000$ g/mol). Moreover, the HLB of G1 (HLB = 4) and G2 (HLB = 4.5) is comparable to copolymer B4 (HLB = 3). Finally, none of the copolymers in Table 1 is water soluble, which is favorable to the permanency of the coalescence barrier in an aqueous environment.

III.2. Preparation of nanoparticles.

Nanoparticles of PLA were prepared by the nanoprecipitation technique.³⁰ The nanoprecipitation of poly(D,L-lactide) (PLA) in the presence of small amounts of amphiphilic P(MMA-*co*-MA) random copolymers has previously been reported.¹⁵ 10 wt% of P(MMA-*co*-MA₂₅) (25 mol% of MA) with respect to PLA were necessary to convert quantitatively PLA into a stable suspension of sub-200nm nanoparticles. The origin of the stability of the nanoparticles against coalescence must be found in their mutual electrostatic repulsion, because the carboxylic acid units of P(MMA-*co*-MA) are ionized at the pH of the phosphate buffer (pH 7.4) used to precipitate PLA. In this study, amphiphilic bioeliminable PCL-*g*-PEO and PEO-*b*-PCL copolymers have been substituted for the non-degradable methacrylic copolymer. The efficiency of the copolymers listed in Table 1 has been compared on the basis of the minimum amount [mg] required to stabilize 100 mg of PLA.

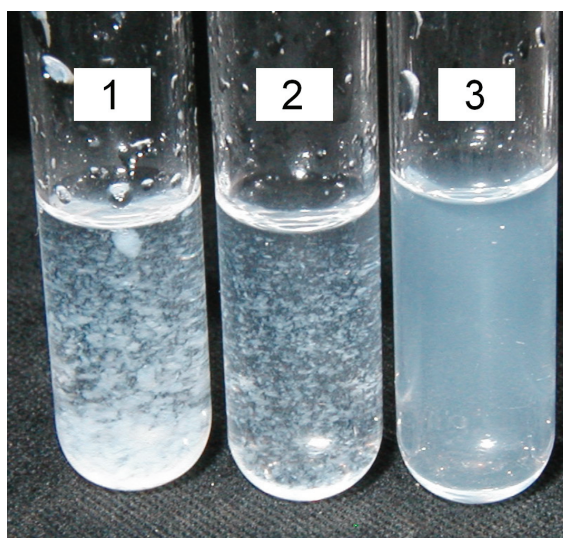


Figure 4. Co-precipitation of PLA with increasing amounts of the copolymer G3 (1) 9 wt%, (2) 17 wt%, (3) 33 wt% (in the copolymer + PLA mixture)

Figure 4 illustrates how PLA is precipitated from DMSO upon addition of the phosphate buffer when the wt% of the copolymer G3 is increased from 9 (sample 1) to 17 (sample 2) and finally to 33 wt% (sample 3) in the (PLA + copolymer) mixture, used at a constant concentration of 16 mg/ml. When the copolymer content is too low, PLA flocculates as observed for samples 1 and 2 in Figure 4. These observations indicate that the amount of copolymer used in the precipitation process has an impact on the surface properties. Each of the 3 graft copolymers is able to stabilize suspensions of PLA NPs in

water, as reported in Table 2, where “0” refers to samples for which no precipitation occurs upon centrifugation (e.g., sample 3 in Figure 4).

Table 2. HLB of the amphiphilic copolymers used in this study and their capacity to stabilize PLA NPs

# ^a	$M_{n,tot}$	HLB	wt% Copol ^c	P ^d
G1	10000 $N^b = 2.3$	4	33	++
			43	+
			50	0
G2	37000 $N = 9.2$	4.5	28	+
			43	0
			50	0
G3	10600 $N = 4.2$	7.5	17	++
			28	+
			33	0
B4	5900	3	50	+++
			83	++
			90	+ ^e
B5	38100	5	50	+++
			83	+ ^e
B6	32300	6	50	+++
			83	+ ^e
B7	6100	7	17	++
			28	+
			50	+
B8	13600	7.5	28	++
			50	0
			50	0
B9	7700	10	28	+
			43	0
			50	0
B10	14500	13	17	+++
			28	+
			33	0
R11	13000	-	9	0
			17	0

[a] "G", "B" and "R" correspond to PCL-*g*-PEO graft, PEO-*b*-PCL diblock and P(MMA-*co*-MA₂₅) random copolymers, respectively, [b] N stands for the average number of PEO grafts ($M_n = 1000$ g/mol or D.P. = 20), [c] wt% of copolymer in the (PLA + copolymer) mixture dissolved in DMSO ($c = 16$ mg/ml), [d] P stands for the relative quantity of gross precipitation compared to stabilization of nanoparticles (scored as 0 (no precipitation), + (low), ++ (much), +++ (major)), [e] conversion of PLA into nanoparticles is never complete, whatever the amount of the copolymer

Table 2 shows that a higher amount of the PCL-*g*-PEO copolymers is needed to stabilize the same amount of PLA compared to the P(MMA-*co*-MA₂₅) copolymer. Indeed, 33 wt% of the most efficient graft copolymer must be used instead of 9 w% of the random methacrylic copolymer. Clearly the steric barrier of PEO grafts ($M_n = 1000$ g/mol) is less

effective than the electrostatic repulsion of the carboxylate groups. It also appears that a graft copolymer with a higher HLB (hydrophilicity) is a better stabilizer for the PLA nanoparticles (comparison of G3 with G1 and G2, in Table 2). Finally, the graft copolymers are more effective stabilizers when the molecular weight is higher at comparable HLB (comparison of G1 with G2, in Table 2). Clearly, a minimum amount (at least 33%) of copolymer is needed to stabilize the PLA nanoparticles, in relation to the hydrophilicity (HLB, PEO content) of the copolymer. Because this amount is high (close to 50% in most of the cases), the nanoparticles do not merely consist of PLA but they are mixed nano-objects of PLA, and PCL containing copolymer. Nevertheless, they will be designated as PLA nanoparticles afterwards. These observations qualitatively agree with a previous study dealing with the nanoprecipitation of PLA in the presence of PCL chains bearing either pendant pyridinium groups or non-ionic hydroxyl groups.¹⁶ Non-ionic hydroxyl-substituted poly(ϵ -caprolactone) was indeed a less effective stabilizer than the positively charged counterpart. Moreover, less copolymer was required to stabilize PLA, when the degree of substitution of the PCL chains, thus their hydrophilicity, was increased. For instance, stabilization of 100 mg of PLA required 50 mg of PCL containing 7 mol% of hydroxyl containing ϵ -CL units (CL-OH) compared to 20 mg for PCL with 23 mol% of CL-OH comonomer.¹⁶

The series of diblock copolymers B4 to B7 (Table 2) are not able to convert PLA into stable nanoparticles. These copolymers B4 to B7 of low HLB (ranging from 3 to 7) cannot prevent the gross precipitation of PLA, even at a copolymer content as high as 83 wt% (500 mg of copolymer for 100 mg of PLA). Only the B8 to B10 diblock copolymers with a HLB higher than 7 are able to stabilize the NP dispersions in water, although at a rate of 33 wt% (50 mg for 100 mg of PLA). Whatever the architecture of the PCL/PEO copolymers (block vs. graft), a higher HLB (at least in the range under consideration) is beneficial for the nanoprecipitation of PLA. However, at a comparable HLB (e.g., HLB = 7), PLA nanoparticles are stabilized by graft copolymers, in contrast to diblock copolymers which are ineffective stabilizers (comparison of G1 and G2 with B4 and B5, in Table 2).

Although the effect of the architecture of amphiphilic copolymers on the stabilization of emulsions has been discussed elsewhere,³⁵⁻³⁸ this work reports for the first time, on the impact of the copolymer architecture on the stabilization of polyester NPs prepared by nanoprecipitation. The graft copolymers do not require an as high HLB as diblocks for being effective stabilizers. An explanation might be found in the non-random grafting of the PCL chains by PEO. Indeed, the actual structure is that of a palm-tree (Figure 3,

copolymer G1 to G3), with a hydrophobic PCL trunk and hydrophilic PEO palms at the top. The PCL trunk would be a more effective anchoring block than a randomly grafted PCL backbone. Moreover, substitution of one long PEO block by several closely connected shorter PEO chains is expected to form a denser, thus more difficult to penetrate, hydrophilic brush as schematized in Figure 5a and Figure 5b.

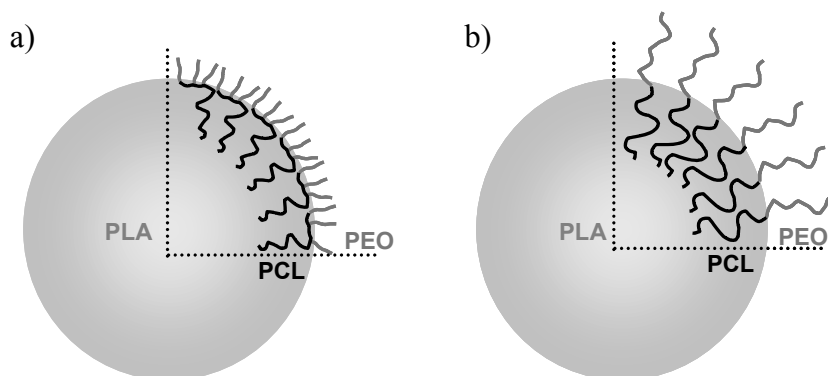


Figure 5. Schematic view of the surface of the nanoparticles organized by a) PCL-*g*-PEO copolymer chains with a gradient structure, b) PEO-*b*-PCL diblock copolymer chains; gray: PEO segments; black: PCL segments, light gray: PLA

So, at comparable amount and hydrophilicity, the copolymer G2 with 4.2 PEO branches forms a denser PEO brush and stabilizes more effectively the PLA nanoparticles than the copolymer G1, with 2.3 PEO branches. The same remark holds for the comparison of the block copolymer B4 (one PEO block of $M_n = 900$ g/mol), which cannot stabilize the NPs and the graft copolymer G1 (2.3 PEO branches of $M_n = 1000$ g/mol and comparable HLB), which is an effective stabilizer. Obviously, the macromolecular architecture plays a key role in the stabilization process rather than the length of the PEO chains. The grafting density of the chains that form the steric barrier seems to be essential because it controls both the surface area occupied by one copolymer chain and the (non)-penetration of the protective shell.

III.3. Size and charge of the nanoparticles.

The average diameter and size distribution (PDI) of the nanoparticles have been measured by dynamic light scattering (DLS) (Table 3).

Table 3. Characteristics of the nanoparticles stabilized by different amphiphilic copolymers

# ^a	Copolymer			Nanoparticles		
	$M_{n,tot}$	HLB	wt% Copol ^c	$D[nm]$ ^d	PDI ^e	$\zeta [mV]$ ^f
G1a	10000	4	43	147	0.18	n.d. ^g
G1b	$N^b = 2.3$		50	188	0.20	-3.1 ± 1.6 ^h
G2a	37000	4.5	43	201	0.10	-1.4 ± 1.3
G2b	$N = 9.6$		50	210	0.20	-0.8 ± 1.1
G3a	10600	7.5	33	122	0.18	n.d.
G3b	$N = 4.2$		43	158	0.16	0.3 ± 0.6
G3c			50	111	0.28	-0.7 ± 0.1
B8a	13600	7.5	50	146	0.15	n.d.
B9a	7670	10	43	158	0.14	n.d.
B9b			50	178	0.14	-1.2 ± 0.4
B10a	14500	13	33	231	0.18	n.d.
B10b			50	217	0.19	n.d.
R11a	13000		9	160	0.20	-56.4 ± 3.2
R11b	MA = 25 mol%		17	140	0.21	-54.8 ± 1

[a] "G" stands for PCL-*g*-PEO graft copolymer, "B" for PEO-*b*-PCL diblock copolymers, "R" for P(MMA-*co*-MA₂₅) random copolymers, [b] N stands for the average number of PEO grafts ($M_n = 1000$ g/mol or D.P. = 20), [c] wt% of copolymer in the (PLA + copolymer) mixture dissolved in DMSO ($c = 16$ mg/ml), [d] average diameter determined by DLS (CONTIN method), averaged on five samples, [e] polydispersity index, [f] zeta potential, [g] not determined, [h] standard deviation

As a rule, the nanoparticles have a diameter in the 100-200 nm range, with a similar size distribution, whatever the architecture and composition of the polymeric stabilizer. These sizes are quite comparable to those observed with the P(MMA-*co*-MA₂₅) random copolymer. In the two series of copolymers, the average diameter tends to increase with the molecular weight of the amphiphilic copolymer (comparison of G1 with G2 and B9 with B10, Table 3). In the graft copolymer series, the average particle size appears to decrease

with increasing HLB (from 4 to 7.5) at constant M_n (comparison of G1 with G3). In a similar study dealing with PLA/PEO-*b*-PLA stealthy NPs, prepared by an emulsion/solvent evaporation technique, Gref *et al.* noted that the particle size decreased from 230 nm to 170 nm upon increasing the PEO content, possibly because the amphiphilic PEO-*b*-PLA (PEO(5k)-*b*-PLA(20k)) copolymer decreased the water/organic phase (methylene chloride) interfacial tension.¹²

Moreover, when the amount of copolymer is increased above the minimum required amount (not shown here), the size of the NPs does not change significantly. Then, part of the copolymer is expected to be located within the PLA core, as confirmed by the amount of PEO located at the surface of the nanoparticles. This characteristic feature has been determined by NMR analysis of the NPs in D₂O, where only PEO at the nanoparticle surface is swollen and detectable in CDCl₃, in which the copolymer is dissolved and the total amount of PEO is measured. According to this method, ~70% of PEO is available at the surface for the nanoparticles prepared with G2, compared to ~25% when the diblock copolymer B8 is the stabilizer. The PEO density at the surface is thus significantly higher in case of stabilization by a graft copolymer rather than a diblock.

Expectedly, the zeta potential of all the nanoparticles is close to zero, consistent with the neutrality of the stabilizing PEO chains (Table 3). In contrast, the nanoparticles stabilized by the P(MMA-*co*-MA₂₅) copolymer are negatively charged, which confirms, if needed, that the surface properties of the nanoparticles are directly governed by the copolymer used as stabilizer.

III.4. Stability of the nanoparticle dispersion.

This technically important characteristic feature has been estimated from the time dependence of the particle size and size distribution, as measured by DLS. As was observed for the PLA nanoparticles electrostatically stabilized by the P(MMA-*co*-MA₂₅) copolymer,¹⁵ the average size and size distribution of the nanoparticles stabilized by PEO containing copolymers do not change significantly for at least 28 days in water stored at 4°C.

III.5. Complement activation.

The stealthiness of the nanoparticles has been assessed *in vitro* by the haemolytic CH50 test and compared to the P(MMA-*co*-MA₂₅) coated nanoparticles. This CH50 test²¹⁻²³ is based on the activation of the complement system by the nanoparticles in normal human serum (diluted 1/4 (v/v)). The amount of serum proteins adsorbed on the NPs' surface decreases with increasing stealthiness. Basically, after exposure of the human normal serum to increasing amounts of nanoparticles, the amount of serum needed to haemolyse 50% of a fixed number of sensitized sheep erythrocytes is determined. By this way, the complement consumption was evaluated after incubation with nanoparticles stabilized by five different amphiphilic copolymers (Table 3, Figure 6). The electrostatically stabilized (non PEO-coated) nanoparticles contain 9% of the P(MMA-*co*-MA₂₅) copolymer (R11). In case of steric stabilization, the polymeric nanoparticles contain either 43 wt% (full line in Figure 6) or 50 wt% (dotted line in Figure 6) of PEO-*b*-PCL and PCL-*g*-PEO. Figure 6 shows that the CH50 consumption increases with the surface area of nanoparticles (thus the amount of nanoparticles), whatever the stabilizer used.

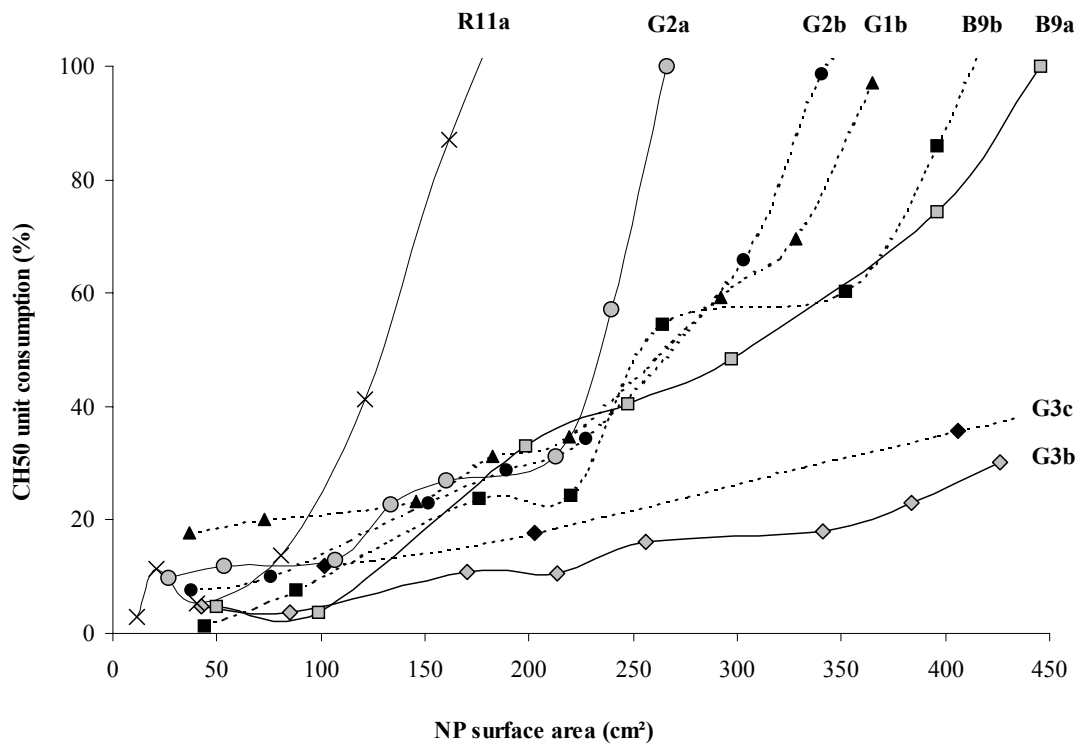


Figure 6. Consumption of CH50 units vs surface area of polymeric nanoparticles stabilized by different amphiphilic copolymers (G1, G2, G3, B9, R11); Wt% of PCL/PEO copolymers in the polymer solution in DMSO: full line = 43wt%, dotted line = 50wt%

Clearly, the nanoparticles stabilized by the P(MMA-*co*-MA) copolymer adsorb larger amounts of serum proteins, i.e., they are strong activators of the complement system. 100% of CH50 units are indeed consumed when the serum protein solution is exposed to only 150 cm² of nanoparticle surface. This consumption is similar to that observed for PMMA nanoparticles,²³ which is consistent with the fact that hydrophobic and negatively charged particles are subject of a rapid clearance from the blood circulation.³⁹ At constant exposed surface, all the nanoparticles stabilized by both PCL-*g*-PEO and PEO-*b*-PCL adsorb less proteins (30% maximum) than the PLA/P(MMA-*co*-MA) nanoparticles. This observation confirms the unique capacity of PEO chains to prevent protein adsorption as a result of specific solution properties and chain conformation in water.⁴⁰ As far as PCL-*g*-PEO copolymers are concerned (copolymers G1, G2, G3, in Table 3), their hydrophobicity plays an important role (at least in the 4 - 7.5 range). Indeed, nanoparticles prepared with the copolymers G1 and G2, of the same HLB and PEO molecular weight, activate the complement system to a similar extent (Figure 6, line G1b and G2a + G2b), whereas the use of the more hydrophilic copolymer G3 results in a substantial decrease in the protein adsorption and thus complement activation. For instance, for a surface of 400 cm², the CH50 unit consumption is 100% for the samples G1b, G2a and G2b, but less than 30% for the samples G3b and G3c. Another relevant parameter is the amount of the amphiphilic copolymer, which is used to prepare nanoparticles. When the surface exceeds 200 cm², the CH50 unit consumption is rapidly smaller for the nanoparticles prepared with PLA containing 50 rather than 43 wt% of the copolymer G2, probably because of the higher density of PEO chains at the NPs' surface. When more hydrophilic copolymers, such as G3 and B9, are the stabilizers, the same effect on the stealthiness of the nanoparticles is no longer observed. It is possible that for the more hydrophilic copolymers an increase of the amount of copolymer has no effect on the surface properties. Indeed, when using 50% of copolymer, the nanoparticles (with a diameter of 100 to 200 nm) consist of ~ 50% of copolymer, which is at least partly located inside the NPs and not on its surface. These observations agree with the results found for the copolymer amount/NP size relationship (no significant decrease of the NP size upon increase of the copolymer amount). In a previous section, diblock copolymers were found less effective compared to graft copolymers with the same HLB in stabilizing PLA nanoparticles. They need a higher HLB for exhibiting a comparable stabilization capacity, which was explained by a higher density of PEO chains at the NPs' surface (Figure 5a and 5b). The same is true when the adsorption of the serum proteins is concerned. When using the diblock copolymer with a

HLB of 10, the nanoparticles (B9, sample B9a and B9b) adsorb serum proteins to a smaller extent compared to the graft copolymers G1 and G2 (HLB = 4.5) at a high surface ($> 250 \text{ cm}^2$), but much more extensively than the graft copolymer G3 (HLB = 7.5), even when a small surface is exposed. These observations are additional evidence that shorter PEO chains with a higher grafting density (as in the case of the gradient (tapered) graft copolymers in this study) are more beneficial than only one PEO chain of higher molecular weight tethered to the surface. The packing density of the PEO chains is crucial for preventing protein adsorption, in accordance with the scientific literature.^{17,38} At a too low density, the surface remains accessible to interaction with proteins. A higher Mn of the PEO chains can however compensate, at least partially, this poorly effective steric barrier. Conversely, the limited efficiency of too short PEO chains in promoting strong steric repulsion can be increased by increasing the packing density of the chains.⁴¹ According to Jeon *et al.*,⁴⁰ the surface density would have a greater effect than the chain length on the steric protection of surfaces. As shown by NMR measurements in D_2O , the amount of PEO actually located at the surface can also be different depending on the copolymer used, which must impact the protein repulsion efficiency.

In conclusion, the graft copolymer G3, which is the most hydrophilic graft copolymer used in this study (HLB = 7.5) with 4.2 PEO graft per PCL chain, is most efficient in preventing protein adsorption.

These pieces of information are useful for the design of long-time circulating nanoparticles, with low interaction with plasma proteins and phagocyte cells. Further studies are however needed to correlate the *in vivo* fate of the nanoparticles considered in this study to the herein reported *in vitro* testing.

IV. Conclusion

A series of PEO-*b*-PCL block copolymers have been synthesized by sequential controlled polymerization of ethylene oxide (propagated by K alkoxide) and ϵ -caprolactone (ϵCL) (propagated by Al alkoxide). PCL-*g*-PEO graft copolymers with a gradient structure have also been prepared by copolymerization of mixtures of ϵCL and ϵCL end-capped PEO chains (macromonomers) initiated by an Al alkoxide. The ability of these amphiphilic copolymers to stabilize PLA nanoparticles prepared by nanoprecipitation depends on both the architecture and HLB of the copolymers. Compared to diblocks,

gradient type graft copolymers are more effective stabilizers. The average diameter of the nanoparticles lies in the 100-200 nm range, depending on HLB and molecular weight of the copolymers. The stealthiness of the PLA/PEO-PCL nanoparticles strongly depends on their surface properties, which are directly governed by the structural characteristics of the stabilizer. Whenever the stabilizer contains a PEO constituent, the adsorption of the serum proteins is significantly decreased compared to other types of amphiphiles, such as P(MMA-co-MA) random copolymers. The gradient graft copolymers are however more effective than the diblocks, as more as their HLB is high.

References.

- ¹ Langer, R.; *Nature* **1998**, *392*, 5
- ² Domb, A. J.; Kumar, N.; Sheskin, T.; Bentolila, A.; Slager, J.; Teomim, D.; in "Polymeric Biomaterials"; Ed. Dumitriu, S., Marcel Dekker, New York, **2001**, Ch. 4
- ³ Uhrich, K. E.; Cannizarro, S. M.; Langer, R. S.; Shakesheff, K. M.; *Chem. Rev.* **1999**, *99*, 3181
- ⁴ Le Roy Boehm, A.-L.; Zerrouk, R.; Fessi, H.; *J. Microencapsulation* **2000**, *17*, 195
- ⁵ Allemann, E.; Leroux, J.-C.; Gurny, R.; *Adv. Drug Deliv. Rev.* **1998**, *34*, 171
- ⁶ Qiu, H.; Rieger, J.; Gilbert, B.; Jerome, R.; Jerome, C.; *Chem. Mat.* **2004**, *16*, 850
- ⁷ Kim, S. Y.; Lee, Y. M.; Shin, H. J.; Kang, J. S.; *Biomaterials* **2001**, *22*, 2049
- ⁸ Jette, K. K.; Law, D.; Schmitt, E. A.; Kwon, G. S.; *Pharm. Res.* **2004**, *21*, 1184
- ⁹ Torchilin, V. P.; *J. Microencapsulation* **1998**, *15*, 1
- ¹⁰ Quintanar-Guerrero, D.; Allemann, E.; Fessi, H.; Doelker, E.; *Drug Dev. Ind. Pharm.* **1998**, *24*, 1113
- ¹¹ Barbault-Foucher, S.; Gref, R.; Russo, P.; Guechot, J.; Bochot, A.; *J. Contr. Release* **2002**, *83*, 365
- ¹² Gref, R.; Lück, M.; Quellec, P.; Marchand, M.; Dellacherie, E.; Harnisch, S.; Blunk, T.; Müller, R. H.; *Colloid Surf. B: Biointerfaces* **2000**, *18*, 301
- ¹³ Gref, R.; Couvreur, P.; Barratt, G.; Mysiakine, E.; *Biomaterials* **2003**, *24*, 4529
- ¹⁴ Cho, C. S.; Cho, K.Y.; Park, I. K.; Sasagawa, T.; Uchiyama, M.; Akaike, T.; *J. Contr. Release* **2001**, *77*, 7
- ¹⁵ Gautier, S.; Grudzielski, N.; Goffinet, G.; De Hassonville, S. H.; Delattre, L.; Jérôme, R.; *J. Biomater. Sci. Polym. Edn.* **2001**, *12*, 429

-
- ¹⁶ Gautier, S.; D'Aloia, V.; Halleux, O.; Mazza, M.; Lecomte, P.; Jérôme, R.; *J. Biomater. Sci. Polymer Edn.* **2003**, *14*, 63
- ¹⁷ Passirani, C.; Benoit, J. P.; in "Biomaterials for Delivery and Targeting of Proteins and Nucleic Acid", Eds: Mahato, R. I., CRC Press, Inc., Boca Raton, Florida, USA, **2005**, Ch.6
- ¹⁸ Lee, J. H.; Lee, H. B.; Andrade, J. D.; *Prog. Polym. Sci.* **1995**, *20*, 1043
- ¹⁹ Torchilin, V. P.; *Adv. Drug. Deliv. Rev.* **2002**, *54*, 235
- ²⁰ Wang, P.; Tan, K. L.; Kang, E. T.; *J. Biomater. Sci. Polym. Edn.* **2000**, *11*, 169
- ²¹ Vittaz, M.; Bazile, D.; Spenlehauer, G.; Verrechia, T.; Veillard, M.; Puisieux, F.; Labarre, D.; *Biomaterials* **1996**, *17*, 1575
- ²² Peracchia, M. T.; Vauthier, C.; Passirani, C.; Couvreur, P.; Labarre, D.; *Life Sciences* **1997**, *61*, 749
- ²³ Passirani, C.; Barratt, G.; Devissaguet, J.-P.; Labarre, D.; *Life Sciences* **1998**, *62*, 775
- ²⁴ Shin, I. G.; Lee, Y. M.; Cho, C. S.; Sung, Y. K.; *J. Contr. Release* **1998**, *51*, 1
- ²⁵ Soo, P. L.; Luo, L.; Maysinger, D.; Eisenberg, A.; *Langmuir* **2002**, *18*, 9996
- ²⁶ Rieger, J.; Bernaerts, K. V.; Du Prez, F. E.; Jérôme, R.; Jérôme, C.; *Macromolecules* **2004**, *37*, 9738
- ²⁷ Rieger, J.; Dubois, P.; Jeusette, M.; Lazzaroni, R.; Jérôme, R.; Jérôme, C.; *Langmuir* **2006**, submitted
- ²⁸ Vangeyte, P.; Jérôme, R.; *J. Polym. Sci., Part A., Polym. Chem.* **2004**, *42*, 1132
- ²⁹ Moineau, G.; Minet, M.; Dubois, P.; Teyssié, P.; Senniger, T.; Jérôme, R.; *Macromolecules* **1999**, *32*, 27
- ³⁰ Fessi, H.; Puisieux, F.; Devissaguet, J. P.; *Eur. Patent 274 961*, **1987**
- ³¹ Vila, A.; Gill, H.; McCallion, O.; Alonso, M.J.; *J. Contr. Release* **2004**, *98*, 231
- ³² Mayer, M. M.; in "Experimental Immunochemistry.", Eds: Kabat E.A.; Mayer, M.M., Springfield, IL, USA **1961**, 133
- ³³ Vermette, P.; Meagher, L.; *Colloid Surf. B: Biointerfaces* **2003**, *28*, 153
- ³⁴ Becker, P.; Schick, M. J.; in "Nonionic surfactants: Physical Chemistry, Surfactant Science Series"; Vol. 23; Ed. Schick, M. J.; Marcel Dekker, New-York, **1987**, 435
- ³⁵ Sela, Y.; Magdassi, S.; Garti, N.; *Colloid Polym. Sci.* **1994**, *272*, 684
- ³⁶ March, G. C.; Napper, D. H.; *J. Colloid Interface Sci.* **1977**, *61*, 383
- ³⁷ Piirma, I.; Lenzotti, J. R.; *Br. Polym. J.* **1989**, *21*, 45
- ³⁸ Gref, R.; Babak, V.; Bouillot, P.; Lukina, I.; Bodorev, M.; Dellacherie, E.; *Colloid Surf. A: Physicochem. Eng. Aspects* **1998**, *143*, 413

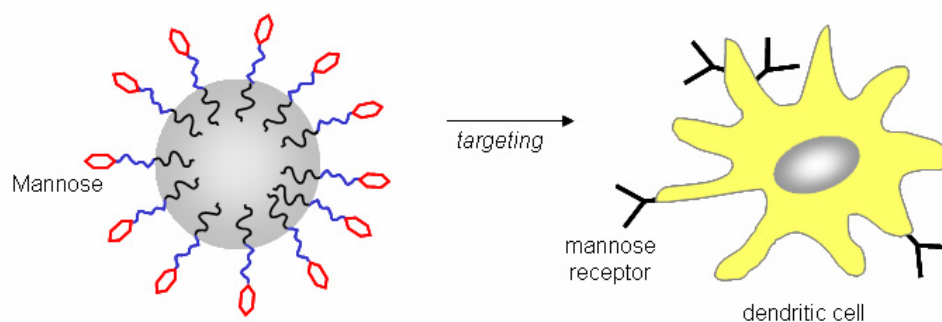
- ³⁹ Passirani, C.; Barratt, G.; Devissaguet, J. P.; Labarre, D.; *Pharm. Res.* **1998**, *15*, 1046
- ⁴⁰ Jeon, S. I.; Lee, J. H.; Andrade, J. D.; De Gennes, P. G.; *J. Colloid Interface Sci.* **1991**, *142*, 149
- ⁴¹ Osterberg, E.; Bergstrom, K.; Holmberg, K.; Schuman, T. P.; Riggs, J. A.; Burns, N. L.; Van Alstine, J. M.; Harris, J. M.; *J. Biomed. Mater. Res.* **1995**, *29*, 741

Chapter 6

**Mannosylated poly(ethylene oxide)-*b*-poly(ϵ -caprolactone) diblock
copolymers: synthesis, characterization, applications for surface
modification of poly(D,L-lactide acid) nanoparticles
and interaction with lectins**

Abstract

*Novel amphiphilic glycopolymers were synthesized by the covalent grafting of mannose derivatives on α -end-functionalized poly(ϵ -caprolactone) and poly(ethylene oxide)-b-poly(ϵ -caprolactone) diblock copolymers (PEO-b-PCL). The different glycopolymers were fully characterized in terms of chemical integrity and purity by high resolution NMR spectroscopy and SEC. They were utilized as amphiphilic bioresorbable surface modifiers for the preparation of poly(D,L-lactic acid) (PLA) nanoparticles by the nanoprecipitation-evaporation technique. The size of the nanoparticles was found to depend on the molar copolymer/ PLA ratio and the nature of the glycopolymer, demonstrating its influence on the formation of the nanoparticles. The surface of the nanoparticles was characterized by $^1\text{H-NMR}$ spectroscopy and zeta potential measurements. Both techniques revealed surface modification of the nanoparticles. Finally, preliminary evidences of the presence and bioavailability of mannose residues on the nanoparticles' surface were obtained by lectin recognition assays, based on the specific interaction of mannose with lectins (*Galanthus nivalis* lectin, GNA). These systems may find potential utility as targeted in vivo vaccine delivery systems.*



Contents

I. INTRODUCTION.....	180
II. EXPERIMENTAL PART.....	181
<i>Materials</i>	181
<i>Synthesis of mannose-derivatives</i>	182
<i>Synthesis of (co)polymers and glycopolymers</i>	187
<i>Preparation of micellar solutions</i>	192
<i>Preparation of nanoparticles</i>	193
<i>Characterization techniques</i>	193
III. RESULTS AND DISCUSSION	197
<i>III.1. Synthesis of the mannose derivatives</i>	199
<i>III.2. Synthesis of α-end-functionalized polymers</i>	200
III.2.1. Synthesis of α -carboxy poly(ϵ -caprolactone).....	200
III.2.2. Synthesis of amphiphilic copolymers	202
III.2.2.1. Synthesis of α -diethylacetal poly(ethylene oxide)- <i>b</i> -poly(ϵ -caprolactone). ..	202
III.2.2.2. Synthesis of α -N,N-dimethylaminoethyl poly(ethylene oxide)- <i>b</i> -poly(ϵ -caprolactone).....	204
<i>III.3. Synthesis of the glycopolymers</i>	205
III.3.1. <i>Approach 1: Peptide-like coupling</i>	205
III.3.2. <i>Approach 2: Reductive amination reaction</i>	208
III.3.2.1. Conversion of the acetal functionality to an aldehyde.....	208
III.3.2.2. Reductive amination.	210
III.3.3. <i>Approach 3: Quarternization reaction</i>	212
III.3.4. General conclusions on the synthesis of glycopolymers.....	214
<i>III.4. Amphiphilic properties of the (glyco)polymers</i>	216
III.4.1. Dynamic interfacial tension measurements.....	216
III.4.2. Micelle formation.	218
<i>III.5. Preparation and characterization of nanoparticles</i>	220
III.5.1. Characterization of size and shape of the NPs.	220
III.5.2. Analysis of the NPs' surface.	225
III.5.2.1. Physico-chemical techniques	225
III.5.2.2. Recognition assays.....	228
III.5.3. Stability.	231
IV. CONCLUSIONS	234

I. Introduction

Cell surface carbohydrates from glycoproteins and glycolipids play an essential role as recognition sites between cells or cells and microorganisms. The recognition mechanism is essentially based on specific interactions between the saccharide residues and soluble or membrane proteins (lectins).¹ Taking advantage of carbohydrates as information molecules, numerous polymeric materials carrying multiple saccharide moieties, such as linear polymers, dendrimers, polymer micelles or nanoparticles, have been developed for analytical, diagnostic and therapeutic purposes. It has been shown that such glycomimetics, that present saccharides in a polyvalent array, may have enhanced binding capacity with lectins based on “the cluster glycoside effect” while the monomeric carbohydrate derivatives exhibit only weak affinity to the same lectins.^{2,3,4,5} In the field of drug delivery, such glycomaterials appear as promising carrier systems allowing the cellular specific targeting of therapeutic agents via membrane lectins, which are capable of internalization of their ligands.⁶ It should be noted, that glycoreceptor (lectin) binding to a particular sugar occurs in a regioselective manner and thus the introduction of glucidic ligands on polymers is generally performed by 1-O substitution of the sugar.

The purpose of this study was to synthesize novel degradable polymeric nanoparticles coated with mannose moieties, which are known to selectively interact with human blood dendritic cells (DC). In fact, the latter express mannose-receptors on their surface. These systems may find potential application as *in vivo* vaccine delivery systems that targeted specifically DC. Indeed, DC are effective in capturing, processing and presenting antigens to native T cells, initiating cellular immune response.⁷ As such, they have been identified as a potent target for vaccine delivery to initiate adaptive immune responses.⁸ Furthermore, in the field of vaccination, nanoparticles have not only carrier function, but they also possess -due to their large size- ‘adjuvant’ properties, i.e., they act in a non-specific manner to increase the specific immunity (to an antigen as compared to that introduced by the vaccine or antigen alone).⁹

Our approach for the synthesis of such nanoparticles relies on the preparation of amphiphilic poly(ϵ -caprolactone) derivatives functionalized at one end by a mannose derivative, in order to be further used as bioresorbable stabilizers and surface modifiers of poly(D,L-lactic acid) (PLA) nanoparticles. PLA has been selected to form the nanoparticle matrix, owing to its biocompatibility, biodegradability and convenient degradation rate.

The synthesis of mannosylated poly(ϵ -caprolactone) derivatives is described herein following two different synthetic pathways; the first one is based on the covalent grafting of a mannose derivative on hydrophobic poly(ϵ -caprolactone) through a hydrophilic oligo(ethylene oxide) spacer. The second route involves the conjugation of a mannose derivative to an amphiphilic poly(ethylene oxide)-*b*-poly(ϵ -caprolactone) diblock copolymer functionalized at its hydrophilic end.

II. Experimental Part

Materials.

All polymerization reactions were carried out under (dry and oxygen-free) argon atmosphere using standard Schlenk techniques. ϵ -Caprolactone (ϵ -CL) (Aldrich, 99%) was dried over calcium hydride under stirring at room temperature for 48 h and purified by vacuum distillation just before use. Toluene and tetrahydrofuran (THF) were purified by distillation under nitrogen after drying over sodium benzophenone ketyl complex. Methylene chloride (CH_2Cl_2) and pyridine were dried by refluxing over calcium hydride for at least 48 h and distilled prior to use. *p*-Methoxy benzyl alcohol (Janssen Chimica, 98%) was dried by repeated azeotropic distillation of toluene just before use. Diethyl ether (Vel), 2-propanol (i PrOH), acetic acid (AcOH), acetone, ethylene oxide (EO) (Messer), 3,3-diethoxy-1-propanol (Aldrich, 98%), 2-dimethylamino ethanol (Aldrich, 99.5%), *N,N*-dimethylformamide (DMF) (Fluka), methylene chloride (Fluka), toluene (Fluka), triethylaluminum (AlEt_3) (Fluka, 1.9M in toluene), 2-[2-(2-Chloroethoxy)-ethoxy]ethanol (Aldrich, 96%), boron trifluoride diethyl etherate (Fluka, 96%) ($\text{BF}_3 \cdot \text{OEt}_2$), sodium azide (NaN_3), 2-Bromoethanol (Fluka, > 95%), *N*-ethyl-diisopropylamine (Fluka, > 98%), Amberlite IR-120[®] (Fluka), methanol (Fluka), ethyl acetate, DMF, ethanol, *N*-hydroxysuccinimide (NHS), 1-ethyl-3-(3-dimethylaminopropyl)carbodiimide (EDC) (Fluka, > 99%), palladium on activated charcoal (10% Pd) (Fluka), and sodium cyanoborohydrate (NaCNBH_3) (Fluka, > 95%) were used as received. Nanoparticles were prepared using acetone (Elvetec[®], 99%), sterile water (Versol[®]) and PLA (BioMérieux, $M_n = 32650$ g/mol, $I_p \sim 1.5$). MilliQ[®] water was used for all other experiments.

Recognition assays were carried out using commercially available lectins and their conjugates. *Concanavalin A* (ConA) from *Canavalis ensiformis* (Sigma, lyophilized

powder, Type IV) was used for aggregation assays of micellar solutions. *Galanthus nivalis* lectin (GNA) coated colloidal gold particles (GNA-gold NP) of a mean diameter of 10 nm (E.Y. Laboratories INC.) were used for cryo-TEM experiments. GNA-biotin conjugate (Biotin conjugated pure *Galanthus nivalis* lectin (GNA) from Snowdrop Bulb, EY Laboratories, INC.), bovine serum albumin (BSA) (Sigma), streptavidine-phosphatase and p-nitrophenyl phosphate (pNPP) were used for the biological recognition assays based on lectin-sugar interactions.

The purity of the synthesized compounds was determined by $^1\text{H-NMR}$ spectroscopy and mass spectrometry (MS) respectively. When no trace of by-products was observed by NMR and MS, the products were described as “>95%” pure (no trace by NMR) and “>99% pure” (no trace by MS), respectively.

Synthesis of mannose-derivatives.

1,2,3,4,6-Penta-*O*-acetyl-*D*-mannopyranose (1).

The synthesis of α -*D*-mannose pentaacetate was carried out according to the procedure described in the literature.¹⁰ The peracetylated sugar was dried by three azeotropic distillations with toluene just before use for the next synthesis step.

Series “a”, introduction of a chloride group.

2-[2-(2-Chloroethoxy)ethoxy]ethyl-2,3,4,6-tetra-*O*-acetyl- α -*D*-mannopyranoside, MannOAc-(EO)₃-Cl (3a).

α -*D*-mannose pentaacetate (6.45 g, 0.0165 mol) was dried by azeotropic distillation with toluene (3×60 ml) and dissolved in 35 ml of CH_2Cl_2 . To this solution, 3.25 ml of 2-[2-(2-Chloroethoxy)-ethoxy]ethanol (0.0224 mol) in 10 ml of CH_2Cl_2 were added under nitrogen. Then, 12 ml of $\text{BF}_3 \cdot \text{OEt}_2$ (0.095 mol) were added drop-by-drop at 0°C over a period of 20 min. The progress of the reaction was followed by Thin Layer Chromatography (TLC; 1:1 ethyl acetate/ cyclohexane). After 24 h of stirring at room temperature under nitrogen, the reaction mixture was slowly added to 45 ml of ice-cooled water.¹¹ The aqueous phase was extracted with 25 ml of CH_2Cl_2 , then the combined organic phases were washed with aqueous saturated NaHCO_3 (1×20 ml), H_2O (2×10 ml) and dried (Na_2SO_4). Solvent was evaporated under vacuum at room temperature and the

crude product was purified by flash chromatography over silica (1:2 ethyl acetate/cyclohexane to give 5.0 g (0.0100 mol) of **3a** as a white solid.

Yield: 60%, purity: > 95%, TLC: $R_f = 0.42$ (7:3 EtOAc/ Cyclohexane) (H_2SO_4)

1H -NMR ($CDCl_3$, 400 MHz) δ (ppm): 1.99, 2.06, 2.11, 2.16 (4×s, 4×3H, CH_3COO), 3.63-3.72 (m, 9H, $OCHHCH_2OCH_2CH_2OCH_2CH_2Cl$), 3.75-3.87 (m, 3H, $OCHHCH_2OCH_2CH_2OCH_2CH_2$), 4.07 (ddd, 1H, H-5), 4.11 (dd, 1H, H-6a), 4.30 (dd, 1H, H-6b), 4.89 (d, 1H, H-1), 5.29 (dd, 1H, H-2), 5.32 (t, 1H, H-4), 5.38 (dd, 1H, H-3). **^{13}C -NMR** ($CDCl_3$, 100 MHz) δ (ppm): 22.04, 22.06, 22.08, 22.20 (4× CH_3COO), 44.20 (OCH_2CH_2Cl), 63.75 (C-6), 67.48 (C-4), 68.70 ($OCH_2CH_2OCH_2CH_2OCH_2CH_2Cl$), 69.72 (C-5), 70.39 (C-3), 70.89 (C-2), 71.39, 71.98, 72.05 ($OCH_2CH_2OCH_2CH_2OCH_2CH_2Cl$), 72.71 ($OCH_2CH_2OCH_2CH_2OCH_2CH_2Cl$), 99.03 (C-1), 171.01, 172.01, 171.35, 172.00 (4× CH_3COO). **ESI-HRMS**: $C_{20}H_{31}ClO_{12}Na$ [$M+Na$] $^+$, M_{theor} m/z : 521.14017, $M_{ESI-RHMS}$ m/z : 521.1399; $C_{20}H_{31}ClO_{12}K$ [$M+K$] $^+$, M_{theor} m/z : 537.11411, $M_{ESI-RHMS}$ m/z : 537.1155.

2-[2-(2-Azidoethoxy)ethoxy]ethyl-2,3,4,6-tetra-*O*-acetyl- α -D-mannopyranoside, MannOAc-(EO) $_3$ -N $_3$ (4a**).**

Compound **3a** (2.0 g, 0.0040 mol) was dissolved in 150 ml of dry DMF at room temperature under nitrogen. 2.0 g of sodium azide (0.032 mol) were added and the reaction mixture was vigorously stirred at 50°C for 42 h. Then, insoluble NaN_3 was filtered off, and the filtrate was concentrated under vacuum. The residual colorless syrup was dissolved in 150 ml of ethyl acetate and the resulting organic phase was washed with H_2O (2×20 ml and 2×10 ml) and dried with Na_2SO_4 . Solvent was evaporated under vacuum to yield **4a** as a colorless syrup/ wax.

Yield: 95%, purity: 93%, TLC: $R_f = 0.41$ (7:3 EtOAc/ Cyclohexane) (H_2SO_4)

1H -NMR ($CDCl_3$, 400 MHz) δ (ppm): 1.99, 2.06, 2.11, 2.16 (4×s, 4×3H, CH_3COO), 3.38 (t, 2H, $OCH_2CH_2N_3$), 3.63-3.71 (m, 9H, $OCHHCH_2OCH_2CH_2OCH_2CH_2N_3$), 3.82-3.87 (m, 1H, $OCHHCH_2OCH_2CH_2OCH_2CH_2N_3$), 4.05 (ddd, 1H, H-5), 4.11 (dd, 1H, H-6a), 4.30 (dd, 1H, H-6b), 4.88 (d, 1H, H-1), 5.29 (dd, 1H, H-2), 5.32 (t, 1H, H-4), 5.35 (dd, 1H, H-3). **^{13}C -NMR** ($CDCl_3$, 100 MHz) δ (ppm): 22.04, 22.06, 22.08, 22.20 (4× CH_3COO), 52.01 ($OCH_2CH_2N_3$), 63.80 (C-6), 67.48 (C-4), 68.78 ($OCH_2CH_2OCH_2CH_2OCH_2CH_2N_3$), 69.80 (C-5), 70.29 (C-3), 70.89 (C-2), 71.39, 71.98, 72.05 ($OCH_2CH_2OCH_2CH_2OCH_2CH_2N_3$), 72.13 ($OCH_2CH_2OCH_2CH_2OCH_2CH_2N_3$), 99.08 (C-1), 171.01, 172.01, 171.35, 172.00

(4×CH₃COO). **ESI-HRMS:** C₂₀H₃₁N₃O₁₂Na [M+Na]⁺, M_{theor} *m/z*: 528.18054, M_{ESI-RHMS} *m/z*: 528.1807; C₂₀H₃₁N₃O₁₂K [M+K]⁺, M_{theor} *m/z*: 544.15448, M_{ESI-RHMS} *m/z*: 544.1548.

2-[2-(2-Azidoethoxy)ethoxy]ethyl- α -D-mannopyranoside, MannOH-(EO)₃-N₃ (5a).

Compound **4a** (1.85 g, 3.66 mmol) was dissolved in 45 ml of dry methanol and 2.0 ml of 0.82 M sodium methoxide (NaOMe) (1.64 mmol) were added under nitrogen. After 5 h of stirring at room temperature, the solution was neutralized with Amberlite IR-120[®] (H⁺) resin and filtered off. Solvent was evaporated to give 1.10 g (0.0032 mol) of **5a** as a colorless wax.

Yield: 89%, purity: 95%, TLC: R_f = 0.21 (4:1 CH₂Cl₂/MeOH) (H₂SO₄)

¹H-NMR (D₂O, 400 MHz) δ (ppm): 3.43 (m, 2H, OCH₂CH₂N₃), 3.56-3.84 (m, 15H, H-2, H-3, H-4, H-6a, H-6b, OCH₂CH₂OCH₂CH₂OCH₂CH₂N₃), 3.84 (m, 1H, H-5), 4.87 (d, 1H, H-1). ¹³C-NMR (D₂O, 100 MHz) δ (ppm): 51.31 (OCH₂CH₂N₃), 62.15 (C-6), 67.48, 68.18, 70.51, 70.75, 70.80, 70.89, 71.23, 71.76, 74.01 (C-2, C-3, C-4, C-5, OCH₂CH₂OCH₂CH₂OCH₂CH₂N₃), 100.08 (C-1). **ESI-HRMS:** C₁₂H₂₃N₃O₈Na [M+Na]⁺, M_{theor} *m/z*: 360.13828, M_{ESI-RHMS} *m/z*: 360.1388; C₁₂H₂₃N₃O₈K [M+K]⁺, M_{theor} *m/z*: 376.11222, M_{ESI-RHMS} *m/z*: 376.1120.

2-[2-(2-Aminoethoxy)ethoxy]ethyl- α -D-mannopyranoside, MannOH-(EO)₃-NH₂ (6a).

Compound **5a** (0.60 g, 1.78 mmol) was dissolved in 45 ml of ethanol. 90 mg of palladium activated on charcoal (10% Pd/C) were added. After 4 h of stirring at room temperature under hydrogen atmosphere, Pd/C was removed by filtration over celite. The filtrate was concentrated under vacuum to yield 0.548 g (1.76 mol) of **6a** as a colorless wax.

Yield: 99%, purity: 80%, TLC: R_f = 0.02 (4:1 2-Propanol/H₂O (1% NH₃)) (Ninhydrin)

¹H-NMR (D₂O, 400 MHz) δ (ppm): 2.75 (t, 2H, OCH₂CH₂NH₂), 3.49-3.84 (m, 15H, H-2, H-3, H-4, H-6a, H-6b, OCH₂CH₂OCH₂CH₂OCH₂CH₂NH₂), 3.89 (dd, 1H, H-5), 4.86 (d, 1H, H-1). ¹³C-NMR (D₂O, 100 MHz) δ (ppm): 41.02 (OCH₂CH₂NH₂), 62.20 (C-6), 67.62, 68.01, 70.62, 70.72, 70.93, 71.20, 71.85, 73.23, 74.01 (OCH₂CH₂OCH₂CH₂OCH₂CH₂NH₂, C-2, C-3, C-4, C-5), 101.15 (C-1). **ESI-HRMS:** C₁₂H₂₅NO₈H [M+H]⁺, M_{theor} *m/z*: 312.1658, M_{ESI-RHMS} *m/z*: 312.1656; C₁₂H₂₅NO₈Na [M+Na]⁺, M_{theor} *m/z*: 334.1478, M_{ESI-RHMS} *m/z*: 334.1493.

Series “b”, introduction of a bromide group.

2-Bromoethyl-2,3,4,6-tetra-O-acetyl- α -D-mannopyroside (MannOAc-Br) (3b).

To a solution of 5.00 g of dried acetylated sugar **1** (0.0128 mol) and 1.84 ml 2-bromoethanol (0.0172 mol) in 30 ml of dry methylene chloride, 11 ml of $\text{BF}_3 \cdot \text{OEt}_2$ (0.0896 mol) were added dropwise at 0°C over a period of 30 min under nitrogen. The progress of the reaction was followed by TLC (7:3 ethyl acetate/ cyclohexane). After 6 h of stirring at room temperature under nitrogen, the reaction mixture was slowly added to 40 ml of ice-cooled water. The aqueous phase was extracted with 20 ml of CH_2Cl_2 , then the combined organic phases were washed with aqueous saturated NaHCO_3 (20 ml), H_2O (2×5 ml) and dried (Na_2SO_4). Solvent was evaporated under vacuum at room temperature and the crude product was purified by flash chromatography over silica (1:2 ethyl acetate/ cyclohexane), to give 4.01 g (8.83 mmol) of **3b** as a white crystalline solid.

Yield: 69%, purity: > 99%, TLC: $R_f = 0.75$ (6.5:3.5 EtOAc/ Cyclohexane) (H_2SO_4)

$^1\text{H-NMR}$ (CDCl_3 , 400 MHz) δ (ppm): 3.52 (t, 2H, CH_2Br), 3.88 (m, 1H, CHHCH_2Br), 3.98 (m, 1H, CHHCH_2Br), 4.12-4.18 (m, 2H, H5, H-6a), 4.29 (m, 1H, H-6b), 4.88 (d, 1H, H-1), 5.26 – 5.38 (m, 3H, H-2, H-4, H-3). $^{13}\text{C-NMR}$ (CDCl_3 , 100 MHz) δ (ppm): 21.98, 22.03, 22.07, 22.19 ($4 \times \text{CH}_3\text{COO}$), 30.09 ($\text{OCH}_2\text{CH}_2\text{Br}$), 63.76 (C-6), 67.28 (C-4), 69.78, 70.19, 70.32, 70.69 ($\text{CH}_2\text{CH}_2\text{Br}$, C-5, C-3, C-2), 99.08 (C-1), 171.01, 171.14, 171.32, 171.99 ($4 \times \text{CH}_3\text{COO}$). **ESI-HRMS**: $\text{C}_{16}\text{H}_{23}\text{O}_{10}\text{BrNa}$ $[\text{M}+\text{Na}]^+$, M_{theor} m/z : 477.03723, $M_{\text{ESI-RHMS}}$ m/z : 477.0358.

2-Azidoethyl-2,3,4,6-tetra-O-acetyl- α -D-mannopyroside (MannOAc-N₃) (4b).

Compound **3b** (0.68 g, 1.49 mmol) was dissolved in 35 ml of dry DMF at room temperature under nitrogen. 0.77 g of sodium azide (12 mmol) were added and the reaction mixture was vigorously stirred at 50°C for 38 h. Then, insoluble NaN_3 was filtered off, and the filtrate was concentrated under vacuum. The residual colorless syrup was dissolved in 40 ml of ethyl acetate and the resulting organic phase was washed with H_2O (1×10 ml, 3×5 ml) and dried (Na_2SO_4). Solvent was evaporated under vacuum to yield 0.584 g (1.40 mmol) of **4b** as a white powder.

Yield: 94%, purity: > 99%, TLC: $R_f = 0.84$ (8.5:1.5 CH_2Cl_2 / MeOH) (H_2SO_4)

¹H-NMR (CDCl₃, 400 MHz) δ (ppm): 1.99, 2.06, 2.11, 2.16 (4×s, 4×3H, CH₃COO), 3.45 (m, 2H, CH₂-N₃), 3.66 (m, 1H, CHH-CH₂-N₃), 3.87 (m, 1H, CHH-CH₂), 4.03 (m, 1H, H-5), 4.14 (dd, 1H, H-6a), 4.29 (dd, 1H, H-6b), 4.86 (d, 1H, H-1), 5.24-5.38 (m, 3H, H-2, H-3, H-4). **¹³C-NMR** (CDCl₃, 100 MHz) δ (ppm): 22.04, 22.06, 22.08, 22.20 (4×CH₃COO), 51.65 (CH₂N₃), 63.75 (C-6), 67.75 (C-4), 68.34 (OCH₂CH₂N₃), 70.15 (C-3, C-5), 70.68 (C-2), 99.04 (C-1), 171.05, 171.10, 171.30, 171.90 (4×CH₃COO). **ESI-HRMS**: C₁₆H₂₃N₃O₁₀Na [M+Na]⁺, M_{theor} *m/z*: 440.12811, M_{ESI-RHMS} *m/z*: 440.1284.

2-Azidoethyl-α-D-mannopyroside (MannOH-N₃) (5b).

Compound **4b** (0.92 g, 2.20 mmol) was dissolved in 20 ml of dry methanol and 1.0 ml of 0.82 M NaOMe (0.82 mmol) were added under nitrogen. After 5 h of stirring at room temperature, the solution was neutralized with Amberlite IR-120[®] (H⁺) resin and filtered off. Solvent was evaporated to give 0.48 g (1.93 mmol) of **5b** as a white powder.

Yield: 87%, purity: > 99%, TLC: R_f = 0.17 (8.5:1.5 CH₂Cl₂/ MeOH)

¹H-NMR (D₂O, 400 MHz) δ (ppm): 3.43 (m, 2H, CH₂CH₂N₃), 3.53-3.92 (m, 8H, OCHH-CH₂-N₃, H-2, H-3, H-4, H-5, H-6a, H-6b), 4.83 (d, 1H, H-1). **¹³C-NMR** (D₂O, 100 MHz) δ (ppm): 51.5 (CH₂N₃), 62.2 (C-6), 67.6, 67.9, 71.2, 71.7, 74.2 (CH₂CH₂N₃, C-2, C-3, C-4, C-5), 101.1 (C-1). **ESI-HRMS**: C₈H₁₅N₃O₆Na [M+Na]⁺, M_{theor} *m/z*: 272.08586, M_{ESI-RHMS} *m/z*: 272.0845; C₈H₁₅N₃O₆K [M+K]⁺, M_{theor} *m/z*: 288.05979, M_{ESI-RHMS} *m/z*: 288.0599.

2-Aminoethyl-α-D-mannopyroside (MannOH-NH₂) (6b).

Compound **5b** (0.14 g, 0.56 mmol) was dissolved in 35 ml of ethanol. 30 mg of 10% Pd/C were added. After 4 h of stirring under hydrogen atmosphere at room temperature, Pd/C was removed by filtration over celite. The filtrate was concentrated under vacuum to yield 0.122 g (0.547 mol) of **6b** as a colorless wax.

Yield: 98%, purity: 92%, TLC: R_f = 0.02 (4:1 2-Propanol/ H₂O (1% NH₃)) (Ninhydrin)

¹H-NMR (D₂O, 400 MHz) δ (ppm): 2.75 (m, 2H, CHCH₂NH₂), 3.45 (m, 1H, OCHHCH₂NH₂), 3.5-3.9 (m, 7H, OCHHCH₂NH₂, H-2, H-3, H-4, H-5, H-6a, H-6b), 4.78 (d, 1H, H-1). **¹³C-NMR** (D₂O, 100 MHz) δ (ppm): 41.2 (OCH₂CH₂NH₂), 62.2 (C-6), 68.1 (C-4), 69.7, 71.2, 71.8, 74.1 (CH₂CH₂NH₂, C-2, C-3, C-5), 101.0 (C-1). **ESI-HRMS**: C₈H₁₈NO₆ [M+H]⁺, M_{theor} *m/z*: 224.11341, M_{ESI-RHMS} *m/z*: 224.1122; C₈H₁₇NO₆Na [M+Na]⁺, M_{theor} *m/z*: 246.09536, M_{ESI-RHMS} *m/z*: 246.0961.

2-Bromoethyl- α -D-mannopyroside (MannOH-Br) (7)

Compound **6b** (1.10 g, 2.41 mmol) was dissolved in 25 ml of dry methanol and 1.6 ml of 0.82 M NaOMe (1.3 mmol) were added under nitrogen. After 35 h of stirring at room temperature, the solution was neutralized with Amberlite IR-120[®] (H⁺) resin and filtered off. Solvent was evaporated to give 0.69 g (2.41 mmol) of **7** as a waxy solid.

Yield: 100%, purity: > 99%, TLC: R_f = 0.02 (7:3 EtOAc/ Cyclohexane) (H₂SO₄).

¹H-NMR (D₂O, 400 MHz) δ (ppm): 3.52-3.60 (m, 3H, CHHCH₂Br, H-4), 3.66-3.95 (m, 7H, CHHCH₂Br, H-2, H-3, H-5, H-6a, H-6b), 4.84 (d, 1H, H-1). ¹³C-NMR (D₂O, 100 MHz) δ (ppm): 32.6 (C_t, OCH₂CHBr), 62.2 (C-6), 67.8 (C-4), 68.8, 71.2, 71.8, 74.2 (CH₂CH₂Br, C-5, C-3, C-2), 101.0 (C-1). **ESI-HRMS**: C₈H₁₅O₆BrNa [M+Na]⁺, M_{theor} *m/z*: 308.99497, M_{ESI-RHMS} *m/z*: 308.9941; C₈H₁₅O₆BrK [M+K]⁺, M_{theor} *m/z*: 324.96891, M_{ESI-RHMS} *m/z*: 324.9674.

Synthesis of (co)polymers and glycopolymers.

Approach 1: Synthesis of an amphiphilic glycopolymer via a peptide-like coupling reaction.

Synthesis of *p*-methoxy benzyl poly(ϵ -caprolactone) (*p*-MeO-Bz-O-PCL) (8).

p-Methoxy benzyl alcohol (*p*-MeO-Ph-CH₂-OH) (1.35 g, 9.77 mmol) was dried by azeotropic distillation with toluene (3 \times 20 ml). The dried product (1.05 g, 7.6 mmol) was then dissolved in 80 ml of dry toluene and poured into a solution of toluene (200 ml) containing AlEt₃ (4 ml, 1.9 M, 7.6 mmol) at 0°C. After 15 min, 7 ml of ϵ -caprolactone (0.063 mol) were added. The reaction mixture was stirred at room temperature for 12 h. The polymerization was quenched by adding an excess of AcOH (1 M in water) and the polymer was recovered by precipitation in heptane and vacuum-dried at room temperature. Yield: 58% (4.2 g), M_{n, NMR} = 1350 g/mol, M_w/M_n (SEC) = 1.42, end functionality > 95% ¹H-NMR (D₂O, 400 MHz) δ (ppm): 1.35 (t, 2H, CH₂-CH₂-CH₂), 1.65 (m, 4H, CH₂-CH₂-CH₂), 2.30 (m, 2H, CH₂-COO), 3.62 (t, 2H, -CH₂-OH), 4.05 (t, 2H, COO-CH₂), 5.04 (m, Ar-CH₂-O), 6.87 (d, 2H, Ar-H), 7.28 (d, 2H, Ar-H).

Conversion of *p*-methoxy benzyl poly(ϵ -caprolactone) into α -carboxy poly(ϵ -caprolactone) (9**).**

Compound **8** (4 g, 29 mmol) was dissolved in 100 ml of acetone and 10% Pd/C (1.6 g) was added. The reaction mixture was stirred under hydrogen atmosphere at room temperature for 21 h. The catalyst was filtered off and the final polymer was isolated by precipitation with an excess amount of heptane and vacuum drying at room temperature.

Yield: 90%, M_n , NMR = 1450 g/mol, M_w/M_n (SEC) = 1.44, end functionality > 95%

$^1\text{H-NMR}$ (CDCl_3 , 400 MHz) δ (ppm): 1.35 (m, 2H, $\text{CH}_2\text{-CH}_2\text{-CH}_2$), 1.65 (m, 4H, $\text{CH}_2\text{-CH}_2\text{-CH}_2$), 2.30 (m, 2H, $\text{CH}_2\text{-COO}$), 3.62 (t, 2H, $-\text{CH}_2\text{-OH}$), 4.05 (t, 2H, COO-CH_2).

Synthesis of poly(ϵ -caprolactone) end-capped by a mannose residue (10**).**

0.50 g of compound **9** were dissolved in 15 ml of dry DMF. Then, 0.10 g of EDC (0.54 mmol), 0.07 g of *N*-ethyl-diisopropylamine (DIPEA) (0.54 mmol) and 0.063 g (0.54 mmol) of NHS dissolved in 3 ml of DMF were added under nitrogen. After 20 h of stirring at room temperature, 0.177 mg of compound **6a** (0.57 mmol) dissolved in 3 ml of DMF was added and the resulting mixture was allowed to stir for further 24 h at room temperature. Then, the solvent was partially evaporated under vacuum to a final volume of 5 ml and 15 ml of milli-Q water was added dropwise to the concentrated reaction mixture under vigorous stirring. The mixture was introduced in a dialyse membrane (Spectra Pro[®] cut off 3500) and dialyzed for 2 days against milli-Q water. Compound **10** (0.495 g) was recovered after freeze-drying as a white powder.

For the preparation of nanoparticles, compound **10** was dissolved in acetone, filtered through Millex LG[®] (Millipore) 0.2 μm , and dried in vacuum.

Yield: 87%, M_n , NMR = 1650 g/mol, M_w/M_n (SEC) = 1.31, end group functionalization = 88%

$^1\text{H-NMR}$ (CDCl_3 , 400 MHz) δ (ppm): 1.35 (m, 2H, $\text{CH}_2\text{-CH}_2\text{-CH}_2$), 1.65 (m, 4H, $\text{CH}_2\text{-CH}_2\text{-CH}_2$), 2.17 (t, 2H, NHCOCH_2), 2.30 (m, 2H, $\text{CH}_2\text{-COO}$), 3.38 (t, 2H, $\text{CH}_2\text{-NH-CO}$), 3.57-3.90 (mannose + 2H ($\text{PCL-CH}_2\text{-OH}$), 3.92 (m, 2H, H-5), 4.05 (t, 2H, COO-CH_2), 4.88 (d, 1H, H-1_{ano}, mannose).

Approach 2: Synthesis of an amphiphilic glycopolymer via a reductive amination reaction.

Synthesis of α -diethylacetal-poly(ethylene oxide) (11a).

In a flame-dried and argon-purged flask, 280 ml of anhydrous THF, 1.9 ml of 3,3-diethoxy-1-propanol (12 mmol) and 20 ml of potassium naphthalene/THF solution (0.6 M) were added under an Argon stream. After vigorous stirring for 15 min at room temperature, this solution was introduced into a 500 ml Parr reactor and 60 g (1.364 mol) of EO were added. After 18 h of polymerization at 30°C, the reaction was treated by 2-propanol, precipitated with an excess amount of diethyl ether and vacuum-dried at 30°C.

Yield: 95%, M_n , NMR = 4650 g/mol, M_w/M_n (SEC) = 1.05, end functionality > 95%

$^1\text{H-NMR}$ (CDCl_3 , 400 MHz) δ (ppm): 1.18 (t, 6H, $\text{CH}_3\text{-CH}_2\text{-O}$), 1.88 (q, 2H, $\text{CH-CH}_2\text{-CH}_2\text{-O}$), 3.55 (m, 4H, $\text{CH}_3\text{-CH}_2\text{-O}$), 3.63 (s, 4H, $\text{O-CH}_2\text{-CH}_2\text{-O}$), 4.62 (t, 1H, CH).

Synthesis of α -diethylacetal-poly(ethylene oxide)-*b*-poly(ϵ -caprolactone)-OH (12a).

4.8 g of compound **11a** were dried by azeotropic distillation with toluene (3 \times 20 ml) and then, 50 ml of dry toluene and AlEt_3 (0.7 ml, 1.9 M) were added. After 30 min at room temperature, 2.4 ml of ϵ -caprolactone (0.022 mol) were added. After 40 h of polymerization at room temperature, the reaction mixture was treated by an AcOH solution (1M in water), precipitated with an excess amount of heptane and vacuum-dried.

Yield: 95%, M_n , NMR = 7250 g/mol, M_w/M_n (SEC) = 1.13, end functionality > 95%

$^1\text{H-NMR}$ (CDCl_3 , 400 MHz) δ (ppm): 1.18 (t, 6H, $\text{CH}_3\text{-CH}_2\text{-O}$), 1.40 (m, 2H, $\text{CH}_2\text{-CH}_2\text{-CH}_2$), 1.64 (m, 4H, $\text{CH}_2\text{-CH}_2\text{-CH}_2$), 1.88 (q, 2H, $\text{CH-CH}_2\text{-CH}_2\text{-O}$), 2.29 (m, 2H, OOC-CH_2), 3.55 (m, 4H, $\text{CH}_3\text{-CH}_2\text{-O}$), 3.63 (m, 4H, $\text{O-CH}_2\text{-CH}_2\text{-O}$), 4.04 (m, 2H, $\text{CH}_2\text{-CH}_2\text{-CH}_2\text{-O}$), 4.21 (m, 2H, $\text{PCL-COO-CH}_2\text{-PEO}$), 4.62 (t, 1H, CH).

Synthesis of α -diethylacetal- ω -methoxy-poly(ethylene oxide)-*b*-poly(ϵ -caprolactone) (13a).

α -Diethylacetal-poly(ethylene oxide)-*b*-poly(ϵ -caprolactone)-OH (**12a**) (2.0 g) was dried by azeotropic distillation with toluene (2 \times 15 ml) and then, 25 ml of dry CH_2Cl_2 and 1.2 ml of Et_3N were added. The mixture was cooled to -10°C and an acetyl chloride solution in CH_2Cl_2 (25.6 ml, 0.33 M) was added dropwise. The reaction mixture was

stirred at room temperature for 23 h. The solvent was removed by evaporation and the residual solid phase was dissolved in toluene. After filtration, the polymer was recovered by precipitation in heptane and vacuum-dried at room temperature. NMR analysis confirmed that the hydroxyl groups were converted quantitatively.

Yield: 85%, $M_{n, NMR} = 7250$ g/mol, M_w/M_n (SEC) = 1.17, end functionality > 95%

^1H NMR (CDCl_3 , 400 MHz) δ (ppm): 1.18 (t, 6H, $\text{CH}_3\text{-CH}_2\text{-O}$), 1.40 (m, 2H, $\text{CH}_2\text{-CH}_2\text{-CH}_2$), 1.64 (m, 4H, $\text{CH}_2\text{-CH}_2\text{-CH}_2$), 1.88 (m, 2H, $\text{CH-CH}_2\text{-CH}_2\text{-O}$), 1.97 (s, 3H, $\text{CH}_3\text{-COO}$), 2.29 (m, 2H, OOC-CH_2), 3.55 (m, 4H, $\text{CH}_3\text{-CH}_2\text{-O}$), 3.63 (m, 4H, $\text{O-CH}_2\text{-CH}_2\text{-O}$), 4.04 (m, 2H, $\text{CH}_2\text{-CH}_2\text{-CH}_2\text{-OOC}$), 4.21 (m, 2H, $\text{PCL-COO-CH}_2\text{-PEO}$), 4.62 (t, 1H, CH).

Synthesis of α -aldehyde PEO-*b*-PCL (15).

The deprotection of the aldehyde group of compound **13a** was conducted by mild acidification of a micellar aqueous solution (6 ml) of α -diethylacetal-PEO-*b*-PCL **13a** ($c = 6.66$ mg/ml, 0.0563 mmol) to pH 2 using a 0.5 M HCl aqueous solution, under moderate stirring. After 2 h of stirring at room temperature, the solution was adjusted to pH 5 by dropwise addition of a 0.1 M NaOH solution. The micellar solution was then immediately used for the reaction with the mannose amine derivative **6b**.

Yield: 83%, $M_{n, NMR} = 7200$ g/mol, M_w/M_n (SEC) = 1.26, end functionality 50 - 90%

^1H NMR (CDCl_3 , 400 MHz) δ (ppm): 1.40 (m, 2H, $\text{CH}_2\text{-CH}_2\text{-CH}_2$), 1.64 (m, 4H, $\text{CH}_2\text{-CH}_2\text{-CH}_2$), 1.97 (s, 3H, $\text{CH}_3\text{-COO}$), 2.29 (m, 2H, $\text{OOC-CH}_2\text{-CH}_2$), 2.67 (t, 2H, CHO-CH_2), 3.63 (m, 4H, $\text{O-CH}_2\text{-CH}_2\text{-O}$), 4.04 (m, 2H, $\text{CH}_2\text{-CH}_2\text{-CH}_2\text{-O}$), 4.21 (m, 2H, $\text{PCL-COO-CH}_2\text{-PEO}$), 9.77 (CHO-CH_2).

Synthesis of PEO-*b*-PCL α -end capped by a mannose residue by a reductive amination reaction (16).

Just after deprotection of the aldehyde group of **13a**, 4 equiv of mannose-amine **6b** were added to the micellar solution of **15** ($c = 6.66$ mg/ml, 0.0563 mmol) and the pH was adjusted to pH 5. Then, a tenfold excess of NaCNBH_3 (3.52 mg, 0.0563 mmol) dissolved in 0.5 ml of water was added, and the resulting mixture was stirred for 4 days under nitrogen atmosphere. Unreacted species were removed by dialysis using a preswollen membrane (Spectra Por[®], molecular cut-off: 6000-8000). The polymer was recovered by freeze-drying, and stored at -20°C .

Yield: 95%, M_w/M_n (SEC) = 1.30, end group functionalization = 23%

^1H NMR (CDCl_3 , 400 MHz) δ (ppm): 1.40 (m, 2H, $\text{CH}_2\text{-CH}_2\text{-CH}_2$), 1.64 (m, 4H, $\text{CH}_2\text{-CH}_2\text{-CH}_2$), 1.78 (quin, 2H, $\text{N-CH}_2\text{-CH}_2\text{-CH}_2$), 1.97 (s, 3H, $\text{CH}_3\text{-COO}$), 2.29 (m, 2H, OOC-CH_2), 2.45 (m, 2H, $\text{N-CH}_2\text{-CH}_2\text{-CH}_2$), 3.19 (m, 2H, $\text{-O-CH}_2\text{-CH}_2\text{-N}$), 3.63 (m, 4H, $\text{O-CH}_2\text{-CH}_2\text{-O}$), 4.04 (m, 2H, $\text{CH}_2\text{-CH}_2\text{-CH}_2\text{-O}$), 4.21 (m, 2H, $\text{PCL-COO-CH}_2\text{-PEO}$), 4.88 (d, 1H, 1-H_{ano} , Mannose).

Approach 3: Synthesis of an amphiphilic glycopolymer via quarternization.

Synthesis of α -*N,N*-dimethylaminoethyl poly(ethylene oxide) ($\text{Me}_2\text{N-PEO-OH}$) (11b**).**

In a flame-dried and argon-purged flask, 200 ml of anhydrous THF, 1.2 ml of *N,N*-dimethylaminoethanol (12 mmol) and 15 ml potassium naphthalene/THF solution (0.8 M) were added under argon stream. After vigorous stirring for 15 min at room temperature, the mixture was introduced into a 500 ml Parr reactor and 60 g of EO (1.364 mol) were added. After 19 h of polymerization at 30°C, 2-propanol was added and the polymer was precipitated with an excess of diethyl ether and vacuum-dried at 30°C.

Yield: 95%, $M_{\text{n, NMR}} = 5470$ g/mol, $M_{\text{w}}/M_{\text{n}}$ (SEC) = 1.06, end functionality > 95%

$^1\text{H-NMR}$ (CDCl_3 , 400 MHz) δ (ppm): 2.22 (s, 6H, $\text{CH}_3\text{-N}$), 2.47 (m, 2H, $\text{CH}_3\text{-N-CH}_2$), 3.62 (m, 4H, $\text{O-CH}_2\text{-CH}_2\text{-O}$).

Synthesis of α -*N,N*-dimethylaminoethyl poly(ethylene oxide)-*b*-poly(ϵ -caprolactone) ($\text{Me}_2\text{N-PEO-}b\text{-PCL-OH}$) (12b**).**

Compound **11b** ($\text{Me}_2\text{N-PEO-OH}$) (1.6 g, 0.3 mmol) was dried by azeotropic distillation with toluene (3×10 ml) and then, 3 ml of dry toluene, 1 drop of pyridine and AlEt_3 (0.25 ml, 1.9 M, 0.475 mmol) were added. After 20 min at room temperature, 3 ml of CH_2Cl_2 and 0.8 ml of ϵ -caprolactone (7.2 mmol) were added. After 36 h of polymerization at room temperature, the reaction was stopped by an excess of AcOH solution (1M in water), and the polymer was recovered by precipitation with a tenfold excess of heptane and vacuum-dried.

For the preparation of nanoparticles, compound **12b** was dissolved in acetone, filtered through Millex LG[®] (Millipore) 0.2 μm , and dried in vacuum.

Yield: 95%, $M_{\text{n, NMR}} = 8300$ g/mol, $M_{\text{w}}/M_{\text{n}}$ (SEC) = 1.10, end functionality > 95%

¹H-NMR (CDCl₃, 400 MHz) δ (ppm): 1.35 (m, 2H, CH₂-CH₂-CH₂), 1.65 (m, 4H, CH₂-CH₂-CH₂), 2.27 (s, 6H, CH₃-N), 2.30 (m, 2H, CH₂-COO), 2.51 (t, 2H, CH₃-N-CH₂), 3.63 (m, 4H, O-CH₂-CH₂-O), 4.05 (t, 2H, COO-CH₂), 4.22 (t, PCL-COO-CH₂-CH₂-O-PEO).

Synthesis of PEO-*b*-PCL end capped by a mannose residue via quarternization (14).

0.46 g of compound **12b** (M_n = 7100 g/mol) was dissolved in 10 ml of dry DMF. Then, 0.28 g of **7** (0.98 mmol) dissolved in 10 ml were added. After 50 h of stirring under nitrogen at 70°C, the reaction mixture was concentrated to 5 ml by partial evaporation of the solvent. Then, 10 ml of water were added and the mixture was introduced in a dialysis membrane (cut-off 3500), and then dialyzed against water Milli-Q for 48 h. The polymer was recovered by freeze-drying as a white solid (0.45 g).

For the preparation of nanoparticles, compound **14** was dissolved in acetone, filtered through Millex LG[®] (Millipore) 0.2 μm, and dried in vacuum. It was stored at -20°C.

Yield: 99%, M_n, NMR = 8600 g/mol, M_w/M_n (SEC) = 1.19, end group functionalization ~ 80%

¹H-NMR (CDCl₃, 400 MHz) δ (ppm): 1.35 (m, 2H, CH₂-CH₂-CH₂), 1.65 (m, 4H, CH₂-CH₂-CH₂), 2.30 (m, 2H, CH₂-COO), 3.40 (s, 6H, CH₃-N), 3.45-4.05 (m, 10 H, Mannose), 3.63 (m, 4H, O-CH₂-CH₂-O-), 4.05 (t, 2H, COO-CH₂), 4.22 (t, 2H, PCL-COO-CH₂-CH₂-O-PEO), 4.9 (s, 1H, H-1, mannose).

Preparation of micellar solutions.

Typically, 50 mg of amphiphilic copolymer were dissolved in 3 ml of THF (c = 16.6 mg/ml). After complete dissolution of the copolymer, 3 ml of doubly distilled water were slowly added. The mixture was dialyzed for 48 hours against water exchanging regularly the surrounding water, using a pre-swollen semi-permeable membrane (cut-off 3500 or 6000-8000 respectively). Similarly, the hydrolysis of the acetal group of α-diethoxyacetal-PEO-*b*-PCL (compound **13a**) was carried out on diluted micellar solutions. Therefore, 80 mg of **13a** were dissolved in 8 ml of THF and 8 ml of water were added progressively before dialysis against water.

Preparation of nanoparticles.

Nanoparticles (NPs) were prepared similar to a nanoprecipitation procedure described previously.^{12,13} Briefly, 0.2 g of PLA (BioMérieux, $M_n = 32650$ g/mol, $I_p \sim 1.5$) and increasing amounts of amphiphilic polymer (9, 46, 137 mol% with respect to PLA) were dissolved in 10 ml of acetone (Elvetec[®], 99%). The mixtures were allowed to stir for 1 h to guarantee complete dissolution of the polymers, then, added dropwise to 7 ml of water (Versol[®]) under slight stirring (250 rpm). Acetone was removed by evaporation under vacuum at room temperature to yield dispersions of nanoparticles. The nanodispersions were stored at 4°C.

Characterization techniques.

NMR spectroscopy. ¹H-NMR and ¹³C-NMR experiments were performed at 298 K using a Bruker DRX400 spectrometer operating at 400 and 100 MHz, respectively. 1D NMR spectra were collected using 16000 data points. All 2D experiments were acquired using 2000 data points and 256 time increments. Chemical shifts are given relative to external tetramethylsilane (TMS = 0 ppm) and calibration was performed using the signals of the residual protons of the solvent as a secondary reference. Deuterium oxide and CDCl₃ were obtained from SDS (Vitry, France). Details concerning experimental conditions are given in the figure captions.

NMR spectra of micellar solutions of copolymer **13a** in H₂O/D₂O (9/1) were acquired using a WATERGATE (Water suppression by GrAdient-Tailored Excitation) experiment. It relies on a spin echo sequence (3-9-13 pulse sequence in the Bruker library) allowing the solvent suppression.¹⁴

¹H-NMR spectroscopy was also used to determine the amount of amphiphilic polymer exposed at the nanoparticles' (NPs') surface. According to a procedure described by Vila *et al.*¹⁵, the aqueous NP dispersions were concentrated by three successive centrifugations, and the water exchanged against D₂O. Typically, 1 ml of NP dispersion was centrifuged three times at 4500 g for 13 min. After each centrifugation step, the supernatant was removed and the solid homogenized with a pipette in 1 ml of D₂O. After the last washing step, the NP precipitate was homogenized in 0.5 ml of D₂O. The dispersion was transferred in a NMR tube and a known amount of a 1.73 M sodium benzoate solution in D₂O was added as an internal standard, and the sample analyzed by

$^1\text{H-NMR}$. Under these conditions, only mobile polymer (PEO) chains of the NPs exposed in the outer aqueous medium could be detected and quantified. Then, the whole content of the NMR tube was freeze-dried, which allowed to determine the exact quantity of PLA and the copolymer. Finally, the solid was dissolved in CDCl_3 and the PLA/ copolymer composition of the NPs determined by $^1\text{H-NMR}$.

Mass spectrometry. Electrospray mass spectra were measured in the positive mode on a ZabSpec TOF (Micromass, UK) mass spectrometer. The mannose derivatives were dissolved in methanol and infused into the electrospray ion source. The capillary voltage was set to 4 kV. Poly(ethylene glycol) standards were used for external calibration.

SEC. The number-average molecular weight (M_n) and polydispersity (M_w/M_n) were determined by size exclusion chromatography equipped with a refractive index detector using THF or DMF as eluent at a flow rate of 1 ml/ min and 45°C on two polystyrene gel columns (columns PL gel $5\mu\text{m}$, porosity: 10^2 , 10^3 , 10^4 , 10^5\AA). The columns were calibrated with standard polystyrene and poly(ethylene oxide) (Polymer Laboratories), respectively.

Thin layer chromatography. Thin layer chromatography was performed on precoated plates of silica gel 60 (F_{254} , Merck) with detection by UV absorption, heating with 5% ethanolic sulfuric acid or ninhydrin solution. **Column chromatography** was performed by the flash technique on silica gel 60 (230 - 400 mesh, 40-63 μm , Merck) with the given solvents.

The size (hydrodynamic diameter, D_H) and size distribution of the NPs were determined at 25°C by quasi-elastic light scattering (QELS) (Zetasizer 3000 HS from Malvern instruments, UK) at an angle of 90° from colloidal dispersions highly diluted in 1mM NaCl aqueous solution. Each value is at least the average of three measurements (polydispersity index of 0.05 for a monodisperse colloid; above 0.5, the dispersion is broadly distributed.¹⁶)

Dynamic light scattering (DLS). The size and size distribution of the micelles were determined by dynamic light scattering (DLS) using an ALV5000 digital correlator in combination with an ALV goniometer and an ALV-SIPC photomultiplier. The incident light source was an ionized argon laser (Spectra Physics 2016) emitting at $\lambda = 488\text{ nm}$. Micellar solutions investigated at 25°C were filtered through Millex[®]-GS filters (porosity

0.22 μm) prior to measurements. The intensity autocorrelation functions ($g_2(t, \theta)$) measured at a given angle (θ) were analyzed thanks to the REPES routine¹⁷ which allows their analysis in terms of a continuous distribution of relaxation times. The average relaxation times components are q^2 dependent along the angular range investigated (from 30 to 140°) meaning that diffusive motions are probed. q is the wave vector defined as $q = 4\pi n/\lambda \sin(\theta/2)$, where n is the refractive index of the solvent.

Zeta potential. Particle surface characterization was performed by measuring the electrophoretic mobilities at pH 6 at constant ionic strength (3×5 measurements) by laser Doppler anemometry using a Zetasizer 3000HS (Malvern Instrument, UK). The conversion to zeta potentials uses the Smoluchowski relation $\zeta = u \times \eta / \varepsilon_0 \varepsilon_r$ where u is the electrophoretic mobility, ε_0 and ε_r are, respectively, the permittivity of the vacuum and the relative permittivity of the medium, η is the viscosity of the medium and ζ is the zeta potential.

Interfacial tension measurements. The interfacial ($\text{CH}_2\text{Cl}_2/\text{H}_2\text{O}$) tension was measured at 20°C with a drop tensiometer (Tracker, ITConcept, Longessaigne, France) equipped with a Bioblock Scientific Polystat CC2. Methylene chloride solutions of the different copolymers at different concentrations were prepared with CH_2Cl_2 preliminary saturated with water Milli-Q (mixing for 24 h). A drop of constant volume (5-10 μl) of each solution was formed in water (6 ml, preliminary saturated with CH_2Cl_2) and the dynamic interfacial tension $\gamma(t)$ was determined by analyzing the axial symmetric shape (Laplacian profile) of the pendant drop in Milli-Q[®] water.

Cryo Transmission Electron Microscopy (Cryo-TEM). The morphology and size of the polymer nanoparticles were examined by cryo-transmission electron microscopy (cryo-TEM). Using methods described elsewhere,^{18,19,20} thin liquid films of NP suspensions (at 1 wt% solid content) were prepared on NetMesh (Pelco, USA) ‘lacey’ carbon membranes and quench-frozen in liquid ethane. Once mounted in a Gatan 626 cryo-holder cooled down with liquid nitrogen, the specimens were transferred in the microscope and observed at low temperature (- 180°C). Images were recorded on Kodak SO163 films, using a Philips CM200 ‘Cryo’ electron microscope operating at 80 kV.

The same technique was also used to study the recognition of mannose-coated polymer NPs by gold nanoparticles surface-decorated by GNA (mannose-specific lectin, aqueous solution, protein concentration 10-20 $\mu\text{g/ml}$). Therefore, 50 μl of the commercial gold-nanoparticle dispersions were diluted with phosphate buffer solution to a final volume of 120 μl , then 12 μl of PLA NP dispersion (solid content of 3 wt%) were added under vigorous stirring and led to interact with the GNA-gold nanoparticles for 12 h.

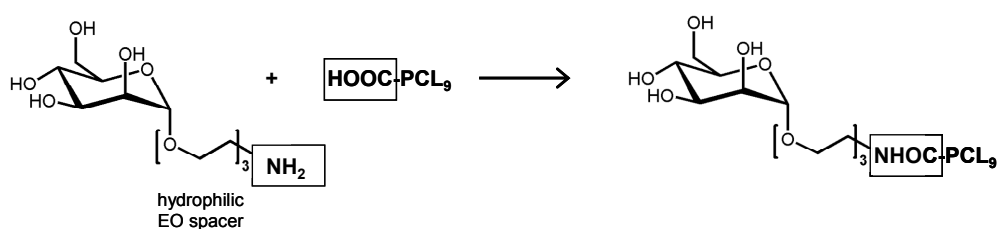
AFM imaging. AFM measurements were performed in “tapping mode” (TMAFM) using a Picoforce (Veeco Instruments) microscope, operating in air at room temperature. Therefore, nanoparticles suspensions (of 0.15 wt% solid content) were deposited on freshly-cleaved mica substrates and analyzed after evaporation of the solvent at room temperature. Image processing and analysis were performed using the Nanoscope software. The treatment was limited to a first order tilt correction of the surface.

Biological lectin recognition assay. Apart from cryo-TEM experiments, the lectin recognition ability of mannose-coated NPs was also examined by a biological assay based on the quantification of the absorbance resulting from the interaction of NP-bound mannose with biotinylated GNA. The detection was achieved by reacting NPs, which had previously been incubated with biotinylated GNA, with streptavidin-phosphatase and then *p*-nitrophenyl phosphate (pNPP). Typically, 50 μl of a nanoparticle dispersion (2% of solid content, 1 mg) was added to 950 μl of phosphate buffer saline (PBS, pH 7.15) containing 0.05% (w/v) Tween 20 (PBST) and 5% (w/v) bovine serum albumin to achieve passivation of the surface and reduce non-specific interactions. The particles were centrifugated at 4000 g for 13 min, the residual 200 μl homogenized in 700 μl PBST containing 3% (w/v) BSA, and incubated with 100 μl of biotin-labeled GNA solution in PBST [$c = 5 \mu\text{l/ml}$ or 10 $\mu\text{l/ml}$] for 1 h at 37°C. The particles were washed twice by centrifugation at 4000 g for another 13 min and redispersed in PBST containing 3% (w/v) BSA, centrifuged again and redispersed in PBST containing 3% (w/v) BSA to a final volume of 900 μl . After this washing step, 100 μl of streptavidin-phosphatase was added (diluted in PBST with 3% (w/v) BSA to 1/1500). After 30 min of incubation at 37°C, the samples were washed twice by centrifugation as described previously and then 850 μl of the supernatant removed. The 150 μl were homogenized with a pipette and then 200 μl of pNPP substrate (1 tablet in 5 ml) were added. After 15 min of incubation at 37°C, the absorbance was measured at 405 nm with a μQuant reader apparatus (Bio Tek instruments).

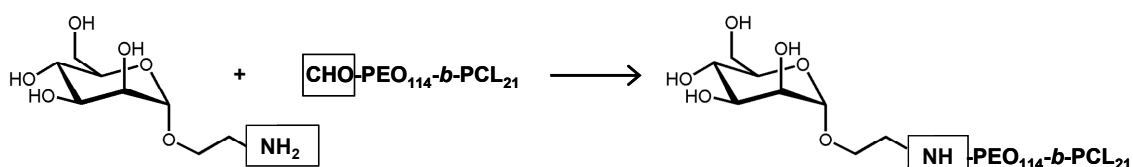
III. Results and discussion

Two main strategies have been employed in order to obtain amphiphilic biodegradable polymers functionalized at the α -end by mannose. As illustrated in Scheme 1, the first one (i) relies on the synthesis of a mannose derivative bearing an amino group attached via a hydrophilic oligo(ethylene oxide) spacer, and its grafting onto a low molecular weight ($M_n \sim 1000$ g/mol) ϵ -caprolactone α -end-capped by a carboxylic acid group. The second synthesis pathway (ii) is based on the synthesis of an amphiphilic poly(ethylene oxide)-*b*-poly(ϵ -caprolactone) *diblock* copolymer (PEO-*b*-PCL), whose hydrophilic chain end is terminated by a functional group (aldehyde or tertiary amine function) suitable for the covalent linking of mannose derivatives (amine or bromine).

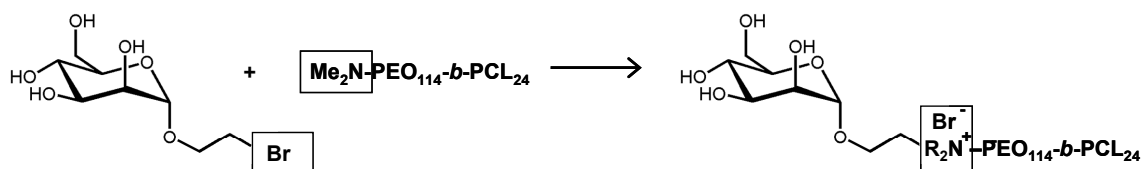
(i) Conjugation of a mannose derivative via a hydrophilic spacer to an ϵ -caprolactone oligomer by amine-acid coupling ("approach 1")



(ii) Conjugation of a mannose derivative to an amphiphilic poly(ethylene oxide-*b*- ϵ -caprolactone) copolymer
a.) by reductive amination reaction ("approach 2")



b.) by quaternization of a tertiary amine ("approach 3")



Scheme 1. Synthetic pathways to mannosylated amphiphilic polymers

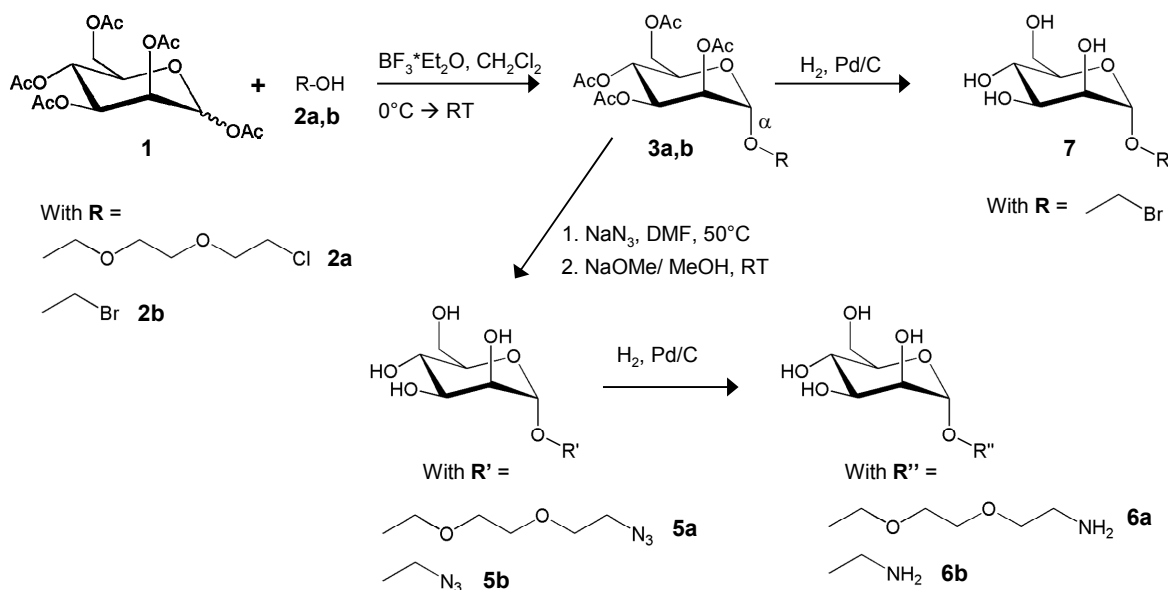
The aim of this work was to use such glycopolymers as surface-modifiers for polymeric nanoparticles (NPs). It was thus important to control precisely the hydrophilic-

hydrophobic balance (HLB) of the polymers. In strategy (i), the size of the hydrophilic segment was given by the length of the commercially available spacer molecule, which consisted here of three hydrophilic ethylene oxide units ($M_n = 132$ g/mol), and the hydrophilic mannose molecule ($M_n = 163$ g/mol). With respect to that, the envisaged length of the hydrophobic poly(ϵ -caprolactone) (PCL) block was fixed to $M_n \sim 1000$ g/mol in order to obtain amphiphilic properties. On the other hand, according to synthesis pathway (ii), both the hydrophilic and the hydrophobic segment could be tailor-made. In order to optimally tune their molecular weight and to reach a narrow molecular weight distribution, the polymers have been synthesized employing controlled polymerization techniques. The hydrophobic block was thus synthesized by ring-opening polymerization (ROP) of ϵ -caprolactone initiated from aluminum alkoxides allowing an optimal control of the polymerization,²¹ whereas the poly(ethylene oxide) block was synthesized by living anionic polymerization of ethylene oxide. End-group functionalities could be introduced by initiating the polymerization from a suitable functional group or its protected precursor. Due to the polymerization mechanism as well as the degradability/ reactivity of the polyester chains, only a limited quantity of functional groups was available, i.e. groups that do not interfere during the polymerization and do not react with the polyester segment. For instance, it had been reported that poly(ϵ -caprolactone) terminated by primary amino group are sensitive to intrachain-reactions, and therefore alternative functional groups have been chosen.²² Another challenge was the covalent coupling of the mannose-derivatives to the end-functionalized polymers. The employed chemical reaction must be selective, efficient and occur under smooth conditions, in order to avoid any degradation of both, the polyester chain and the carbohydrate.

With this in mind, three different coupling reactions have been employed: an amine-acid coupling (i), “*approach 1*”, a reductive amination reaction between aldehyde and amine derivatives (ii.a.), “*approach 2*”, and a quaternization reaction of a tertiary amine (ii.b.), “*approach 3*” (Scheme 1).

The different pathways to mannose functionalized amphiphilic glycopolymers involved thus (i) the synthesis of a mannose derivative possessing a functional end-group (amine or bromide group), (ii) the preparation of (co)polymers terminated by the desired functional group and (iii) the grafting of the latter by mannose derivatives. The different synthesis steps are described in detail in the following section.

III.1. Synthesis of the mannose derivatives.



Scheme 2. Synthesis of the mannose derivatives

Scheme 2 shows the synthesis of the targeted mannose derivatives, either functionalized by a bromide group **7** or a primary amino group (**6a**, **6b**). Two different halogenated alcohols (**2a** and **2b**) were used for the first glycosylation step in order to introduce a chloride or a bromide reactive group attached (**2a**) or not (**2b**) via a hydrophilic spacer. These leaving groups open up the possibility to introduce other functionalities as can be seen in scheme 2. The glycosylation reactions were performed using the boron trifluoride etherate method that allows, in one single step, the efficient regioselective conversion of (per)acetylated sugars into the corresponding 1,2-trans glycosides.²³ These reactions occurred in methylene chloride by reaction of penta-*O*-acetyl- β -D-mannopyranoside (**1**) (synthesized from mannose by the ‘Helferich method’¹⁰) with 2-[2-(2-chloroethoxy)-ethoxy]ethanol (**2a**) or 2-bromoethanol (**2b**) in the presence of a large excess of the Lewis acid boron trifluoride etherate. After purification by flash chromatography, compounds **3a** and **3b** could be obtained in 60% and 69% yield, respectively.

Compounds **3a** and **3b** were converted in the corresponding azide derivatives by reaction with a large excess of sodium azide.²⁴ The azide derivatives **4a** and **4b** were recovered after extraction with ethyl acetate and deacetylated under Zemplén conditions to yield quasi quantitatively compounds **5a** and **5b**. The reduction of the azide function of **5a** and **5b** occurred in ethanol under hydrogen atmosphere in the presence of palladium on

activated charcoal. Compound **6a** was obtained with 89% yield and an overall yield of 45%, and compound **6b** in 98% yield and overall yield of 80% starting from compound **1**.

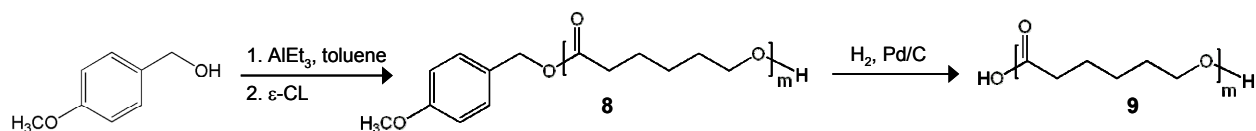
The 2-bromoethyl- α -D-mannopyroside (**7**) was quantitatively obtained by deacetylation of compound **3b** under Zemplén conditions.

At each synthesis step, the mannose derivatives have been analyzed by $^1\text{H-NMR}$, $^{13}\text{C-NMR}$ and ESI-HRMS (Electrospray ionization- high resolution mass spectrometry), and the values are reported in the experimental section.

III.2. Synthesis of α -end-functionalized polymers.

III.2.1. Synthesis of α -carboxy poly(ϵ -caprolactone) (**9**).

Low molecular weight poly(ϵ -caprolactone) α -terminated by a carboxylic acid group was synthesized in two steps as illustrated in scheme 3. The first step consisted in the ROP polymerization of ϵ -caprolactone using a benzyl alcohol derivative as initiator. The resulting ester derivative was hydrolyzed under hydrogen atmosphere in the presence of Pd/C.



Scheme 3. Synthesis of α -carboxy poly(ϵ -caprolactone)

The progress of the polymerization of ϵ -caprolactone was assisted by $^1\text{H-NMR}$ and the reaction was stopped at 100% monomer conversion. The number average molecular weight (M_n) of the polyester backbone (**8**) was determined by $^1\text{H-NMR}$ from the relative intensity of the proton signals at 4.05 ppm of PCL ($I_{4.05\text{ppm}}/2$) and at 3.62 ppm of the methylene ω -end groups ($-\text{CH}_2-\text{CH}_2-\text{OH}$) ($I_{3.62}/2$), which corresponded to the intensity of protons of the benzyl α -end-group at 6.87 ppm ($I_{6.87}/2$) (not shown). As reported in Table 1, the M_n ($M_{n,\text{NMR}} = 1350$) determined by NMR was slightly higher than the theoretical value ($M_{n,\text{th}} = 1084$), possibly due to the loss of the *p*-methoxy benzyl alcohol during the drying step by azeotropic distillation of water with toluene. SEC measurements revealed that the molecular weight distribution (M_w/M_n) was quite narrow (1.42). (Table 1, Figure

4, trace A). The molecular weight M_n ($M_{n,SEC} = 1100$ g/mol) was close to the theoretical value.

Table 1. Macromolecular characteristics of *p*-methoxy-benzyl poly(ϵ -caprolactone) (8), α -carboxy poly(ϵ -caprolactone) (9) and its mannose conjugate (10).

#	PCL derivative	$M_{n,theor}$	$M_{n,RMN}$	$M_{n,SEC}$	M_w/M_n^e
8	PCL-O-Bz-OMe	1084 ^a	1350 ^b	1100 ^c	1.42
9	PCL-COOH	945	1450	1050 ^c	1.44
10	PCL-CONH-(EO) ₃ -Mannose	1255	1750	2850 ^d	1.31

^a $M_{n,theor} = [\epsilon\text{-CL}]_0/\text{ROH} \times \text{MW}_{\epsilon\text{-CL}} + M_n$ (*p*-methoxy benzyl alcohol) at 100% of conversion; ^b $M_{n,RMN} = \text{DP}(\text{PCL}) \times 114 + [M_n$ (*p*-methoxy benzyl alcohol)]; ^c as determined by SEC in THF calibrated by PS Standards and converted into PCL according to equation $M_n(\text{PCL}) = 0.259 \times M_n(\text{PS})^{1.073}$; ^d as determined by SEC in THF calibrated by PS Standards; ^e as determined by SEC in THF

Furthermore, ¹H-NMR spectroscopy provided evidence of the quantitative removal of the benzyl alcohol group (Figure 1), showing the presence of the four characteristic peaks of the polyester chain, and the proton signal at 3.62 ppm characteristic of the methylene group of the ω -chain-end, but no signal of the aromatic ring. M_w/M_n did not change significantly, indicating that no degradation of the polymer chain took place during the hydrogenolysis step (Table 1).

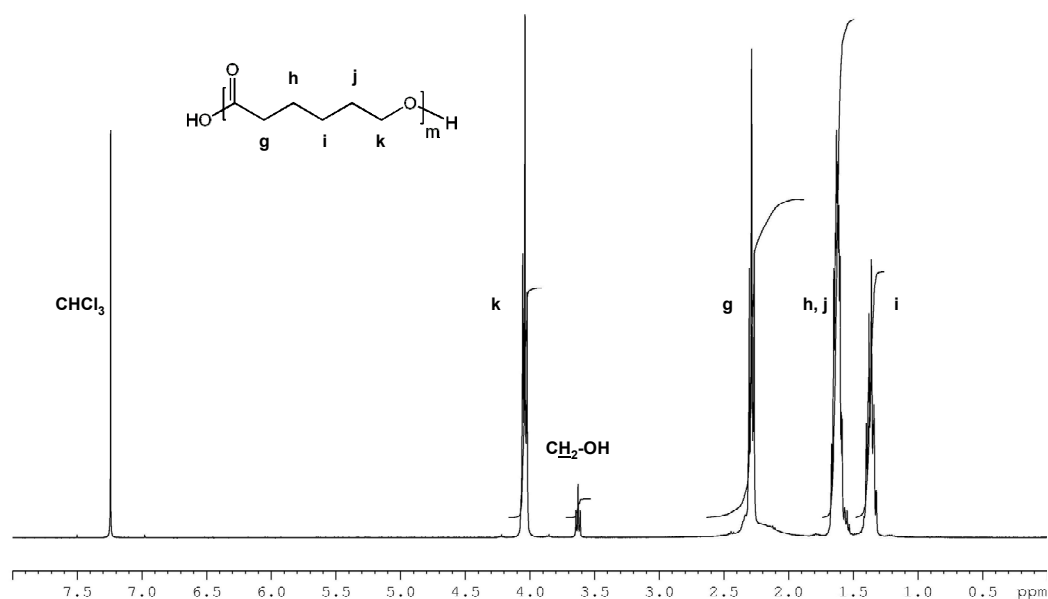
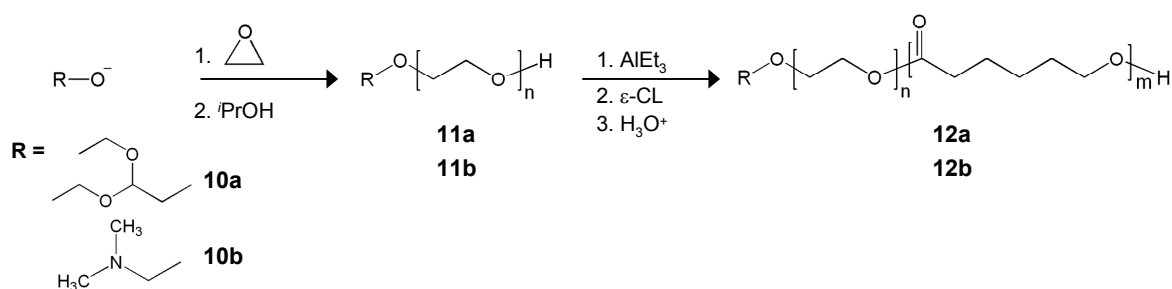


Figure 1. ¹H-NMR spectrum (400 MHz, 25°C, CDCl₃) of α -carboxy poly(ϵ -caprolactone).

III.2.2. Synthesis of amphiphilic copolymers α -end capped by a reactive group (12a, 12b).

The first step to amphiphilic poly(ethylene oxide)-*b*-poly(ϵ -caprolactone) block copolymers functionalized at the hydrophilic end by either a protected aldehyde or a tertiary amine was the anionic polymerization of ethylene oxide, initiated by alcohols bearing the desired functional group or their precursor. Ethylene oxide was thus polymerized from the alkoxides of *N,N*-dimethylaminoethanol and 3,3-diethoxypropanol (Scheme 4). In a second step, the ω -hydroxyl group of the PEO chain was reacted with AlEt_3 , leading to the corresponding alkoxide which was then used as a macroinitiator for the ring-opening polymerization of ϵ -caprolactone, as previously reported by Vangeyte *et al.*²⁵ The length of the PCL block was controlled by the ϵ -caprolactone over PEO-Al alkoxide molar ratio. Both polymer blocks were thus synthesized by controlled polymerization techniques in order to achieve the desired molecular weight and narrow molecular weight distribution. After each synthesis step, the polymers were characterized by $^1\text{H-NMR}$ spectroscopy and SEC.



Scheme 4. General synthetic pathway to amphiphilic copolymers α -end capped by a functional group

III.2.2.1. Synthesis and characterization of α -diethylacetal poly(ethylene oxide)-*b*-poly(ϵ -caprolactone) (12a).

After polymerization of the first PEO block, a small volume was sampled and analyzed by SEC and $^1\text{H-NMR}$. The number-average molecular weight (M_n) and the polydispersity index M_w/M_n were found to be 4500 g/mol (using PEO standard) and 1.05, respectively. The M_n value agreed quite well with the theoretical calculated value of 5000 g/mol ($[\text{EO}]_0/[\text{I}]_0$) (Table 2).

Table 2. Macromolecular characteristics of the α -diethylacetal-PEO (11a), α -diethylacetal PEO-*b*-PCL (12a) and CHO-PEO-*b*-PCL (15).

#	<i>polymer</i>	$M_{n,theor}$	$M_{n,RMN}$	$M_{n,SEC}^d$	M_w/M_n^d
11a	acetal-PEO-OH	5150 ^a	4650	4500	1.05
12a	α -acetal-PEO-PCL	7550 ^b	7250 ^c	6100	1.13
13a	α -acetal- ω -methoxy PEO-PCL	7550	7250 ^c	6050	1.17
15	α -aldehyde PEO-PCL	7500	7200	“6300”	1.26

^a $M_{n,theor} = [EO]_0/ROH \times MW_{EO} + M_n(3,3\text{-diethoxypropanol})$ at 100% of conversion; ^b $M_{n,theor} = [\epsilon\text{-CL}]_0/ROH \times MW_{\epsilon\text{-CL}} + 5150$; ^c $M_{n,RMN} = DP(PCL) \times 114 + 4650$; ^das determined by SEC in THF calibrated by PEO standards

The α -diethoxyacetal PEO-*b*-PCL diblock copolymer was eluted in a single unimodal and narrow fraction by SEC, which is shifted to higher molecular weights compared to α -diethylacetal-PEO-OH 11a. The ¹H-NMR spectrum of the copolymer in Figure 2, shows the characteristic peaks of the PEO and the PCL block and the typical signals of the acetal group at the α -end, at 1.18 ppm (methyl group), 4.62 ppm (triplet attributed to the acetal methine protons) and at 1.88 ppm (methylene groups).

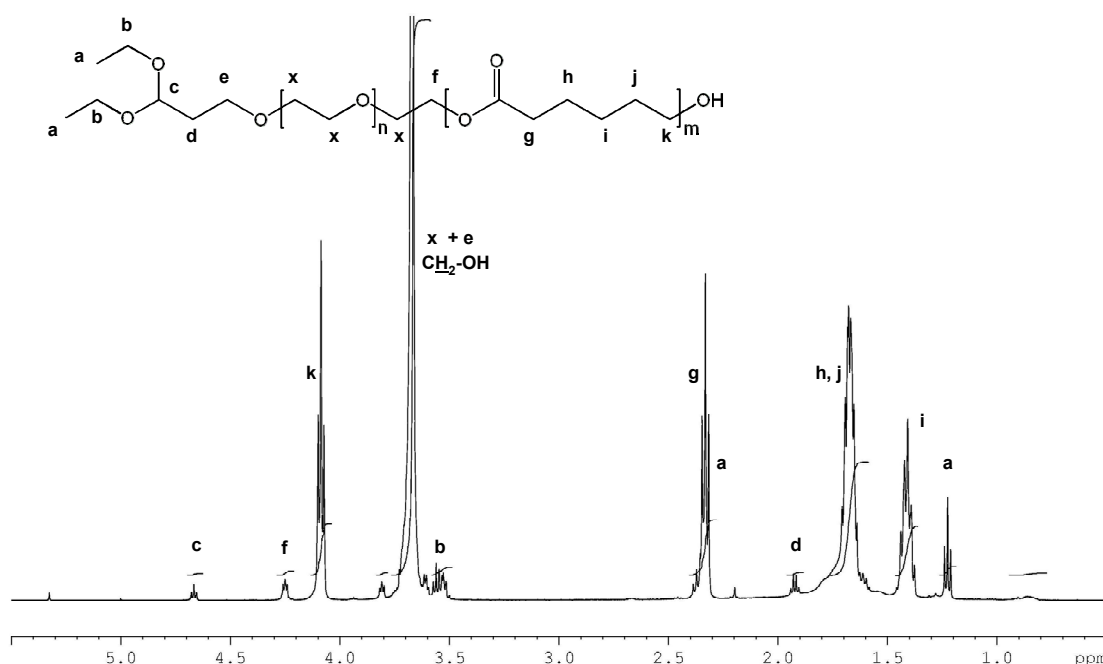


Figure 2. ¹H-NMR spectrum (400 MHz, 25°C, CDCl₃) of α -diethylacetal poly(ethylene oxide)-*b*-poly(ϵ -caprolactone) (compound 12a).

The length of the PCL segment was calculated from the integration of the proton signals of the PEO segment at 3.6 ppm and the α -methylene protons of PCL at 4.05 ppm. It was determined as 2600 g/mol, and agreed thus well with the theoretical value (2400

g/mol). Finally, the ω -end group of compound **12a** was protected quantitatively by reaction with an excess of acetyl chloride in order to avoid side reactions during the following hydrolysis step. As reported in Table 2, no degradation of the polymer chain was observed by SEC and NMR.

III.2.2.2. Synthesis and characterization of α -*N,N*-dimethylaminoethyl poly(ethylene oxide)-*b*-poly(ϵ -caprolactone) (*Me*₂*N*-PEO-PCL) (**12b**).

The number average molecular weight (M_n) of the poly(ethylene oxide) chain **11b** was determined by ¹H-NMR from the relative intensity of the proton signals of the PEO chain at 3.62 ppm ($I_{3.62\text{ppm}}/4$) and of the methyl groups (CH_3N) of the tertiary amine end-function at 2.22 ppm ($I_{2.22\text{ppm}}/6$) (Table 3). Size exclusion chromatography (SEC) showed that the product was eluted in a single and narrow fraction (chromatogram not shown). Table 3 reveals that the molecular weights determined by NMR and SEC (using PEO standard) agreed well with the theoretical ones, confirming the control of the polymerization.

Table 3. Macromolecular characteristics of the α -*N,N*-dimethylaminoethyl PEO (11b**), α -*N,N*-dimethylaminoethyl PEO-*b*-PCL (**12b**) and glycopolymer (**14**).**

#	<i>polymer</i>	$M_{n,theor}$	$M_{n,RMN}$	$M_{n,SEC}$	M_w/M_n^e
11b	Me ₂ N-PEO-OH	5090 ^a	5470	5050 ^e	1.06
12b	Me ₂ N-PEO- <i>b</i> -PCL	7830 ^b	8300 ^d	7100 ^e	1.10
14	Mannose-N ⁺ -PEO- <i>b</i> -PCL	8120 ^c	8600	7440 ^e	1.19

^a $M_{n,theor} = [\text{EO}]_0/\text{ROH} \times \text{MW}_{\text{EO}} + M_n$ (*N,N*-dimethylaminoethanol) at 100% of conversion; ^b $M_{n,theor} = [\epsilon\text{-CL}]_0/\text{Me}_2\text{N-PEO-OH} \times \text{MW}_{\epsilon\text{-CL}} + 5090$; ^c $M_{n,theor} = \text{MW}(2\text{-bromoethyl-}\alpha\text{-D-mannoside}) + 7830$; ^d $M_{n,RMN} = \text{DP}(\text{PCL}) \times 114 + 5470$; ^e as determined by SEC in THF calibrated by PEO standards

After purification by precipitation in heptane, the diblock copolymer **12b** was characterized by SEC and ¹H-NMR (Figure 3). The trace of the copolymer in the size exclusion chromatogram is narrow ($M_w/M_n = 1.10$) and unimodal (see Figure 4, trace 'A'), indicating the complete initiation of the polymerization of ϵ -caprolactone from the PEO macroinitiator. In addition, the molecular weight determined by ¹H-NMR was close to the theoretical one, confirming a good control of the polymerization (Table 3). The ¹H-NMR spectrum (Figure 3) shows the characteristic peaks corresponding to the proton signals of

the methyl protons (2.27 ppm), and the methylene protons (2.51 ppm) vicinal to the α -amino group, the methylene protons (4.22 ppm) in α -position of the ester group between the PEO and PCL block (PEO-CH₂-CH₂-OOC-CH₂-CH₂-PCL), respectively.

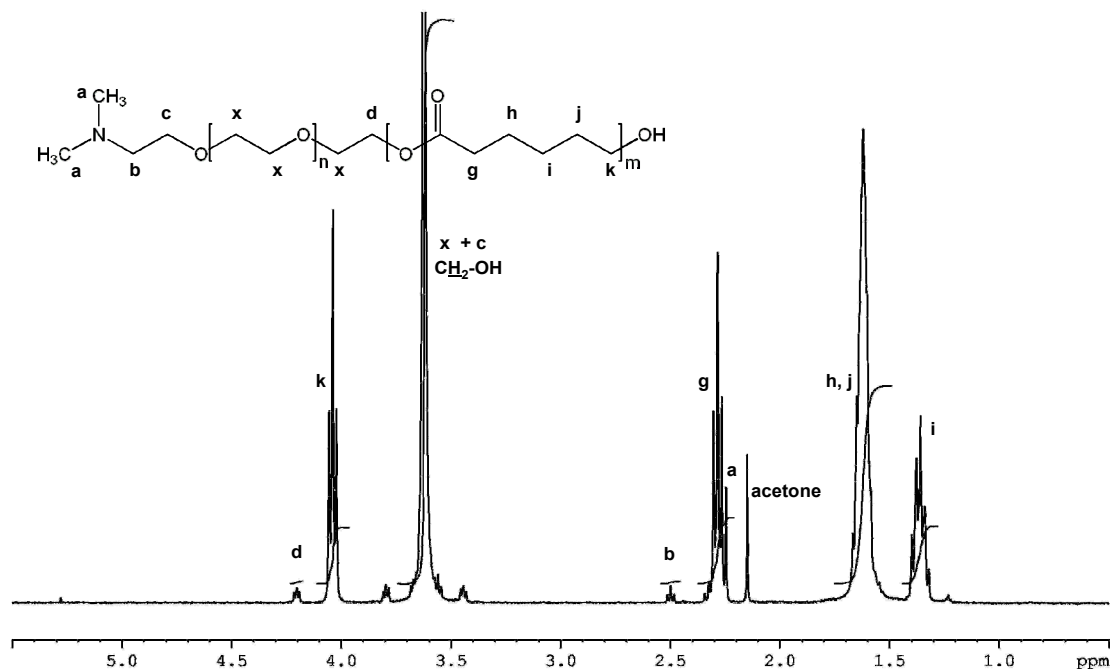


Figure 3. ¹H-NMR spectrum (400 MHz, 25°C, CDCl₃) of α -N,N-dimethylaminoethyl poly(ethylene oxide)-*b*-poly(ϵ -caprolactone) (12b).

III.3. Synthesis of the glycopolymers.

III.3.1. Approach 1: Synthesis of PCL end-capped by a mannose-derivative via a peptide-like coupling reaction.

Acid-amine coupling is universally employed in peptide chemistry, and known for its efficiency under smooth conditions. The first synthesis pathway to reach a mannose end-capped amphiphilic polymer relies thus on the formation of an amide linkage by reaction of a low molecular weight ϵ -caprolactone terminated by a *carboxylic acid* group, α -carboxy poly(ϵ -caprolactone) (**9**), with a mannose derivative bearing an amine function linked via a hydrophilic ethylene oxide spacer **6a** (see Scheme 1, *approach 1*). The reaction was based on the nucleophilic attack of the amine end-group of **6a** on the activated ester formed by reaction of α -carboxy poly(ϵ -caprolactone) with *N*-hydroxysuccinimide (NHS) in the presence of a slight excess of a water-soluble

carbodiimide (1-ethyl-3-(3-dimethylaminopropyl)carbodiimide, EDC).²⁶ The carbodiimide and its by-product formed during the reaction could be easily removed from the reaction medium by washing with water/ dialysis against water.

In order to avoid any degradation of the polyester chain, the coupling reaction was carried out under mild conditions, i.e. at room temperature, using only a slight excess of coupling agent and amine (1.5 and 1.6 equiv with respect to the carboxylic acid group, respectively) and in anhydrous solvent (DMF). Figure 4 shows the SEC traces of the functional PCL (trace A) and the PCL-mannose conjugate (trace B). Both peaks are quite narrow, with a similar M_w/M_n , indicating that the polymer chain did not suffer from degradation (see Table 1). Furthermore, the elution of the carbohydrate-conjugate is shifted to smaller elution volumes. This might be related to the increase of molecular weight, and therefore size, of the molecule or else to the presence of the carboxyl group.

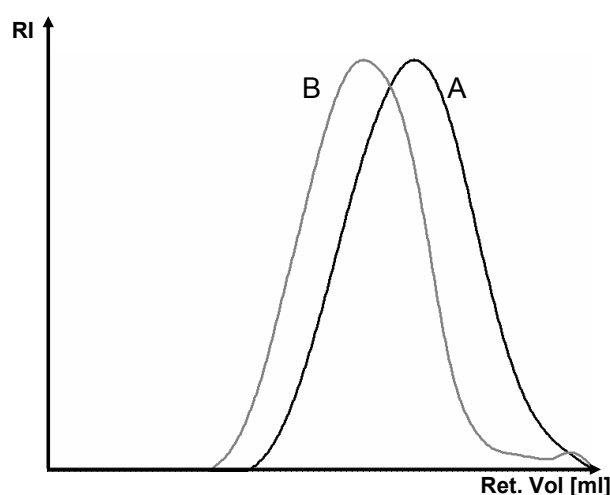


Figure 4. SEC traces for α -carboxy poly(ϵ -caprolactone) 9 (A) and the corresponding mannosylated glycopolymer 10 (B).

Figure 5 shows the $^1\text{H-NMR}$ spectra of the glycopolymer performed in CDCl_3 . Beside the peaks that are characteristic of the proton signals of the polyester chain (at 1.35 (H_i), 1.65 (H_h+H_j), 2.30 (H_g), 3.62 ($-\text{CH}_2\text{-OH}$), 4.05 (H_k)), additional peaks at 4.88 ppm and between 3.6 and 3.9 ppm are observed, which can be attributed to the glycosidic moiety. Indeed, the signal at 4.88 ppm is characteristic of the anomeric proton (H_1) of mannose. In addition, a peak at 3.38 ppm appears, i.e., in the range of chemical shift typical of the methylene protons of amides. Two-dimensional $^1\text{H-NMR}$ (COSY) experiments confirmed the attribution of the signals.

In addition, no proton signal can be observed at about 2.75 ppm, which is characteristic of the methylene group ($\text{CH}_2\text{-NH}_2$) vicinal to the amine function of the mannose derivative **6a**.

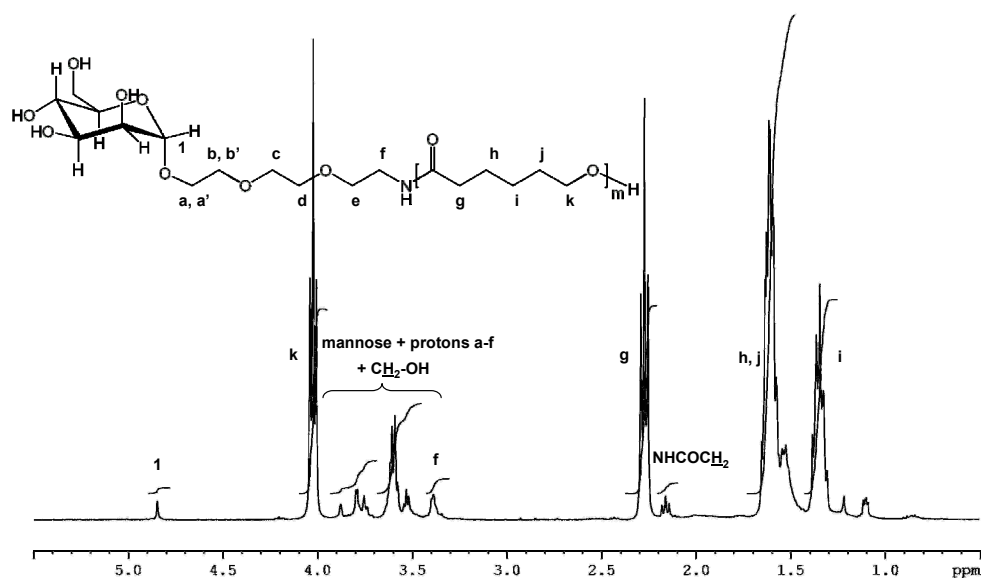


Figure 5. $^1\text{H-NMR}$ spectrum (400 MHz, 25°C, CDCl_3) of poly(ϵ -caprolactone) end-capped by a mannose residue (**10**).

The functionalization yield of the coupling reaction was determined by $^1\text{H-NMR}$ integration of the anomeric proton H_1 of the mannose moiety at 4.88 ppm ($I_{4.88}$) and the methylene protons H_k in α -position of the ester at 4.05 ppm ($I_{4.05}/2$), taking into account the degree of polymerization obtained from compounds **8** and **9** ($\text{DP}_{\text{PCL-COOH}} = 13$). According to equation 1, it was found to be 88%.

$$\% (\alpha\text{-functionality}) = \frac{I_{4.88 \text{ ppm}}}{I_{4.05 \text{ ppm}} / (2 \times 13)} \times 100 \quad \text{eqn. 1}$$

In conclusion, a mannose moiety could be successfully linked via a hydrophilic spacer to a biodegradable hydrophobic polyester chain.

III.3.2. Approach 2: Synthesis of PEO-*b*-PCL end-capped by a mannose residue via a reductive amination reaction.

The second approach relies on the conjugation of a copolymer, that is α -terminated by an aldehyde group, to an amino derivative of mannose, using a **reductive amination reaction**. This strategy had been proposed by Kataoka *et al.* for the conjugation of biomolecules to CHO-PEO-*b*-PLA diblock copolymers.^{27,28, 29}

III.3.2.1. Conversion of the acetal functionality to an aldehyde (15).

The hydrolysis of an acetal end group of amphiphilic copolymers into the corresponding aldehyde under acidic conditions has been reported to be susceptible to side reactions. In case of α -acetal- ω -hydroxyl-end-capped polymers, one possible side reaction relies on the acid catalyzed reaction of the formed aldehyde with the ω -hydroxyl group of the PCL segment by formation of a hemiacetal. Therefore, the ω -hydroxyl group of PEO-*b*-PCL diblock copolymer **12a** was protected by reaction with acetyl chloride.

In addition, it is known that two aldehyde groups possessing a methylene group in α -position undergo “aldol addition” and “condensation” under acidic (and alkaline) conditions. Therefore, Kataoka *et al.* performed the hydrolysis of the α -acetal end group of PEO-*b*-PLA copolymers on micellar solution, in order to reduce the mobility of the PEO chains and to decrease undesired reactions.²⁷ Thus, micelles from ‘water insoluble’ copolymer **13a** were prepared by a dialysis technique, and the pH of the solution was adjusted to pH 2 with 0.5 M hydrochloric acid. The conversion of acetal into aldehyde was monitored by ¹H-NMR in D₂O as shown in Figure 6a. The progress of the reaction can be followed by the appearance of the end-aldehyde proton (CHO) at 9.77 ppm and the α -methylene proton vicinal at 2.67 ppm (CHO-CH₂-), and the disappearance of the acetal methine proton (CH-CH₂) at 4.62 ppm. The conversion could thus be determined by integration of the proton signal at 2.67 ppm ($I_{2.7\text{ppm}}/2$) (or 9.77 ppm ($I_{9.6\text{ppm}}/1$)) and the oxymethylene groups of the PEO segment ($I_{3.6\text{ppm}}/(4 \times \text{DP})$). After 1 h of hydrolysis at pH 2, more than 50% of the acetal groups were converted to the corresponding aldehyde. Longer reaction times (> 3 h) however led to a decrease of the rate of conversion, likely due to side reactions, such as the formation of aldols (“aldol reaction/ addition” and “condensation”) under acidic conditions.

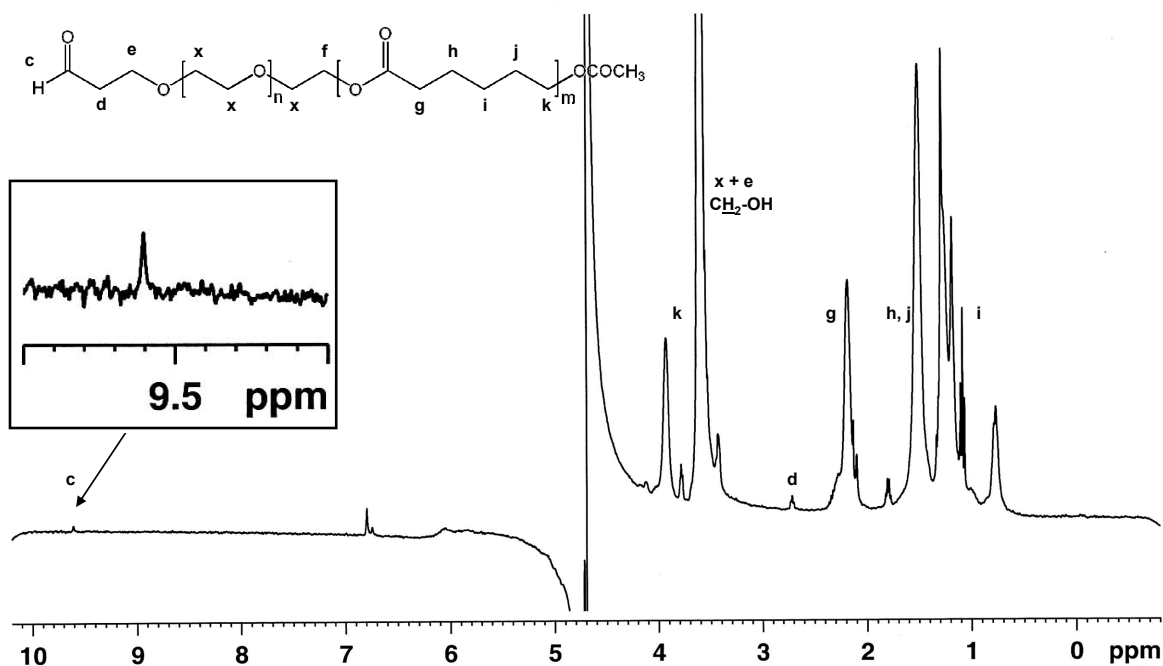


Figure 6a. $^1\text{H-NMR}$ (400 MHz, 25°C , in (9:1 $\text{H}_2\text{O}/\text{D}_2\text{O}$) of an aqueous micellar solution (R_H (DLS) = 11 nm) of α -diethylacetal-PEO-*b*-PCL after 65 min of hydrolysis at pH 2.

The micellar solutions after 2 h of reaction were lyophilized and analyzed by NMR and SEC. $^1\text{H-NMR}$ of the dried product in CDCl_3 confirmed the conversion of 50% obtained from the WATERGATE experiments (Figure 6b).

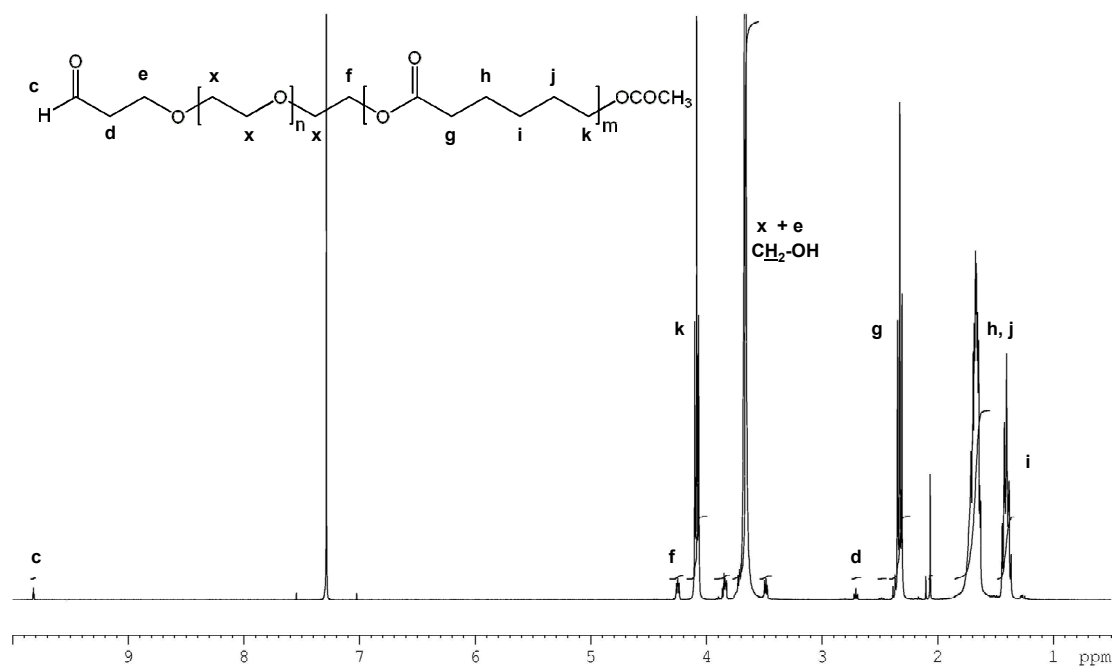


Figure 6b. $^1\text{H-NMR}$ spectrum (400 MHz, 25°C , CDCl_3) of α -aldehyde poly(ethylene oxide)-*b*-poly(ϵ -caprolactone) (15).

In addition, SEC analysis (Figure 7) of the product showed a bimodal molecular weight distribution, with a second distribution at higher molecular weight than the initial copolymer **12a** seemingly indicating the formation of dimers by “aldol addition”, i.e. reaction between the enolate of an aldehyde with the α -carbonyl of a second aldehyde with formation of a β -hydroxy aldehyde. Finally, it must be noted that this reaction was very hard to control and that the yields of conversions of the acetal group into an aldehyde were not reproducible, ranging from 50 to 90%.

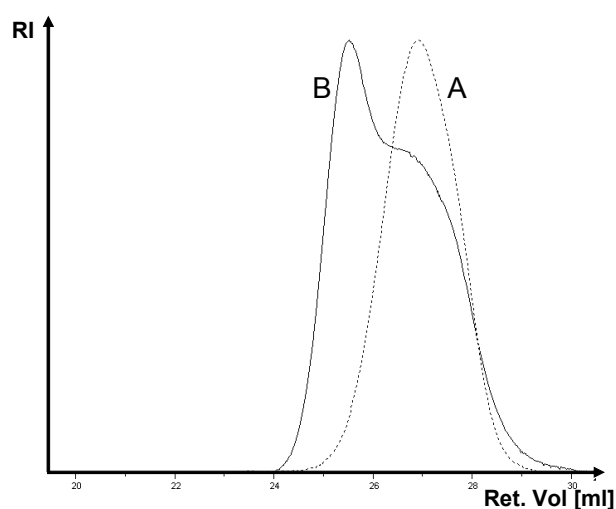


Figure 7. SEC analysis of the copolymer (A) before and (B) after acetal hydrolysis.

III.3.2.2. Reductive amination (16).

At pH 5, the primary amine of the mannose derivative **6b** reacts with the aldehyde group of the copolymer **13a** affording a Schiff base. The latter can then be reduced to a secondary amine using an excess of NaCNBH_3 . The mannose functionality was determined from $^1\text{H-NMR}$ (Figure 8). The calculation was based on the ratio of the intensities of the H-1 proton signal of mannose (4.88 ppm) and the α -methylene proton signal (4.04 ppm) of the PCL block and revealed a functionality of 23%. Considering an aldehyde functionality of 50%, the conversion was thus close to 50%.

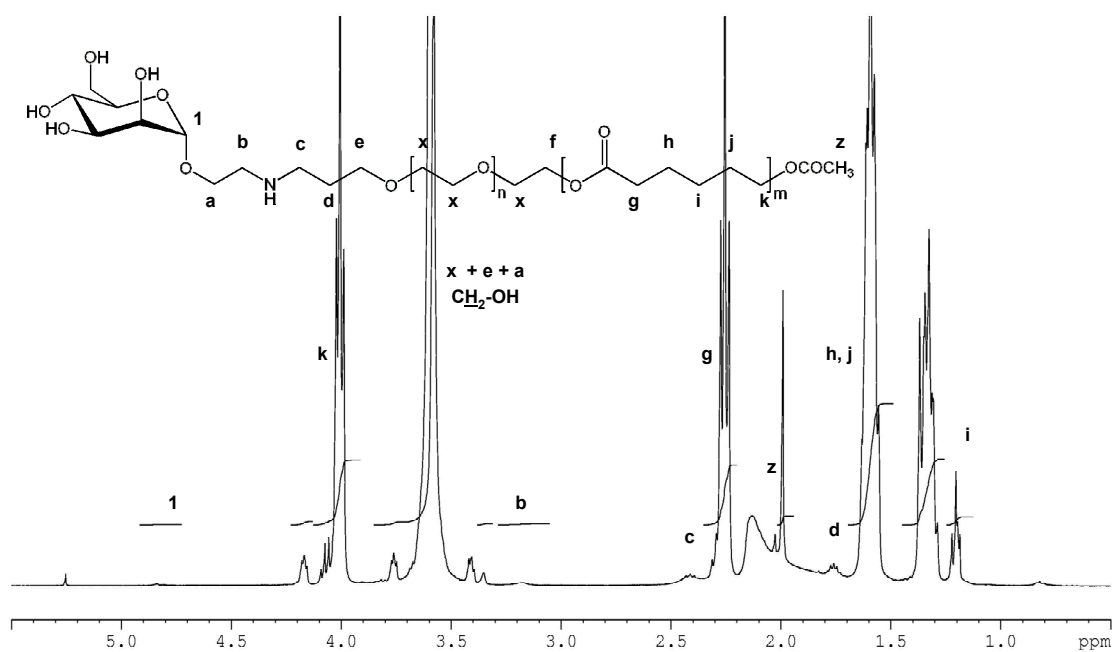


Figure 8. $^1\text{H-NMR}$ spectrum (400 MHz, 25°C, CDCl_3) of α -aldehyde poly(ethylene oxide)-*b*-poly(ϵ -caprolactone) after reductive amination reaction (16).

III.3.3. Approach 3: Synthesis of PEO-*b*-PCL end-capped by a mannose residue via “quarternization” of (R₃N⁺-PEO-PCL Br⁻) (14).

The third strategy towards mannosylated amphiphilic copolymers relies on the quarternization of the tertiary amino end-group of a PEO-*b*-PCL copolymer using a brominated mannose derivative (Scheme 1, 2b). In fact, it had been reported earlier that poly(ϵ -caprolactone) bearing pendant bromide groups, poly(ϵ -caprolactone)-*co*-poly(γ -bromo- ϵ -caprolactone), could be selectively and quantitatively converted to the corresponding pyridinium salt by quarternization with pyridine.^{30,31,32} This way, amphiphilic or water-soluble polyesters could be obtained in good yields (90%) without degradation of the polymer chain. Quaternary ammonium bromides are usually obtained by reaction of a brominated compound with a tertiary amine at high temperatures, and they are based on the nucleophilic attack of a tertiary amine and as such preferably conducted in anhydrous conditions. According to the literature, high yields have been obtained in polar solvents such as ethanol or methanol.³³

The covalent linking of brominated mannose derivative **7** (Br-R) to the tertiary amino end-group of the amphiphilic PEO-*b*-PCL copolymer **12b** was thus achieved by simply mixing the two compounds in an appropriate solvent and heating, without recourse to any activating agent. As summarized in Table 4, different reaction conditions (different solvents, Br-R' to R₂N-R'' ratio and temperature) were tested in order to obtain the corresponding ammonium salt in high yields, by avoiding any degradation of the polyester chain.

Table 4. Yields of the quarternization reaction between α -N,N-dimethy-aminoethyl PEO-*b*-PCL (12b) and 2-bromoethyl- α -D-mannopyranoside as a function of the reaction conditions.

#	<i>solvent</i>	<i>equiv Br-R^a</i>	<i>temp</i>	<i>time</i>	<i>F^b</i>
A	micelles in H ₂ O	14 equiv	50°C	70 h	17%
B	DMF	10 equiv	50°C	24 h	14%
C	MeOH	10 equiv	60°C	72 h	18%
D	DMF	17 equiv	70°C	72 h	80%
E	DMF	15 equiv	70°C	50 h	70-80%
F	DMF	17 equiv	70°C	5 d	80% ^c

^a molar equivalents of bromoethyl- α -D-mannopyranoside (Br-R) with respect to the tertiary amine (R₂N-R'') (12b); ^b α -end group functionalization yield; ^c SEC revealed degradation of the polymer chain

It was found that a large excess of 2-bromoethyl- α -D-mannopyranoside (Br-R) is necessary. Moreover, high reaction temperatures and long reaction time significantly increase the conversion of the reaction. The best functionalization yields were obtained in dry DMF, at 70°C using a large excess of the brominated mannose-derivative (15 equiv).

For the removal of the excess of mannose, the reaction mixture was concentrated by evaporation of a large quantity of the solvent and micellar solutions were formed by dropwise addition of the same volume of water. These solutions were then dialyzed against water for 48 h, and the product recovered in good yield by lyophilization (Yield = 99%). The conversion of the reaction and the removal of the excess of mannose reaction were confirmed by $^1\text{H-NMR}$ spectroscopy. Figure 9 shows the $^1\text{H-NMR}$ spectrum of the product in CDCl_3 after purification by dialysis.

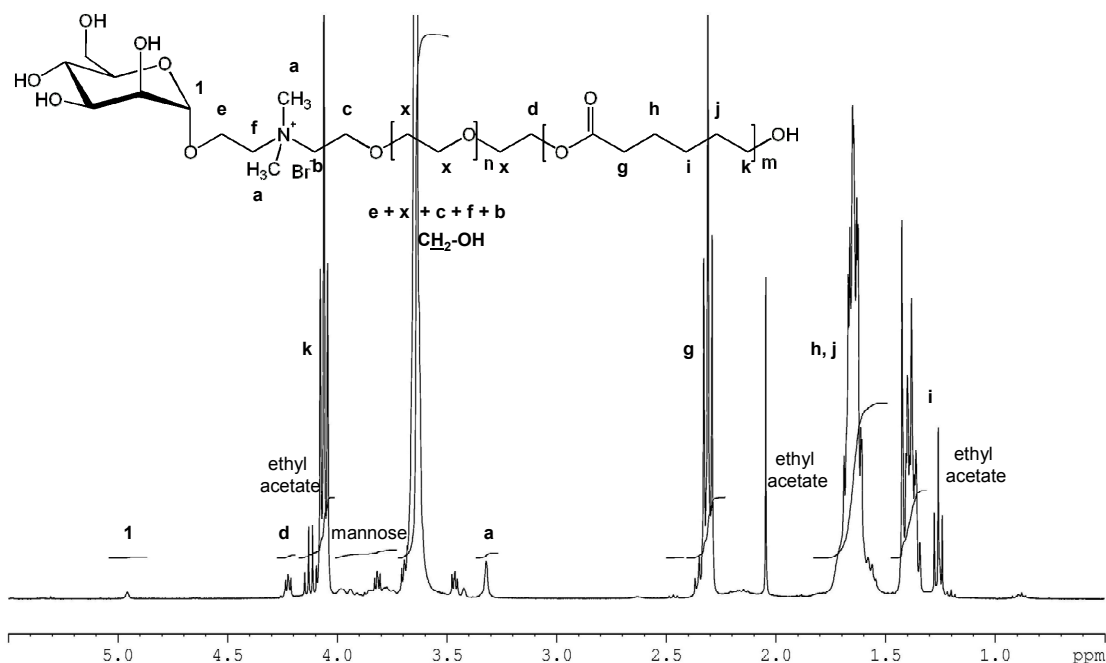


Figure 9. $^1\text{H-NMR}$ spectrum (400 MHz, 25°C, CDCl_3) of α -mannosylated poly(ethylene oxide)-*b*-poly(ϵ -caprolactone) 14 from copolymer (12b).

Compared to the spectrum of the copolymer before derivatization (Figure 3), new resonances in the range of 3.4 ppm to 5.0 ppm appeared, which are characteristic of the protons of the mannose moiety. The signal at 4.9 ppm can be attributed to the anomeric proton of mannose (H_1). Furthermore, the two peaks at 2.27 ppm (6H, $\text{CH}_3\text{-N}$) and at 2.51 ppm (2H, N-CH_2) characteristic of the tertiary amino end-group of PEO-*b*-PCL (20) before quarternization disappeared, indicating the quantitative conversion in the ammonium salt.

In addition, we observed a new resonance at 3.40 ppm. The integration of this peak was found six times that of the anomeric proton H₁ of mannose. The resonance at 3.40 ppm was thus attributed to the methyl protons of the quaternary ammonium salt and agrees with the chemical shift values of methyl group of quaternary ammonium salts found in the literature.³⁴ The ratio of 1:6 of the integrals evidences the successful elimination of excess mannose. In addition, two-dimensional ¹H-NMR experiments (COSY) confirmed its attribution to the methyl group in α -position of the amine, as no coupling of this proton signal (at 3.40 ppm) was observed.

Figure 10 shows the SEC chromatograms of copolymer **12b** (trace A) and the corresponding glycopolymer **14** (trace B) prepared according to reaction conditions “E” (Table 4). The chromatogram of the glycopolymer remains unimodal and narrow, consistent with the absence of degradation and side reactions ($M_n/M_w = 1.19$). Longer reaction times led to degradation of the polymer. (SEC trace not shown, see Table 4, entry F)

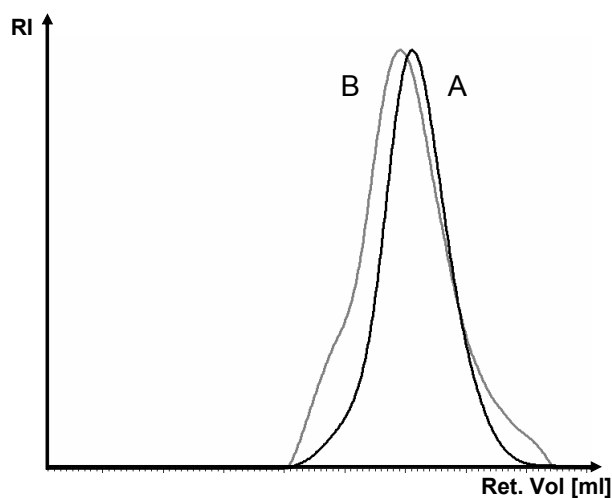


Figure 10. SEC chromatograms for α -*N,N*-dimethylaminoethyl PEO-*b*-PCL copolymer before (A) and after quaternization in DMF at 70°C for 50 h according to (reaction conditions “E”) (B).

III.3.4. General conclusions on the synthesis of glycopolymers 10, 16 and 14.

Comparing the different synthesis pathways to mannosylated amphiphilic glycopolymers, it comes clear that the first approach (acid-amine coupling, NH₂-mannose to COOH-end-capped PCL) was simple and led in good yields to the desired glycopolymer without degrading the polyester chain. However, the length of the hydrophilic segment of

the glycopolymer is determined by the length of the commercially available hydrophilic spacer molecule. Thus, the amphiphilic properties can hardly be tuned. The second approach, based on a reductive amination reaction, revealed to be very difficult. It required the use of protecting groups, and led to side reactions. The conversion to the glycopolymer was very low. In contrast, the third approach, based on the quarternization of the tertiary amino group of R₂N-PEO-*b*-PCL by Br-mannose, seems the most promising pathway, as the reaction proceeded in good yields and without recourse to protecting chemistry.

III.4. Amphiphilic properties of the (glyco)polymers: Dynamic interfacial tension measurements and micelle formation.

III.4.1. Dynamic interfacial tension measurements.

The amphiphilic properties of the polymers **10**, **12b** and **14** have been investigated by measurements of the interfacial tension γ at a CH_2Cl_2 / water interface with a pendant drop tensiometer (TRACKER). Figure 11 displays the dynamic interfacial tension isotherms $\gamma(t)$ corresponding to different concentrations C_s of solutions of the PEO-*b*-PCL diblock copolymer **12b**, before (Fig. 11 A, **12b**) and after quarternization with mannose-bromide (Fig. 11 B, **14**) in CH_2Cl_2 .

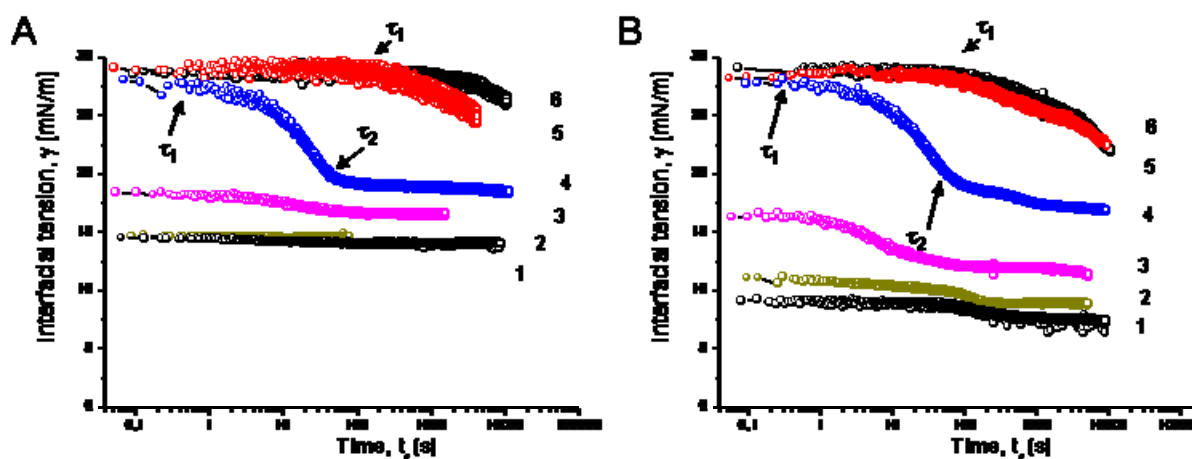


Figure 11. Kinetic curves for A) copolymer “12b”, R_2N -PEO-*b*-PCL for different bulk concentrations C_s (1) 1 ; (2) 0,5 ; (3) $5 \cdot 10^{-2}$; (4) $5 \cdot 10^{-3}$; (5) $5 \cdot 10^{-4}$; (6) $5 \cdot 10^{-6}$ mg/ ml and B) copolymer “14”, R_3N^+ -PEO-*b*-PCL, Br^- for (1) 5 ; (2) 0,5 ; (3) $5 \cdot 10^{-2}$; (4) $5 \cdot 10^{-3}$; (5) $5 \cdot 10^{-4}$; (6) $5 \cdot 10^{-6}$ mg/ml.

In general, the curves $\gamma(t)$ show several stages of adsorption with different characteristic relaxation times: the induction stage (*lag stage* for $t < \tau_1$), the post-induction stage (*post-lag stage* for $\tau_1 < t < \tau_2$) and the final stage ($t > \tau_2$). As indicated in Figure 11, the *lag time* τ_1 is well distinguished for relatively low bulk concentrations C_s ($< 5 \times 10^{-3}$ mg/ml), and is characterized by a slow decrease of the $\gamma(t)$ (curves 6, 5, 4 in Figure 11) at the beginning of the adsorption process. This induction time corresponds to the diffusion of the macromolecules from the bulk to the interface. Generally, after having achieved the interface (by diffusion), macromolecules such as polysoaps or proteins,^{35,36,37} unfold at the interface and may adsorb irreversibly by anchoring their hydrophilic part in the polar

phase. The *post-lag stage* of adsorption is characterized by a fast decrease of the interfacial tension ($d\gamma/dt$). During this period, the first layer adsorbed for $t < \tau_1$ is “compacted” by newly arriving polymer chains which interpose between the already adsorbed molecules.

At the end of the post-lag stage, the formed adsorption layer begins to act as a repulsive barrier against newly arriving macromolecules. This is manifested by a remarkable decrease of $d\gamma/dt$ after time τ_2 .

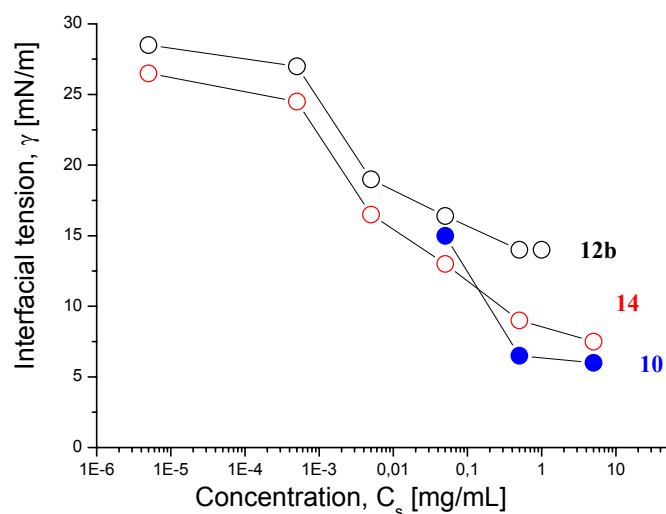


Figure 12. (Adsorption) Isotherms of the interfacial tension γ at the H_2O/ CH_2Cl_2 interface for the samples of copolymer 12b, copolymer 14 and polymer 10 measured for the ageing time of adsorption layers 10^3 s.

Figure 12 shows the interfacial tension in function of the polymer bulk concentration C_s after 1000 s of aging of the CH_2Cl_2 drop. It compares thus the effectiveness of the PEO-*b*-PCL diblock copolymer, before (Fig. 12, **12b**) and after quarternization with mannose-bromide (Fig. 12, **14**) in reducing the oil-water interfacial tension γ . Both PEO-*b*-PCL diblock copolymers exhibit strong interfacial activity, and lead to a significant decrease of the initial γ , $\gamma(H_2O/ CH_2Cl_2) \sim 30$ mN/m. However, the quarternized copolymer -bearing the mannose moiety- seems more efficient. Indeed, for high concentrations of copolymer **14** ($c > 1$ mg/ml) γ is decreased so much that the values come close to the limit of measurability by the pendant drop method (drop felt down after several minutes.) Figure 12 shows also some preliminary results of the low molecular weight mannosylated PCL (Fig. 12, **10**). This glycopolymer displays also interfacial activity but additional measurements would be necessary to compare it with the diblock copolymers. It must

however be emphasized, that the graph displays the concentrations in mg/ml, which pretends an effectiveness in favor to the low molecular copolymer **10**.

III.4.2. Micelle formation.

Micelles from PEO-*b*-PCL diblock copolymers **12b** and **14** were prepared using a dialysis method. These colloidal solutions were investigated by DLS (dynamic light scattering) analysis. For both types of micelles, the apparent diffusion coefficient ($D_{app} = 1/\tau \times q^2$) did not depend on the angle of measurement, indicating a low size dispersity of the objects. The hydrodynamic radius R_H for both types of micelles, from copolymers **12b** (Figure 13 a, curve A) and **14** (Figure 13 b, curve A), was determined as 11 nm. This R_H agrees well to that of micelles made of PEO-*b*-PLA diblock³⁸ or PEO-*b*-PCL³⁹ diblock copolymers reported in the literature. So, well-defined unimodal spherical micelles with a small diameter could be prepared from amphiphilic PEO-*b*-PCL diblock copolymers.

In order to investigate whether mannose is exposed and bioavailable at the surface of the micelles prepared from glycopolymer **14**, an aggregation assay was performed. This assay relies on the interaction of mannose with *Concanavalin A* (ConA), a lectin which forms complexes with mannose by multivalent interaction. In case of availability of mannose at the surface of the micelles, the micelles would be “cross-linked” and the formation of large aggregates is expected to be detectable by DLS, for instance. Micelles prepared from copolymer **12b** were used as a negative reference sample. The semi-logarithmic plots obtained from “REPES routine” treatment of the raw DLS results (Figure 13) show the size distributions for a) micelles prepared from the mannose-conjugated copolymer **14** (Figure 13 a) and b) from copolymer **12b** (Figure 13 b) before and after addition of an excess of ConA. Figure 13 a shows that upon addition of an excess of ConA to the sugar-containing micelles, a second population at higher molecular weight appeared (curve B, in gray), whereas micelles of the initial size ($R_H = 11$ nm) were still detected. The more ConA was added the more aggregates were formed. When the same experiment was carried out on non-mannosylated micelles (Figure 13 b), the formation of aggregates were also observed coexisting with the initial micelles (Fig. 13b, curve B in gray). It must however be mentioned, that for the same reaction conditions, i.e. the same quantity of ConA and micelles, the extent of the second population (calculated from the micelle/

aggregate surface ratio) reached up to 30% in case of micelles from the mannosylated copolymer **14**, compared to only 10 to 15% for copolymer **12b**.

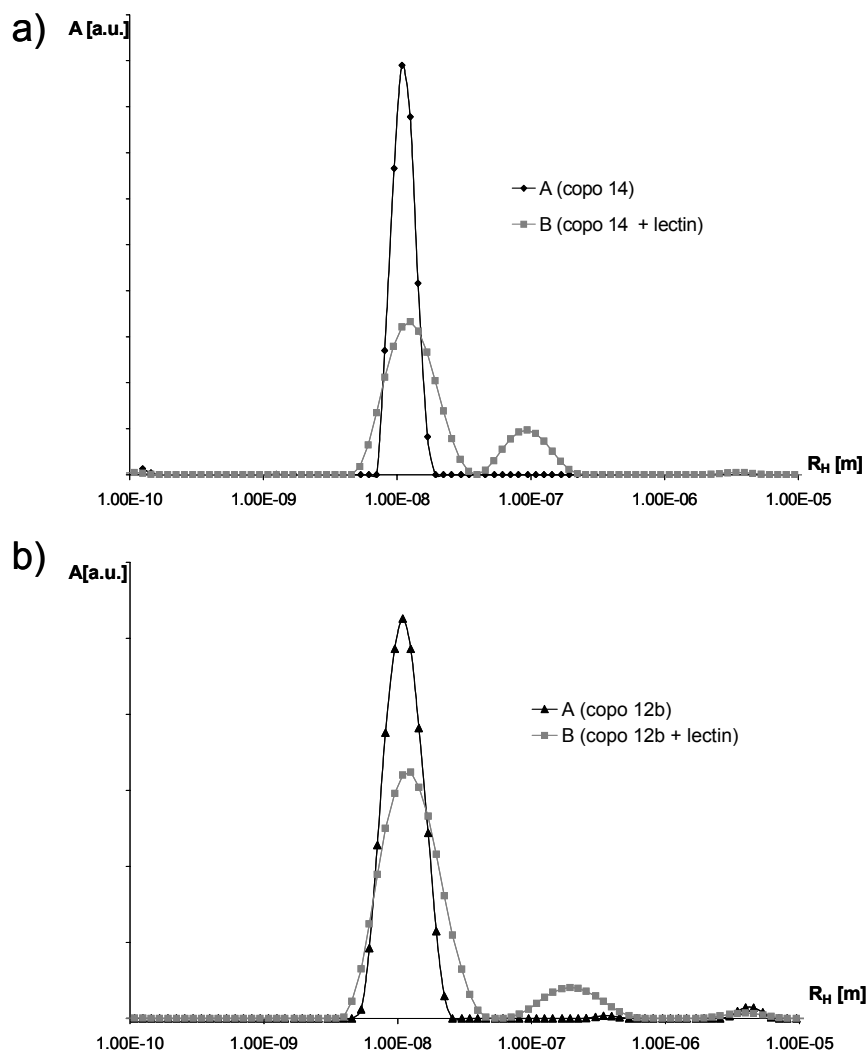


Figure 13. DLS of micellar solutions prepared from a) mannosylated PEO-*b*-PCL diblock copolymer “14” and b) reference PEO-*b*-PCL diblock polymer “12”; curves “A” before addition of the lectin; curves “B” after addition of the lectin.

In both cases, the lectin induces thus the formation of aggregates, partly probably due to non-specific interactions between the micelles and the ConA. However, the difference of the extent of the reactions might be a first indication of the existence of specific interactions between exposed mannose and the lectin.

III.5. Preparation and characterization of nanoparticles.

III.5.1. Characterization of size and shape of the NPs.

It has been reported that amphiphilic copolymers could be used as stabilizers and surface-modifiers of polymeric nanoparticles (NPs), using various preparation techniques.^{13,40,41} As reported in the previous section, polymers **10**, **12b** and **14** show interfacial activity. The glycopolymers **10** and **14** seem thus promising candidates to modify the surface of NPs by mannose.

In this work, fully bioresorbable polymeric NPs are prepared by a nanoprecipitation-evaporation procedure,¹³ which relies on the use of water-miscible volatile organic solvent, which dissolves well the (water-insoluble) polymer. Then, upon addition of this organic solution to a large quantity of water under stirring, the solvent diffuses into the water phase and induces the precipitation of the polymer into NPs. In our study, PLA and mixtures of PLA with increasing amounts of polymer **10**, **12b** and **14** (9, 46, 137, 233 mol% with respect to PLA) were dissolved in acetone and ‘nanoprecipitated’ in water. Due to their interfacial activity, the glycopolymers were expected to be at least partially localized at the NPs’ surface.

First of all, it must be mentioned that PLA alone could be converted into stable NPs. Moreover, the addition of the amphiphilic (co)polymers **10**, **12b** and **14**, did generally not hinder the formation of NPs at least up to 137 mol% with respect to PLA. These NPs have then been analyzed by cryo-TEM, AFM and DLS.

The left hand side of Figure 14 shows typical cryo-TEM images of aqueous dispersions of NPs prepared from solutions of PLA (Fig. 14 a), and mixtures of PLA and 46 mol% (with respect to PLA) of copolymer **12b** (Fig. 14 b) and **14** (Fig. 14 c), respectively. All the NPs are spherical and no aggregation was observed. At a closer look, the NPs prepared in presence of copolymer **12b** (“NP PLA + copo 12b”) seem smaller than ‘pure’ PLA NPs (“NPs PLA”) or NPs prepared in presence of glycopolymer **14** (“NPs PLA + copo 14”). The right hand side of Figure 14 shows the size-distribution histograms of the three different types of NPs determined by measuring the diameter of 800 NPs. As reported in Table 5, the number-average diameter (D_n) of NPs “NPs PLA + copo 12b” is about 60 nm in contrast to a D_n of about 100 nm for the two other sorts of NPs. The standard deviation (std) is large for all types of NPs.

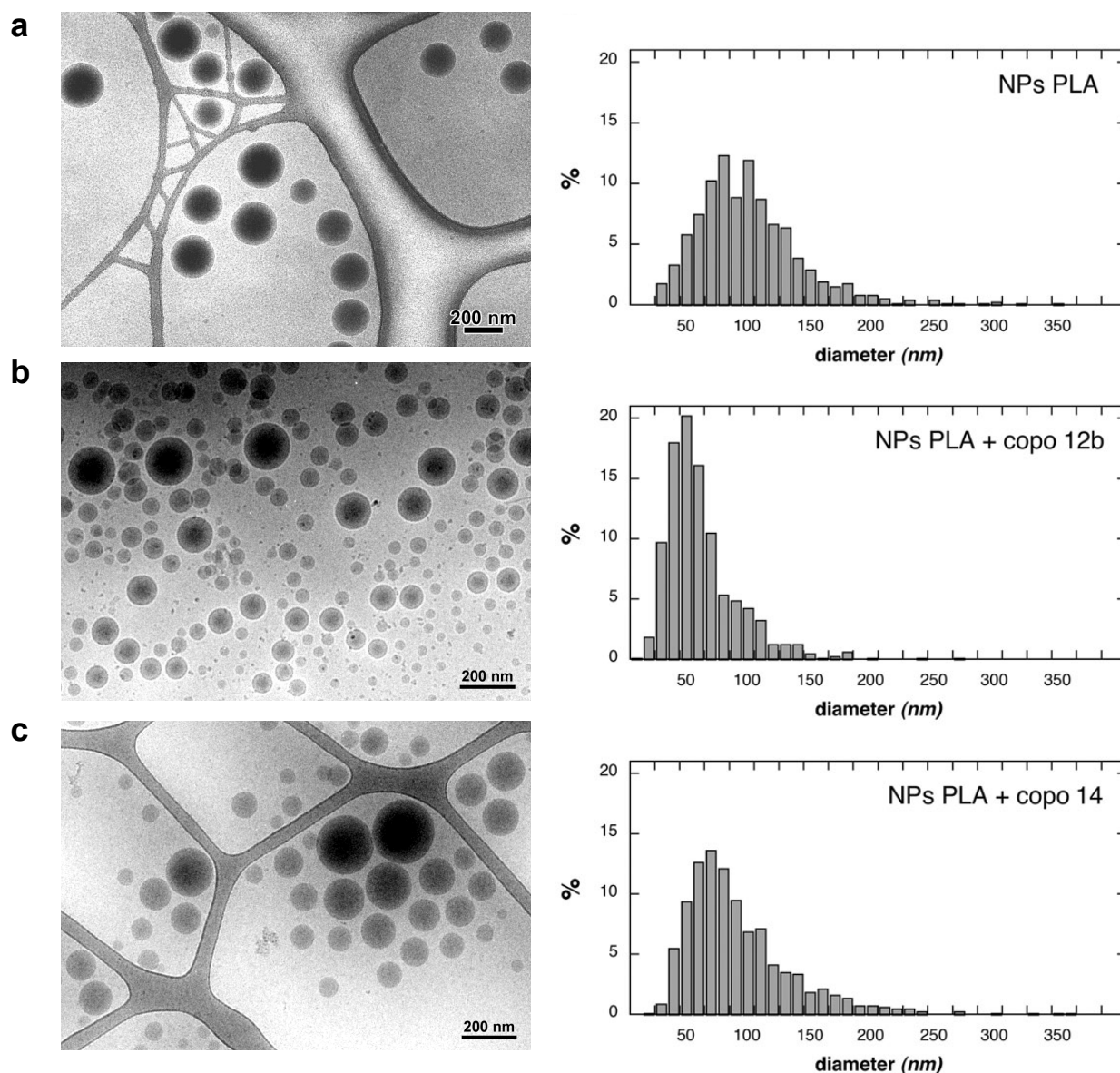


Figure 14. left : Cryo-TEM pictures of nanoparticles (NPs) made from a) PLA, b) PLA with 46 mol% of copolymer 12b (NR₂-PEO-*b*-PCL) and c) PLA with 46 mol% of copolymer 14 (Mannose-N⁺-PEO-*b*-PCL Br⁻) embedded in vitreous ice; **right:** size-distribution histograms determined by measuring the diameter of 800 NPs from cryo-TEM images.

Table 5. Number-average diameter (D_n) and standard deviation (std) of the different NPs.

	<i>NPs PLA</i>	<i>NPs PLA +12b</i>	<i>NPs PLA +14</i>
D_{n-TEM} [nm]	101	63	93
std [nm]	44	30	46

Furthermore, the NPs have been analyzed by AFM (Figures 15 and 16). Figure 15 shows a typical AFM picture of closely packed NPs (sample prepared from mixtures of PLA with 46 mol% of copolymer **14**). This experiment confirms the dimensions obtained by cryo-TEM (spherical, of about 50 to 200 nm) and provides additional information about the 3D structure of the NPs.

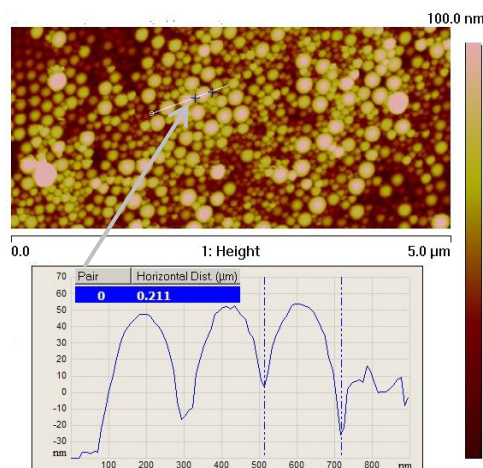


Figure 15. Topography and horizontal cross-section of nanoparticles prepared from PLA with 46 mol% of copolymer **14** observed by tapping mode AFM. The height color scale is on the right side of the picture.

The analysis of three NPs in Figure 16, taking into account the size of the apex of the AFM tip, gives a corrected width of around 190 nm and a maximum height of about 90 nm. These measurements reveal a very low deformation of the nanospheres and prove that they are quite rigid objects.

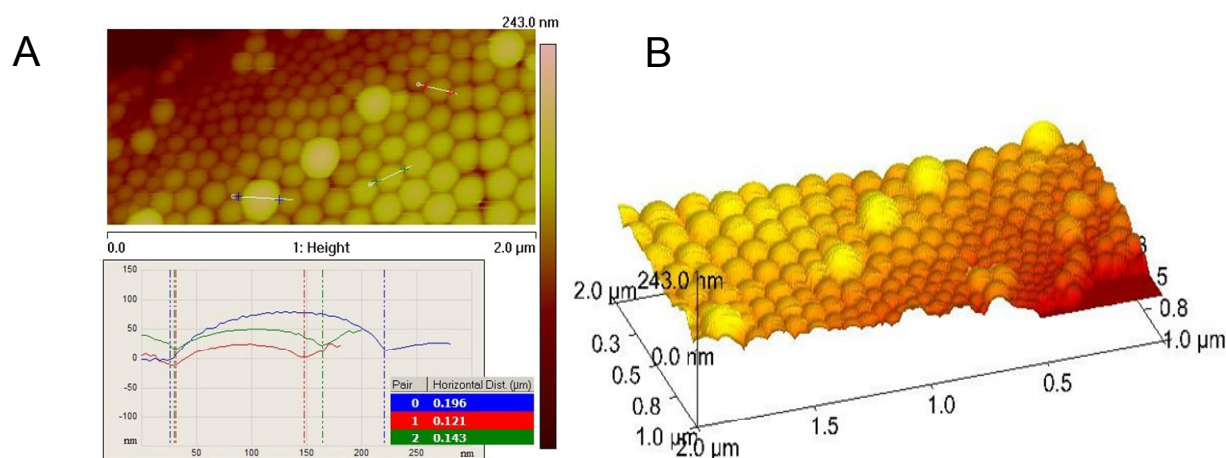


Figure 16. (A) Topography and horizontal cross-section of PLA nanoparticles with 46 mol% of copolymer **14** observed by tapping mode AFM. The height color scale is on the right side of the picture. (B) 3D rendering view of (A) combining the color height scale and extra illumination for the shadows.

It can thus be concluded that the NPs resist to the compressive forces during the preparation of the cryo-TEM samples and hence that the sizes determined by cryo-TEM are reliable.

Table 6 summarizes the conversion (“conv”) of the polymer material dissolved in acetone into NPs. It was for all samples in the range of 80 to 90%. However, when 233 mol% of polymer **10** (with respect to PLA) were added, rough precipitation was observed, i.e. the formation of the NPs seems to be strongly disrupted. Furthermore in contrast to the other types of NPs, all the NPs prepared with polymer **10** lacked stability and aggregated with time. (A possible explanation is given later in the text, section III.5.2.1.)

Table 6. Characteristics of polymer nanoparticles prepared from acetone solutions containing different amounts of (co)polymers (with respect to PLA).

#	(co)polymer	copo/ PLA ^{theor} [mol%]	conv ^a [%]	t _s ^b [%]	D _H ^c [nm]	PDI ^d	zeta pot [mV]
0	Reference sample “blank”	PLA without copo	82	2.7	191	0.13	-56
1a	10	9	90	2.9	194	0.10	-58
1b		46	86	3.0	191	0.10	-55
1c		137	88	3.5	198	0.14	-53
1d		233	67	2.5	178	0.14	N.D. ^e
2a	12b	9	82	3.0	180	0.13	-49
2b		46	88	3.2	156	0.12	-13
2c		137	86	4.2	140	0.08	15
3a	14	9	86	2.7	199	0.10	-41
3b		46	89	3.0	225	0.15	7
3c		137	83	3.4	258	0.14	21

^a mass of solid transformed in nanoparticles [g]/ mass of polymer [g] initially dissolved in acetone × 100; ^b solid rate in g/ 100 ml; ^c hydrodynamic diameter averaged on 5 × 10 measurements; ^d PDI = polydispersity index; ^e N.D. = not determined

Cryo-TEM experiments revealed that the size distribution of the NPs were quite large. Table 6 reports the polydispersity index (PDI) for the different samples calculated by QELS. They ranged from 0.1 to 0.15. Indeed, a PDI of 0.05 is characteristic of a monodisperse colloid, whereas for values above 0.5 the dispersion is broadly size distributed.¹⁶ No evidence of the influence of co-polymer used on the size distribution could be observed.

Figure 17 demonstrates the influence of the quantity and nature of the (co)polymer on the *size* of the NPs. It clearly shows that the addition of glycopolymer **10** does not influence their dimensions. However, the amphiphilic PEO-*b*-PCL *diblock* copolymers **12b** and **14** do have an impact on the size of the NPs. Indeed, the addition of copolymer **12b**, which is α -end-capped by a tertiary amino group, decreases the NPs' size. On the other hand, copolymer **14**, bearing a mannose group attached via a positively charged quaternary ammonium group, increases the size of the NPs. The higher the copolymer/ PLA ratio, the stronger are these effects. The properties (charge, size) of the end-group seem thus to have a great impact on the NPs' formation. At this stage, it is however difficult to propose an explanation. In order to better understand the role of the (co)polymers, the surface of the NPs was analyzed.

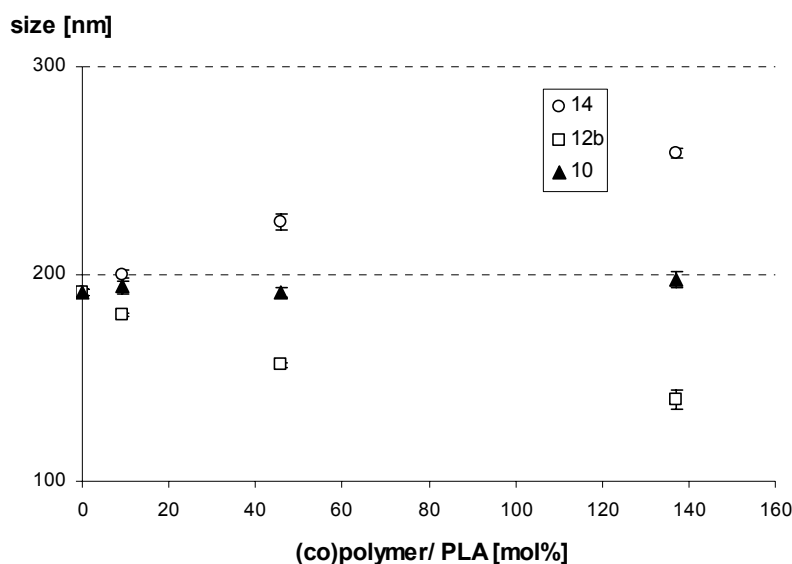


Figure 17. Effect of the quantity and nature of the copolymer on the NP size (“10” = Mannose-(EO)₃-PCL; “12b” = Me₂N-PEO-*b*-PCL; “14” = Mannose-N⁺-PEO-*b*-PCL Br⁻).

III.5.2. Analysis of the NPs' surface.

The NPs' surface properties were characterized by *physico-chemical techniques* such as zeta potential measurements and NMR spectroscopy. Let's remind that the aim of this study was to decorate polymeric nanoparticles by mannose moieties allowing the specific targeting of cells that express mannose receptors at their surface. Therefore, *recognition assays* based on the mannose-lectin interaction have also been employed.

III.5.2.1. Physico-chemical techniques.

Zeta potential measurements. Figure 18 shows the influence of the nature and the quantity of the (co)polymer on the zeta potential of the different nanoparticles (NPs).

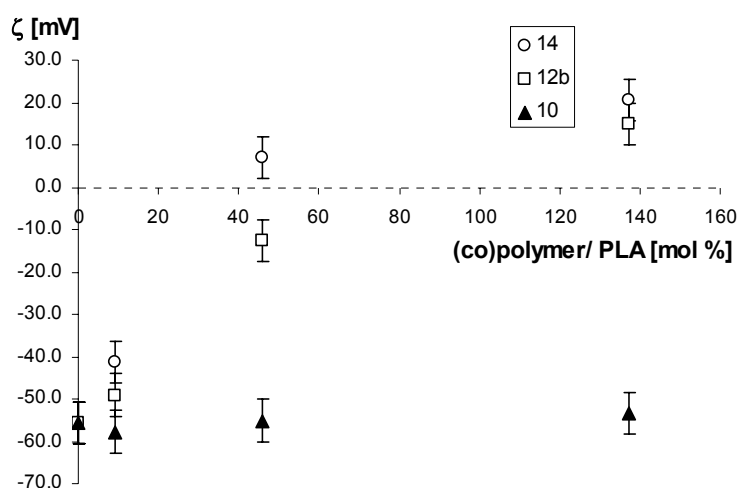


Figure 18. Zeta potential [mV] at pH 6 vs. (co)polymer/PLA ratio (“10” = Mannose-(EO)₃-PCL; “12b” = Me₂N-PEO-*b*-PCL; “14” = Mannose-N⁺-PEO-*b*-PCL Br⁻).

All measurements were performed at pH 6. First of all, it must be noted that ‘pure’ PLA NPs are negatively charged, which contributes to their stability. The negative charge comes from the carboxyl groups at the α -end of the polymer, which has a number-average molecular weight (M_n) of 32650 g/mol and was synthesized by polyaddition. Furthermore, the addition of the small neutral glycopolymer **10** did not significantly change the value of the zeta potential, at least for the copolymer/PLA ratios investigated here. On the other hand, upon addition of copolymers bearing a tertiary (**12b**) or quaternary (**14**) amine the zeta potential increases. Whenever high copolymer/PLA ratios are used negatively charged PLA NPs become positively charged, while preserving the stability of the NPs. Indeed, copolymer **14** bears a quaternary ammonium group, thus a permanent positive

charge, and copolymer **12b** a tertiary amine group. It must be noted that the latter (**12b**) is highly protonated at pH 6 (in 1 mM NaCl solution) due to its high pK_a ($pK_a \sim 9.3$). These measurements provide thus one first evidence of the ability of amphiphilic polymers to modify the surface properties of NPs when used as “co-polymer” (in addition to PLA) in a nanoprecipitation technique.

$^1\text{H-NMR}$ analysis. In order to determine the amount of amphiphilic polymer present at the NPs’ surface, $^1\text{H-NMR}$ experiments have been carried out on NP dispersions in D_2O . Therefore, water was exchanged against D_2O by three successive centrifugations, and the dispersions were concentrated to “solid contents” up to 6% (6 g/ 100 ml). These dispersions in D_2O were then analyzed by liquid $^1\text{H-NMR}$ spectroscopy and the amount of PEO at the surface determined using an internal standard. Using this technique, PEO chains entrapped in the solid core of the NPs are not detected. The real copolymer/ PLA composition of the NPs recovered after the centrifugation step (Table 7, “copo/ PLA_{expt}”), was determined by $^1\text{H-NMR}$ spectroscopy in CDCl_3 , after freeze-drying of the dispersions in D_2O and re-dissolution of the samples in CDCl_3 . The results are summarized in Table 7.

Table 7. Composition of the NPs determined by $^1\text{H-NMR}$ in CDCl_3 and percentage of PEO at the surface of the NPs (determined in D_2O).

#	“co-polymer”	copo/ PLA _{theor} [mol%] ^a	copo/ PLA _{expt} [wt%] ^b	loss of copo ^c [%]	PEO at NPs’ surface [%] ^d
1a		9	7	22	\ll ^e
1b	10	46	37	20	8
1c		137	NPs not stable, N.D.	N.D.	N.D. ^f
2a		9	5	44	66
2b	12b	46	28	40	85
2c		137	41	70	98
3b	14	46	12	74	94
3c		137	12	91	98

^a copolymer/ PLA ratio in the acetone used for the nanoprecipitation process; ^b copolymer/ PLA ratio of the NPs determined by $^1\text{H-NMR}$ after dissolution of precipitated NPs in CDCl_3 ; ^c loss of the copolymer in the supernatant upon centrifugation; ^d percentage of soluble PEO located at the NPs’ surface with respect to the total amount of PEO in the NPs; ^e \ll below the limit of detection; ^f N.D. = not determined

It becomes clear that the experimentally determined copolymer/ PLA ratio (“copo/ PLA_{expt}”), of the NP’s composition was always lower than the theoretical one (“copo/

PLA_{theor}”), independently of the copolymer used. Compared to PLA, the copolymers were preferentially lost in the supernatant during centrifugation. Actually, this step leads to the concentration of heavier, i.e. bigger, NPs and the loss of smaller particles in the supernatant. Due to the discrepancy between theoretical and experimental copolymer/ PLA ratio, one can thus conclude that the objects of small size in the supernatant contain more copolymer compared to bigger particles of the centrifugate. This might be related to the high surface/volume ratio of smaller NPs compared to bigger ones, considering that the amphiphilic copolymer is preferentially localized at the NPs’ surface. Another explanation might be the formation of two kinds of ‘nanoobjects’ during the nanoprecipitation, one of very small size, such as micelles, composed of the copolymer, and a second population composed of a mixture of both polymers, PLA and the copolymer.

In contrast to diblock copolymers **12b** and **14**, the experimentally determined compositions of NPs prepared with polymer **10** are quite close to the theoretical values, indicating that this polymer is poorly lost during the centrifugation steps. It should be mentioned that NPs prepared with **10** aggregated easily, especially upon –even gentle– centrifugation. Actually, analysis of such NP dispersions after two successive centrifugations at 4000 g (7000 rpm) by QELS revealed that the distribution of the size was bimodal and the formation of bigger aggregates (900 nm) was evidenced. The formation of bigger aggregates rather than the loss of copolymer might thus explain the correspondence of the theoretical and experimental copolymer/PLA ratio.

Table 7 also lists the amount of “PEO at the NPs’ surface”, which is the percentage of soluble PEO coating around the particles with respect to the total amount of PEO in the NPs. Actually, the majority, i.e. 65 to 100%, of the PEO chains is localized at the surface, except for glycopolymer **10** (8%), the PCL oligomer capped by a mannose via a hydrophilic spacer. This copolymer seems thus localized in the core of nanoparticle. One possible explanation might be found in the molecular characteristics of glycopolymer **10**. In contrast to diblock copolymers **12b** and **14**, **10** possesses only a very short hydrophilic ethylene oxide chain. However, the latter is probably the driving force for the polymer’s migration to the surface of the PLA NPs. Due to the lack of this long hydrophilic chain, glycopolymer **10** may precipitate together with PLA (during the NPs’ preparation) and remain entrapped in the core of the NPs. Hence, the oligo(ethylene oxide) chains would be hidden in the polymer aggregates and not detectable by liquid ¹H-NMR. This tentative of explanation, indicating a random distribution of polymer **10** in the NPs (instead of a preferential localization of the polymer at the surface), agrees well with the fact that the

loss of **10** in the supernatant upon centrifugation is less (about 20%) compared to the copolymers **12b** and **14** (40-90%). It must thus be concluded, that this technique provides evidences of the presence of PEO chains at the NPs' surface, and thus the presence of mannose moieties at the NPs' surface seems probable.

III.5.2.2. Recognition assays.

The previously described characterization techniques allowed demonstrating the presence of the hydrophilic segment of the copolymer at the surface of the NPs. However, biological assays based on the recognition of mannose by a mannose-specific lectin (*Galanthus nivalis*, GNA) are necessary in order to prove the presence and bioavailability of mannose.

Interaction of the mannose-decorated polymeric NPs (~200 nm) with GNA-gold nanoparticles (10 nm) studied by cryo-TEM. In order to demonstrate the bioavailability of mannose on the NPs' surface, PLA NPs prepared with 46 mol% of glycopolymer **14** (Mannose-N⁺-PEO-*b*-PCL Br⁻, sample "3b" in Table 7), were mixed with GNA coated-gold nanoparticles (10 nm) and observed by cryo-TEM. In case of complex formation between the NPs' mannose with the lectins of the gold NPs, the association of both types of NPs should be detectable by cryo-TEM.

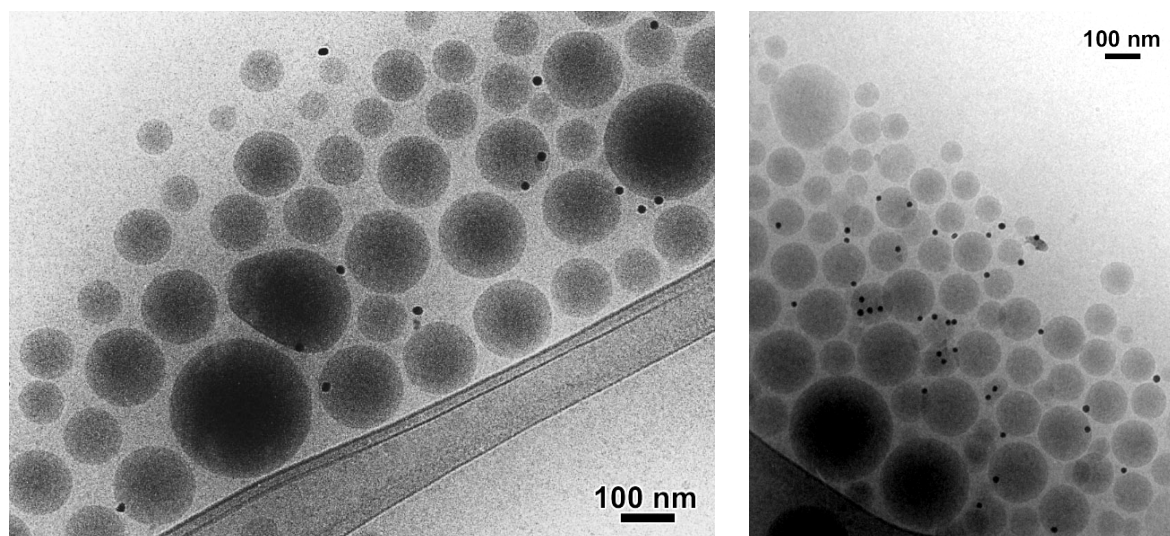


Figure 19. Cryo-TEM images of NPs prepared from PLA with 46 mol% of copolymer **14** (Mannose-N⁺-PEO-*b*-PCL Br⁻ "14") after incubation with GNA-coated gold nanoparticles (10 nm).

The images in Figure 19 clearly demonstrate the adsorption of the gold-nanoparticles (dark dots of about 10 nm diameter) on the surface of the polymer NPs (in gray).

The same experiment was also performed with “blank” “non-mannosylated” NPs, i.e. NPs prepared from mixtures of PLA and copolymer **12b** (46 mol% R₃N-PEO-*b*-PCL, sample “2b” in Table 7). It was found that GNA-gold NPs also adsorbed on this kind of polymeric NPs. However, the extent of adsorption seemed smaller, and “free” non-associated gold nanoparticles could also be observed. The unspecific adsorption of the GNA protein on the NPs’ surface might be a consequence of its strong interfacial activity as shown by measurements with a pendant drop tensiometer (TRACKER) at the CH₂Cl₂/water interface (Figure 20).

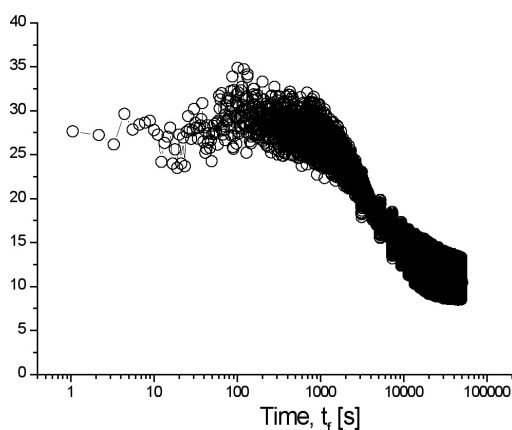


Figure 20. Kinetics of lectin’s adsorption ($1.7 \cdot 10^{-4}$ mg/ ml) at the CH₂Cl₂/ water interface (after 1000 s, $\gamma = 25$ mN/m; after 10000s, $\gamma = 15$ mN/m).

Biological assay based on lectin-sugar interaction. Biological assays, based on specific lectin-sugar interactions, are currently employed to quantify colorimetrically the amount of bioavailable sugars at a surface. As demonstrated schematically in Figure 21, the use of a biotinylated lectin allows for its complexation with a streptavidin-enzyme conjugate and the spectrometric quantification of the formed complex.

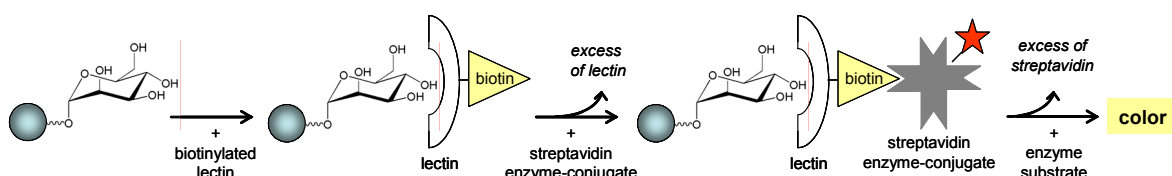


Figure 21. Scheme for the multistep titration of particle-fixed mannose by biotin-labeled biotin.

In a typical assay, biotinylated lectins (GNA-lectin conjugates) were incubated with an aqueous NP dispersion, and then the excess was removed by centrifugation. The next step consisted in the addition of a streptavidin-enzyme conjugate, which complexes with the lectin-bound biotin. After removal of the excess of the streptavidin enzyme-conjugate (streptavidin-phosphatase), the substrate for the enzyme (*p*-nitrophenyl phosphate, pNPP) was added, converted to a colored compound, which could then be quantified by colorimetry. This allows the determination of the amount of mannose that is bioavailable at the surface of the NPs.

The first experiments revealed that both proteins, i.e. the lectin and the streptavidin derivative, non-selectively adsorbed on all types of NPs. In the following assays the NPs were thus pre-incubated with the protein BSA in order to prevent this non-specific adsorption (of lectin and streptavidin) at the NPs' surface ("passivation"). Non-adsorbed BSA was then removed by washing of the NPs by centrifugation.

Figure 22 shows the absorbance of the solutions (relying on the amount of the colored product in the sample) for the different types of NPs. Pure PLA NPs and particles prepared from mixtures of PLA with 46 mol% of **12b** (R₂N-PEO-*b*-PCL copolymer) were used as references. It reveals that the absorbance for NPs containing glycopolymers (**10** and **14**) is much higher than that measured for the references. However, even the reference particles were detected as "mannose-positive", as shown by the coloration of the medium. This might indicate the non-specific adsorption of the lectin, or an inefficiency of the removal of the excess proteins through the washing steps.

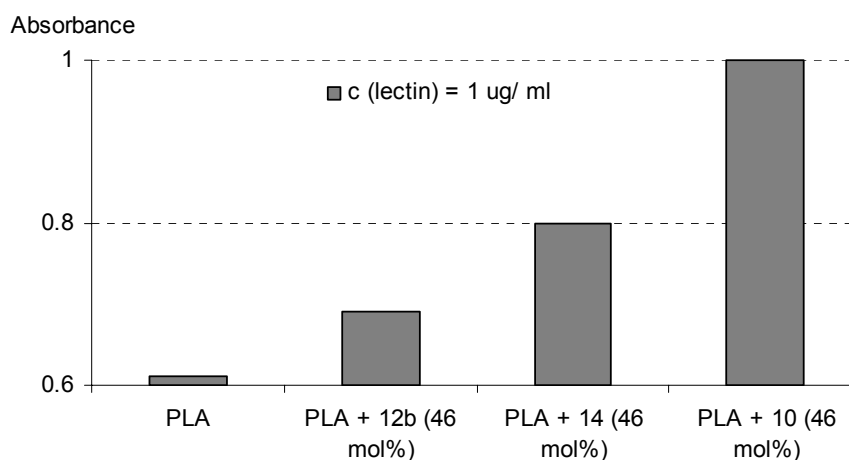


Figure 22. Absorbance measured from the interaction of nanoparticles with GNA-biotin conjugate labeled with phosphatase, in the presence of *p*-nitrophenyl phosphate.

The next assays were thus performed using additional reference samples (“blanks”). These “blanks” were not incubated with the biotinylated lectin, however the following steps of the assay were performed as for the other samples. Figure 23 displays the results of a typical assay. For NP that had been mixed with the lectin (columns in gray), the intensity of absorbance for the samples prepared with the mannosylated polymers, “PLA + 14” and “PLA + 10”, is almost the double of that for the sample without mannose (“PLA + 12b”). This indicates that the adsorption of GNA is mediated via specific interaction of mannose moieties with the lectin. However, even NPs that had not been incubated with lectins (“blanks”, columns in white) led to a slight coloration of the medium, due to the presence of streptavidin. It must thus be considered that the NPs adsorbed the protein streptavidin, or that the latter had not been removed completely by the washing steps.

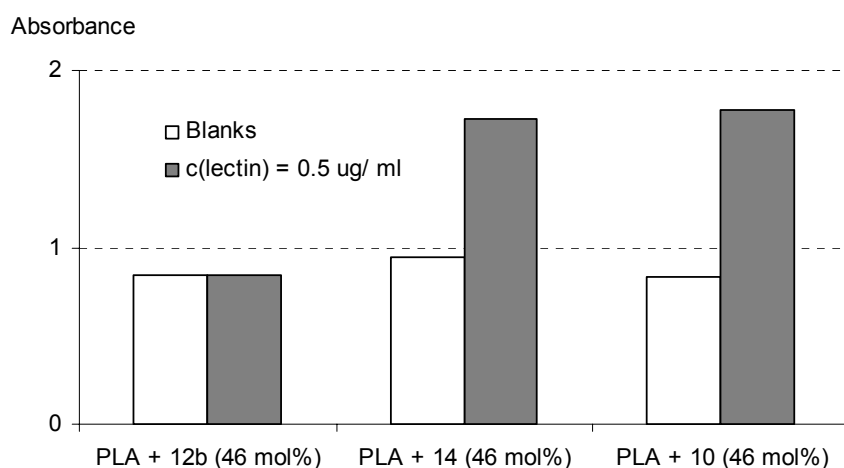


Figure 23. Absorbance measured from the interaction of nanoparticles with GNA-biotin conjugate labeled with phosphatase, in the presence of *p*-nitrophenyl phosphate. “Blanks”: samples that were not incubated with the GNA-conjugate.

In conclusion, similarly to cryo-TEM experiments we were faced to non-specific interactions of proteins, i.e. lectin and streptavidin, with the NPs’ surface. However, these preliminary results indicate that mannose-moieties are bioavailable on the surface of the NPs, but they do not allow drawing quantitative conclusions.

III.5.3. Stability.

The colloidal stability of nanodispersions stored at 4°C was observed over a period of two months. Macroscopically, nanodispersions prepared with PLA alone or mixtures of PLA and copolymer **12b** and **14** (independently of the amount of copolymer) were stable.

Cryo-TEM confirmed the good colloidal stability and the absence of aggregates after 2 month. In contrast, NPs prepared with glycopolymer **10** formed large aggregates as shown in Figure 24. The formation of aggregates seems to be directly related to the amount of **10** used in the nanoprecipitation. As a rule, the more polymer **10** was added, the stronger seemed the tendency of the NPs to aggregate. As already reported earlier (section III.5.1.), the addition of large amounts of polymer **10** (**10**/PLA ratio = 233 mol%) did even hinder the formation of NPs. One possible explanation was derived from the results obtained by NMR analysis of the NP's surface (see section III.5.2.1.). They revealed that low molecular weight polymer **10** was preferentially located in the PLA NPs' core rather than on their surface. It seems possible, that the presence of two different polymers (PLA and **10**) in the NPs' core may destabilize the colloidal system and lead to the formation of aggregates with time.

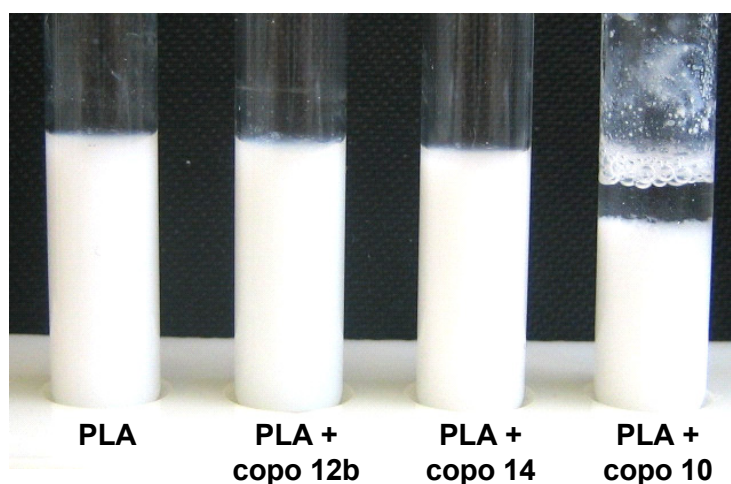


Figure 24. Stability of the nanoparticle solution after 3 month. (PLA with 46 mol% of copolymer).

It should be mentioned, that after two months of storage, the sample containing NPs prepared from PLA and 46 mol% of the mannosylated copolymer **14** had been incubated with GNA-coated gold nanoparticles, in order to demonstrate the interaction of GNA-nanogolds with mannose moieties of the PLA NPs' surface (detailed explanation see section III.5.2.). The cryo-TEM image of the sample (in Figure 25) shows well separated PLA NPs with gold nanoparticles adsorbed at their surface.

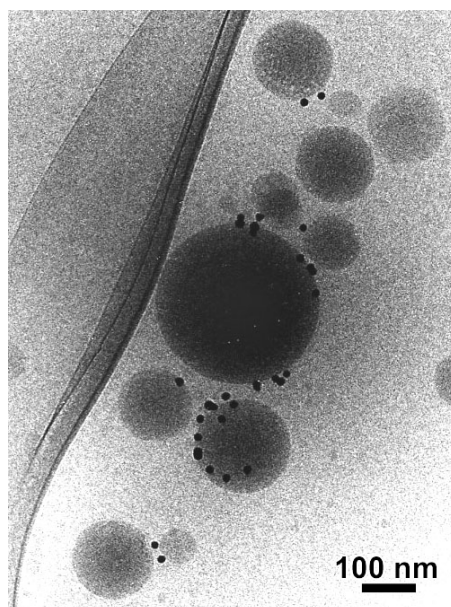


Figure 25. Cryo-TEM image of nanoparticles of 2-month old NPs prepared from PLA with 46 mol% of copolymer 14 after incubation with GNA-coated gold nanoparticles (10 nm).

Interestingly, besides the PLA NPs, objects of a tubular shape were observed (Figure 26). As illustrated in the cryo-TEM images of Figures 26, GNA-coated gold nanoparticles seemed to associate preferentially with them.

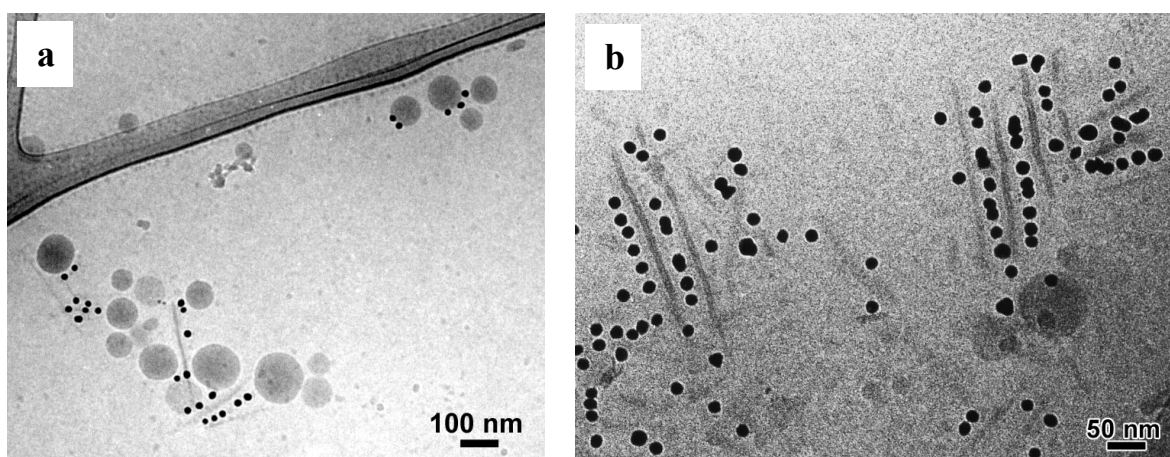


Figure 26. a) and b) Cryo-TEM images of nanoparticles and tubular objects of 2-month old NPs prepared from PLA with 46 mol% of copolymer 14 after incubation with GNA-coated gold nanoparticles (10 nm).

At a closer look (Figure 26 b), the objects consist of an electron-dense core with a width of about 7 nm. On both sides of this elongated core, a layer of very low density and a width of about 6 nm can be seen. The GNA-gold particles seem in contact with this

external layer, rather than with the core region. The total width of the elongated objects is close to 20 nm.

As described in section III.4.2., the hydrodynamic radius (R_H) of spherical micelles formed from copolymer **14** was 11 nm. Considering this size, the elongated objects in the 2 month-old NPs dispersions might be tubular copolymer micelles, with an electron-dense core corresponding to the PCL block and a light outer layer corresponding to a corona made of PEO. That would explain the high affinity of the GNA-functionalized gold particles with the micelles exposing mannose moieties at their surface.

IV. Conclusions

In conclusion, amphiphilic biodegradable/bioeliminable glycopolymers have been synthesized through grafting of mannose derivatives on either α -end-functionalized poly(ϵ -caprolactone) or PEO-*b*-PCL diblock copolymers. Three synthesis pathways have been employed, relying on (i) an acid-amine coupling, (ii) a reductive amination reaction or (iii) a quaternization reaction, leading to neutral, ionisable or permanently charged polymers. Best grafting yields were obtained for the acid-amine coupling and the quaternization reaction. The reductive amination reaction however, proved to be less effective, related to the appearance of side reactions. The polymers revealed interfacial activity as shown by measurements at a water/ CH_2Cl_2 interface. The amphiphilic glycopolymers were then used to coat PLA nanoparticles (NPs) by mannose as targeting moieties. It was found, that the size and zeta potential of the NPs was directly linked/ related to the type and the quantity of the amphiphile. NMR spectroscopy also revealed their role as surface modifiers of the NPs. Moreover, the presence and bioavailability of mannose moieties on the NPs was demonstrated by interaction with a mannose-specific lectin (GNA). However, a quantitative interpretation of the results was not possible due to non-specific adsorption of the lectin/ proteins on the NPs' surface. Further investigation would thus be necessary for the quantification of the recognition of surface-exposed mannose by a mannose-specific lectin.

References.

- ¹ Dwek, R.A.; *Chem. Rev.* **1996**, *96*, 683-720
- ² Nishimura, S.I., Matsuoka, K., Kurita, K.; *Macromolecules* **1990**, *23*, 4182-4184
- ³ Nishimura, S.I., Matsuoka, K., Furuike, T., Ishii, S., Kurita, K., Nishimura, K. M.; *Macromolecules* **1991**, *24*, 4236-4241
- ⁴ Roy, R., Pon, R.A., Tropper, F.D., Andersson, F.O.J. Chem. Soc., *Chem. Commun.* **1993**, 264-265
- ⁵ Zeng, X., Murata, T., Kawagishi, H., Usui, T., Kobayashi, K.; *Carbohydr. Res.* **1998**, *312*, 209-217
- ⁶ Smart, J.D.; Nicholls, T.J.; Green, K.L.; Rogers, D.L.; Cook, J.D.; *J. Pharm. Sci.* **2000**, *9*, 93-99
- ⁷ McGreal, E.P.; Miller, J.L.; Gordon, S.; *Curr. Opin. Immunol.* **2005**, *17*, 18-24
- ⁸ Guernonprez, P.; Valladeau, J.; Zitvogel, L.; Thery, C.; Amigorena, S.; *Annu. Rev. Immunol.* **2002**, *20*, 621-667
- ⁹ Warren, H.S.; Leclerc, C.; Adjuvants, in "Encyclopedia in Immunology"; Delves, P.J.; Roitt, I.M. (Eds.), 2nd ed.; Vol. 1, Academic press, San Diego, **1998**, pp. 36-39
- ¹⁰ Conchie, J.; Levvy, G.A.; *Meth. Carbohydr. Chem.* **1963**, *II*, 345-347
- ¹¹ Dahmen, G.; Noori, G.; *Carbohydr. Res.* **1983**, *116*, 303-307
- ¹² Fessi, H.; Puisieux, F.; Devissaguet, J.Ph.; Ammoury, N.; Benita, S.; *Int. J. Pharm.* **1989**, *55*, R1-R4
- ¹³ Stolnik, S.; Davies, M.C.; Illum, L.; Davis, S.S.; Boust, M.; Vert, M.; *J. Control. Rel.* **1994**, *30*, 57-67
- ¹⁴ Sklenar, M.; Piotto, M.; Leppik R.; Saudek, V.; *J. Magn. Reson.* **2003**, *Series A 102*, 241-245
- ¹⁵ Vila, A.; Gill, H.; McCallion, O.; Alonso, M.J.; *J. Contr. Release* **2004**, *98*, 231-244
- ¹⁶ Coombes, A.G.A.; Tasker, S.; Linblad, M.; Holmgren, K.; Hoste, K.; Toncheva, V.; Schacht, E.; Davies, M.C.; Illum, L.; Davis, S.S.; *Biomaterials* **1994**, *15*, 673-680
- ¹⁷ Stepanek, P. "Dynamic Light Scattering"; Brown, W., Ed.; Oxford University Press: New York, **1993**; Chapter 4
- ¹⁸ Dubochet, J.; Adrian, M.; Chang, J.J.; Homo, J.C.; Lepault, J.; McDowell, A.W.; Schultz, P.; *Quart. Rev. Phys.* **1988**, *21*, 129-228
- ¹⁹ Harris, J.R. "Negative Staining and Cryoelectron Microscopy: the Thin Films Techniques", Bios Scientific Publishers, Oxford, UK, **1997**

-
- ²⁰ Negrete-Herrera, N.; Letoffe, J.M.; Putaux, J.L.; David, L.; Bourgeat-Lami, E.; *Langmuir* **2004**, *20*, 1564-1571
- ²¹ Duda, A.; Penczek, S.; *Makromol. Chem., Macromol. Symp.* **1991**, *47*, 127-140
- ²² Stassen, S.; Archambeau, S.; Dubois, P.; Jerome, R.; Teyssie, P.; *J. Polym. Sci. Part A: Polym. Chem.* **1994**, *32*, 2443 - 2455
- ²³ Magnusson, G.; Noori, G.; Dahmén, J.; Frejd, T.; Lave, T.; *Acta Chemica Scandinavica B*, **1981**, *35*, 213-216
- ²⁴ Lindhorst, T.K.; Kötter, S.; Krallmann-Wenzel, U.; Ehlers, S.; *J. Chem. Soc., Perkin. Trans.* **2001**, *1*, 823-831
- ²⁵ Vangeyte, P.; Jérôme, R.; *J. Polym. Sci. Polym. Chem.* **2004**, *42*, 1132-1142
- ²⁶ Yamada, H.; Imoto, T.; Fujita, K.; Okazaki, K.; Motomura, M.; *Biochemistry* **1981**, *20*, 4836-4842
- ²⁷ Nagasaki, Y., Okada, T.; Scholz, C.; Iijima, M.; Kato, M.; Kataoka, K.; *Macromolecules* **1998**, *31*, 1473-1479
- ²⁸ Yamamoto, Y.; Nagasaki, Y.; Kato, M.; Kataoka, K.; *Colloid Surf. B: Biointerfaces* **1999**, *16*, 135-146
- ²⁹ Jule, E.; Nagasaki, Y.; Kataoka, K.; *Langmuir* **2002**, *18*, 10334-10339
- ³⁰ Detrembleur, C.; Mazza, M.; Lou, X.; Halleux, O.; Lecomte, P.; Mecerreyes, D.; Hedrick, J.L.; Jérôme, R.; *Macromolecules* **2000**, *33*, 7751-7760
- ³¹ Detrembleur, C.; Mazza, M.; Halleux, O.; Lecomte, P.; Mecerreyes, D.; Hedrick, J.L.; Jérôme, R.; *Macromolecules* **2000**, *33*, 14-18
- ³² Gautier, S.; D'Aloia, V.; Halleux, O.; Mazza, M.; Lecomte, P.; Jérôme, R.; *J. Biomater. Sci. Polym. Edn.* **2003**, *14*, 63-85
- ³³ Streitwieser, A.; *Chem. Rev.* **1956**, *56*, 571-732
- ³⁴ Hazziza-Laskar, J.; Nurdin, N.; Helary, G.; Sauvet, G.; *J. Appl. Polym. Sci.* **1993**, *50*, 651-662
- ³⁵ Ybert, C.; Di Meglio, J.-M.; *Langmuir* **1998**, *14*, 471-475
- ³⁶ Beverung, C.J.; Radke, C.J.; Blanch, H.W.; *Biophys. Chem.* **1998**, *70*, 121-132
- ³⁷ Beverung, C.J.; Radke, C.J.; Blanch, H.W.; *Biophys. Chem.* **1999**, *81*, 59-80
- ³⁸ Hagan, S.A.; Coombes, A.G.A.; Garnett, M.C.; Dunn, S.E.; Davies, M.C.; Illum, L.; Davis, S.S.; Harding, S.E.; Purkiss, S.; Gellert, P.R.; *Langmuir* **1996**, *12*, 2153- 2161

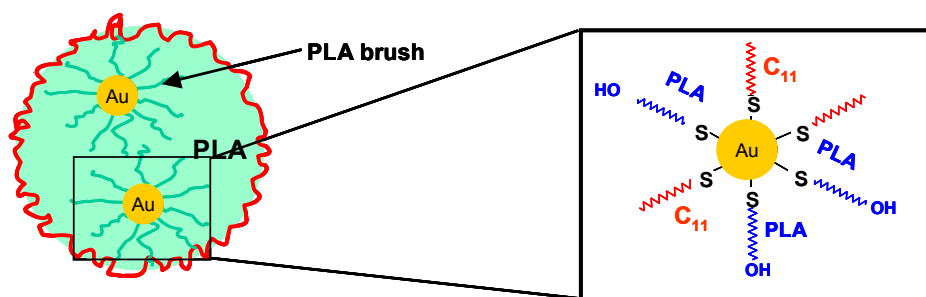
- ³⁹ Vangeyte, P.; Gautier, S.; Jérôme, R.; *Colloid Surf. A, Physicochem. Eng. Asp.* **2004**, *242*, 203–211
- ⁴⁰ Davis, S.S.; Illum, L.; Stolnik, S.; *Curr. Opin. Colloid Interf. Sci.* **1996**, *1*, 660-666
- ⁴¹ Lemarchand, C.; Gref, R.; Couvreur, P.; *Eur. J. Pharm. Biopharm.* **2004**, *58*, 327-341

Chapter 7

**PLA-coated gold nanoparticles
for the labeling of PLA biocarriers**

Abstract

Poly(D,L-lactide) end-capped by a protected thiol was synthesized by bulk ring-opening polymerization (ROP) of D,L-lactide initiated by the reaction product of aluminum isopropoxide $[Al(iOPr)_3]$ with α -(2,4-dinitrophenylsulfenyl)ethanol. After the thiol deprotection, PLA-SH was used to stabilize gold nanoparticles. Either these nanoparticles were prepared in the presence of PLA-SH, or PLA-SH was substituted for part of the undecanethiol ($C_{11}SH$) that stabilized preformed gold nanoparticles. In contrast to $C_{11}SH$ coated nanoparticles, those ones stabilized by PLA-SH were successfully entrapped into 100 nm PLA nanocarriers prepared by nanoprecipitation. This is an easy technique to label PLA biocarriers and therefore trace their fate in vivo.



Contents

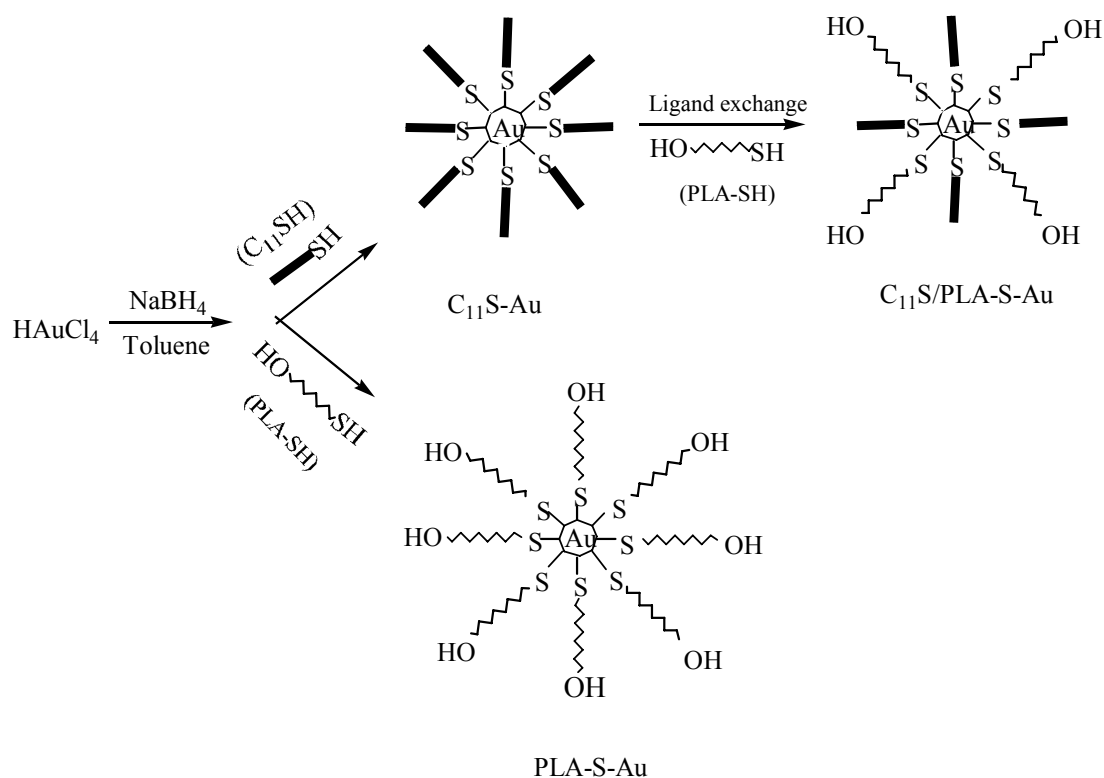
I. INTRODUCTION.....	245
II. EXPERIMENTAL PART.....	246
<i>Materials</i>	246
<i>Synthesis of α-(2,4-dinitrophenylthio) ethanol (A)</i>	247
<i>Synthesis of poly(D,L-lactide) end-capped by a protected thiol (PLA-A)</i>	247
<i>Deprotection of the thiol end-group of PLA-A</i>	247
<i>Preparation of gold nanoparticles stabilized by C₁₁SH and PLA-SH</i>	247
<i>“Ligand-exchange” for the preparation of C₁₁S/PLA-S stabilized gold NPs</i>	248
<i>Characterization</i>	248
III. RESULTS AND DISCUSSION	249
<i>III.1. Poly(D, L-lactide) end-capped by thiols</i>	249
<i>III.2. Gold nanoparticles stabilized by thiol end-capped PLA</i>	252
<i>III.3. Labeling of PLA nanocarriers</i>	257
IV. CONCLUSION	258

I. Introduction

Biocompatibility and biodegradability of polylactides make them well suited to drug delivery¹ and tissue engineering.² Although PLA nanocarriers are suitable for drug delivery, their fate in vivo remains an open question as long as they cannot be directly observed by TEM in histological sections. The labeling of PLA nanocarriers by a “contrasting” agent, such as gold nanoparticles, is thus highly desirable.

Gold nanoparticles are already frequently used as TEM contrast agents (immunogold technique³) in immunocytochemistry. For instance, antibodies adsorbed on gold nanoparticles are routinely used in histology⁴, which allows for the biospecific labeling of tissues and TEM observations.⁵ Gold-based autometallography⁶ is also a very specific method to detect molecules in biological specimens.

This paper aims at labeling PLA nanocarriers by the direct incorporation of gold nanoparticles, thus on the occasion of PLA nanoprecipitation. PLA nanocarriers result indeed from the rapid addition of water to a binary solution of PLA and a stabilizing copolymer in DMSO.⁷ The strategy proposed in this work consists in grafting PLA at the surface of gold nanoparticles, which are then dispersed in the DMSO solution of PLA and co-precipitated with formation of gold-labeled PLA nanocarriers. Two methods for the grafting of PLA at the surface of gold nanoparticles have been tested, i.e., the direct formation⁸ of gold nanoparticles in the presence of thiol end-capped poly(D,L-lactide) (PLA-SH), and the partial substitution, or ligand-exchange,⁹ of the alkylthiol ligands of preformed gold nanoparticles by PLA-SH, which results in a mixed alkyl/PLA stabilizing shell (Scheme 1). Gold nanoparticles have been prepared and stabilized by PLA-SH of different molecular weights according to each technique, and incorporated into PLA nanocarriers by nanoprecipitation.



Scheme 1. Synthetic route of gold nanoparticles stabilized by both undecanethiol and/or poly(lactide) thiol

II. Experimental Part

Materials.

Toluene was dried by refluxing over sodium and distilled under nitrogen before use. D,L-Lactide was purchased from Boehringer and purified by recrystallization from a 40 wt% solution in dry toluene. It was dried at room temperature, under reduced pressure, for 24 h before polymerization. Aluminum isopropoxide [$\text{Al}(\text{iOPr})_3$] was sublimated, and then dissolved in dry toluene (0.25 M) under nitrogen. Lactide was bulk polymerized as reported elsewhere.¹⁰ Mercaptoethanol was dried over anhydrous magnesium sulfate (MgSO_4) and distilled just before use. All the other reagents were used as received: $\text{H[AuCl}_4\text{]} \times \text{H}_2\text{O}$ (Strem, 99.9 %); $\text{N}(\text{C}_8\text{H}_{17})_4\text{Br}$ (Aldrich, 98 %); NaBH_4 (Janssen, 98 %); C_{11}SH (Aldrich, 98 %).

Synthesis of α -(2,4-dinitrophenylthio) ethanol (A).¹¹

A solution of 0.39 g of mercaptoethanol (5.0 mmol) in 4.0 ml of CHCl_3 was slowly added to a solution of 0.94 g (5.0 mmol) of 2,4-dinitrofluorobenzene mixed with 1.4 ml of triethylamine (10.0 mmol) in 6.0 ml of chloroform. The reaction mixture was stirred at room temperature for 15 h. It was neutralized with HCl (1.0 M) and then washed twice with water. Yellow crystals were collected from the organic phase and recrystallized from CHCl_3 . (Yield :68 %)

^1H NMR (CDCl_3): δ 9.06 (s, 1H, -Ar), δ 8.27 (d, 1H, -Ar), δ 7.75 (d, 1H, -Ar), δ 4.05 (t, 2H, $-\text{SCH}_2\text{CH}_2\text{OH}$), δ 3.30 (t, 2H, $-\text{SCH}_2\text{CH}_2\text{OH}$).

Synthesis of poly(D,L-lactide) end-capped by a protected thiol (PLA-A).

The initiator was prepared by reaction of 1 equiv. of $\text{Al}(\text{}^i\text{OPr})_3$ with 3 equiv. of compound **A** in toluene. The solvent was distilled off regularly in order to displace the isopropanol formed as a by-product. It was replaced by freshly dried toluene, and the azeotropic distillation was repeated (2 times). D,L-lactide was bulk polymerized at 130°C, in a previously flamed and nitrogen purged flask, for 20 h. End-functional poly(D,L-lactide) (Table 1; entries 1, “PLA1”, and 3, “PLA2”) was dissolved in THF, precipitated in heptane, and dried in vacuo. (Yield: 82 %.)

Deprotection of the thiol end-group of PLA-A.

PLA end-capped by a protected thiol was dissolved in CHCl_3 in the presence of 1-propanethiol (100 equiv). Triethylamine was added until pH was 8. The reaction mixture was stirred under nitrogen for 15 h. After elimination of the unreacted 1-propanethiol, it was poured in heptane, and the thiol end-capped PLA (PLA-SH) was precipitated (Table 1; entries 2, “PLA1-SH”, and 4, “PLA2-SH”).

Preparation of gold nanoparticles stabilized by C_{11}SH and PLA-SH, respectively.

Gold nanoparticles were prepared according to Brust *et al.*⁸ except for the Au/S molar ratio 3.5:1 as recommended by D.V. Leff *et al.*¹² In a typical experiment, 25.48 mg of $\text{HAuCl}_4 \times \text{H}_2\text{O}$ was dissolved in 2.46 ml of deionized water. 1.65 ml of a $\text{N}(\text{C}_8\text{H}_{17})_4\text{Br}$ solution in toluene (0.10 M) was added to the aqueous solution under rapid stirring ($\text{N}(\text{C}_8\text{H}_{17})_4\text{Br}/\text{Au} = 2.22:1$). The two-phase mixture was vigorously stirred until the tetrachloroaurate was completely transferred to the organic phase, which was then

separated from the slightly orange aqueous phase. The organic solution was added with 0.51 ml of a C₁₁SH solution in toluene (0.042 M), followed by the slow addition of 2.0 ml of a freshly prepared aqueous solution (0.41 M) of NaBH₄ (NaBH₄/Au =11.0:1) under vigorous stirring for 12 h. The organic phase was separated and concentrated until 1.0 ml was left, and finally added into 75 ml of ethanol (96 %). This mixture was kept at -20°C for 48 h, and the dark brown precipitate was collected by centrifugation and dried *in vacuo* (Table 2; entry 1, “C₁₁S-Au”). When PLA-SH was used instead of C₁₁SH, the reaction time was 4 h (Table 2; entries 4, “PLA1-S-Au” and 5 “PLA2-S-Au”).

“Ligand-exchange” for the preparation of C₁₁S/PLA-S stabilized gold nanoparticles.

The “ligand-exchange” reaction⁹ was carried out by adding PLA-SH to the C₁₁S-Au dispersion in toluene. In a typical experiment, 4.0 mg of C₁₁S-Au in 2.0 ml of toluene were added to 6.4 mg of PLA-SH (Mn = 2400), and stirred for 48 h at room temperature. The solvent was removed *in vacuo*, and the collected material was washed abundantly with absolute ethanol and recovered by centrifugation (Table 2; entries 2, “C₁₁S/PLA1-S-Au” and 3, C₁₁S/PLA2-S-Au”). The Au/S atomic ratio was 4.2 for the C₁₁S-Au nanoparticles according to the data reported elsewhere.¹²

Characterization.

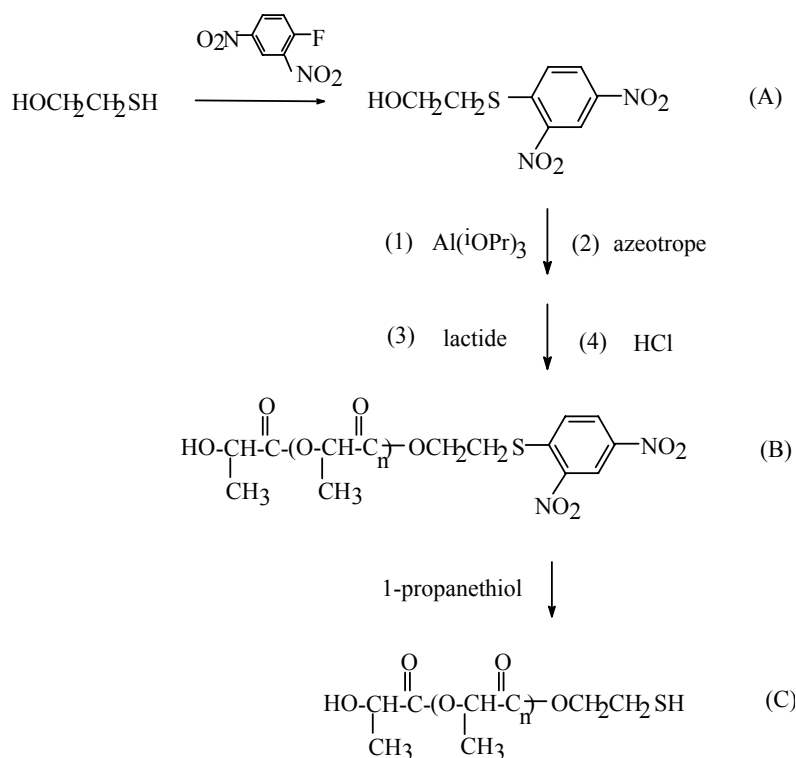
Poly lactide was analyzed by ¹H NMR spectroscopy with a Bruker AM 400 apparatus at 25°C, in deuterated chloroform added with tetramethylsilane as an internal reference. Number-average molecular weight was calculated from the intensity ratio for the CH protons of the lactide units ($\delta= 5.2$) and the CH₂ protons adjacent to the sulfide end-group ($\delta= 3.3$) (see Fig. 1A). It was also determined by size exclusion chromatography (SEC) in THF with a HP 1090 liquid chromatograph, equipped with a HP 1037 A refractive index detector and four PL GEL columns of various pore sizes (10⁵, 10⁴, 500 and 100 Å). Absolute molecular weights were calculated by using polystyrene standards and the Mark-Houwink equations for polystyrene ($K_{PS}=1.25\times 10^{-4}$ dl/g, $\alpha_{PS}=0.707$) and poly lactide ($K_{PLA}=5.49\times 10^{-4}$ dl/g and $\alpha_{PLA}=0.639$), respectively.

Transmission electron micrographs (TEM) were recorded with a Philips CM-100 microscope. Samples were prepared by spreading a drop of a dilute dispersion of particles on a copper grid coated with Formvar. UV-vis spectra were recorded for gold nanoparticles dispersed in chloroform and DMSO. Raman spectra of gold nanoparticles were recorded

with a LabRam spectrometer (Jobin-Yvon) equipped with a confocal microscope and a liquid N₂ cooled “Open electrode” CCD. The spectral resolution was 2 cm⁻¹. The excitation laser beam (514.5 nm) was focused on the sample, previously deposited onto a glass plate and dried. In order to prevent the coloured sample from being burnt, the power of the laser was kept at the minimum value (0.5 mW), and the integration time was increased accordingly (100 sec.). Because of the grafting dispersion and the length of the CCD detector (1 inch), the full spectrum was recorded in two parts, covering the 200-1800 cm⁻¹ and 2400-3700 cm⁻¹ ranges, respectively. Dynamic light scattering (DLS) was carried out with a Brookhaven instrument (Ar laser, 488nm) with a suspension diluted by filtered deionized water until a PLA concentration of 50µg/ml was reached. The size distribution was calculated by the Contin method.

III. Results and Discussion

III.1. Poly(D, L-lactide) end-capped by thiols (Scheme 2).



Scheme 2. Synthetic route for the thiol end-capping polylactide

A few examples of thiol end-capped chains have been reported in the scientific literature.¹³ In this work, a method reported for poly(ϵ -caprolactone) (PCL) by J. L. Hedrick *et al.*¹¹ has been extended to PLA. As shown in Scheme 2, the thiol has been protected by 2,4-dinitrofluorobenzene (Sangers reagent), which is highly reactive towards a variety of functional groups.¹⁴ Deprotection is possible under mild conditions as discussed hereafter. Moreover, the aromatic protecting group can be unambiguously identified by ^1H NMR, which is an advantage for monitoring both the end-capping and the deprotection reactions. In this respect, Figure 1A shows the ^1H NMR spectrum for PLA end-capped by the protected thiol. Resonances typical of PLA are observed at 5.16 and 1.56 ppm,^{10, 15} respectively.

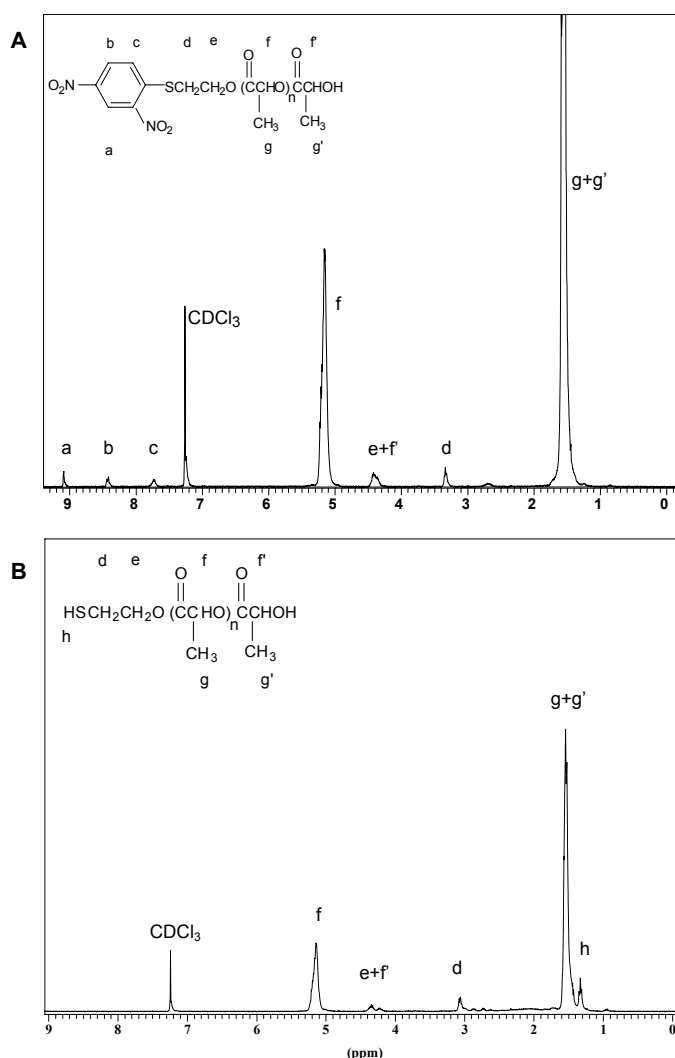


Figure 1. ^1H NMR spectra for thiol end-capped poly(lactide): (A) before, (B) after deprotection

The aromatic protons of the 2, 4-dinitrophenylsulfenyl moiety are observed at 9.09, 8.42 and 7.73 ppm, respectively. The chemical shifts for the protons of the two methylene groups between the O and S atoms are at 4.43 and 3.33 ppm, respectively, thus different from the values noted for 2, 4-dinitrophenylsulfenyl ethanol, i.e. $\delta = 4.05$ and 3.31 ppm. This peaks assignment allows for the molecular weight of PLA to be calculated (intensity ratio of peaks f and d) and compared to SEC data as shown in Table 1. Bulk polymerization of LA at 130°C results in a broad molecular weight distribution ($M_w/M_n = 4.0$ for low M_n (1200 g/mol) and 2.1 for $M_n = 3500$ g/mol). A slow initiation compared to propagation together with the slow dissolution of the initiator in the molten monomer contribute to this effect.

Table 1. Characteristic features of thiol-functionalized polylactide

<i>polylactide</i>	<i>type</i>	$[M_0]/[Al]$	<i>conv.</i> %	M_n^a		<i>Polydispersity</i>
				^1H-NMR	SEC	M_w / M_n
PLA1	protected	64	100	3500	3800	2.10
PLA1-SH	deprotected			4700	4800	1.55
PLA2	protected	25	100	1200	800	4.00
PLA2-SH	deprotected			2100	2400	1.50

^a M_n : number average molecular weight; conv. stands for conversion

The thiol end-group of PLA has been deprotected by a large excess of 1-propanethiol in chloroform. This solvent is needed for the deprotection of PLA of the higher M_n (3500 g/mol) to be quantitative. The 1H NMR spectrum (Figure 1B) confirms the successful deprotection of PLA. The resonance peaks (a, b and c) for the phenyl group have disappeared, in contrast to peak d (-S-CH₂-) which has been shifted significantly from $\delta = 3.33$ to $\delta = 3.10$ ppm. Consistently, an additional peak assigned to -SH is observed at $\delta = 1.32$ ppm. Unexpectedly, M_n of PLA is higher and the polydispersity is lower after deprotection. The only reasonable explanation is that the shorter chains are lost when PLA is purified by reprecipitation in heptane. More PLA is recovered when it is precipitated at low temperature rather than at room temperature, which confirms that the PLA solubility is very sensitive to molecular weight at least in the temperature range under consideration.

III.2. Gold nanoparticles stabilized by thiol end-capped PLA.

C₁₁S-Au nanoparticles have been prepared by an *in-situ* method⁸ and used as a reference to investigate whether PLA-SH can have a beneficial effect on the stability of dispersion of gold nanoparticles in various solvents. These particles are waxy with a dark-brown color. They are repeatedly dispersible in non or weakly polar solvents, such as heptane, toluene and chloroform, but not at all in more polar solvents, such as DMSO (Table 2).

Table 2. Dispersions of gold nanoparticles in organic solvents

<i>Properties</i> <i>Nanoparticles</i>	<i>Solvent</i>					<i>Size (nm)</i>
	<i>Water</i>	<i>Heptane</i>	<i>Toluene</i>	<i>Chloroform</i>	<i>DMSO</i>	
C₁₁S-Au	-	+	+	+	-	7±2
C₁₁S/PLA1-S-Au	-	-	+	+	+	2±1
C₁₁S/PLA2-S-Au	-	-	+	+	+	3±1
PLA1-S-Au	-	-	-	-	+	6±1
PLA2-S-Au	-	-	-	-	+	5±1

+: Dispersible; -: not dispersible; DMSO: dimethylsulfoxide; 1: PLA1-SH with Mn = 2400 and PLA1-S/C₁₁S ratio = 0.4 ; 2: PLA2-SH with Mn = 4800 and PLA2-S/C₁₁S ratio = 0.6. The size was estimated by measurements of 100 nanoparticles on enlarged TEM images.

PLA-SH has then been exchanged for the ligand of the C₁₁S-Au nanoparticles (Scheme 1), according to two PLA-S/C₁₁S ratios, i.e., 0.4 and 0.6, respectively. The particles then appear as a solid with a light brown color. They are dispersible in toluene, chloroform and highly polar DMSO, but no longer in heptane which is a non-solvent for PLA (Table 2). This observation is valid to the set of PLA chains listed in Table 1. Whenever PLA-S-Au nanoparticles are prepared in a direct way (*in-situ* method; Scheme 2), Table 2 shows that they can be redispersed after purification only in DMSO with a deep purple color. These gold nanoparticles have been dispersed in two-phase heptane/DMSO mixtures as illustrated in Figure 2.

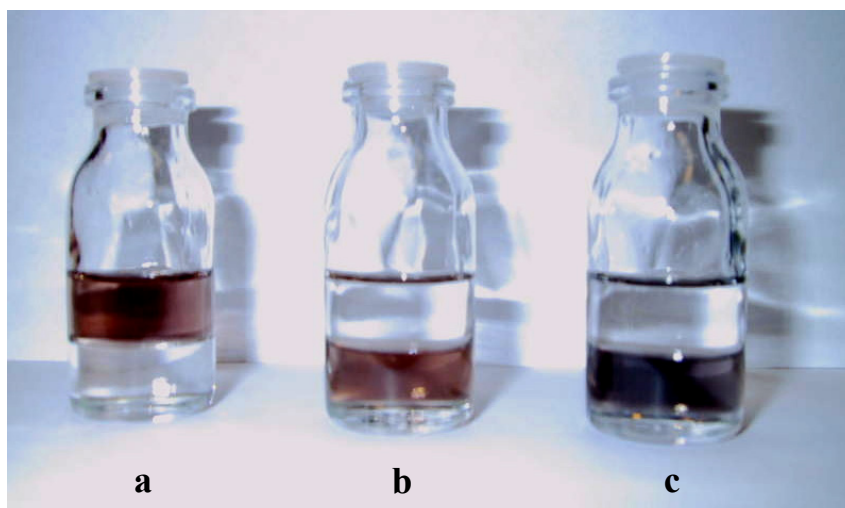


Figure 2. Dispersion of gold nanoparticles in two-phase heptane (top)/DMSO (bottom) mixtures. Stabilization by a) undecanethiol, b) mixed undecanethiol/poly lactide-thiols, c) poly lactide-thiol.

These observations indicate that the dispersion stability closely depends on the amount of PLA-SH adsorbed onto the gold nanoparticles. Indeed, stability is noted in solvents of increasing polarity (heptane < toluene and chloroform < DMSO) when the undecanethiol ligand ($C_{11}SH$) is replaced partly (29 % and 38 %, as confirmed by 1H NMR) and then completely by PLA-SH.

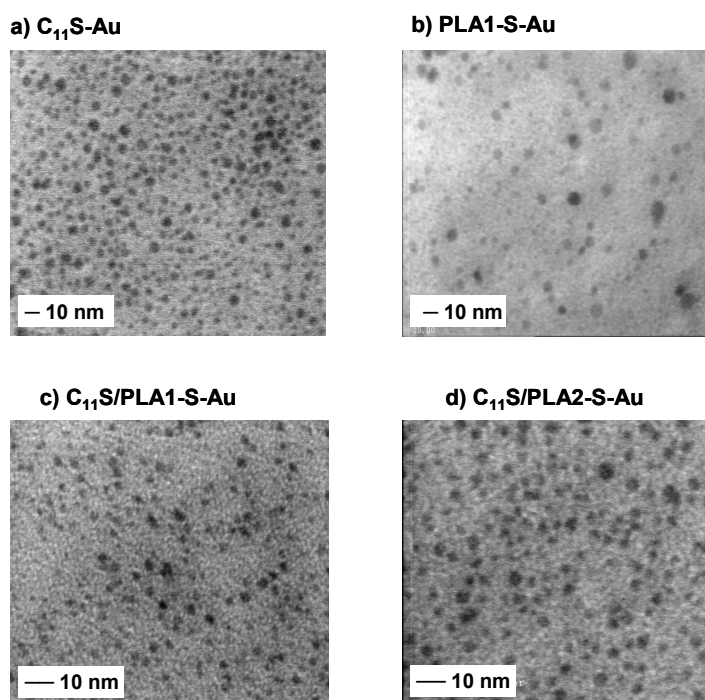


Figure 3. TEM of gold nanoparticles stabilized by: a) undecanethiol, b) poly lactide- thiol c) mixed undecanethiol/poly lactide ($M_n = 2400$) thiol and d) mixed undecanethiol/poly lactide ($M_n = 4800$) thiols

Gold nanoparticles have been observed by transmission electron microscopy (TEM). Figure 3 shows spherical nanoparticles, of which the size is reported in Table 2. Nanoparticles with a corona of mixed ligands ($C_{11}S$ and PLA-S) are significantly smaller (Figures 3c and 3d) than the $C_{11}S$ -Au coated particles (figure 3a) with a more uniform size distribution. This modification is typical for particles prepared by the “ligand-exchange” method,¹⁶ more likely because they are recovered by centrifugation after reaction. The non (or not extensively enough) modified $C_{11}S$ -Au nanoparticles would not precipitate in the excess of ethanol, so leading to size fractionation. Although the difference is not very important ($\pm 15\%$), the PLA1-S-Au nanoparticles are smaller than the $C_{11}S$ -Au ones, which could be reasonably explained by a simple molecular packing model as shown in Figure 4. The solvated PLA chains are supposed to be coiled, compared to the short C_{11} alkyl radicals, which would be rather rod-shaped.¹⁷ Therefore, the PLA chains are less densely packed at the gold surface, with the consequence that the occupied area is larger, and the gold nanoparticles are smaller. The space conformation of the ligand can thus affect the size of the stabilized gold nanoparticles.¹⁸

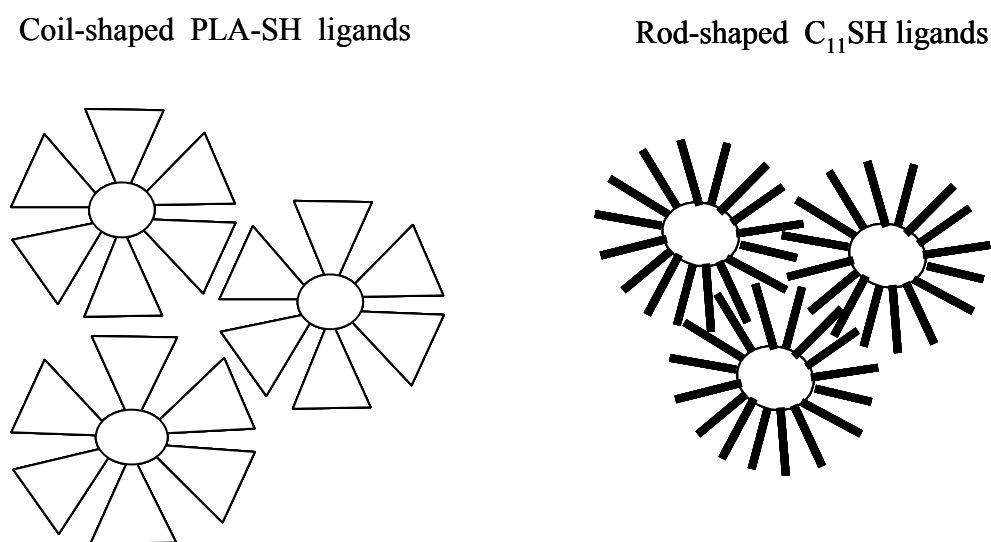


Figure 4. Molecular packing model for gold nanoparticles stabilized by PLA-SH and $C_{11}SH$

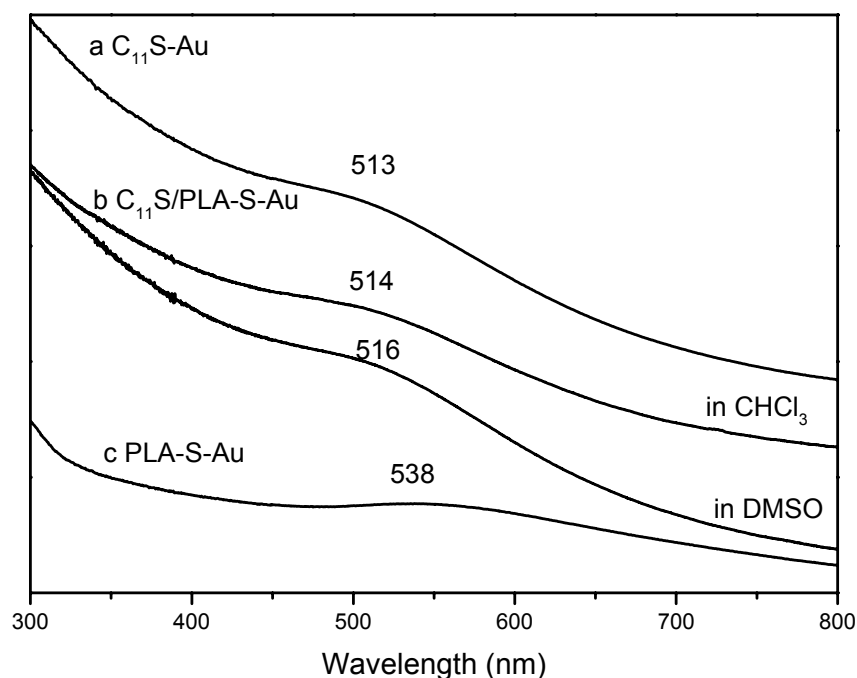


Figure 5. UV-vis spectra for thiol-stabilized gold nanoparticles in different solvents at room temperature: a) undecanethiol (CHCl₃), and b) undecanethiol/poly lactide (Mn : 2400) thiol (CHCl₃ and DMSO), c) poly lactide (Mn: 2400) thiol (DMSO)

UV-vis spectroscopy was used to characterize the gold nanoparticles (Figure 5). The maximum of absorption, which corresponds to the gold plasmon resonance,¹⁹ is known to depend on several factors including particle size, surface functionality, solvent and temperature.²⁰ No significant modification is observed in the maximum absorption for the C₁₁S-Au and C₁₁S/PLA-S-Au particles, whereas a bathochromic shift is observed for the PLA-S-Au ones. This shift cannot be accounted for by a solvent effect (comparison of CHCl₃ and DMSO in Figure 5b), and it is exceedingly large for being explained by the difference in the particles size reported in Table 2. A possible explanation might be found in the way that the ligands (C₁₁S-Au and PLA-S) interact with the gold surface. Although the C₁₁ alkyl substituents have no reason to interact with the metal, this is not the case for the ester of the PLA monomer units (Figures 5a and 5c). However, when the two types of ligands coexist (Figure 5b), only the chemisorption of the thiol would be effective.

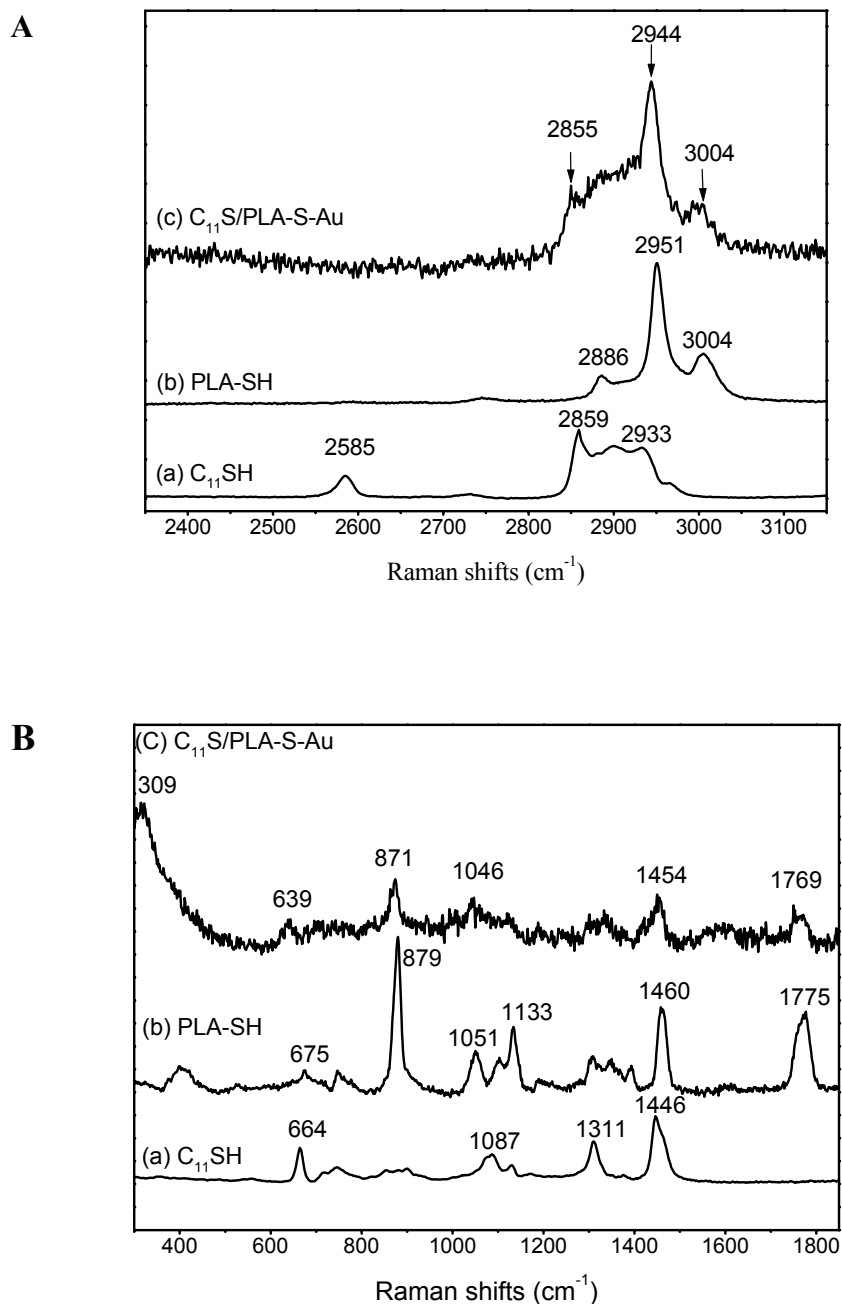


Figure 6. Raman spectra in the $2350-3150\text{ cm}^{-1}$ region (6A) and in the $300-1850\text{ cm}^{-1}$ region (6B), for liquid undecanethiol (a), and solid polylactide thiol (b) and gold nanoparticles stabilized by undecanethiol/poly lactide ($M_n = 2400$) thiol (c).

Thiol-stabilized nanoparticles have been characterized by Raman spectroscopy in the scientific literature.²¹ In this study, Raman spectra have been recorded to confirm that the ligand exchange of PLA-SH for $C_{11}SH$ is efficient. Figure 6 shows bands characteristic of the C-H binding at $2859 - 2933\text{ cm}^{-1}$ for (unadsorbed) $C_{11}SH$ (Figure 6A-a), and at 2886

and 2951cm^{-1} for (unadsorbed) PLA-SH (Figure 6A-b). The bands of C_{11}S and PLA-S remain visible in case of the $\text{C}_{11}\text{S}/\text{PLA-S-Au}$ nanoparticles (Figure 6A-c). Moreover, the band assigned to S-H of C_{11}SH at 2585cm^{-1} is no longer observed for the $\text{C}_{11}\text{S}/\text{PLA-S-Au}$ nanoparticles, in agreement with the formation of a S-Au bonding. Figure 6 B shows the C-S stretching region, which provides structural information on the fragment adjacent to the sulfur head group.²² The band at 639cm^{-1} is typical of the C-S bonding,²² when S is linked to gold in the $\text{C}_{11}\text{S}/\text{PLA-S-Au}$ nanoparticles. The Raman spectrum for the $\text{C}_{11}\text{S}/\text{PLA-S-Au}$ nanoparticles also shows bands at 1769cm^{-1} characteristic of the PLA ester groups and at 1454 , 1046 and 871cm^{-1} , which confirms the contribution of PLA-SH to the stabilization of the gold nanoparticles. Moreover, the Au-S bonding is observed at 309cm^{-1} , which confirms that the nanoparticles are stabilized by thiols.

III.3. Labeling of PLA nanocarriers.

The gold nanoparticles stabilized by the mixed $\text{C}_{11}\text{SH}/\text{PLA-SH}$ shell have been successfully dispersed in DMSO, without alteration of size and /or shape, thus without aggregation. They have been encapsulated in polylactide nanocarriers prepared by nanoprecipitation as reported by S. Gautier *et al.*⁷ (Figure 7). Briefly, the PLA nanocarriers were prepared by rapid addition of water (4 fold excess) to a DMSO solution of poly(D,L-lactide) (16 mg/mL; Mn 50000) and poly(methyl methacrylate-co-methacrylic acid) (PMMA-co-MA) (1.6 mg/mL; Mn = 13000, MA content = 25 mol%). The average size of the accordingly formed PLA nanocarriers is about 100 nm.

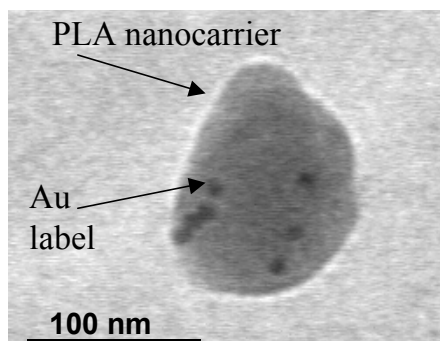


Figure 7. TEM of polylactide nanocarriers labeled by $\text{C}_{11}\text{S}/\text{PLA-S-Au}$ nanoparticles (Mn of PLA: 2400).

Labeling of PLA nanocarriers by addition of conventional negatively-charged Au-citrate nanoparticles²³ or commercially available (Sigma) hydrophilic Au-streptavidin nanoparticles to the aqueous phase used to (nano)precipitate PLA, was not successful. Indeed, a weak affinity for PLA and a highly stable dispersion in water prevent these hydrophilic gold-nanoparticles from co-precipitating with PLA. In contrast, when C₁₁S-/PLA-S-Au (ca. 2.44 nm) or PLA-S-Au (ca.5.56 nm) nanoparticles are dispersed in the DMSO solution, they are successfully encapsulated in the PLA nanocarriers (Figure 7). DLS measurements have shown that the size (136±12nm) and size distribution of the PLA nanocarriers are not significantly modified by the gold nanoparticles. Moreover, the gold-labeled nanocarriers do not exhibit higher propensity to aggregation than the neat nanoparticles in solution. The PLA-S- shell makes gold nanoparticles appropriate to the labeling of PLA nanocarriers and their tracing within tissues. *In vivo* experiments are under current investigation.

IV. Conclusion

Thiol end-capped PLA has been synthesized by ROP of lactide initiated by a protected thiol containing alcohol, followed by deprotection. The efficiency of the end-capping and deprotection reactions has been confirmed by ¹H NMR. After deprotection of the thiol end-group, Mn is increased and the polydispersity is decreased, as result of fractionation when the thiol end-capped PLA is reprecipitated in heptane. Gold nanoparticles have been successfully stabilized by PLA-SH, either directly by the “*in-situ*” method in a two-phase system or by a “ligand-exchange” reaction. Stability of dispersions of PLA-SH coated gold nanoparticles in DMSO increases with the amount of PLA-SH attached to the surface (PLA-S-Au > C₁₁S/PLA-S-Au > C₁₁S-Au). TEM shows that the average size lies in 7-2 nm depending on the structure and size of the ligand(s). These C₁₁S/PLA-S-Au and PLA-S-Au nanoparticles can be successfully encapsulated in PLA nanocarriers, which are accordingly labeled and could be traced by autometallography of TEM sections.⁶

References.

- ¹ Kreuter, J. *J. Control. Rel.* **1991**, *16*, 169. Alleman, E.; Gurny, R.; Doelker, E. *Eur. J. Pharm. Biopharm.* **1993**, *39*, 173. Deng, X.; Liu, Y.; Yuan M.; Li X.; Lin, L.; Jia, W. X. *J. Appl. Polym. Sci.* **2002**, *86*, 2557.
- ² Kulkarni, R. K.; Moore, E. G.; Hegyeli, F.; Leonard, F. *J. Biomed. Mater. Res.* **1971**, *5*, 163. Pitt, C. G.; Marks, T. A.; Schlinder, A. In *Biodegradable Drug Delivery Systems Based on Aliphatic Polyesters: Application of Contraceptives and Narcotic Antagonists, Controlled Release of Bioactive Materials*; Baker, R., Ed.; Academic, New York, **1980**.
- ³ De Mey, J. *Immunocytochemistry, practical application in pathology and biology*; Polak, J. M.; Van Naarden, S., Eds.; Wright-PSG, **1983**, Chapter 6, 83.
- ⁴ Kreuter, J. In *Microcapsules and Nanoparticles in Medicine and Pharmacy*; Donbrow, M., Ed.; CRC, Boca Raton, **1992**.
- ⁵ Safer, D.E.; Bolinger, L.; Leigh, J. S. *J. Inorg. Biochem.* **1986**, *26*, 77. Safer, D. E.; Hainfeld, J.; Wall, J. S.; Reardon, J. E. *Science* **1982**, *218*, 290. Hainfeld, J. F.; Furuya, F. R. *J. Histochem., Cytochem.* **1992**, *40*, 177.
- ⁶ Weipoltshammer, K.; Schofer, C.; Almeder, M.; Wachtler, F.; *Histochem. Cell. Biol.* **2000**, *114*, 489.
- ⁷ Gautier, S.; Grudzielski, N.; Goffinet, G.; Hassonville, S. H. D.; Delattre, L.; Jérôme, R. *J. Biomater. Sci. Polymer Edn.* **2001**, *12*, 429. Grandfils, C.; Nihant, N.; Jérôme, R.; Teyssié, P. *Patent US* **1999**, No. 5,962, 566.
- ⁸ Brust, M.; Walker, M.; Bethell, D.; Schiffrin, D. J.; Whyman, R. *J. Chem. Soc., Chem. Commun.* **1994**, 801.
- ⁹ Hostetler, M. J.; Green, S. J.; Stokes, J. J.; Murray, R. W. *J. Am. Chem. Soc.* **1996**, *118*, 4212.
- ¹⁰ Degée, P.; Dubois, P.; Jérôme, R. *Macromol. Symp.* **1997**, *123*, 67.
- ¹¹ Trollsas, M.; Hawker, C. J.; Hedrick, J. L. *Macromolecules* **1998**, *31*, 5960.
- ¹² Leff, D. V.; Ohara, P. C.; Heath, J. R.; Gelbart, W. M. *J. Phys. Chem.* **1995**, *99*, 7036.
- ¹³ Stouffer, J. M.; McCarthy, T. J. *Macromolecules* **1988**, *21*, 1204. Premachandran, R.; Banerjee, S.; John, V. T.; McPherson, G. L. *Chem. Mater.* **1997**, *9*, 1342. Hirao, A.; Shione, H.; Wakabayashi, S.; Nakahama, S.; Yamagushi, K.; *Macromolecules* **1994**, *27*, 1835. Tohyama, M.; Hirao, A.; Nakahama, S.; *Makromol. Chem. Phys.* **1996**, *197*, 3135. Corbierre, M. K.; Cameron, N. S.; Sutton, M.; Mochrie, S. G. J.; Lurio, L. B.; Rühm, A.; Lennox, R. B. *J. Am. Chem. Soc.* **2001**, *123*, 10411. Nuss, S.; Böttcher, H.;

- Wurm, H.; Hallensleben, M. L.; *Angew. Chem., Int. Ed.* **2001**, *40*, 4016. Chiefari, J.; Chong, Y. K.; Ercole, F.; Krstina, J.; Jeffery, J.; Le, T. P.T. Mayadunne, R. T. A.; Meijs, G. F.; Moad, C. L.; Moad, G.; Rizzardo, E.; Thang, S. H. *Macromolecules* **1998**, *31*, 5559. Sumerlin, B. S.; Donovan, M. S.; Mitsukami, Y.; Lowe, A. B.; McCormick, C. L.; *Macromolecules* **2001**, *34*, 6561. Mitsukami, Y.; Donovan, M. S.; Lowe, A. B.; McCormick, C. L. *Macromolecules* **2001**, *34*, 2248. Donovan, M. S.; Lowe, A. B.; Sumerlin, B. S.; McCormick, C. L.; *Macromolecules* **2002**, *35*, 4123. Donovan, M. S.; Sanford, T.; Lowe, A. B.; Mitsukami, Y.; Sumerlin, B. S.; McCormick, C. L. *Macromolecules* **2002**, *35*, 4570.
- ¹⁴ Sanger, F. *Biochem. J.* **1945**, *39*, 507. Zahn, H.; Trautmann, K. Z. *Naturforsch.* **1954**, *9B*, 578. Siepmann, E.; Zahn, H. *Biochim. Biophys. Acta* **1964**, *82*, 412. Prisco, G. D. *Biochem. Biophys. Res. Commun.* **1967**, *26*, 148. Shaltiel, S. *Biochem. Biophys. Res. Commun.* **1967**, *29*, 178.
- ¹⁵ Degée, P.; Dubois, P.; Jérôme, R. *Macromol. Chem. Phys.* **1997**, *198*, 1973.
- ¹⁶ Brown, L.O.; Hutchison, J. E. *J. Am. Chem. Soc.* **1999**, *121*, 882. Martin, J. E.; Wilcoxon, J. P.; Odinek, J.; Provencio, P. *J. Phys. Chem. B* **2000**, *104*, 9475.
- ¹⁷ Ullman, A. *Chem. Rev.* **1996**, *96*, 1533. Yonezawa, T.; Onoue, S.; Kunitake, T. *Polym. Prepr. Jpn.* **1999**, *48*, 3547.
- ¹⁸ Yonezawa, T.; Yasui, K.; Kimizuka, N. *Langmuir* **2001**, *17*, 271.
- ¹⁹ Henglein, A. *J. Phys. Chem.* **1993**, *97*, 5457.
- ²⁰ Hostetler, M. J.; Wingate, J. E.; Zhong, C. J.; Harris, J. E.; Vachet, R.W.; Clark, M.R.; Londono, J. D.; Green, S. J.; Stokes, J. J.; Wignall, G. D.; Glish, G. L.; Porter, M. D.; Evans, N. D.; Murray, R.W. *Langmuir* **1998**, *14*, 17. Link, S.; El-Sayed, M. A. *J. Phys. Chem. B* **1999**, *103*, 4212. Shipway, A. N.; Katz, E.; Willner, I. *Chem Phys Chem* **2000**, *1*, 18.
- ²¹ Lee, P. C.; Meisel, D. *J. Phys. Chem.* **1982**, *86*, 3391. Xu, H.; Tseng, C. H.; Vickers, T. J.; Mann, C. K.; Schlenoff, J. B. *Surf. Sci.* **1994**, *311*, L707.
- ²² Hosteter, M. J.; Stokes, J. J.; Murray, R.W. *Langmuir* **1996**, *12*, 3604.
- ²³ Jana, N. R.; Gearheart, L.; Murphy, C. J. *Langmuir* **2001**, *17*, 6782.

General Conclusions and Perspectives

The main target of this work was the surface modification of polymeric nanoparticles by novel biocompatible amphiphilic copolymers, composed of hydrophilic poly(ethylene oxide) (PEO) and hydrophobic poly(ϵ -caprolactone) (PCL).

The first part of this work was devoted to the controlled synthesis of the copolymers and their complete characterization. Their amphiphilic properties were then analyzed, and they were employed as stabilizers and surface modifiers for the nanoparticles. The main results are summarized hereafter.

1. Controlled synthesis and characterization of amphiphilic copolymers of various architectures composed of PEO and PCL

As shown in Scheme 1, PEO/ PCL copolymers of three different **architectures**, (i) *diblock*, (ii) *graft* (gradient or random) and (iii) *star*-shaped copolymers were synthesized by controlled polymerization techniques.

(i) PEO-*b*-PCL *diblock* copolymers α -terminated by either a methoxy group or a functional group protected or not, were prepared by sequential polymerization. The anionic polymerization of ethylene oxide was initiated by a potassium alkoxide containing the envisioned α end-group. Then, the ω -hydroxy end-group of PEO was converted into an Al alkoxide in order to initiate the ϵ -caprolactone (ϵ -CL) polymerization in a controlled manner. PEO-*b*-PCL diblock copolymers with the expected molecular characteristics and a narrow molecular weight distribution were accordingly prepared. In addition, diblock copolymers terminated by either a tertiary amine or an aldehyde group were reacted with mannose derivatives with formation of amphiphilic glycopolymers.

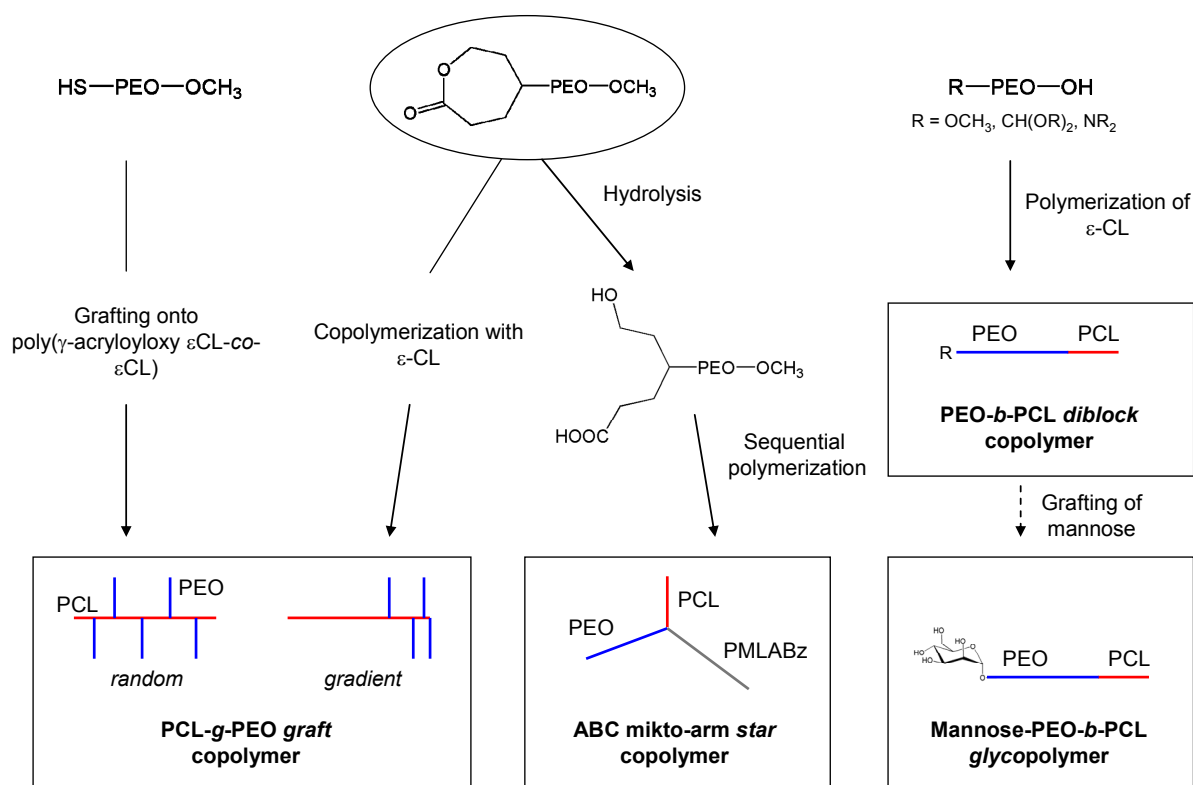
(ii) PEO-*g*-PCL *graft* copolymers were successfully synthesized by two strategies, (a) the “macromonomer method”, using a PEO macromonomer, (b) the “grafting onto” approach based on the "Michael addition".

The strategy (a) requires the synthesis of a novel PEO macromonomer copolymerizable by ring-opening polymerization. An original pathway for end-capping PEO chains by an ϵ -caprolactone unit was proposed, based on the controlled anionic polymerization of ethylene oxide initiated by an alkoxide derivative of cyclohexanone, which is a precursor of ϵ -CL. Attention was paid to the complete conversion of the ω -

hydroxyl end-group into a methoxy group in order to prevent the macromonomer (co)polymerization from being perturbed. The reactivity ratios of the macromonomer (γ PEO.CL) and ϵ -CL showed the preferential incorporation of ϵ -CL in the growing chains. The copolymer has thus a "gradient" or "palm-tree" structure.

In the second strategy (b), a copolymer bearing pendant reactive groups was synthesized by copolymerization of ϵ -caprolactone with a functional comonomer: γ -(acryloyloxy)- ϵ -caprolactone. A random copolymer was formed as supported by reactivity ratios similar for the two comonomers. The pendant acrylates were reacted with the thiol groups of α -methoxy- ω -mercapto PEO chains (Michael addition) with formation of *random* PCL-g-PCL graft copolymers.

(iii) Finally, a third type of copolymers with a *star-shaped* structure was prepared by using the γ PEO.CL macromonomer. Indeed, the alkaline hydrolysis of the lactone end-group released a carboxylate group, suitable for the anionic polymerization of benzyl β -malolactonate (MLABz), and a hydroxyl group, able to initiate the ring opening polymerization of ϵ -CL. $^1\text{H-NMR}$ and SEC confirmed the synthesis of the desired ABC mikto-arm star copolymer.



Scheme 1. Overview of the PEO derivatives and copolymers synthesized in this work.

2. Amphiphilic properties of the block and gradient graft copolymers and their use as stabilizers and surface modifiers in the preparation of polymeric nanoparticles

The amphiphilic properties of the PEO/PCL diblock and gradient graft copolymers were investigated by measurement of the interfacial tension γ at an oil/water interface. All the copolymers decreased γ significantly. However the extent of the interfacial activity was influenced mainly by the copolymer architecture and the hydrophilic-lipophilic balance (HLB) of the copolymers, and only slightly by the total molecular weight and degree of grafting.

It must be emphasized that both building blocks of the copolymers are biocompatible. Moreover PCL is biodegradable and PEO is bioeliminable and known for protein-repellent properties. Because of these unique properties and their interfacial activity, these copolymers were used as stabilizers and/ or surface modifiers for polymeric nanoparticles.

The first series of experiments aimed at preparing “stealthy” polymeric nanoparticles (NPs). Such NPs adsorbed proteins very weakly and did not activate importantly the complement system, which is part of the human immune system and responsible for the rapid removal of foreign bodies from the blood circulation. Both the PEO containing diblock and graft copolymers stabilized PLA nanoparticles. The surface properties, and thus the stealthiness of the NPs, were directly governed by the structural characteristics of the copolymers used as stabilizers. The gradient graft copolymers were found more effective in preventing protein adsorption than the diblocks, and the best results were observed for the most hydrophilic graft copolymer, i.e., the copolymer containing most ethylene oxide units.

A further aim of this study was the preparation of nanoparticles that target selectively dendritic cells, which possess receptors for mannose molecules at their surface. PEO-*b*-PCL diblock copolymers terminated by a mannose unit at the PEO extremity were used in order to decorate the surface of PLA nanoparticles with mannose. Zeta potential measurements and $^1\text{H-NMR}$ spectroscopy confirmed the presence of the copolymers at the NPs' surface. Finally, the bioavailability of mannose residues at the nanoparticle surface was supported by recognition assays (Enzyme-Linked Lectin Assay (ELLA) and labeling

by gold nanoparticles (for CryoTEM)), based on the specific recognition by mannose-specific lectins.

Perspectives

In the frame of this work, some copolymers and their synthesis raised interest. The novel α -(ϵ -caprolactone) PEO macromonomer is a very versatile macromolecule. It was used as a PEO macromonomer in *Chapters 1 and 2* and as precursor of a α -double-headed PEO chain in *Chapter 4*. All the possibilities have however not been exploited. For instance, the hydrolysis of α -(ϵ -caprolactone) PEO, ω -end-capped by a hydroxyl group should lead to an α,α' -(hydroxy, carboxy)- ω -hydroxy PEO, that could find application in the synthesis of dendrimers by polycondensation.

Moreover, a novel ABC mikto-arm star copolymer composed of PEO, PCL and PMLABz arm was synthesized. In a next step, the carboxyl groups of the PMLABz block should be deprotected, so leading to copolymers that are biocompatible and bioeliminable/biodegradable on top of being pH-responsive. It would be very interesting to investigate the properties of this type of amphiphilic star-shaped terpolymer in water, e.g., micellization as a function of pH.

Because of largely different reactivity ratios, the PEO macromonomer and ϵ -caprolactone (ϵ -CL) led to gradient graft copolymers (*Chapter 2*). Therefore, copolymerization of the macromonomer with monomers of a closer reactivity, such as lactides (LA), might be considered. PLA-*g*-PEO copolymers could be used as stabilizers and surface modifiers for PLA nanoparticles rather than PCL-*g*-PEO.

Targeting of specific tissues or organs by nanoparticles is a challenge that was addressed in this study. Indeed, PCL-*b*-PEO copolymers with mannose attached as a probing molecule to PEO were synthesized. Moreover, graft copolymers proved to be very efficient surface modifiers. It would thus be interesting to synthesize PCL-*g*-PEO graft copolymers, with a biomolecule attached at the end of the PEO chains. These copolymers could be synthesized by a Michael-type addition of bifunctional PEO chains, such as biotin-PEO-SH.

It was shown that the surface of PLA nanoparticles could be modified by small quantities of mannosylated amphiphilic copolymers. However, the bioavailability and the specific recognition of the mannose molecules at the surface of the NPs by lectins could not be demonstrated firmly, because of non-specific adsorption of the recognition proteins (lectins) at the NPs' surface. Two strategies might be employed in the future. Firstly, larger quantities of PEO containing copolymers (e.g., mixture of PEO-*b*-PCL copolymers and mannosylated copolymers), should be used in order to make the nanoparticles stealthy. Secondly, the specific interaction of the NPs by lectines should be studied by more specific techniques, such as isothermal titration calorimetry (ITC).

The loading of the nanoparticles by bioactive compounds/drugs, and the study of the release profiles should complete this study. Finally, toxicity tests and *in vivo* recognition tests are crucial on the way to the biomedical application of these systems.